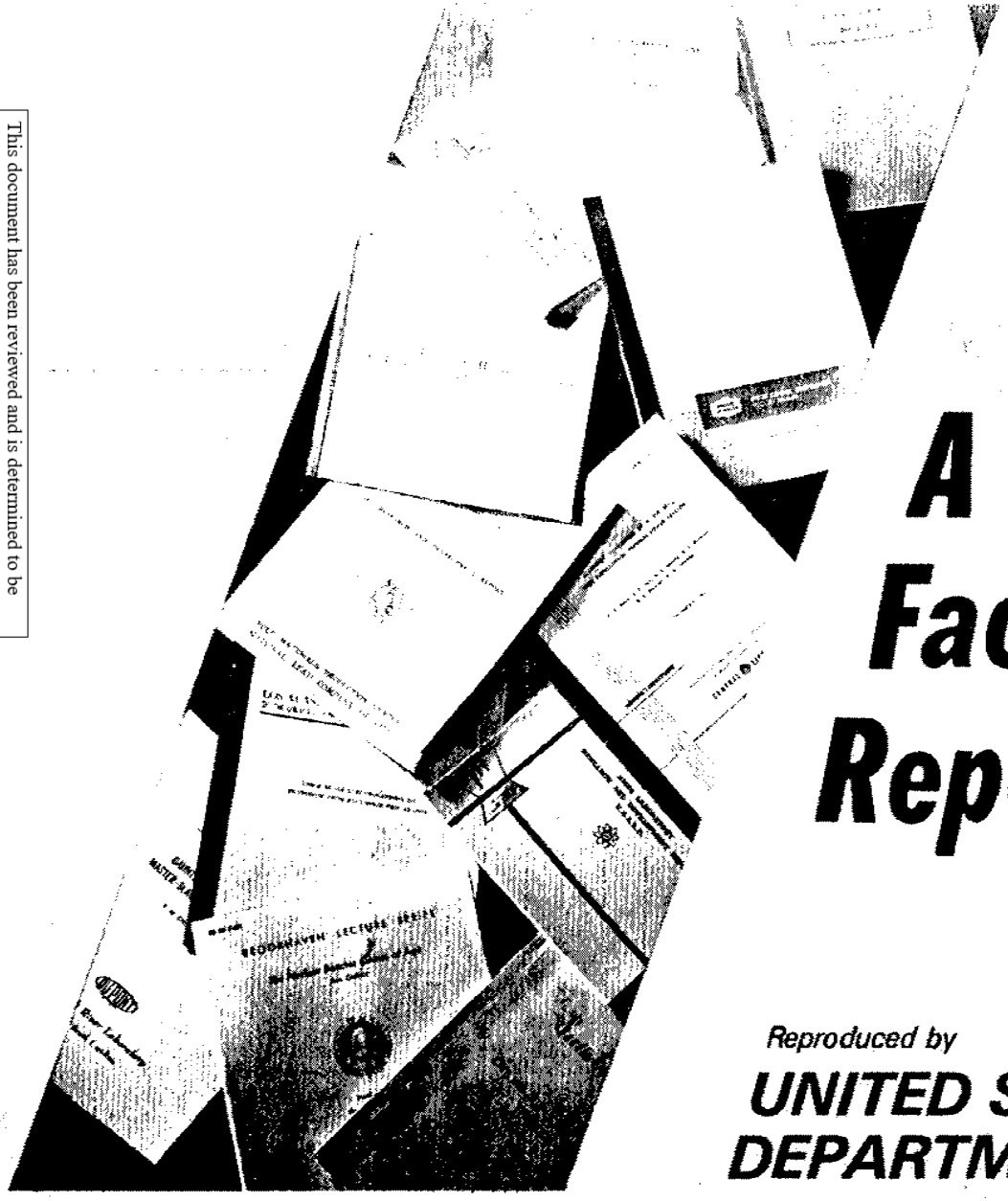

A Facsimile Report

Reproduced by

UNITED STATES DEPARTMENT OF ENERGY

Office of Scientific and Technical Information

Post Office Box 62 *Oak Ridge, Tennessee 37831*

ORNL-5676
Dist. Category UC-86

Contract No. W-7405-eng-26

Consolidated Fuel Reprocessing Program

THE SCRUBBING OF GASEOUS NITROGEN OXIDES IN PACKED TOWERS

R. M. Counce
Chemical Technology Division

This report was prepared as a dissertation and submitted to the faculty of the Graduate School of the University of Tennessee in partial fulfillment of the degree of Doctor of Philosophy with a major in chemical engineering.

Date Published: November 1980

OAK RIDGE NATIONAL LABORATORY
Oak Ridge, Tennessee 37830
operated by
UNION CARBIDE CORPORATION
for the
DEPARTMENT OF ENERGY

ACKNOWLEDGMENTS

The advice and encouragement during all phases of this research from the author's major professor, Joe Perona, are deeply appreciated. The support and encouragement of the author's supervisor, Bill Groenier, and colleague, Denny Holland, are also appreciated. Additionally, appreciation is expressed for the comments and suggestions of the Doctoral Committee: Jack Watson, Charlie Moore, and Wayne Davis.

The major portion of the experimental phase of this study was conducted by the late Ed Brantley; Ed died of a heart attack during one of the final series of experiments in this study. Ed paid particularly close attention to experimental details and his observations were always extremely helpful. The work of other people connected with the experimental phase of this study, Lee Thompson, Elsie White, Robert Coggins, Tim Scott, Tom Yount, and Rick Yates is gratefully acknowledged.

The secretarial assistance of Janice Allgood and the editorial comments of Mary Guy are especially appreciated.

This work was performed at the Oak Ridge National Laboratory for the U.S. Department of Energy under Contract W-7405-eng-26 with Union Carbide Corporation, Nuclear Division. This work was part of the Consolidated Fuel Reprocessing Program; in this regard, the author is appreciative of the efforts of Bill Burch, the Oak Ridge National Laboratory Consolidated Fuel Reprocessing Program Director.

ABSTRACT

Gaseous nitrogen oxides were scrubbed with water at 298 K and at near atmospheric pressure in towers packed with 6- and 13-mm Intalox saddles. Nitrogen oxide removal efficiencies from 55 to 97% were obtained over a wide variation of packing depths. Other studies concerning the depletion of nitrous acid in packed towers are also presented.

A mathematical model was developed based on the mass-transfer information for packed towers and chemical-reaction and mechanistic phenomena specific to the NO_x-HNO_x-H_2O system. Calculated NO_x removal efficiencies utilizing this model agree with the observed experimental phenomena fairly closely. The model is presented and discussed along with the results of the experimental activities.

TABLE OF CONTENTS

LIST OF TABLES

TABLE PAGE

LIST OF FIGURES

SYMBOLS AND ABREVIATIONS

a	gas-liquid interfacial area, m^{-1}
a_i	activity of ith specie, kg·mol m^{-3}
a_t	total surface area of packing per unit volume, m^{-1}
C_i	bulk liquid concentration of component i, kg·mol m^{-3}
C_i^*	interfacial concentration of component i, kg·mol m^{-3}
d	differential operator
D_G	diffusivity in the gas phase, m^2 s^{-1}
$\mathcal{D}_i$	diffusivity of component i in water, m^2 s^{-1}
$\mathcal{D}$	diffusivity, m^2 s^{-1}
D_L	diffusivity in the liquid phase, m^2 s^{-1}
e,exp	natural exponential function
E_j	enhancement factor, the factor by which the absorption of component j is increased by liquid reaction
F	molar flow rate, kg·mol s^{-1}
g	gravational constant m^2 s^{-1}
(g)	gas
G	volumetric gas flow rate m^3 s^{-1}
G'	superficial mass velocity of gas, kg m^{-2} s^{-1}
H	height, m
ΔH	enthalpy change
H	Henry's law constant, m^3 atm kg·mol^{-1}
H_j	Henry's law constant for jth specie in water, m^3 atm kg·mol^{-1}
HNO_x	HNO_2 + HNO_3
(i)	gas-liquid interface

I	ionic strength, kg·ion m^{-3}
k	a first-order or a pseudo-first-order rate constant, s^{-1}
k', k'', k'''	arbitrary reaction-rate constants, defined as used
k_G	gas-phase mass-transfer coefficient, kg·mol m^{-2} atm^{-1} s^{-1}
$k_{G,i}$	gas-phase mass-transfer coefficient for component i, kg·mol m^{-2} atm^{-1} s^{-1}
k_L	liquid-phase mass-transfer coefficient, m s^{-1}
$k_{L,i}$	liquid-phase mass-transfer coefficient for component i, cm s^{-1}
k_j	forward reaction rate constant for reaction j
k_{-j}	backward reaction rate constant for reaction j
K_j	equilibrium constant for reaction j
K_{-j}	equilibrium constant for the reverse order of reaction j
$K_{a,j}$	activity equilibrium constant for reaction j
$K_{c,j}$	concentration equilibrium constant for reaction j
$K_{p,j}$	pressure equilibrium constant for reaction j
log	base 10 logarithmic function
ℓn	base e logarithmic function
L	liquid flow rate, m^3 s^{-1}
L'	superficial mass velocity of liquid kg m^{-2} s^{-1}
(ℓ)	liquid
NO*	$NO + N_2O_3 + (1/2)\ HNO_2$
NO_2^*	$NO_2 + 2N_2O_4 + N_2O_3 + (1/2)\ HNO_2$
NO_x	$NO^* + NO_2^*$
0	beginning

P_i	bulk gas partial pressure of component i, atm
P_i^*	interfacial partial pressure of component i, atm
r_i	reaction rate for component i, kg·mol m^{-3} s^{-1} or atm s^{-1}
R	gas law constant, m^3 atm kg·mol^{-1} K^{-1}
$\overline{R}_i$	absorption rate for component i, kg·mol m^{-2} s^{-1}
R*	molar ratio of HNO_3 produced to HNO_2 disappearing, inherently negative or zero
R**	molar ratio of NO produced to HNO_2 disappearing, inherently negative or zero
ΔS	entropy change
t	time, s
V	column
V_{COL}	volume of packing, m^3
V_L	volume of liquid, m^3
$V_{L,T}$	total liquid volume in system
V	volume, m^3
w	weight %
x	distance, m
X_i	Fractional conversion of component i, i.e., $X_{NO_x} = [(P_{NO_x})_{in} - (P_{NO_x})_{out}]/[(P_{NO_x})_{in} + \varepsilon(P_{NO_x})_{out}]$
Y_i	gaseous mole fraction of component i
ΔV	incremental column volume, m^3
ϕ	reaction rate constant
β	molar excess of HNO_2 over HNO_3
γ	activity coefficient
Δ	signifies a difference in the final and initial values

δ	film thickness, m
ε	fractional volume change due to conversion
ε_L	liquid holdup, $m^3\ m^{-3}$
ζ	dimensionless film thickness
ϕ	arbitrary mass-transfer constants
μ_G	viscosity of liquid, kg $m^{-1}\ s^{-1}$
μ_L	viscosity of liquid, kg $m^{-1}\ s^{-1}$
ρ_G	density of gas, kg·mol m^{-3}
ρ_L	density of liquid, kg·mol m^{-3}
σ	surface tension, kg s^{-1}
σ_c	critical surface tension, kg s^{-1}
Ψ_i	stoichiometric factor
τ	residence time, s

Other nomenclature is used from time to time in this report. Any deviation from the above list or unidentified nomenclature will be explained immediately after usage in the text.

CHAPTER I

INTRODUCTION AND SIGNIFICANCE

The absorption of nitrogen oxides into aqueous media is important in many industrial processes, as well as in the production of nitric acid. Interest in this process is increasing due to current interest in air pollution abatement and resource recovery. There is an enormous amount of "piece-wise" literature, both of a fundamental and of an applied nature, on this subject. However, an integrated understanding of the basic mechanisms involved in this process has not been available. In a recent article, Dr. Robert L. Pigford (1978) states, "...today we still don't know how to design a nitric acid absorber reliably. We aren't sure whether the size of the absorber is influenced more by the rate of oxidation of nitric oxide in the gas space between plates, the rate of decomposition of nitrous acid in the liquid on the trays, or the rates of mass-transfer-limited reactions between N_2O_4 and N_2O_3 with water at the interface between phases."

An experimental study of the absorption of gaseous nitrogen oxides into dilute nitric acid in packed towers has been completed. A mathematical model has been developed based on mass-transfer information for packed towers and chemical reaction and mechanistic phenomena specific to the NO_x-HNO_x-H_2O system. This model agrees with the experimental results quite well. The experimental work and the mathematical model are presented and discussed in this report. This mathematical model will be useful for NO_x scrubber design and for other process simulation activities.

The terms NO_x or other specie conversion or removal efficiency, as used in this study, indicate the mole fraction of gaseous NO_x or other specie absorbed or otherwise converted; the use of these terms is not to be confused with plate, tray, or stage efficiencies, which have been explicitly defined in terms of an approach to some equilibrium value. Due to there being several nitrogen oxides of interest, the terms chemical nitric oxide (NO*) and chemical nitrogen dioxide (NO_2^*) are used (see also symbols and abbreviations); the important gaseous nitrogen oxide species may be represented in terms of equivalent NO* or NO_2^* species. In referencing the numbered equilibrium reactions (equations) in this report, if the number is followed by a b, the backward reaction is of interest; whereas, if the number is followed by an f, the forward reaction is of interest; on the other hand, if the number is followed by a B, then the inverse equilibrium is of interest. Standard conditions as used in this study are taken to be at a temperature and a pressure of 298 K and 1 atm.

CHAPTER II

LITERATURE REVIEW

The scrubbing of NO_x compounds from gas streams and the chemistry involved in this operation have been the subject of many experimental investigations. Much of this work was directed toward the development and optimization of nitric acid production equipment for the "oxidation of ammonia" process, which was demonstrated commercially just prior to World War I (Chilton, 1960). The process is based on the production of gaseous NO_x by the catalytic oxidation of ammonia and the absorption and reaction of these NO_x species by liquid water. The development of the theory of combined absorption and chemical reaction (Astarita, 1967; Danckwerts, 1970) was of tremendous importance to the understanding of the absorption of nitrogen oxides (Wendel and Pigford, 1958) and is currently used in intrepretation of laboratory scale nitrogen oxide absorption data and design calculations for nitrogen oxide scrubber design (Sherwood, Pigford, and Wilke, 1975; Hoftyzer and Kwanten, 1972; Counce, 1979).

The purpose of this literature review is to present a compilation of the literature relevant to nitrogen oxide scrubbing operations and to determine what experimental work is necessary for the design of an aqueous scrubber to remove moderate partial pressures of nitrogen oxides at atmospheric pressure. Other reviews on the aqueous scrubbing of nitrogen oxides are presented by Hoftyzer and Kwanten (1972) and Sherwood, Pigford, and Wilke (1975).

1. The NO_x-HNO_x-H_2O System

The NO_x-HNO_x-H_2O chemical system can be described for engineering purposes by considering the important species to be NO, NO_2, N_2O_3, N_2O_4, HNO_2, HNO_3, and H_2O. The relative homogeneous and heterogeneous equilibrium proportions and the reactivity of these compounds in the gas and liquid phases form the theoretical basis for this study. This portion of the literature review first considers the important gas-phase reactions, then briefly contrasts the solubilities of the various NO_x species, and finally presents the important liquid-phase chemical reactions. The study of the liquid-phase chemical reactions first focuses on those reactions that contribute in a positive manner to the absorptive flux of NO_x species from the gas to the liquid phase. Attention will then be directed to the decomposition and/or depletion of aqueous HNO_2 produced by those previously mentioned reactions; this decomposition or depletion is believed to produce the desorptive flux of NO_x species that is associated with the scrubbing of NO_x species from gas streams.

Gas Phase Reactions

The following gas-phase reactions are of interest when describing the NO_x-HNO_x-H_2O system:

$$2NO_2\ (g) \leftrightarrow N_2O_4\ (g)\ , \tag{1}$$

$$NO\ (g) + NO_2\ (g) \leftrightarrow N_2O_3\ (g)\ , \tag{2}$$

$$NO\ (g) + NO_2\ (g) + H_2O\ (g) \leftrightarrow 2HNO_2\ (g)\ , \tag{3}$$

$$3NO_2\ (g) + H_2O\ (g) \leftrightarrow 2HNO_3\ (g) + NO\ (g)\ , \tag{4}$$

and

$$2NO\ (g) + O_2\ (g) \rightarrow 2NO_2\ (g)\ . \tag{5}$$

The results of experimental investigations to determine equilibrium and rate constants are presented for a number of investigations for each of the above reactions. Other reviews on this subject have been done by Beattie (1963) and Gray (1958).

The NO_2-N_2O_4 Equilibrium Reaction. Bodenstein (1922) studied the reaction between NO_2 and N_2O_4 at temperatures from 282 to 404 K. Data are expressed in the following equation for the log of the pressure equilibrium constant that best described this work, according to Bodenstein:

$$\log K_{-1} = -\frac{2692}{T} + 1.75 \log T + 0.00483T - 7.144 \times 10^{-6}T^2 + 3.062\ . \tag{6}$$

Verhoek and Daniels (1931) also investigated Reaction (1) but varied the temperature from 298 to 318 K. The following equation expresses their data for the log of the pressure equilibrium constant at low partial pressures of N_2O_4.

$$\log K_{-1} = 9.8698 - \frac{3198}{T}\ . \tag{7}$$

Corrections for increasing N_2O_4 partial pressures are given at 308 and 318 K similar to the following equation at 298 K:

$$K_{-1} = 0.1426 - 0.03103\ P_{N_2O_4} . \quad (8)$$

The heat of dissociation was calculated to be 14,000 kcal kg·mol^{-1}.

Hoftyzer and Kwanten (1972) give the following correlation for K_1 without temperature restrictions, derived from considerations of the work of Verhoek and Daniels (1931) and the JANAF Thermochemical Tables (1971):

$$K_1 = (0.707 \times 10^{-9}) \exp (6866/T) . \quad (9)$$

The rate of dissociation of gaseous N_2O_4 was studied by Carrington and Davidson (1953) at total pressures from 0.5 to 7 atm and temperatures of 253 to 301 K. At 298 K, a first-order dissociation rate constant was determined to be $8.3 \pm 1.3 \times 10^4$ s^{-1}, and the bimolecular association rate of NO_2 was calculated to be 5.2×10^8 m^3 kg·mol^{-1} s^{-1}, using equilibrium constants calculated from the work of Verhoek and Daniels (1931).

The NO-NO_2-N_2O_3 Equilibrium Reaction. Abel and Proisl (1929) studied the reaction of NO and NO_2 over a wide range of temperatures. At zero pressure, K_{-2} was found to be 0.539 and 2.39 atm at 281 and 308 K. The heat of dissociation was calculated to be 9600 kcal kg·mol^{-1}.

Verhoek and Daniels (1931) studied Reaction (2) and calculated values of 2.105, 3.673, and 6.880 atm for the equilibrium constant K_{-2} for very low N_2O_3 partial pressures at 298, 308, and 318 K respectively.

The heat of dissociation was calculated as 10,160 kcal kg·mol^{-1}. Correction for this equilibrium constant at higher N_2O_3 partial pressures is also given.

Reaction (2) was also studied by Beattie and Bell (1957). They calculated values of K_{-2} of 0.595, 1.082, 1.916, 3.097, and 5.193 atm at low N_2O_3 partial pressures and temperatures of 278, 288, 298, 308, and 318 K. The heat of dissociation was calculated as 9527 ± 96 kcal kg·mol^{-1}. The values of K_{-2} decreased with increasing partial pressures of NO_2. This work by Beattie and Bell was expressed in equation form by Hoftyzer and Kwanten (1972) as:

$$K_2 = (66.15 \times 10^{-9}) \exp (4740/T) \ . \qquad (10)$$

The $NO-NO_2-H_2O-HNO_2$ Equilibrium Reaction. Wayne and Yost (1951) investigated the reaction of NO, NO_2, and H_2O as well as the dissociation of HNO_2 and N_2O_3 at 298 K. These reactions were found to be very fast. The forward reaction rate constant of the following equation, combining Reactions (2) and (3),

$$N_2O_3 \ (g) + H_2O \ (g) \leftrightarrow 2HNO_2 \ (g) \ , \qquad (11)$$

was found to be 1.1×10^5 atm^{-2} s^{-1}, apparently catalyzed by water. The reverse reaction rate constant was found to be 6.6×10^{-4} atm^{-2} s^{-1}, again apparently catalyzed by water. The dissociation rate constant for N_2O_3 was found to be 150 s^{-1}. Their value for K_3 is given in Table 1.

Ashmore and Tyler (1961) investigated Reaction (3) at 293, 313, 333, and 353 K. Their data for K_3 are presented in Table 1. The calculated heat of reaction was -18,820 ± 200 kcal kg·mol^{-1}.

Table 1. Equilibrium constants for the gas phase reaction of NO, NO_2, HNO_2, and H_2O

Temperature (K)	Values of K_3 (atm^{-2}) obtained by various researchers			
	Wayne and Yost	Ashmore and Tyler	Karavaev and Skvortsov	Waldorf and Babb
293		1.56		
298	1.74		1.60	2.38
313		0.641		
325			0.445	
333		0.250		
350			0.156	
353		0.112		
375			0.609×10^{-1}	
400			0.267×10^{-1}	
425			0.132×10^{-1}	
450			0.704×10^{-2}	
475			0.398×10^{-2}	
500			0.236×10^{-2}	

Sources:

1. L. G. Wayne and D. M. Yost, *J. Chem. Phys.* 19: 41 (1951).
2. G. Ashmore and B. J. Tyler, *J. Chem. Soc.* 1017 (1961).
3. M. Karavaev and G. A. Skvortsov, *Russ. J. Phys. Chem.* 36: 566 (1962).
4. D. M. Waldorf and A. L. Babb, *J. Chem. Phys.* 39: 432 (1963).

The equilibrium constant for Reaction (3) was later investigated by Karavaev and Skvortsov (1962). Their data are presented in Table 1. The heat of reaction was computed as -18,000 kcal $kg \cdot mol^{-1}$.

Reaction (3) was later investigated by Graham and Tyler (1972) at 298 K and higher temperatures. At 298 K, their value of the forward reaction rate constant for Reaction (3) is 3.1×10^3 atm^{-2} s^{-1}, again catalyzed by water.

Kaiser and Wu (1977) investigated Reaction (3) at 300 K and found the results to be complicated by adsorption of HNO_2 and H_2O. Using straight-forward rate expressions, they found upper bounds for the forward and reverse reaction rate constants for Reaction (3) of 7×10^{-49} atm^{-2} s^{-1} and 4×10^{-25} atm^{-1} s^{-1} respectively. These values are considerably different from the previously mentioned researchers.

Waldorf and Babb (1963) investigated Reaction (3) at 298 K. Their data point is presented in Table 1.

Hoftyzer and Kwanten (1972) present the following equation for K_3 based on the work of Wayne and Yost (1951), Ashmore and Tyler (1961), Karaveav and Skvortsov (1962), and Waldorf and Babb (1963):

$$K_3 = 0.187 \times 10^6 \exp (4723/T) \quad . \tag{12}$$

The NO_2-H_2O-HNO_3-NO Equilibrium Reaction. There is confusion as to the importance of the gas-phase reaction between NO_2 and water, Reaction (4). Much of the confusion is due to the gas-phase reaction being thermodynamically limited; however, the two-phase system can occur spontaneously and the overall reaction:

$$3NO_2\ (g) + H_2O\ (g) \leftrightarrow 2HNO_3\ (\ell) + NO\ (g)\ , \qquad (13)$$

is thermodynamically favored (Forsythe and Giauque, 1942). This additional phase formation is commonly observed as a mist or fog to some extent by almost all researchers studying the NO_x-HNO_x-H_2O system; it is formed spontaneously when the gas-phase concentration of HNO_3 exceeds about 50 ppm at ambient conditions (Goyer, 1963) or if the gas-phase concentration or partial pressure over aqueous solutions exceeds its vapor pressure. The researcher is at an extreme disadvantage in these studies because if the gas-phase reaction is limited so as not to produce a second phase, the extent of the reaction may be scarcely detectable.

The gas-phase reaction of NO_2^* and H_2O was successfully studied, however, by England and Corcoran (1974) at low partial pressures of HNO_3, ambient temperature, and pressure. These data were best described by the following equation:

$$dP_{NO_2^*}/dt = -2k_{15}\ P_{NO_2}^2\ P_{H_2O} + 2k_{-15}\ P_{HNO_2}\ P_{HNO_3}\ , \qquad (14)$$

where the proposed overall reaction is:

$$2NO_2\ (g) + H_2O\ (g) \leftrightarrow HNO_2\ (g) + HNO_3\ (g)\ . \qquad (15)$$

The values of k_{15} and k_{-15} at 298 K are 184 ± 9.8 $atm^{-2}\ s^{-1}$ and 478 ± 26 $atm^{-1}\ s^{-1}$. The activation energy was -978 kcal $kg{\cdot}mol^{-1}$. This paper presents a very interesting analysis of their observations and those of others based on basic theoretical concepts of the NO_x-HNO_x-H_2O system.

The reverse of the NO_2^*-H_2O reaction, that is, the reaction of NO and HNO_3 was studied by Smith (1947) at low pressures over a temperature range of 273 to 303 K. The production of NO_2 in the gas-phase was approximately represented by the following equation:

$$dP_{NO_2^*}/dt = k_{-4} P_{NO} P_{NO_2} P_{HNO_3} , \quad (16)$$

apparently catalyzed by NO_2. Water vapor also increased the reaction rate. Smith believed that the effect of water vapor was due to a heterogeneous reaction. The value of k_{-4} was about 3×10^2 atm^{-2} s^{-1} at 298 K. The reaction rate decreased over the temperature range of 273 to 303 K.

The reaction of NO and HNO_3 was treated as an instantaneous reaction by Lefers, et al (1980) in wetted-wall column studies in which gaseous NO was contacted with concentrated aqueous HNO_3. These studies were conducted at 1 atm and 293 K; the NO partial pressure at the inlet was 0.02 to 0.12 atm, and the nitric acid strength was 60 to 80 wt %. In these experimental studies, the NO is oxidized to NO_2 by HNO_3 in the gas-phase, followed by the absorption of N_2O_4 into the acid solutions. These studies show good agreement between theoretical computations and experimental results.

The Oxidation of NO. The oxidation of NO was studied by Bodenstein (1918) at 273, 303, 333, and 363 K; the partial pressure of NO was varied from 0.08 to 0.14 atm in excess oxygen. Bodenstein confirmed the third-order kinetics consistent with the following rate equation:

$$r_5 = k_5 P_{NO}^2 P_{O_2} . \quad (17)$$

Rate constants are given in Table 2.

Under conditions comparable to those used by Bodenstein, Hasche and Patrick (1925) examined the kinetics of the reaction of NO and oxygen at 273 and 303 K and found that a third-order reaction occurs consistent with Equation (17). The reaction appears to be catalyzed by the presence of glass wool. Reaction rate constants are presented in Table 2.

Treacy and Daniels (1955) also found a third-order reaction consistent with Equation (17) in their analysis of the reaction kinetics of NO and oxygen at 273, 298, and 338 K. The NO partial pressure was varied from 0.006 to 0.02 atm, and the oxygen partial pressure was varied from 0.026 to 0.006 atm. Reaction rate constants are listed in Table 2.

The reaction rate constant of Morrison, Rinker, and Corcoran (1966), who investigated the oxidation of NO at 300 K, is also presented in Table 2. The NO concentration was varied from 2 to 75 ppm; the oxygen concentration ranged from 0.03 to 0.25 atm. The reaction appeared to proceed at third-order kinetics, consistent with Equation (17).

Greig and Hall (1967) used similar parameters to investigate the oxidation of NO. In their work, temperatures of 293, 322, 352, and 372 K were used; the partial pressure of NO varied from 0.05 to 0.11 atm, and the partial pressure of oxygen ranged from 0.01 to 0.28 atm. These workers also confirmed third-order kinetics consistent with Equation (17). Rate constants are presented in Table 2.

Solubilities of NO, NO_2, N_2O_3, N_2O_4, HNO_2, and HNO_3 in Water

An indication of the role of the individual NO_x and HNO_x species in aqueous absorption technology can be seen by comparing the individual

Table 2. Experimental values of the reaction rate constant for the oxidation of NO

Reaction rate constant	Temperature (K)											Investigators
	273	293	298	300	303	322	333	338	352	363	372	
k_5 (atm^{-2} sec^{-1})	34.75				22.95		14.86			10.16		Bodenstein
	43.24				26.19							Hasche and Patrick
	25.9		13.4					9.75				Treacy and Daniels
				21.47								Morrison, Rinker, and Corcoran
		34.8				24.1			18.2		15.0	Greig and Hall

Sources:

1. M. Bodenstein, *Z. Elektrochem.* 24: 183 (1918).
2. R. L. Hasche and W. A. Patrick, *J. Am. Chem. Soc.* 46: 1207 (1925).
3. J. C. Treacy and F. Daniels, *J. Am. Chem. Soc.* 77: 2033 (1955).
4. M. E. Morrison, R. C. Rinker, and W. H. Corcoran, *Ind. Eng. Chem., Fundam.* 5: 175 (1966).
5. J. D. Greig and P. G. Hall, *Trans. Faraday Soc.* 63: 655 (1967).

specie solubilities presented in Table 3. These heterogeneous equilibriums, ranked by solubility from least to highest are

$$NO\ (g) \leftrightarrow NO\ (\ell)\ , \tag{18}$$

$$NO_2\ (g) \leftrightarrow NO_2\ (\ell)\ , \tag{19}$$

$$N_2O_3\ (g) \leftrightarrow N_2O_3\ (\ell)\ , \tag{20}$$

$$N_2O_4\ (g) \leftrightarrow N_2O_4\ (\ell)\ , \tag{21}$$

$$HNO_2\ (g) \leftrightarrow HNO_2\ (\ell)\ , \tag{22}$$

and

$$HNO_3\ (g) \leftrightarrow HNO_3\ (\ell)\ . \tag{23}$$

These equilibrium (Henry's Law) constants vary over several orders of magnitude ranging from very soluble to extremely insoluble species. Another review of this subject was authored by Schwartz and White (1980).

Liquid-Phase Mechanisms and Reactions

In the liquid phase, the following reactions appear to be important to the absorption flux:

$$2NO_2\ (\ell) + H_2O\ (\ell) \rightarrow HNO_3\ (\ell) + HNO_2\ (\ell)\ , \tag{24f}$$

$$N_2O_4\ (\ell) + H_2O\ (\ell) \rightarrow HNO_3\ (\ell) + HNO_2\ (\ell)\ , \tag{25f}$$

and

$$N_2O_3\ (\ell) + H_2O\ (\ell) \rightarrow 2HNO_2\ (\ell)\ . \tag{26f}$$

The reaction of NO_2 and water is sufficiently slow to be considered as a bulk-phase reaction; thus, the absorption rate is related to the transfer

Table 3. Henry's Law constants at 298 K

Species	H_i ($m^3 \cdot atm\ kg \cdot mol^{-1}$)
NO	518.0[a]
NO_2	24.4[b]
N_2O_3	2.59[c]
N_2O_4	0.769[d]
HNO_2	0.0305[e]
HNO_3	8.2×10^{-13}[f]

[a] A. G. Loomis, *International Critical Tables III*, 255 McGraw Hill, New York (1928).

[b] Andrews and Hanson, *Chem. Eng. Sci.* 14: 105 (1961).

[c] C. E. Corriveau, Jr., Master's Thesis in Chemical Engineering, University of California, Berkeley (1971).

[d] H. Kramers, M. P. P. Blind, and E. Snoeck, *Chem. Eng. Sci.* 14: 115 (1961).

[e] E. Abel and E. Neusser, *Monatsh. Chem.* 54: 855 (1929).

[f] P. J. Hoftyzer and F. J. G. Kwanten, *Processes for Air Pollution Control*, 2nd ed., Chemical Rubber Co., Cleveland (1972).

of NO_2 into the bulk liquid phase (Andrews and Hanson, 1961). However, the hydrolysis of N_2O_4 and N_2O_3 are sufficiently fast to take place in the liquid film (see also Appendix F).

The bulk of material presented in this section, however, deals with the absorption of NO_2^* and NO* into water under conditions that make the hydrolysis of N_2O_4 and N_2O_3 the primary liquid-phase reactions that positively contribute to the absorptive flux.

The Equilibrium Absorption of NO_2-N_2O_4 into Water. The equilibrium reaction of NO_2-N_2O_4 and water was investigated by early researchers in order to provide information for the design of nitric acid production columns. These reactions were usually written as:

$$2NO_2\ (g) + H_2O\ (\ell) \leftrightarrow HNO_2\ (\ell) + HNO_3\ (\ell)\ , \tag{27}$$

$$3HNO_2\ (\ell) \leftrightarrow HNO_3\ (\ell) + H_2O\ (\ell) + 2NO\ (g)\ . \tag{28}$$

The overall reaction is then

$$3NO_2\ (g) + H_2O\ (\ell) \leftrightarrow 2HNO_3\ (\ell) + NO\ (g)\ . \tag{29}$$

In 1959, Carberry pointed out that in view of the mounting body of evidence which indicated that N_2O_4 was the reactive specie, Reaction (1) should be included in the above scheme,

$$2NO_2\ (g) \leftrightarrow N_2O_4\ (g)\ .$$

The overall equilibrium reaction now becomes:

$$3/2\ N_2O_4\ (g) + H_2O\ (\ell) \leftrightarrow 2HNO_3\ (\ell) + NO\ (g)\ . \tag{30}$$

The equilibrium expression,

$$K_{30} = \frac{a_{HNO_3}^2 \; P_{NO}}{a_{H_2O} \; P_{N_2O_4}^{3/2}} , \tag{31}$$

may be put in a more useful form defining a portion of K_{30} to be:

$$K_c = \frac{P_{NO}}{P_{N_2O_4}^{3/2}} , \tag{32}$$

a function of the nitric acid strength. Values of K_c have been obtained by various researchers (Abel et al., 1930; Burdict and Freed, 1932; Chambers and Sherwood, 1937; Denbigh and Prince, 1947; Epshtein, 1939; and Tereshchenko et al., 1968). However, it was Carberry (1959) and Menegus (1959) who discovered that when the overall reaction was expressed in terms of N_2O_4 instead of NO_2 the equilibrium expression K_c became independent of temperature. This plot, by Carberry, is presented in Figure 1. Another useful representation of this information is an equation for K_c as a function of the weight percent nitric acid presented by Beattie (1963) and Sherwood, Pigford, and Wilke (1975):

$$\log K_c = 7.412 - 20.28921 \; w + 32.47322 \; w^2 - 30.87 \; w^3 . \tag{33}$$

One fact often overlooked in applying the equilibrium constant, K_c, is that the indicated reaction sequence explicitly requires that nitrous acid be present in the liquid phase. The sequence of reactions that produce 1/3 mole NO from the reaction of 3/2 mole N_2O_4 must produce and

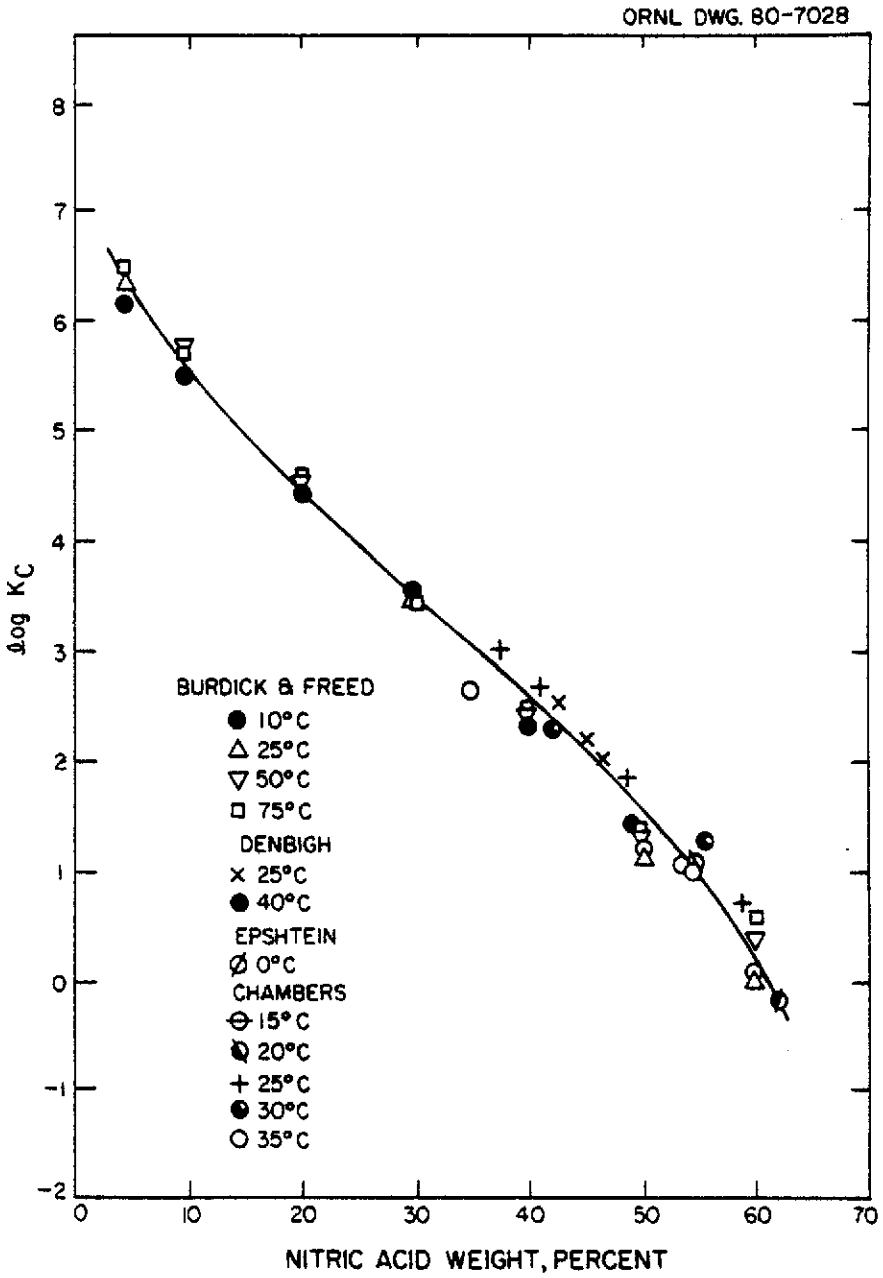

Figure 1. Equilibrium between phases for Reaction (29).
Source: J. Carberry, *Chem. Eng. Sci.* 9: 189.

maintain a steady-state HNO_2 concentration in the liquid phase. Although this is a simple point, it is generally overlooked. Makhotkin and Shamsutdinov (1976) state that in atmospheric pressure nitric acid production columns, the HNO_2 concentration varied from 0.02 to 0.07 kg·mol m^{-3} as the HNO_3 concentration varied from 1.3 to 10.4 kg·mol m^{-3}.

In other experimental studies by Makhotkin and Shamsutdinov (1976), using a laboratory-scale apparatus at 293 K and atmospheric pressure, 0.01 atm NO_2 in N_2 was bubbled through an aqueous solution. The results are seen in Figure 2. The ratio of NO produced to NO_2 absorbed reaches about 33% only when the steady-state HNO_2 concentration is attained.

The Non-Equilibrium Absorption of NO_2-N_2O_4 into Aqueous Solutions. The hydrolysis of N_2O_4 during the absorption of N_2O_4 into water or dilute nitric acid is essentially irreversible due to low concentrations of HNO_2 and HNO_3 in the liquid phase, Reaction (25f):

$$N_2O_4\ (\ell) + H_2O\ (\ell) \rightarrow HNO_3\ (\ell) + HNO_2\ (\ell)\ .$$

Chambers and Sherwood (1937) studied the absorption of NO_2-N_2O_4 from nitrogen into water and aqueous solutions of HNO_3 and NaOH at 298 K using both a wetted-wall column and a semi-batch system. The partial pressure of NO_2^* was varied from 0.04 to 0.58 atm. The HNO_3 concentration was varied up to 18 kg·mol m^{-3}; the NaOH concentration was varied up to 11.6 kg·mol m^{-3}. The results from the wetted-wall column showed the mass-transfer coefficient varied as the 0.8 power of the gas Reynolds number, indicating that the gas-phase resistance controlled the absorption rate. However, the mass-transfer coefficients were lower than expected

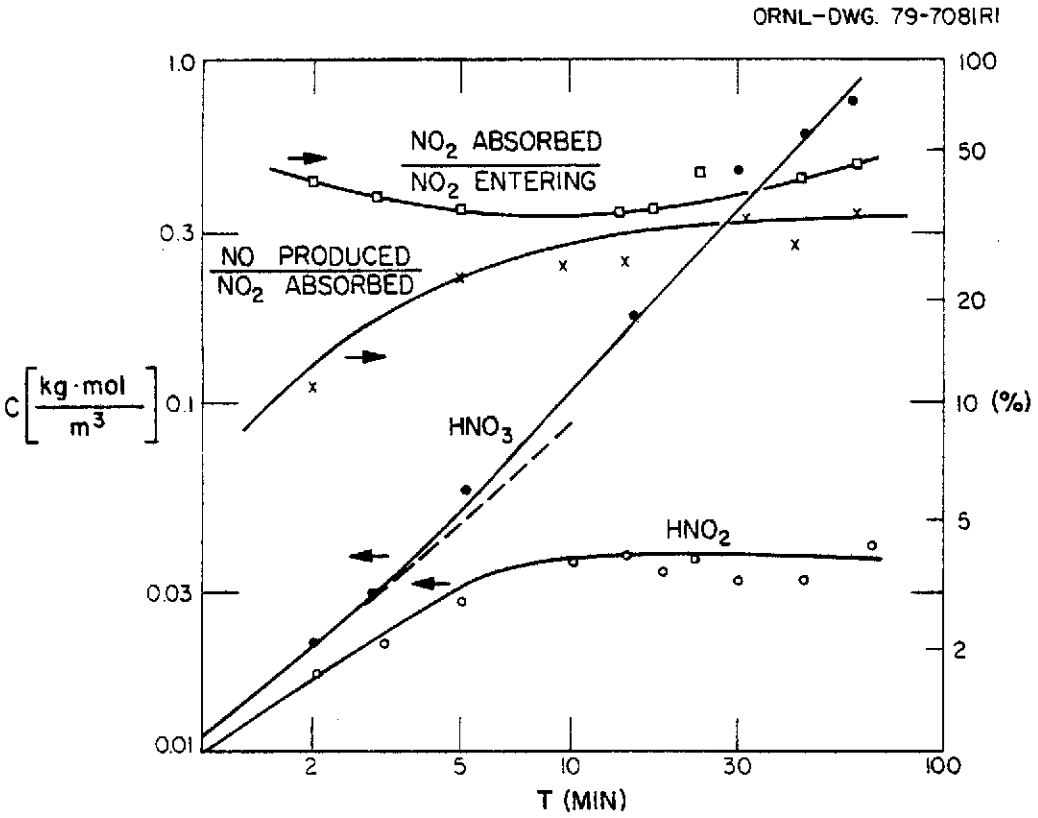

Figure 2. Results of semi-batch NO_2^* absorption studies.

Source: A. F. Makhotkin and A. M. Shamsutdinov, *Khim. i. Khim. Tekhn.* XIX: 1411 (1976).

based on data of water vaporization under similar conditions. Further, NO was found in the off-gas from these experiments, even when aqueous NaOH was used as the absorbent. If the reaction of NO_2^* and water took place in the liquid phase, one should expect that the reaction,

$$2NO_2\ (\ell) + 2NaOH\ (\ell) \rightarrow NaNO_2\ (\ell) + NaNO_3\ (\ell) + H_2O\ (\ell)\ , \qquad (34)$$

should prevent the formation of gaseous NO. Chambers and Sherwood assumed that nitric acid mist was formed in the gas-film due to the reaction of NO_2^* and water vapor, and the increased resistance was due to the diffusion of NO_2^* through this mist. A decrease in the NO_2^* absorption rate with increased NaOH or HNO_3 strength was also observed.

The effects of system temperature, NO_2^* concentration, and acid molarity on the absorption rate of NO_2-N_2O_4 from NO_2^*-N_2 gas mixtures into HNO_3 using a wetted-wall column in a closed system with complete recirculation were investigated by Denbigh and Prince (1947). Temperatures of 298 and 313 K were used; the NO_2^* partial pressure ranged from 0 to 0.27 atm; and the acid molarity was varied from 1.7 to 13.0 kg·mol m^{-3}. For acid strengths up to 5.7 kg·mol m^{-3}, the absorption rate of NO_2^* can be reasonably represented as a linear function of the partial pressure of N_2O_4:

$$\overline{R}_{NO_2^*} = \phi\ P_{N_2O_4}\ . \qquad (35)$$

Their values of ϕ at 298 and 308 K are 7.36×10^{-4} and 8.29×10^{-4} kg·mol m^{-2} atm^{-1} s^{-1}. At higher acid strengths, the absorption rate takes into consideration the reaction reversibility:

$$\overline{R}_{NO_2^*} = \phi \left(P_{N_2O_4} - K' P_{N_2O_4}^{1/4} P_{NO}^{1/2} \right) , \tag{36}$$

where

$$K' = K_{30}^{3/4} / K_c^{1/2} . \tag{37}$$

Liquid and gas phases were analyzed; the gas phase was analyzed continuously for NO_2-N_2O_4 using a calibrated photo cell. The results were assumed to be controlled by chemical kinetics in the region of the gas-liquid interface. Little HNO_2 was found in the liquid at the end of the experiment.

A wetted-wall column was also used by Caudle and Denbigh (1953) to experimentally measure the rate of NO_2^* absorption from nitrogen into water, 2.8 kg·mol m^{-3} NaOH, and calcium chloride solutions. The system featured closed recirculating gas and liquid streams. The variables examined were gas composition, temperature, and gas and liquid flow rates. The absorption rate was highest when water was the absorbent. No effect of liquid flow rate was observed over a range of liquid Reynolds numbers from 3500 to 12,000 except for the local eddying and mixing effects in the liquid phase that appeared to be functions of the gas flow rate. The absorption rate of NO_2^* can be calculated as a linear function of the partial pressure of N_2O_4, except when NO was present and a small N_2O_3 absorption flux was indicated. At 298 K, the rate constant from Equation (35) was between 8.2×10^{-4} and 3.3×10^{-3} kg·mol m^{-2} atm^{-1} s^{-1}.

Caudle and Denbigh (1953) suggested that the hydrolysis of N_2O_4 occurs at the gas-liquid interface because (a) the absorption rate is

proportional to the interfacial area instead of the volume of bulk phases; and (b) NO is liberated primarily in the column, with a small amount being evolved from the exiting liquor, when N_2O_4 is absorbed in column. No NO was evolved from NO_2^* absorption into NaOH solutions. The absorption rate was determined by photometric gas analysis.

Peters and Holman (1955) used both nitrogen and air as the diluent gas in their wetted-wall column experiments on the absorption of NO_2-N_2O_4 into water, NaOH, and NaCl solutions. No significant difference was noted in the results with nitrogen or air. The NO_2^* partial pressure was maintained at 0.048 atm; all runs were made at atmospheric pressure and at temperatures ranging from 301 to 329 K. The concentrations of NaOH and NaCl were 2.8 and 4.8 kg·mol m^{-3} respectively. The absorption rate of NO_2^* was higher when water was the absorbing liquid and lowest when NaCl solutions were used. The absorption rate decreased significantly with increasing temperature in all cases. Both the gas and liquid phases were analyzed, and inlet and outlet NO_2^* and HNO_3 or NaOH concentrations were determined by chemical methods. The presence of NO in the off-gas when an NaOH solution is the absorbent liquid may suggest a gas-phase reaction for the hydrolysis of NO_2^*. However, no proportionality of NO_2^* removal rate to water vapor fugacity was interpreted as an indication of the presence of a liquid-phase reaction; thus, both liquid- and gas-phase reactions may contribute to NO_2^* absorption.

Wendel and Pigford (1958) studied the absorption of NO_2-N_2O_4 into water using a wetted-wall column and nitrogen as the diluent gas. The NO_2^* partial pressure was varied up to 0.20 atm. The range of gas rates covered Reynolds numbers from 170 to 350; water rates were varied

to allow contact times between gas and liquid from 0.03 to 0.3 s; and temperatures of 298 and 313 K were used. No effects of gas or liquid flow rates or of contact time on the two reaction rates were observed. The indicated rate-controlling step was the hydrolysis of N_2O_4. The results were interpreted using the penetration theory and assuming that Reaction (25f) occurs in the liquid film,

$$\overline{R}_{NO_2^*} = 2(\sqrt{\mathcal{D}k}/H)_{N_2O_4} P^*_{N_2O_4} \quad . \tag{38}$$

Other experimental results are presented in Table 4. It is noteworthy that this is the first application of the penetration theory to the understanding of the absorption of NO_2^*.

In a literature review in 1959, Carberry concluded that, in cases where N_2O_4 is dissolved in solvents of high dielectric strength, ionization occurs according to the reaction:

$$N_2O_4\ (\ell) \rightarrow NO^+\ (\ell) + NO_3^-\ (\ell)\ , \tag{39}$$

and N_2O_4 exists in these solutions in the ionized form. In light of this conclusion, the reaction of dissolved N_2O_4 and water may be written as:

$$N_2O_4\ (\ell) + H_2O\ (\ell) \rightarrow NO^+\ (\ell) + OH^-\ (\ell) + H^+\ (\ell) + NO_3^-\ (\ell)\ , \tag{40}$$

or

$$N_2O_4\ (\ell) + H_2O\ (\ell) \rightarrow HNO_2\ (\ell) + H^+\ (\ell) + NO_3^-\ (\ell)\ . \tag{41}$$

Table 4. Values of terms in Equation (38) at the various temperatures used in studying the absorption of N_2O_4 into water

Term	Temperature (K)					Investigators
	293	298	303	308	313	
$\left(\sqrt{Dk}/H\right)_{N_2O_4}\left(\frac{kg\cdot mole}{atm\ m^2\ s}\right)$		5.8×10^{-4}			5.4×10^{-4}	Wendel and Pigford
		1.1×10^{-3}		1.0×10^{-3}		Dekker, Snoeck, and Kramers
	7.7×10^{-4}		8.9×10^{-4}			Kramers, Blind, and Snoeck
		$1.0\text{-}1.1 \times 10^{-3}$				Gerstacker
		0.903×10^{-4}				Hoftyzer and Kwanten
		5.7×10^{-4}				Corriveau
		6.85×10^{-4}				Kameoka and Pigford
$k\ (s^{-1})$		290.0			1340.0	Wendel and Pigford
		290.0				Moll
	1.0×10^3					Grätzel, Henglein, Lilie, and Beck
	250.0		330.0			Kramers, Blind, and Snoeck
$H\left(\frac{atm\ m^3}{kg\cdot mole}\right)$		1.04			2.86	Wendel and Pigford
	0.72		0.81			Kramers, Blind, and Snoeck
$D\left(\frac{m^2}{s}\right)$	1.23×10^{-9}		1.59×10^{-9}			Kramers, Blind, and Snoeck

Sources:

1. M. M. Wendle and R. L. Pigford, *AIChE J.* 4: 249 (1958).
2. W. A. Dekker, E. Snoeck, and H. Kramers, *Chem. Eng. Sci.* 11: 61 (1959).
3. H. Kramers, M. P. P. Blind, and E. Snoeck, *Chem. Eng. Sci.* 14: 115 (1961).
4. Gerstacker, *Chem. Eng. Sci.* 14: 124 (1961).
5. P. J. Hoftyzer and F. J. G. Kwanten, *Processes for Air Pollution Control*, 2nd ed., p. 164, Chemical Rubber Company, Cleveland (1972).
6. C. E. Corriveau, Master's Thesis in Chemical Engineering, University of California, Berkeley (1971).
7. Y. Kameoka and R. L. Pigford, *Ind. Eng. Chem. Funda.* 16: 163 (1977).
8. A. J. Moll, PhD. Dissertation, University of Washington (1966).
9. M. Grätzel, A. Henglein, A. Lilie, and G. Beck, *Ber. Bunsengles.* 73, 646 (1969).

The ionization of N_2O_4 not only supports the kinetic and chemical equilibrium data, but it also provides significant corroboration for the argument that a purely gas-phase reaction between N_2O_4 and water vapor is an unlikely occurrence.

Dekker, Snoeck, and Kramers (1959) investigated NO_2-N_2O_4 absorption in a wetted-wall column for contact times of 0.2 to 0.4 s, inlet NO_2^* partial pressures of 0.03 to 0.15 atm, and operating temperatures of 298 to 308 K. The absorption rate data were correlated with an equation similar to Equation (38); contact time had little effect on the absorption rate. The experimental results, presented in Table 4 are fairly consistent with the following model:

1. In the gas phase, NO_2 and N_2O_4 are in continuous equilibrium with each other.
2. At the gas-liquid interface, only N_2O_4 is dissolved in water.
3. The diffusion of N_2O_4 into water is accompanied by a rapid pseudo-first-order chemical reaction between N_2O_4 and water.

Absorption of NO_2^* was measured by photometric analysis of the gas phase and titration of the liquid acid phase for both HNO_3 and HNO_2.

A stirred-tank reactor was used by Peters and Koval (1959) to study the absorption of NO_2^* from NO_2^*-air mixtures into water. In their study, the partial pressure of NO_2^* (NO_2-N_2O_4) was varied from 0.4 to 4.4 atm; both the gas and the liquid phases were analyzed to determine NO_2^* absorption. They found that removal efficiency improved with increased NO_2^* concentration and/or increased agitation. The agitator was designed to break up large gas bubbles into smaller ones. The data can be correlated with the following rate equation:

$$\overline{R}_{NO_2^*} = \phi\ P^*_{N_2O_4} + \phi_2\ P^*_{NO}\ P^*_{NO_2} \ . \qquad (42)$$

Equation (42), in contrast to Equation (38), adds a term to account for N_2O_3 reactions.

This experiment differs from the work with bubble-cap, sieve-plate, or wetted-wall columns in that the stirred tank provides for greater gas-liquid contact time and contact area. Under these conditions, the reaction of N_2O_3 with water cannot be ignored.

Koval and Peters (1960) examined the absorption of NO_2^* from feed-gas mixtures of NO_2^*-NO*-N_2 into water at 304 K in a long wetted-wall column at atmospheric pressure. The NO_2^* partial pressure was varied up to 0.04 atm. Chemical analysis of the gas and liquid phases revealed that the presence of NO had a marked effect on the HNO_3-HNO_2 split, greatly increasing the production of HNO_2 at the expense of HNO_3 production. The chemical stoichiometry is described by the following equation:

$$(2 + \beta/4)N_2O_4\ (g) + (2 + \beta/2)H_2O\ (\ell) \rightarrow 2HNO_3\ (\ell) + 2(1 + \beta/2)HNO_2\ (\ell) - (\beta/2)NO\ (g) \ , \qquad (43)$$

where β refers to the molar excess of HNO_2 over HNO_3. The following rate equation describes the experimental data:

$$\overline{R}_{NO_2^*} = \phi\ P^*_{N_2O_4} + \phi_2\ P^*_{NO}\ P^*_{NO_2} - \phi_3 C^2_{HNO_2} \ . \qquad (44)$$

Equation (44) allows for an additional absorption flux and a desorption flux to Equation (38).

Kramers, Blind, and Snoeck (1961) used a laminar water jet to study the absorption of NO_2-N_2O_4 from an inert carrier gas into water at 293 and 303 K. Gas-phase resistance was eliminated by using pure NO_2^* at reduced pressures. They determined the absorption rate by chemical analysis of the liquid phase for HNO_2 and HNO_3. The absorption rate data were correlated with Equation (38); experimental results are given in Table 4.

Moll (1966) investigated the rate of hydrolysis of N_2O_4 over the temperature range 300 to 318 K. He injected liquid N_2O_4 directly into a flowing water stream and measured the resulting temperature rise downstream of the injection point. From these temperature profiles, he determined k_{25f}, a pseudo-first-order rate constant. His rate constant at 298 K is presented in Table 4, and his correlation of k_{25f} with the temperature from 300 to 318 K is:

$$\ell n\ k_{25f} = 16.38 - 3163/T. \qquad (45)$$

His work is the first direct evidence that the hydrolysis of N_2O_4 occurs as Equation (25f), a pseudo-first-order reaction.

In some pulse radiolytic investigations by Grätzel (1969), the liquid-phase reaction rate constant of N_2O_4 and water was found to be considerably higher than that determined from other investigators. Their data point at 293 K is given in Table 4.

Hoftyzer and Kwanten (1972) investigated the absorption of NO_2-N_2O_4 by using laminar jets. In their works, the following variables were studied: the partial pressure of NO_2^*, 0.05 to 1.70 atm; temperature, 276 to 348 K; and acid molarity. Data were correlated using Equation (38).

The experimentally determined value of $(\sqrt{Dk}/H)_{N_2O_4}$ is given in Table 4 for 298 K, and the following correlation represents their data for temperatures from 276 to 348 K:

$$\log [(\sqrt{Dk}/H)_{N_2O_4}] = - 0.52 - 760/T \ . \qquad (46)$$

These investigators found that the value of $(\sqrt{Dk}/H)_{N_2O_4}$ decreased with increasing acid molarity. This decrease was attributed to the increase in the Henry's Law constant with increasing ionic strength. They stated that the values of H could be corrected by using the factor exp (-0.075 I), where I is the ionic strength.

Chilton and Knell (1972) studied the absorption of NO_2-N_2O_4 into water, NaOH solutions of 1 and 5.7 kg·mol m^{-3}, and KI solutions of 1 kg·mol m^{-3} (normality was 0.2 due to presence of NaOH also). These tests were conducted at 298 K and atmospheric pressure using a long wetted-wall column. The partial pressure of NO_2^* was varied between 0.01 and 0.07 atm. Standard chemical analyses of the gas and liquid phases were in excellent agreement. Their absorption rate data for NO_2^* absorption into water were in agreement with other researchers — the mass-transfer resistance assumed to be in the liquid phase. The absorption of NO_2^* into KI was approximately twice as fast as into water and was thought to be limited by gas-phase resistance of the transfer of NO_2^* to gas-liquid interface. The reaction of NO_2^* and iodine is thought to be

$$NO_2 \ (\ell) + KI \ (\ell) \rightarrow KNO_2 \ (\ell) + I \ (\ell) \ . \qquad (47)$$

The absorption rate of NO_2^* into aqueous NaOH was lower than that of water. This is thought to be due to decreased solubility and diffusivity of N_2O_4, reduced activity of water, and less rippling of film due to increased viscosity.

Using a wetted five-sphere laboratory absorber, the absorption of NO_2-N_2O_4 into water and aqueous solutions of H_2SO_4, NaOH, and Na_2SO_4 was studied by Kameoka and Pigford (1977). These studies were to evaluate the alkaline absorption of simulated oxidized flue gases from stationary combustion facilities. The NO_2^* partial pressure was varied from 0.01 to 0.02 atm in a N_2 carrier gas. The results were based on liquid-phase chemical analysis.

The absorption rate into water correlated well with Equation (38) and the results are presented in Table 4. The absorption rate was unaffected by the presence of H_2SO_4 in concentrations of 0.09 kg·mol m^{-3}. The absorption rate in aqueous solutions of 0.2 kg·mol m^{-3} NaOH was about 7% higher than for water alone. This increase in absorption rate with the addition of NaOH apparently conflicts with the results of Chambers and Sherwood and Chilton and Knell; however, both of these papers deal with more concentrated NaOH solutions. Apparently, the increase in NO_2 reactivity more than compensates for the loss of solubility at low NaOH molarities. The absorption rate with appropriate rate constants for these studies was

$$\overline{R}_{N_2O_4} = (P^*_{N_2O_4}/H_{N_2O_4}) \sqrt{D_{N_2O_4} (k_{25f} C_{H_2O} + k' C_{OH^-})} . \qquad (48)$$

The reaction rate of NO_2^* in 0.1 kg·mol m^{-3} NaOH and 0.042 through 0.153 kg·mol m^{-3} solutions of Na_2SO_3 was expressed as

$$\overline{R}_{N_2O_4} = (P_{N_2^*O_4}/H_{N_2O_4}) \sqrt{\mathcal{D}_{N_2O_4} (k_{25f} C_{H_2O} + k' C_{OH^-} + k'' C_{SO_3^=})} \quad . \tag{49}$$

Using Kramer's (1961) values for $\mathcal{D}_{N_2O_4}$ and $H_{N_2O_4}$, the following is calculated:

$$k_{25_f} C_{H_2O} = 194 \ s^{-1} \ ,$$

$$k' = 147 \ m^3 \ kg \cdot ion^{-1} \ s^{-1} \ ,$$

and

$$k'' = 8690 \ m^3 \ kg \cdot mol^{-1} \ s^{-1} \ .$$

These rate equations indicate parallel aqueous reaction paths for N_2O_4 reacting with H_2O, OH^-, and SO_3^{--}.

Makhotkin and Shamsutdinov (1976) studied the effects of HNO_2 on NO_2^* absorption into water, nitric acid, and other aqueous solutions in a film column at 293 K. The absorption rate of NO_2^* at HNO_2 partial pressures of 0.2 to 0.75 vol % generally decreased to zero as the aqueous nitric acid concentration approached about 55 wt %; however, all curves exhibit a maximum at 4 to 5 wt % nitric acid. The absorption rate of NO_2^* at gas concentrations of 0.1 to 5 vol % decreased as the nitrous acid concentration of the absorbing solution was increased from zero to 0.046 kg·mol m^{-3}; this decrease is more pronounced at gaseous NO_2^* concentrations below 1 vol %. The NO_2^* absorption rate was also studied for various solutions. The highest absorption rate was observed for tributyl phosphate, water saturated with tributyl phosphate, and tributyl phosphate with 0.27 kg·mol m^{-3} HNO_3 and 0.18 kg·mol m^{-3} HNO_2. In order

of decreasing NO_2^* absorption rates, the other solutions were 5 wt % nitric acid, water, 17 wt % HNO_3, 42 wt % HNO_3, and 10 wt % KOH. The NO_2^* absorption rate into water saturated with tributyl phosphate was definitely a function of the gas velocity over a range of 0.3 to 3.0 m s^{-1} at NO_2^* concentrations of 0.5 to 2 vol %; at lower NO_2^* concentrations there is a change in the relationship between NO_2^* absorption and gas velocity.

The Non-Equilibrium Absorption of N_2O_3 into Water. Using a laboratory absorber of five wetted spheres, Corriveau (1971) studied the absorption of gaseous mixtures of NO_2^* and NO* into water at 298 K and atmospheric pressure. The major absorbing species were found to be N_2O_4 and N_2O_3 over interfacial partial pressures of $(9.0 - 2.9) \times 10^{-5}$ atm and $(1.0 - 4.0) \times 10^{-4}$ atm respectively. Experimental results were based on an analysis of NO_2^* in the feed gas, and HNO_2 and the total acid in the liquid phase. The absorption of HNO_2 was found to be negligible in these experiments, and a value of $(\sqrt{Dk}/H)_{N_2O_3}$ of 1.59×10^{-3} kg·mol m^{-2} atm^{-1} s^{-1} was obtained; k and H were found to be 1.2×10^4 s^{-1} and 0.39 kg·mol m^{-3} atm^{-1}. Corriveau's values of $(\sqrt{Dk}/H)_{N_2O_4}$ are presented in Table 4. No absorption of HNO_2 was observed during these experiments although HNO_2 was thought to act as a transport specie in the gas-phase.

The Decomposition/Desorption of Aqueous HNO_2. During the removal of nitrogen oxides from gas streams by absorption into water, aqueous HNO_3 and HNO_2 are produced. Nitric acid is fairly stable in comparison with HNO_2, which can spontaneously decompose in the liquid-phase to HNO_3 and NO or transfer back to the gas-phase due to the relatively high vapor pressure of HNO_2 over aqueous solutions. This desorption phenomena

is a well-known characteristic in the aqueous scrubbing of nitrogen oxides. The literature concerning the mechanisms and reactions involved in the disappearance of aqueous HNO_2 has been extensively investigated as this area appears to be the least understood of the NO_x-HNO_x-H_2O system phenomena.

The reversible nature of the depletion of nitrous acid from aqueous solutions was confirmed by Montemartini (1890) to be Reaction (28):

$$3HNO_2\ (\ell) \leftrightarrow HNO_3\ (\ell) + H_2O\ (\ell) + NO\ (g)\ .$$

This work was conducted primarily at 300 K and atmospheric pressure in open and closed vessels with a quiescent liquid phase. Nitrous acid for the decomposition studies was prepared in total concentrations up to 0.005 kg·mol m^{-3} with initial HNO_3 concentrations near zero. [Total nitrous acid (HNO_2^*) is the sum of HNO_2 in all its aqueous equilibrium forms.] The depletion was first order with respect to aqueous HNO_2 with the rate constant decreasing by about 1/3 for each 15 K. The ratio of HNO_3 produced to HNO_2 disappearing from solution, R*, was about -1/3 for decomposition studies conducted in a continuously replaced inert atmosphere; for similar studies conducted in open vessels, R* was slightly lower than -1/3, and the rate constants were also slightly lower. The equilibrium, as expressed in Reaction (28), was also approached from the right.

The decomposition of nitrous acid was later investigated in a sparged flask at 291 K at ambient pressure by Montemartini (1892). Total nitrous acid solutions of 0.005 kg·mol m^{-3} were generated by adding KNO_2 to HNO_3 solutions in concentrations up to 13 kg·mol m^{-3}. The sparge gas was H_2. The effluent gas was bubbled through a KOH solution, which removes the NO_2^* by:

$$2NO_2\ (g) + 2KOH\ (\ell) \rightarrow KNO_2\ (\ell) + KNO_3\ (\ell)\ . \qquad (50)$$

The NO present in the gas phase would not be absorbed to a great extent in the KOH solution. The overall decomposition reaction for HNO_3 concentrations from 0.8 to 5.6 kg·mol m^{-3} was first order with respect to the HNO_2^* concentration and is in agreement with Reaction (28); for higher HNO_3 strengths, the decomposition was Reaction (27b):

$$HNO_2\ (\ell) + HNO_3\ (\ell) \rightarrow 2NO_2\ (g) + H_2O\ (\ell)\ .$$

The formation and decomposition of nitrous acid were further investigated by Valey (1892) using laboratory glassware. "The experiments were conducted in dull and generally foggy weather, advantageous at least for them, as concentrated nitric acid is decomposed by direct sunlight." Valey studied the formation of liquid HNO_2^* produced by sparging nitric acid solutions with gaseous NO. The initial HNO_3 concentration was varied from 1.0 to 16.9 kg·mol m^{-3}. The temperature was varied from 282 to 325 K under ambient pressure conditions. The concentrations of HNO_2^* and HNO_3 in the liquid phase were analyzed continuously until steady-state had been established. The proportional quantity of total nitrous acid at steady-state increased with increased nitric acid concentration. With more dilute acids, this proportional quantity of total nitrous acid increases then decreases with temperature; for concentrated acids, this decrease with temperature is uniform. The reaction of NO and HNO_3 was commonly observed to produce liquids of blue to greenish-blue in color. For HNO_3 molarities 4.6 to 9.2 kg·mol m^{-3}, the steady-state HNO_2^*-HNO_3 mixtures were blue in color. For HNO_3 molarities of greater than

10.8 kg·mol m^{-3}, it appeared that NO_2^* was formed first in the liquid, then HNO_2 was formed because the liquid turned yellow at first, then deep green. For HNO_3 strengths less than 5.6 kg·mol m^{-3}, the reaction is as described by Reaction (28b):

$$2NO\ (g) + HNO_3\ (\ell) + H_2O\ (\ell) \rightarrow 3HNO_3\ (\ell)\ .$$

Total nitrous acid in concentrations up to 1 kg·mol m^{-3} in water was prepared for the decomposition experiments by a variety of methods: (1) the decomposition of recrystallized $AgNO_2$ in a slight difficiency of HCl, (2) the absorption and subsequent reaction of gaseous NO and liquid HNO_3, (3) the absorption and subsequent reaction of gaseous NO_2^* and liquid H_2O, and (4) the passing of fumes from arsenious oxide and nitric acid through liquid H_2O. These experiments were conducted in a quiescent environment with continuous replacement of the inert atmosphere. The temperature was varied from 284 to 304 K. The decomposition with respect to HNO_2^* was second order, doubling for every 20-degree temperature increase, and was inversely proportional to the concentration of liquid HNO_3.

From the work of Valey, Reaction (28B),

$$2NO\ (g) + HNO_3 + H_2O \leftrightarrow 3HNO_2\ ,$$

appears to be reversible with a ratio of steady-state HNO_3:HNO_2 of 9:1. This reversibility appeared, however, to be true only with HNO_3 concentrations less than 5.6 kg·mol m^{-3}.

The equilibrium reaction (28B) was later investigated by Sapozhnikova (1900) using laboratory glassware at 291 K and essentially atmospheric

pressure. The equilibrium was approached by decomposing liquid HNO_2^* with initial concentrations of 0.1 to 0.6 kg·mol m^{-3} in a gaseous NO atmosphere. The HNO_2^* was prepared by acidifying nitrite salts and dissolving N_2O_3 in H_2O. Agitation decreased the time required to reach equilibrium from 275 to 4 h. The decomposition reaction was followed by measuring the pressure of NO and appeared to be second order with respect to HNO_2^*. Sapozhnikova defined an equilibrium constant as:

$$K_{28} = \frac{C_H + C_{NO_3} - C_{NO}^2}{C_{HNO_2}^3} \quad . \tag{51}$$

He was able to reach an order of magnitude agreement in K_{28} with these tests.

Sapozhnikova (1901) then approached the equilibrium by the absorption and reaction of gaseous NO and liquid HNO_3. These experiments were conducted at 298 K with initial HNO_3 concentrations of 0.05 to 3.0 kg·mol m^{-3}. The experiment was again conducted in an atmosphere of NO at essentially ambient pressure; the reaction was followed by measuring the experimental pressure. A vibrated gas-liquid contactor was used as a reactor. Some HNO_2^* was initially introduced into the liquid by dissolving N_2O_3 in H_2O. Sapozhnikova reported difficulty in producing pure N_2O_3 due to the dissociation equilibrium:

$$2N_2O_3\ (\ell) \leftrightarrow N_2O_4\ (\ell) + 2NO\ (\ell) \quad . \tag{52}$$

At equilibrium, the color of the solution was related to the specific gravity of nitric acid: blue, 1.2; blue-green, 1.275; green, 1.375;

dark green, 1.4; reddish brown, 1.5. His equilibrium constant, K_{28}, varied regularly from 232 to 88 for a final HNO_2 concentration of 0.02813 to 2.81 kg·mol m^{-3} respectively.

Trautz (1904) studied the decomposition of liquid HNO_2^* because of its effect on the lead-chamber process for the production of sulfuric acid. The production of H_2SO_4 is limited by the decomposition of liquid HNO_2. Initial concentrations of HNO_2^* of 0.08 to 0.021 kg·mol m^{-3} were decomposed in a glass apparatus with a nitrogen sparge of the solution at 298 K. The sparge was used after observing the unagitated reaction to be slow. From these experiments, Trautz concluded that Reaction (28f) occurs very fast and is limited by the escape of NO from solution.

Trautz also describes a near fatal accident involving the breathing of NO_2^* fumes. His physical ordeal, following this exposure, is recounted in graphic detail. This experience left him with permanent emphysema and sensitivity to NO_2^*. A remedy that proved effective in eliminating his physical discomfort following this experience was "inhalation and the drinking of very strong alcoholic beverages."

Lewis and Edgar (1911) studied equilibrium Reaction (28B) at 298 K in laboratory glassware. The equilibrium was approached from the HNO_3 side. Pure gaseous NO was bubbled through initially 0.1 kg·mol m^{-3} mixtures of HNO_3. The reaction was followed by measuring the electro-conductivity of the mixture. The reaction velocity increased proportional to the gas rate. The reaction was presumed to be autocatalytic because the maximum reaction velocity was not reached until several hours after the beginning of the experiment. The equilibrium constant,

$$K_{28B} = \frac{C^2_{HNO_2}}{C_{H^+}\, C_{NO_3^-}}, \qquad (53)$$

was found to be 0.0267 corrected to a partial pressure of NO equal to 1.0.

The author has been unable, thus far, to secure a copy of the dissertation of H. Liebmann, Dresden (1914). In view of its apparent importance, a quote is inserted from a review of this work by Abel and Schmid (1928a): "H. Liebmann ... conducted some research of the kinetics of nitrous acid, which, in spite of numerous investigations, still posed a number of questions. Liebmann ... paid particular attention to the influence of the inducted flow of nitrogen on (the decomposition of HNO_2). The decomposition itself, he states, stops being trimolecular in flowing gases, the reaction decreases during its occurrence, beginning between a molecularity of 2 and 3 and decreases to bimolecularity and then to monomolecularity ... Liebmann attempts to explain the mechanism of this process by the assumption of two tautomer forms of nitrous acid."

Ray, Dey, and Ghosh (1917) studied the decomposition of liquid HNO_2 in unagitated laboratory glassware at 273, 294, and 313 K. The initial HNO_2 concentration was 0.032 kg·mol m^{-3}, and the atmosphere of the experiment was air. The decomposition reaction was first order with rate constants of 1.4×10^{-4}, 2.2×10^{-4}, and 5.7×10^{-4} s^{-1} respectively.

Knox and Reid (1919) provide a substantial study of the decomposition of liquid HNO_2 in laboratory glassware at ambient pressure under an atmosphere of air. Variables in the study were temperature, 273 to 323 K; HNO_2^* concentration, 0.05 to 2.51 kg·mol m^{-3}; HNO_3 concentration, 0 to

7.25 kg·mol m^{-3}; surface area, agitation, and CO_2 vs air sparging. The base experimental conditions were temperature, 293 K; $C_{HNO_2^*}$ (initial), 0.05 kg·mol m^{-3}; and C_{HNO_3} (initial), 0. The decomposition rate increased with agitation and surface area as shown in Figure 3. The decomposition rate also increased with temperature. No HNO_3 was present initially in these runs. The order of the reaction appeared to be second order with respect to HNO_2^* at HNO_3 concentrations of 0.05 kg·mol m^{-3} and temperatures from 273 to 323 K. Variation in the initial HNO_3 concentration had little overall effect on the decomposition rate. However, the extent of the reaction in the first 5 min of the experiment increased with increasing HNO_3 concentration. A comparison of air vs CO_2 sparged experiments reveals a higher rate constant for the air case; however, the reaction order remained approximately second order. The overall reaction describing these experiments is represented by Equation (28f).

The decomposition of aqueous HNO_2 was next studied by Klemenc and Pollak (1922) at atmospheric pressure and temperatures of 273 to 303 K in a glass flask sparged with N_2. Total nitrous acid concentrations of 0.05 to 0.23 kg·mol m^{-3} were prepared by adding acid to aqueous solutions of $NaNO_2$. Rate constants were based on undissociated HNO_2.

At 288 K, studies were conducted using HNO_2 prepared by the addition of CH_3COOH to aqueous $NaNO_2$. With excess $NaNO_2$, the rate constant increased with increasing hydrogen ion activity. The rate constant in these experiments is also found to increase with the concentration of undissociated HNO_2 and temperature, doubling approximately every 15 degrees. The rate constant was found to be proportional to the 2/3

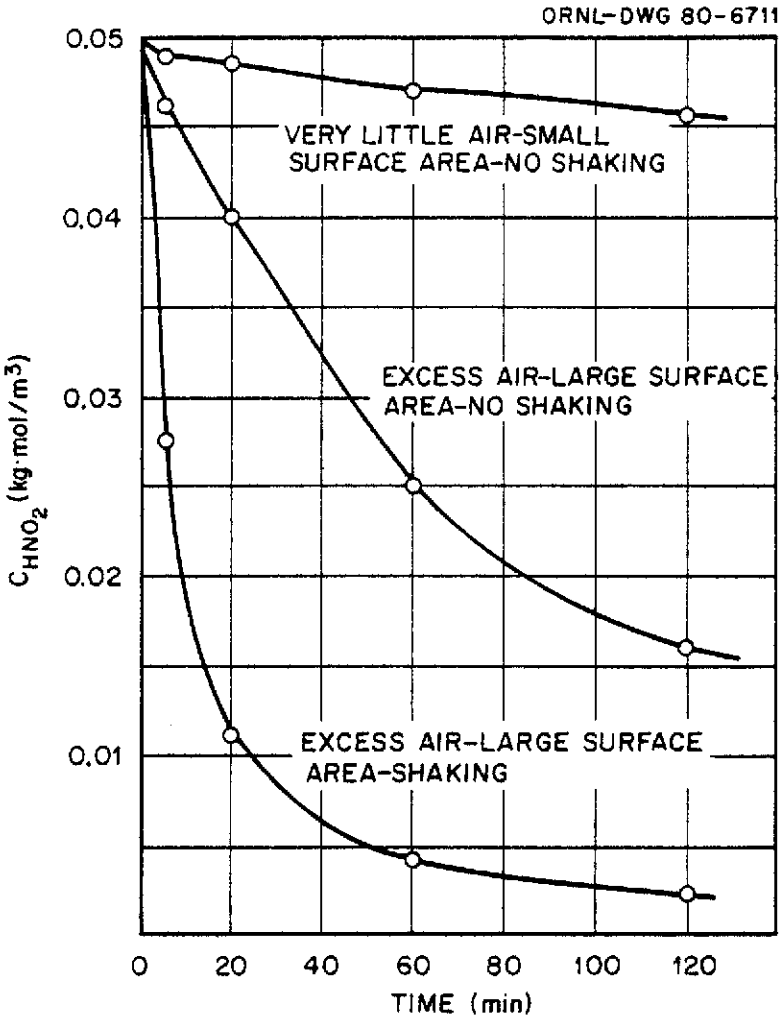

Figure 3. The effect of shaking and surface on the decomposition of 0.05 kg·mol m^{-3} nitrous acid.

Source: J. Knox and D. M. Reid, *J. Chem. Soc. Ind.* 38 (9): 105T (1919).

power of the gas velocity. The order of the reaction was difficult to determine at low-gas sparge rates (somewhere between first and third order) but definitely approached first order at higher gas flow rates.

In some experiments involving H_2SO_4 and HNO_3 as the strong acid, the reaction rate constant increased with increasing acid strength from 0.1 to 3 kg·mol m^{-3}. Other experiments involving mineral acids showed that the rate constant decreased with increased partial pressures of NO in the sparge gas.

The decomposition reaction sequence was assumed to be:

$$HNO_2\ (\ell) \leftrightarrow NO\ (\ell) + OH\ (\ell)\ , \tag{54}$$

and

$$NO\ (\ell) \leftrightarrow NO\ (g)\ . \tag{18B}$$

The rate of Reaction (54) was assumed to be limited by the escape of NO from solution.

The decomposition of aqueous HNO_2 was later studied by Taylor, Wignall, and Cowley (1927) at atmospheric pressure and temperatures of 273 and 298 K. The initial concentration of HNO_2 was 1 kg·mol m^{-3} prepared by adding $Ba(NO_2)_2$ to aqueous H_2SO_4. The reaction was studied in a stirred device under a layer of "medicinal paraffin." They reported that HNO_2 was stabilized with increased H_2SO_4 concentrations up to 7 kg·mol m^{-3}. The reaction was observed to proceed very fast at first, and then to proceed as a first-order reaction to a pseudo-stable HNO_2 concentration. These concentrations were 0.4 and 0.2 kg·mol m^{-3} at 273 and 298 K respectively. The overall reaction was consistent with Equation (28) and the following equilibrium reactions were postulated:

$$2HNO_2\ (\ell) \leftrightarrows N_2O_3\ (\ell) + H_2O\ (\ell)\ , \tag{26B}$$

and

$$N_2O_3\ (\ell) \leftrightarrows NO\ (\ell) + NO_2\ (\ell)\ . \tag{55}$$

Abel and Schmid (1928a, 1928b, 1928c, and 1929), Abel, Schmid, and Babad (1928 and 1929), and Abel, Schmid, and Roemer (1930) performed a remarkable series of experiments on the formation and decomposition of aqueous nitrous acid in an atmosphere of gaseous NO. They succeeded in establishing both the equilibrium constant and the forward and backward rate constants for Reaction (28) in an NO atmosphere. These equilibrium and rate constants have widespread acceptance among those knowledgeable in NO_x-HNO_x chemistry.

In Part I of the "Kinetics of Nitrous Acid," Abel and Schmid (1928a) provide a literature search and develop the theoretical concepts that further distinguish this work. The decomposition reaction sequence is as follows:

$$4HNO_2\ (\ell) \leftrightarrows N_2O_4\ (\ell) + 2NO\ (\ell) + 2H_2O\ (\ell)\ , \tag{56}$$

and

$$N_2O_4\ (\ell) + H_2O\ (\ell) \rightarrow HNO_2\ (\ell) + H^+\ (\ell) + NO_3^-\ (\ell)\ , \tag{57}$$

where Reaction (57) is the rate controlling step. The formation reactions are

$$N_2O_4\ (\ell) + 2NO\ (\ell) + 2H_2O\ (\ell) \rightarrow 4HNO_2\ (\ell)\ , \tag{58}$$

and

$$HNO_2\ (\ell) + H^+\ (\ell) + NO_3^-\ (\ell) \rightarrow N_2O_4\ (\ell) + H_2O\ (\ell)\ , \tag{59}$$

where Reaction (59) is the rate limiting step. The overall equilibrium is generally expressed as:

$$3HNO_2\ (\ell) \leftrightarrows H^+\ (\ell) + NO_3^-\ (\ell) + 2NO\ (g) + H_2O\ (\ell)\ . \qquad (60)$$

The general differential equation, based on the HNO_2 concentration, can be written as:

$$\mp \frac{dC_{HNO_2}}{dt} = \pm k_{-60} \frac{C_{HNO_2}^4}{P_{NO}^2} \mp k_{60}\, C_{HNO_2}\, C_{H^+}\, C_{NO_3^-}\ . \qquad (61)$$

In "Kinetics of Nitrous Acid," Part II, Abel and Schmid (1928b) conduct their orienting experiments. They recognized in the beginning that the removal of NO from solution could control the decomposition reaction.

The decomposition of aqueous HNO_2 was first investigated with a quiescent and a stirred liquid in an N_2 atmosphere. The following salt-acid combinations were used to generate HNO_2 in this and subsequent experiments: $NaNO_2 + HNO_3$, $NaNO_2 + HNO_4$, and $Ba(NO_2)_2 + H_2SO_4$. The results were obscured by an apparent oversaturation of NO in the liquid phase.

When NO was introduced into the sparge gas, the decomposition rate velocity was noted to be a function of the sparge gas velocity.

A gas-liquid contactor agitated by vibration proved to be effective in maintaining equilibrium between the gas and liquid phases for this system. There was a noticeable increase in the decomposition rate of HNO_2 for NO partial pressures of 0.3 atm versus the case when the NO partial pressure was 0.5 atm, and the orienting experiments were concluded.

In the "Kinetics of Nitrous Acid," Part III, Abel and Schmid (1928c) studied the decomposition reaction at 298 K and atmospheric pressure. The HNO_2 concentration varied between 0.025 to 0.100 kg·mol m^{-3}, the hydrogen ion concentration varied from 0 to 0.08 kg·mol m^{-3}, and the ionic strength was varied from 0 to 3.0 kg·ion m^{-3}. The reaction sequence was assumed to be as presented in Equations (56) and (57). The rate constants are given in Table 5 and are consistent with the following equation:

$$\frac{dC_{HNO_2}}{dt} = k_{-60} \frac{C^4_{HNO_2}}{P^2_{NO}} . \tag{62}$$

The rate constant k_{-60} increased linearily with the ionic strength as:

$$k_{-60} = (0.77 + 0.18\ I)\ m^9\ kg{\cdot}mol^{-3}\ s^{-1}\ atm^{-2} . \tag{63}$$

Abel credits this increase to a decrease in the solubility of gaseous NO.

In "The Decomposition of Nitrous Acid," Part IV, Abel, Schmid, and Babad (1928) investigated the formation of nitrous acid at 298 K and 0.5 and 1.0 atm pressures. The HNO_2 concentration was approximately 0.01 kg·mol m^{-3}, the hydrogen ion concentration varied up to 0.25 kg·mol m^{-3}, and the ionic strength was varied from 0 to 1.1 kg·mol m^{-3}. The reaction sequence was assumed to be as presented in Equations (56) and (57). The rate constant is given in Table 5 and is consistent with the following equation:

$$\frac{dC_{HNO_2}}{dt} = k_{60}\ C_{HNO_2}\ C_{H^+}\ C_{NO_3^-} . \tag{64}$$

Table 5. Experimentally determined values of constants k_{60}, k_{-60}, and K_{60} at various temperatures and zero ionic strength

Reaction rate constant	Temperature (K)								
	273	283	285.5	288	293	298	303	313	333
k_{-60} $\left(\frac{m^9\ atm^2}{kg \cdot mol^3\ s}\right)$	0.010[a]	0.0605[a]			0.365[a]	0.767[b]	1.98[a]	8.75[a]	85.5[a]
k_{60} $\left(\frac{m^6}{kg \cdot mol^2\ s}\right)$				0.011[a]		0.027[c]			
K_{60} $\left(\frac{m^3\ atm^2}{kg \cdot mol}\right)$			13.3[d]	14.1[a]		28.7[e]	39.6[d]		

[a] E. Abel, H. Schmid, and E. Rommer, *Z. Physik. Chem.* 148: 337 (1930).

[b] E. Abel, and H. Schmid, *Z. Physik Chem.* 134: 279 (1928).

[c] E. Abel, H. Schmid, and S. Babad, *Z. Physik. Chem.* 136: 135 (1928).

[d] A. Kelmenc and E. Hayek, *Z. Anorg. U. Allgem. Ch.* 186: 181 (1930).

[e] E. Abel and H. Schmid, *Z. Physik. Chem.* 136: 430 (1929).

This constant decreased from 0.027 to 0.013 $m^6\ kg{\cdot}mol^{-2}\ s^{-1}$ as the ionic strength increased from 0 to 1.1 $kg{\cdot}ion\ m^{-3}$. The rate equation expresses the autocatalytic nature of the reaction. The pressure of NO had no effect on the reaction as long as it is present in sufficient quantity for the reaction to proceed.

In the "Kinetics of Nitrous Acid," Part VI, Abel and Schmid (1929) calculate an equilibrium constant for Reaction (60), assuming superposition of the two rate constants involved, that is,

$$K_{a,60} = \frac{k_{60}}{k_{-60}} = \frac{C_{H^+}\ C_{NO_3^-}\ P_{NO}^2}{C_{HNO_2}^3} . \tag{65}$$

The relationship of the rate coefficients to the ionic strength disappears with the appropriate activity coefficients,

$$K'_{60} = \frac{a_{H^+}\ a_{NO_3^-}\ P_{NO}^2}{a_{HNO_2}^3} . \tag{66}$$

Their data are presented in Table 5. The activity coefficients for HNO_3 were those determined by Abel, Redlich, and Lengyel (1928). Activity coefficients for HNO_2 were calculated but were essentially unity. At zero ionic strength, K_{60} = 29.0 $m^3\ kg{\cdot}mol^{-1}\ atm^{-2}$ at 298 K as compared with 31 predicted earlier by Lewis and Randall (1923).

The effect of temperature on the decomposition of aqueous HNO_2 was investigated in an NO atmosphere at temperatures from 273 to 333 K at very low hydrogen ion concentrations and ionic strengths up to

4 kg·ion m^{-3} by Abel, Schmid, and Roemer (1930). The formation reaction of aqueous HNO_2 was investigated at 288 K, and an equilibrium constant was calculated. The procedure was as presented previously. The results of these and other experiments are presented in Table 5. The decomposition reaction varied with temperature and ionic strength as:

$$\log k_{60} = - \frac{6250}{T} + 24.43 + 0.078\ I\ . \tag{67}$$

The following equation expresses the activity coefficient of HNO_2:

$$\log \gamma_{HNO_2} = 1/3 \log \frac{46 + 11\ I}{46}\ . \tag{68}$$

The values for the heats of reaction of the formation and equilibrium were 21.2×10^3 kcal kg·mol^{-1} and 11.9×10^3 kcal kg·mol^{-1}.

The vapor pressure of nitrous acid above its aqueous solutions was studied at 298 K by Abel and Neusser (1929) in an NO atmosphere. A value of 0.0352 m^3 atm kg·mol was found at an ionic strength of 1.4 kg·ion m^{-3}. In terms of the activity of HNO_2, the Henry's Law coefficient was found to be 0.0305 m^3 atm kg·mol^{-1} and increased slightly with ionic strength.

Lang and Aunis (1951a) studied the depletion of aqueous HNO_2 at 298 K in open beakers. Some experiments were conducted using a stirrer. Aqueous HNO_2^* solutions of 0.001 to 0.1 kg·mol m^{-3} were prepared by the acidification of $NaNO_2$. Hydrogen ion concentrations were varied up to 5 and 2 kg·mol m^{-3} for HNO_2^* concentrations of 0.001 and 0.1 kg·mol m^{-3}.

For experiments involving no agitation, the reproducibility was poor. Liquid analysis varied with the depth of the liquid. The decomposition rate was interpreted as being first order, and the rate constant was proportional to the surface area as:

$$\frac{C_{HNO_2^*}}{C_{HNO_2^*,O}} = a\, e^{-kt} , \tag{69}$$

where

$$k = k'a ,$$

and

k' = a first-order rate constant,

a = interfacial area,

although the second-order analysis was probably equally valid with their data.

For the agitated case, the depletion was first order at least for high agitation rates. The rate increased with agitation and the concentration of aqueous HNO_2. The depletion rate increased with pH up to 0.01 kg·mol m^{-3} for various acids after which pH had little effect. The type of acid used to acidify the $NaNO_2$, HCl, H_2SO_4, or HNO_3 had no effect on the reaction rates. The ratio, R*, varied from -0.14 to -0.44, generally decreasing with the increased concentration of HNO_2 and increasing with increased agitation.

Lang and Aunis (1951b) later studied the decomposition of aqueous HNO_2^* at 298 K with a constant agitation of 500 rpm. The shapes of the vessels were varied; the degree to which the vessels were open to the

atmosphere was varied; and additionally, gas streams were introduced at the bottom of the liquid and just above its surface.

The removal rate of HNO_2^* without a gas stream and for 0.1 kg·mol m^{-3} was measured in open and closed atmospheres. The decomposition rate for the open vessels was first order and insensitive to the vessel height. The value for R* in these tests was -0.33. For the tests with the closed vessels, the rate was much slower and appeared to be displaced from first toward second order. The value of R* for the closed tests was -0.775. For some tests with 0.01 kg·mol m^{-3} solutions of HNO_2^*, the respective rates were lower; R* is higher for both open and closed atmospheres. However, the gross observations were as noted previously for the tests with 0.1 kg·mol m^{-3} HNO_2^*.

When a gas stream is introduced in the bottom of the liquid for the open vessel, nitrogen and air give similar values of k′ [as used in Equation (69)] for the open vessel and for 0.1 kg·mol m^{-3} HNO_2. However, the values of R* vary greatly, being substantially lower for air. Oxygen considerably increases k′ and gives very low R* values. The rate appeared to be first order for all of these cases.

When a gas stream is introduced in the bottom of the liquid and is held up over the solution, there is little difference in the rate of HNO_2^* disappearance for air or N_2 for solutions of 0.1 kg·mol m^{-3} HNO_2^*. However, at high gas rates the HNO_2^* disappearance rate in air approaches that in O_2.

In general, for open or semi-open vessels, increasing the sparge gas rate has a similar effect to increasing the agitation rate — the rate of disappearance of HNO_2^* is increased and R* increases.

When a gas stream is introduced a little above the liquid surface of a 0.1 kg·mol m^{-3} solution of HNO_2^*, the stream accelerates the disappearance of HNO_2^* although less than when the gas is introduced as a sparge of the liquid. The quantity R* is larger than for a similar gas flow bubbling through the liquid.

Because of the rate increases as oxygen is bubbled through the solution rather than air and the fact that in open vessels the sparge of air produces a similar rate of HNO_2^* removal to N_2 at the same rate, oxidation in the liquid phase is considered to be significant only when near pure O_2 exists in the gas phase.

The depletion of aqueous HNO_2^* was studied further by Komuro (1953). Komuro studied aqueous HNO_2 depletion at temperatures of 293 to 308 K at ambient pressure in a 1-liter bottle. Agitation was provided by stirring. The concentration of HNO_2^* in these studies was approximately 0.05 kg·mol m^{-3}, prepared by the acidification of $NaNO_2$ with HNO_3. The concentration of HNO_3 was varied from 0 to 6 kg·mol m^{-3}.

At 298 K, the first-order rate constant divided by the interfacial area was approximately 2.3×10^{-2} m^{-2} s^{-1}, measured at the HNO_2^* concentration of 0.01 to 0.05 kg·mol m^{-3} and an HNO_3 concentration of 1.0 kg·mol m^{-3}. The activation energy was found to be 5.98×10^3 kcal kg·mol^{-1}. The rate constant was found to be proportional to the first order of the undissociated HNO_2 concentration controlled by the equilibrium:

$$HNO_2 + H^+ \leftrightarrow H_2O + NO^+ \ , \ K = 0.4 \ . \qquad (70)$$

The rate constant increased with acid strength up to about 1 kg·mol m^{-3}, remaining essentially constant for higher acid strengths.

Komuro attributed the HNO_2 disappearance from solution to the physical desorption of HNO_2 given by Reaction (19b):

$$HNO_2\ (\ell) \rightarrow HNO_2\ (g)\ .$$

Suzawa, Hondo, Manabe, and Hinokiyama (1955) investigated the removal of aqueous HNO_2^* at temperatures of 273 to 313 K in a stirred laboratory reactor under a H_2 atmosphere at ambient pressure. Aqueous HNO_2 at 0.1 and 0.01 kg·mol m^{-3} was prepared by the addition of HCl to $NaNO_2$ solutions. The pH of the solution was varied from 0 to 2. Reactor vessels having cross-sectional areas 50.2 and 132.7 cm^2 were used. The stirrer speed was varied from 100 to 500 rpm.

The disappearance of HNO_2 from the solution was interpreted as first order, although the rate constants increased slightly with HNO_2 concentration. The rate constant for the removal of HNO_2 from solution (with no gas sparge) at 273 K was approximately 6.33×10^2 m^{-2} s^{-1} at a stirrer speed of 200 rpm. The removal rate constant increased linearly with the stirrer speed.

The rate constant increased with pH; the log of the rate constant and pH were in linear agreement. Below 283 K, the ratio of the moles of NO produced to the moles of HNO_2 disappearing, R**, was -0.5; above 283 K this ratio was -0.67. The chloride ion had no apparent effect on the measured HNO_2 disappearance rates.

The experimenters view the limiting physical phenomena in these experiments as the diffusion of HNO_2 through the liquid film.

Andrews and Hanson (1961) observed the presence of aqueous HNO_2 in an important series involving experiments of NO_x absorption in a single-sieve plate column. In these studies, conducted at 298 K and atmospheric

pressure, the liquid was recirculated through the column until steady-state was established. These researchers developed rate equations from basic diffusional, kinetic, and equilibrium constants that are in good agreement with the measured NO_x absorption efficiency of their sieve tray.

The mechanism describing the depletion of HNO_2 from the liquid phase was related to the absorbing NO_2^* partial pressure in the gas phase, and hence the concentration of HNO_2 in the liquid phase. For gas phase NO* concentrations of less than 5.0×10^{-4} kg·mol m^{-3}, the predominate mechanism was the kinetics of HNO_2 decomposition, as indicated previously by Abel and co-workers, and the rate of NO diffusion indicated by:

$$r_{HNO_2} = -3/4\ k_L a\ (C_{NO} - C^*_{NO}) \ . \tag{71}$$

By neglecting the concentration of NO at the gas-liquid interface, the following desorption rate may be derived from Equation (71):

$$r_{HNO_2} = -3/4\ (k_L a)^{2/3}\ V^{1/3}\ (2k_{25f}\ H_{N_2O_4}\ H^2_{NO}/K_1)^{1/3}\ p^{2/3}_{NO_2}\ p^{2/3}_{NO} \ . \tag{72}$$

This decomposition reaction sequence for HNO_2, as described earlier by Abel and co-workers, was found to be in the slow reaction regime as defined by Shah and Sharma (1976).

In a series of experiments very similar to those performed by Abel and his associates, Usabillaga (1962) studied the decomposition of aqueous HNO_2 at temperatures of 273, 283, 298, and 313 K. The initial

concentrations of HNO_2 for the decomposition and formation studies were 0.05 to 0.21 and 0.01 to 0.04 kg·mol m^{-3} respectively. The HNO_3 concentration was varied from 0.5 to 4.5 kg·mol m^{-3}. These experiments were conducted essentially at ambient pressure using a stirred batch reactor and a gaseous NO atmosphere. The variation in the pressure over the reaction was followed in order to monitor the reaction progress. Usabillaga found an additional second-order decomposition reaction to the kinetics of Abel and his associates:

$$2HNO_2\ (\ell) \leftrightarrow NO_2\ (\ell) + NO\ (\ell) + H_2O\ (\ell)\ , \tag{73}$$

and

$$2NO_2\ (\ell) + H_2O\ (\ell) \rightarrow HNO_2\ (\ell) + H^+\ (\ell) + NO_3^-\ (\ell)\ . \tag{74f}$$

His differential equation for the formation and decomposition is

$$\mp \frac{dC_{HNO_2}}{dt} = \pm k_{-60} \frac{C^4_{HNO_2}}{p^2_{NO}} \pm k'_{-60} \frac{C^2_{HNO_2}}{p_{NO}} \mp k_{60}\, C_{HNO_2}\, C_{H^+}\, C_{NO_3^-}\ . \tag{75}$$

His data are given in Table 6. Note, however, that K_{60} is computed using k_{60} and k_{-60}. A comparison with Abel's data from Table 5 shows no real surprises.

Schmid and Baehr (1964) studied Reaction (28b) at temperatures of 273 to 298 K in HNO_3 concentrations up to 5 kg·mol m^{-3}. Dilute HNO_2 concentrations were generated by injecting $NaNO_2$ into the HNO_3 solution. The reaction was studied in a stirred and vibrated reactor under NO atmospheres of 0.5 and 1 atm.

Table 6. Experimentally determined values of constants k_{-60}, k'_{-60}, k_{60}, and K_{60} at various temperatures

Reaction constants	Temperature (K)			
	273	283	298	313
$k_{-60}\left(\frac{m^9\ atm^2}{kg \cdot mol^3\ s}\right)$	0.00577	0.0505	0.520	50.52
$k'_{-60}\left(\frac{m^3\ atm}{kg \cdot mol\ s}\right)$	0.00012	0.00032	0.00083	0.0025
$k_{60}\left(\frac{m^6}{kg \cdot mol^2\ s}\right)$	0.00128	0.00393	0.0193	0.0662
$K^a_{60}\left(\frac{m^3\ atm^2}{kg \cdot mol}\right)$	4.53	12.8	26.9	100.0
$^aK_{60} = k_{-60}/k_{60}$				

Source: A. Usabillaga, *Kinetics of Nitrous Acid Formation and Decomposition*, Dissertation, University of Illinois (1962).

No deviation from the Abel and Schmid kinetics was found. At 293 K, the rate constant, k_{-60}, is approximately 0.0168 m^6 kg·mol^{-2} s^{-1} up to 1 kg·mol m^{-3} HNO_3. This rate constant increases markedly with increased HNO_3 concentrations.

The decomposition of aqueous HNO_2 was subsequently studied by Safin, Makhotkin, and Galeev (1970) at 298 K and ambient pressure. These studies were carried out in an agitated batch reactor and a film column. Aqueous HNO_2^* was prepared by the dissolution of N_2O_4 in H_2O.

Studies in the batch reactor with no agitation indicated that the decomposition rate of aqueous nitrous acid is proportional to the surface area and increases with increased liquid volume. Subsequent experiments with the agitated reactor and initial concentrations of HNO_2^* and HNO_3 at 0.02 kg·mol m^{-3} indicated that as the partial pressure of NO was increased, the disappearance of HNO_2^* continued with no generation of HNO_3 in the liquid. This again brings up the possibility of physical desorption of HNO_2.

Studies with the film column and HNO_2^* concentrations of 0.1 to 0.15 kg·mol m^{-3} and similar concentrations of HNO_3 yield no clear conclusions.

The researchers do have some theoretical insight into the described phenomena that appears to be noteworthy. The decomposition of HNO_2 in the liquid phase and the desorption of HNO_2 are two mutually connected processes, determining the kinetics of the HNO_2 loss from aqueous solutions. They define the term:

$$\phi = \delta \sqrt{\frac{k_{-60}\, C_{HNO_2}^4}{H_{NO}^2\, C_{NO}^2\, \mathcal{D}_{HNO_2}}} . \qquad (76)$$

The quantity ϕ^2 is the relation between the rate of chemical conversion in the liquid film and the rate of molecular diffusion of the reacting specie. When $\phi << 1$, the disappearance of HNO_2 occurs primarily as the result of physical desorption of HNO_2. When $\phi >> 1$, the reduction of HNO_2 is primarily due to the decomposition reaction in the liquid phase. The following mass transfer equation is said to describe the loss of HNO_2 in the film column:

$$\overline{R}_{HNO_2} = -k_L a \, (C_{HNO_2} - C^*_{HNO_2}) \, , \tag{77}$$

provided $\phi >> 1$.

The depletion of aqueous HNO_2 was further studied by Kobayashi, Takezawa, Hara, Nikki, and Kitano (1976) at temperatures of 273 to 295 K with a quiescent and agitated (vibrated) liquid phase. Aqueous HNO_2 concentrations of 0.004 to 0.04 kg·mol m^{-3} were generated by the acidification of $NaNO_2$ with HNO_3. Both the liquid phase and gas phase were analyzed. These experiments were conducted under a flowing N_2 atmosphere.

Studies were first conducted with a quiescent liquid phase. The nitrogen cover gas flow rate has no effect on the decomposition reaction. The reaction velocity in this series of experiments was found to be independent of the liquid volume, but is reported to be proportional to the surface area. The reaction was approximately first order with respect to the HNO_2 concentration. The reaction rate increased slightly with ionic strength and was independent of the H^+ concentration below 0.1 kg·mol m^{-3}. The gaseous reaction product ratio of NO to NO_2 was unity. The following overall reaction describes the observed phenomena:

$$2HNO_2\ (\ell) \rightarrow NO\ (g) + NO_2\ (g) + H_2O\ (\ell)\ . \qquad (78)$$

In experiments involving vibration of the liquid phase, the reaction velocity was 10 times that observed for the quiescent condition. The reaction velocity was independent of the N_2 flow rate, and the ratio of gaseous $NO:NO_2$ produced from the disappearance of aqueous HNO_2 was greater than unity. The reaction order of these experiments decreased from 1.35 to 1.23 as the temperature increased from 273 to 295 K. No effect of the H^+ concentration was observed below 0.1 kg·mol m^{-3}; however, a slight increase in the reaction velocity was noted for increasing ionic strength. The reaction sequence in this phenomena was thought to be:

$$HNO_2\ (\ell) \rightarrow HNO_2\ (i)\ , \qquad (79)$$

$$2HNO_2\ (i) \leftrightarrow N_2O_3(i) + H_2O\ (i)\ , \qquad (80)$$

$$N_2O_3\ (i) \leftrightarrow N_2O_3\ (g)\ , \qquad (81)$$

and

$$N_2O_3\ (g) \leftrightarrow NO\ (g) + NO_2\ (g)\ . \qquad (2B)$$

The following rate equations correlated well with the data:

$$\overline{R}_{HNO_2} = -k_L a\ (C_{HNO_2} - C^*_{HNO_2})\ , \qquad (77)$$

although some compensation was required for the reverse reaction of N_2O_3 and water at the gas-liquid interface.

In experiments primarily focused on determining the effect of HNO_2 on the absorption of NO_2^*, Makhotkin and Shamsutdinov (1976) made some relevant observations on the formation and decomposition of aqueous HNO_2. These studies were conducted at 293 K in a sparged batch reactor and in a film column. The studies using the sparged batch reactor were previously described.

In studies involving the decomposition of aqueous HNO_2^* in a film column, both gaseous NO and NO_2 are produced probably indicating the desorption of some HNO_2 or N_2O_3. However, substantially more NO than NO_2 is present in the effluent gas.

The oxidation of aqueous HNO_2 was investigated by Pogrebnaya, Usov, and Baranov (1976) at 298 K in a stirred batch reactor in O_2 at pressures up to 50 atm. The concentration of HNO_2^* was 0.005 kg·mol m^{-3} generated by the acidification of $NaNO_2$. The pH was varied between 2.9 to 4.0. The reaction is represented by:

$$2HNO_2\ (\ell) + O_2\ (\ell) \rightarrow 2HNO_3\ (\ell)\ , \tag{82}$$

and of the form,

$$dC_{HNO_2}/dt = -k'C^2_{HNO_2}\ . \tag{83}$$

The variation in the reaction rate with pH could be explained by making the concentration of HNO_2 to be the non-ionized HNO_2 as:

$$dC_{HNO_2}/dt = -k'_{82}\left(\frac{C_{H^+}}{K_{85} + C_{H^+}}\right) C^2_{HNO_2^*}\ . \tag{84}$$

The rate constant, k'_{82}, was found to be (0.58 ± 0.04) m^3 kg·mol^{-1} s^{-1}. The value of the equilibrium constant for

$$HNO_2\ (\ell) \leftrightarrow H^+\ (\ell) + NO_2^-\ (\ell) \qquad (85)$$

was found to be $(7.31 \pm 0.1) \times 10^{-4}$ kg·mol m^{-3} at 298 K by a potentiometic titration procedure.

Komiyama and Inoue (1978) used two different gas-liquid contactors in their study of the depletion of HNO_2 from aqueous solutions. These studies were conducted at ambient pressure and temperatures of 288 and 298 K, using a bubbling contactor and a stirred flat surface contactor. These studies were conducted in a helium atmosphere with HNO_2 in concentrations of 0.004 to 0.2 kg·mol m^{-3} prepared by adding H_2SO_4 to a $NaNO_2$ solution. Both the gas and liquid phases were analyzed.

Using the bubbling contactor, k_La was varied from 0.003 to 0.25 s^{-1} by varying the gas rate and the method of introduction. The experimental results were found to agree with the following equation:

$$r_{HNO_2} = -k'(k_La)^{2/3}\ C_{HNO_2}^{4/3} \ . \qquad (86)$$

At 288 and 298 K, the values of k' were 1.45×10^{-2} and 2.39×10^{-2} kg·$mol^{-1/3}$ $s^{-1/3}$ m^1. Because the evolution of gaseous NO in these experiments was about two-thirds of the depletion rate of HNO_2, the overall stoichiometry, as expressed in Reaction (28), is valid. The following assumptions were used to develop a model for the depletion of HNO_2 in the bubbling contactor data:

1. Desorption of components other than NO may be neglected.
2. The transport of NO in the liquid phase is given by:

$$\overline{R}_{NO} = -k_La\ (C_{NO} - C_{NO}^*) \ . \qquad (87)$$

3. The following equilibria are set up in the bulk liquid:

$$2HNO_2\ (\ell) \leftrightarrow NO\ (\ell) + NO_2\ (\ell) + H_2O\ (\ell)\ , \tag{88}$$

$$2NO_2\ (\ell) \leftrightarrow N_2O_4\ (\ell)\ , \tag{89}$$

$$N_2O_4\ (\ell) + H_2O\ (\ell) \rightarrow HNO_2\ (\ell) + HNO_3\ (\ell)\ , \tag{25f}$$

and

$$NO\ (\ell) + NO_2\ (\ell) \leftrightarrow N_2O_3\ (\ell)\ . \tag{90}$$

4. The process is at steady state.

With assumptions 1, 2, and 4, the depletion of HNO_2 may be expressed as:

$$r_{HNO_2} = -3\ k_{25f}\ C_{N_2O_4}\ , \tag{91}$$

and

$$r_{HNO_2} = -3/2\ k_L a\ (C_{NO} - C^*_{NO})\ . \tag{92}$$

Utilizing K_{87} and K_{88} yields:

$$r_{HNO_2} = -3\ k_{25f}\ K^2_{88}\ K_{89}\ C^4_{HNO_2}/C^2_{NO}\ , \tag{93}$$

a rate equation very similar to that obtained by Abel and Schmid and Andrews and Hanson. Combining Equations (92) and (93) and assuming C^*_{NO} to be negligible yields:

$$C_{NO} = 4^{1/6}\ (k_{25f}\ K^2_{88}\ K_{89})^{-1/3}\ C^{4/3}_{HNO_2}\ . \tag{94}$$

Substituting Equation (93) into (94) yields:

$$r_{HNO_2} = -(3/2)^{2/3} (k_{25f} K_{88}^2 K_{89})^{1/3} (k_L a)^{2/3} C_{HNO_2}^{4/3} , \quad (95)$$

an equation very similar to that obtained by Abel and Schmid (1928a). A comparison of combined constant of $(k_{25f} K_{88}^2 K_{89})$ with that derived from Abel and Schmid's work is fairly close at 298 K.

The flat surface contactor was equipped with a cone in the center of the liquid surface to keep it flat. The gas and liquid phases were independently agitated. The liquid-phase mass-transfer coefficient, ranging from 4.23 to 5.17 $\times 10^{-4}$ s^{-1}, was reported to be almost independent of the agitation speed in both phases. The gas-phase coefficient, as reported, was not dependent on the gaseous flow rate but rather on the agitation rate. The depletion rate was found to be a function of α, where α is defined as

$$\alpha = \frac{(1/k_L a)}{(1/k_G a) + (V_L/G)} . \quad (96)$$

The ratio of nitric acid produced to nitrous acid depletion decreased as α was increased, indicating some change from the overall stoichiometry of Equation (28). The overall depletion rate of aqueous HNO_2 for the flat-surface contactor data required additional mechanisms to the simultaneous hydration of N_2O_4 and evolution of NO as proposed earlier. These additional mechanisms are the desorption of nitrous acid molecules and the decomposition of HNO_2 into NO and NO_2 in the vicinity of the gas-liquid interface.

The decomposition of HNO_2 into NO and NO_2 was expressed in Equation (88). Values of the forward and reverse rate constants were determined to be as follows:

	Temperature (K)	
	288	298
k_{88} (m^3 kg·mol^{-1} s^{-1})	45.6	136
k_{-88} (m^3 kg·mol^{-1} s^{-1})	6.9×10^7	1.12×10^8

Values of α ranged from 1 to 350. For low values of α, the depletion of HNO_2 was shown to be due to the simultaneous hydration of N_2O_4 and desorption of NO; for an intermediate α, all three mechanisms apply, and for high α, the depletion is due to the desorption of HNO_2.

The Ionization and Dehydration of Aqueous HNO_2. Calculations at 298 K were made for the ionization of nitrous acid,

$$HNO_2\ (\ell) + H^+\ (\ell) \leftrightarrow NO_2^-\ (\ell)\ , \tag{97}$$

and the dehydration of nitrous acid,

$$2HNO_2\ (\ell) \leftrightarrow N_2O_3\ (\ell) + H_2O\ (\ell)\ , \tag{26B}$$

by Turney and Wright (1958). The values of K_{97} and K_{26B} were found to be 7×10^{-5} and 9×10^{-3} respectively.

Bunton and Stedman (1968), experimentally investigated the dehydration of nitrous acid in perchloric acid at 298 K. Their value of the concentration equilibrium constant,

$$K_{26B} = \frac{C_{N_2O_3}}{C^2_{HNO_2}} , \tag{98}$$

are given below for various molarities:

C_{HClO_4}	4.2	5.1	6.1	6.75	7.2	7.6
K_{26B}	0.057	0.19	0.49	0.56	0.29	0.36

Turney (1960) later calculated the activity equilibrium constant for this data to average 0.19.

The dehydration of nitrous acid was also investigated by Turney (1960) in perchloric acid at 298 K. The values of the activity constant, $K_{a,26B}$ was determined experimentally to be 0.20 m^3 $kg \cdot mol^{-1}$.

The activity coefficient of HNO_2 and the equilibrium constant of N_2O_3 formation were experimentally determined by Schmid and Kremayr (1966) at 293 K for the dehydration of nitrous acid. The activity equilibrium constant was found to be 16 m^3 $kg \cdot mol^{-1}$. This constant can be used at 298 K because of the effect of temperature for this case being smaller than the average error in arriving at the equilibrium constant. The activity coefficient of nitrous acid, valid for temperatures of 273 to 333 K and ion concentrations up to 12 kg·ions m^{-3}, is:

$$\gamma_{HNO_2} = 1 + 0.067\ I\ . \tag{99}$$

The concentration equilibrium constant,

$$K_{85} = \frac{C_{H^+}\ C_{NO_2^-}}{C_{HNO_2}} . \tag{100}$$

was determined spectrophotometrically by Ho (1977) at unit ionic strength at temperatures of 288, 298, and 308 K for aqueous HNO_2. The values were $(0.94 \pm 0.02) \times 10^{-3}$, $(1.02 \pm 0.02) \times 10^{-3}$, and $(1.11 \pm 0.04) \times 10^{-3}$ kg·mol m^{-3} respectively. The ΔH and ΔS for the dissociation at 298 K were found to be 1.47×10^3 kcal kg·mol^{-1} and -8.8×10^3 kcal kg·mol^{-1} respectively.

Further discussion of material presented in this section may be found in a recent review by Stedman (1979).

2. Studies with Prototype and Full-Scale NO_x Scrubbing Equipment

Early NO_x scrubbing studies were directed toward increasing the efficiency of nitric acid production columns that were associated with the production of nitric acid by the "oxidation of ammonia process" (Chilton, 1960). These columns, usually with bubble-cap plates, were designed with equilibrium and emperical information on the reaction of NO_2 and water, Reaction (29),

$$3NO_2\ (g) + H_2O\ (\ell) \leftrightarrow 2HNO_3\ (\ell) + NO\ (g)\ ,$$

and kinetic information on the oxidation of NO, Reaction (5),

$$2NO\ (g) + O_2\ (g) \rightarrow 2NO_2\ (g)\ .$$

The most familiar of the modern nitric acid production columns is a 30- to 50-plate water-cooled bubble-cap tower, 18 to 40 m tall, with diameters of 1.5 to 4 m (Hoftzyer and Kwanten, 1972). These towers operate at pressures of 5 to 8 atm and at temperatures determined by available cooling water. The feed and tail gases of such a unit have

NO_x concentrations of about 9.3 and 0.5 to 0.1 vol %, respectively; the product stream is usually 58 to 70% HNO_3. Nitric acid production towers have undergone a sixty year optimization process; however, because the design basis for these pieces of equipment incorporates a great deal of empirical information, extrapolation to different NO_x scrubbing tasks has been extremely difficult.

In the mid 1950s, the analysis of NO_x scrubbing studies in prototype equipment began to incorporate developments in the understanding of NO_x-HNO_x-H_2O chemistry (Peters et al., 1955); in the early 1960s, efficiencies for NO_2^* removal were successfully predicted (Andrews and Hanson, 1961) using the developing theory of gas absorption accompanied with chemical reaction (Astarita, 1967; Danckwerts, 1970). Application of the theories of absorption accompanied by chemical reaction and a detailed knowledge of system chemistry seem to be the most promising route toward a greater understanding of nitrogen oxide scrubbing operations.

An industrial-scale bubble-cap column was used by Fauser (1928) to measure the effects of temperature and pressure on NO_2^* absorption. He found that absorption rates increase with decreasing operating temperatures (288 to 259 K) and with increasing operating pressures (up to 5 atm).

Taylor, Chilton, and Handforth (1931) studied the effects of temperature and pressure on NO_x absorption in a pilot-plant-scale bubble-cap column. They also found that column efficiency could be increased by reducing the operating temperature or by increasing the operating pressure. The column performance was accurately predicted using Bodenstein's data for the oxidation of NO and existing equilibrium data for the NO_2-N_2O_4 equilibrium.

Peters, Ross, and Klein (1955) studied NO_2^* absorption in a single-plate 0.19-m-ID bubble-cap column equipped with seven bubble caps. The experiment was conducted at acid concentrations of 0 and 2.6 kg·mol m^{-3} and NO_2^* partial pressures up to 0.10 atm. Runs were made at liquid flow rates of 5.0×10^{-6} and 10.0×10^{-6} m^3 s^{-1} and gas rates of 5.71×10^{-4} and 1.14×10^{-3} m^3 s^{-1}. All runs were conducted at atmospheric pressure and at temperatures from 292 to 297 K. No significant difference in the results was noted from the use of nitrogen or air as the diluent gas. These investigators assumed that overall Reaction (29) applied for the hydrolysis of N_2O_4 and that a model developed from chemical reaction rates was adequate. Their results showed that the rate of removal of NO_2^* was proportional to the concentration of N_2O_4 in the gas phase. NO_2^* removal efficiencies are presented in Figure 4. The fraction of entering oxides converted to HNO_3 was found to decrease as the contact time between gas and liquid decreased. Neither the liquid flow rate nor the acid molarity of the scrubbing liquid had any effect on removal efficiency; however, increasing the humidity in the feed gas increased removal efficiency. They concluded that the absorption reactions occur at the gas-liquid interface.

Peters (1955) compared the absorption of NO_2-N_2O_4 from air into water and dilute HNO_3 (<2.6 kg·mol m^{-3}) in the following devices: a single-plate bubble-cap column previously described (Peters et al., 1955); a 0.025-m-ID column, packed with 6-mm glass raschig rings to a height of 1.17 m; a 0.14-m-ID single-plate fritted bubbler column consisting of 12 medium-frit glass rods sealed into the plate; a 0.025-m-ID, 1.32-m-high spray tower equipped with a single spray nozzle; and a

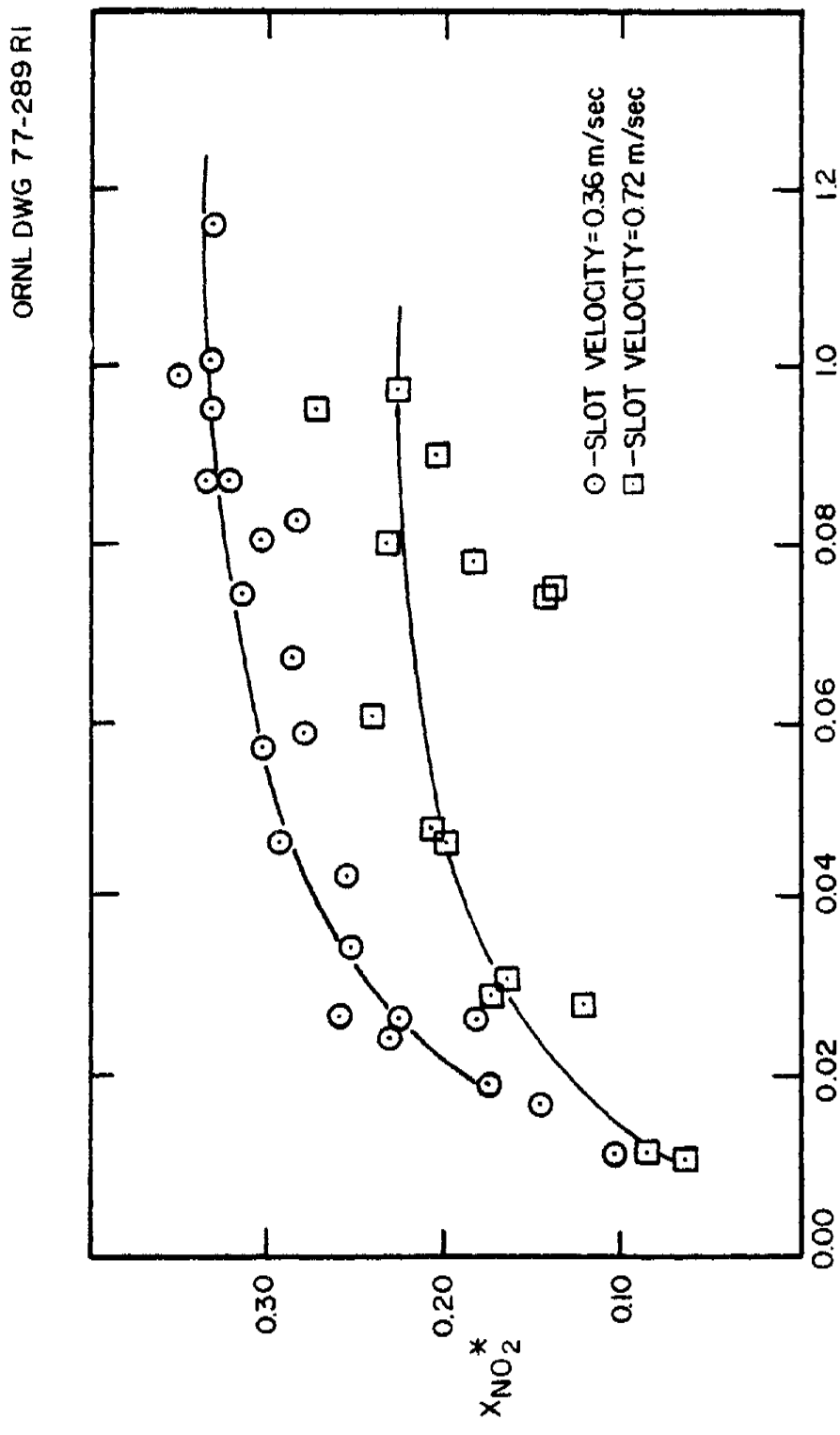

Figure 4. Efficiency of NO_2^* removal by bubble-cap column vs NO_2^* partial pressure obtained by Peters, Ross, and Klein.

Source: M. S. Peters, C. P. Ross, and J. E. Klein, *AIChE J.* 1: 105 (1955).

0.025-m-ID bed of silica gel packed to a height of 0.3 m. The partial presure of NO_2^* was varied from 0.002 to 0.02 atm, but the total pressure was maintained at 1.0 atm. The temperature was maintained at 298 K. Efficiencies of the packed beds were reported in terms of 0.3 m of packing. Operating parameters were chosen to permit a fair comparison of the removal efficiencies of various types of contactors. The removal efficiency was found to be independent of the liquid rate in the bubble-cap and fritted bubbler columns as long as the HNO_3 concentration of the liquid did not increase above 2.8 kg·mol m^{-3}. The spray column was operated at a liquid flow rate that would yield a finely divided mist, and the packed column was operated at approximately 90% of flooding.

The experimental results are presented in Figure 5. The performance of the bubble-cap column improved with increasing NO_2^* concentration, and its removal efficiency is significantly surpassed only by that of the fritted bubbler column. The removal efficiency of the fritted bubbler column was higher than that of other devices except at NO_2^* concentrations of less than 0.004 atm. However, the pressure drop through this plate was about 30 times higher than that of the bubble-cap plate. Removal efficiencies with the packed column were lower than those found with the bubble-cap column or the fritted bubbler column. However, the decrease in efficiency with reduction in NO_2^* concentration is fairly gradual, and the performance of the packed column at NO_2^* partial pressures of less than 0.002 atm becomes comparable to that of other types of equipment. Results obtained with the spray column indicate that removal efficiencies at NO_2^* concentrations less than 0.001 atm are poor, but at higher concentrations are comparable to those obtained with other types of equipment.

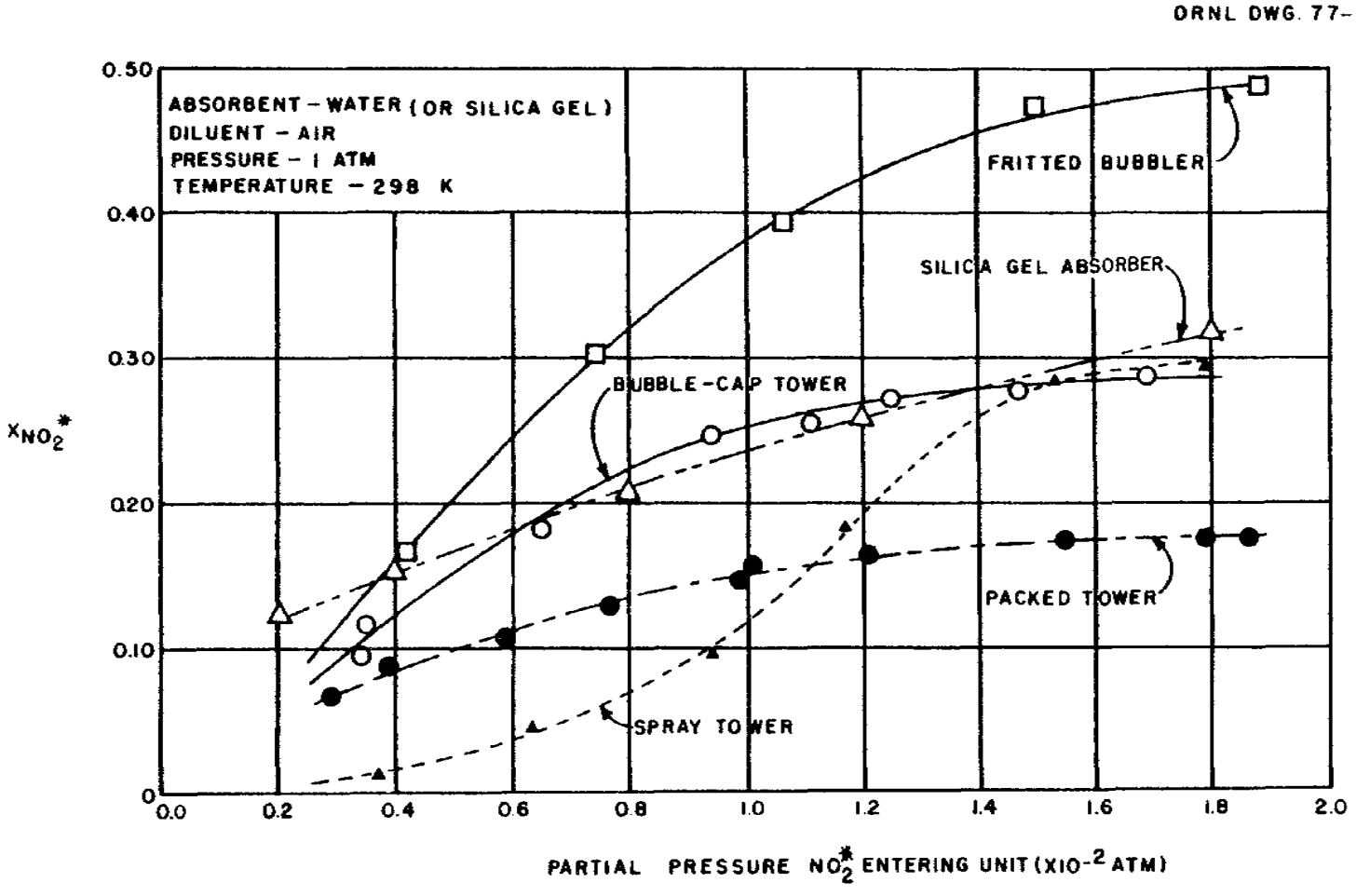

Figure 5. Efficiency of NO_2^* removal from dilute gas with different types of equipment obtained by Peters.

Source: M. S. Peters, *University of Illinois Engineering Experiment Report No. 14*, USAEC-COO-1015 (1955).

The silica gel adsorber provides the best removal efficiency of the units tested at concentrations of less than 0.004 atm.

Peters (1955) also studied NO_2^* absorption from air into water and dilute HNO_3 (<2.6 kg·mol m^{-3}) in a three-stage bubble-cap column. A typical plate was described previously (Peters et al., 1955). The distance between the plates was 0.3 m; the partial pressure of NO_2^* in the feed varied from 0.005 to 0.08 atm. Distilled water was fed into the top of the column at the rate of 5.0×10^{-6} m^3 s^{-1}. The gas flow rate was 5.9 m^3 s^{-1}. Other operating conditions were as described above. The efficiencies of the three plates are presented in Figure 6. The efficiency increases as the gas moves up the tower for any given NO_2^* partial pressure in the feed.

Atroshchenko, Konvisar, and Kordysh (1960) studied the absorption of NO_x compounds in a 0.03-m-ID bubble-cap column. Their results showed that Murphree plate efficiency generally increases with increasing NO_2^* partial pressures and with increasing interplate distance. Atroshchenko, Konvisar, and Ivakhnenko (1965) later investigated the effects of plate hole size, the ratio of open area to total plate area, and the gas flow rate on gaseous NO_x absorption in a sieve-plate column. In general, they discovered that plate efficiencies increase with decreased plate open area and decreased gas flow rates.

In 1960, Chilton presented an extensive review of the "Dupont Pressure Process" for The Manufacture of Nitric Acid by the Oxidation of Ammonia. He presents an extensive literature review and empirical observations on the optimization of high pressure nitrogen oxide absorption in bubble-cap towers. His observations on plate spacing, temperature,

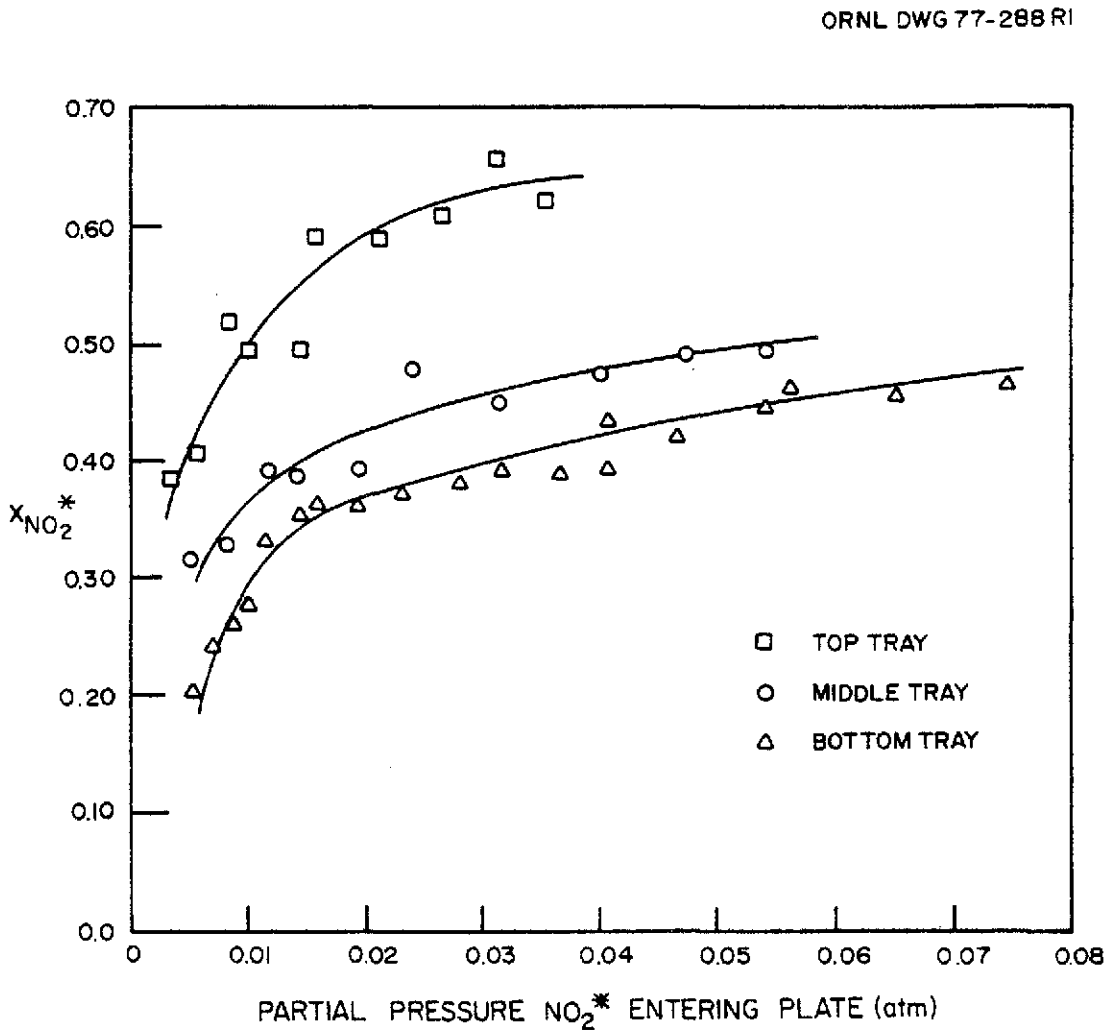

Figure 6. Effect of NO_2^* partial pressure in entering gases on NO_2^* conversion with a three-plate bubble-cap column obtained by Peters.

Source: M. S. Peters, *University of Illinois Engineering Experiment Report No. 14*, USAEC-COO-1015 (1955).

and presssure are also explainable based on the observations on NO oxidation and N_2O_4 being the absorbing specie.

Graham, Lyons, and Faucett (1964) applied the Dupont Pressure Process in the construction of a bubble-cap HNO_3 production column. They give performance data of this design for a column rated at 50,000 kg of HNO_3 produced per day.

Andrews and Hanson (1961) studied the absorption of NO_2^* from air-NO_2^* and air-NO_2^*-NO* gaseous mixtures into dilute HNO_3 using a recirculating acid stream and a small single-sieve-tray column at 298 K. The partial pressure of NO_2^* was varied up to 0.10 atm. For NO_2^* concentrations greater than 0.01 atm, the predominant absorption mechanism is the solution of N_2O_4 into the liquid followed by its rapid hydrolysis to HNO_3 and HNO_2. The work of Andrews and Hanson, however, is the first attempt to use existing knowledge of chemical reaction rates, diffusional rates, and equilibrium data to calculate the conversion of NO_2^*. Their definition of NO_2^* conversion is the ratio of NO_2^* absorbed to that entering the plate. Andrews and Hanson associated steady-state absorption and desorption mechanisms and add the resulting partial NO_x conversions for an overall NO_x conversion. The term steady-state is important because Andrews and Hanson waited until the aqueous HNO_2 concentration reached a steady value before taking data. Their model reflects this logic. The descriptive overall reactions for the four important combined absorption mechanisms are (a) Equations (101) and (102), (b) Equation (103), (c), Equations (104) through (106), and (d) Equations (107) and (108).

$$2N_2O_4\ (g) + 2H_2O\ (\ell) \rightarrow 2HNO_3\ (\ell) + 2HNO_2\ (g)\ , \quad (101)$$

$$2N_2O_4\ (g) + H_2O\ (\ell) \rightarrow 2HNO_3\ (\ell) + N_2O_3\ (g)\ , \quad (102)$$

} a

$$4NO_2\ (g) + 2H_2O\ (\ell) \rightarrow 2HNO_3\ (\ell) + 2HNO_2\ (g)\ , \quad (103)$$

} b

$$3NO_2\ (g) + H_2O\ (g) \rightarrow 2HNO_3\ (g) + NO\ (g)\ , \quad (104)$$

followed by

$$6HNO_3\ (g) \rightarrow 6HNO_3\ (\ell) \quad (105)$$

or

$$2HNO_3\ (g) + H_2O\ (g) \rightarrow 2HNO_3\ (\text{mist}) \rightarrow 2HNO_3\ (\ell)\ , \quad (106)$$

} c

$$3N_2O_3\ (g) + H_2O\ (\ell) \rightarrow 2HNO_3\ (\ell) + 4NO\ (g)\ , \quad (107)$$

and

$$6HNO_2\ (g) \rightarrow 2HNO_3\ (\ell) + 4NO\ (g) + 2H_2O\ . \quad (108)$$

} d

The predicted component and overall conversions are presented in Figure 7. The overall or total plate NO_x conversion is compared with the experimental data in Figure 8.

The absorption mechanisms of Andrews and Hanson (1961) were combined with a desorption stipulation of 1/3 mole of NO* for every mole NO_2^* absorbed in a model for NO_x absorption in packed columns by Hoftyzer and Kwanten (1972). The model is reported to work with fair success at predicting the NO_x removal efficiency in high-pressure absorbers.

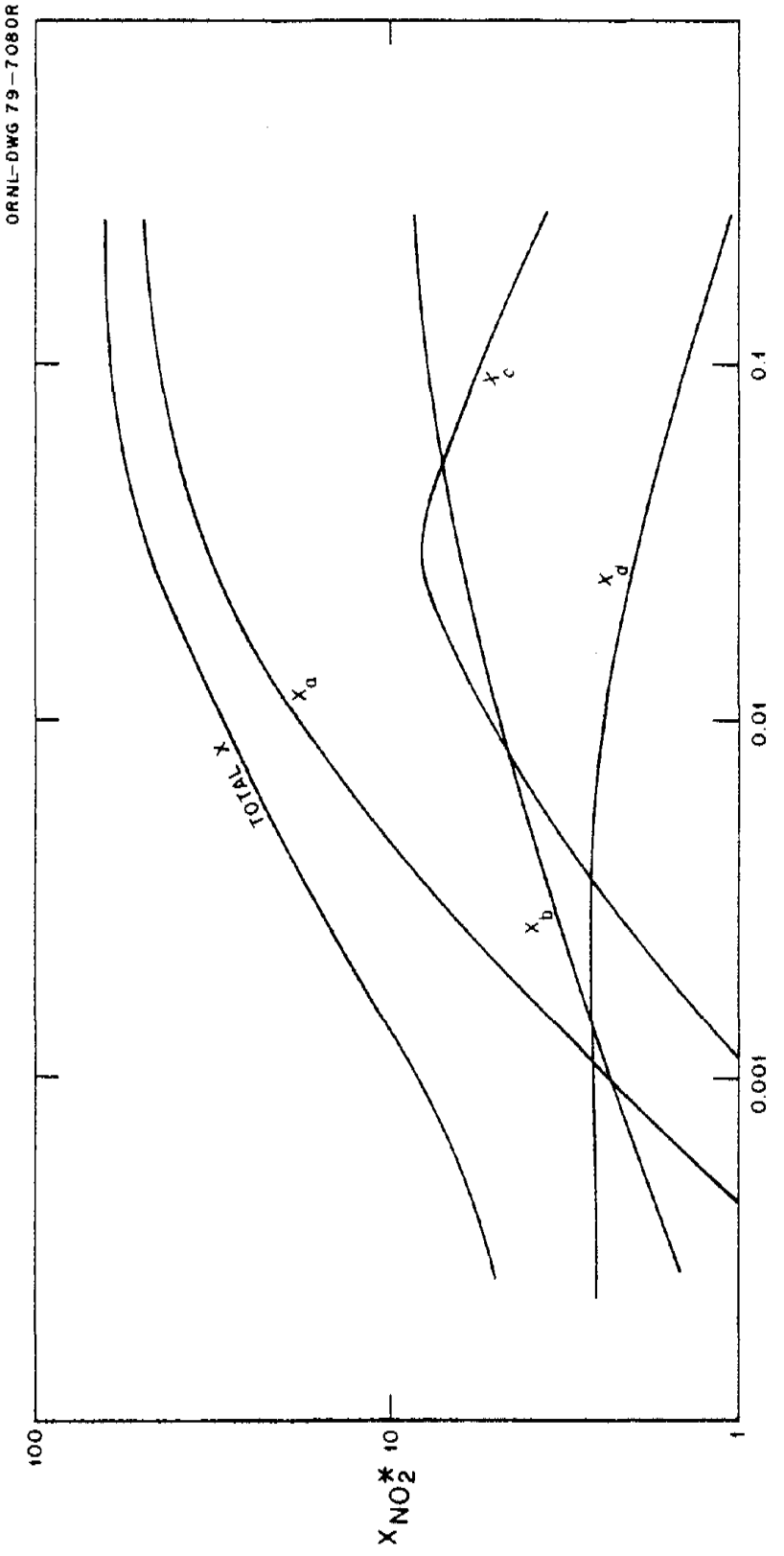

Figure 7. Predicted component and total NO_2^* conversion obtained by Andrews and Hanson.

Source: S. P. Andrews and D. Hanson, *Chem. Eng. Sci.* 14: 105 (1961).

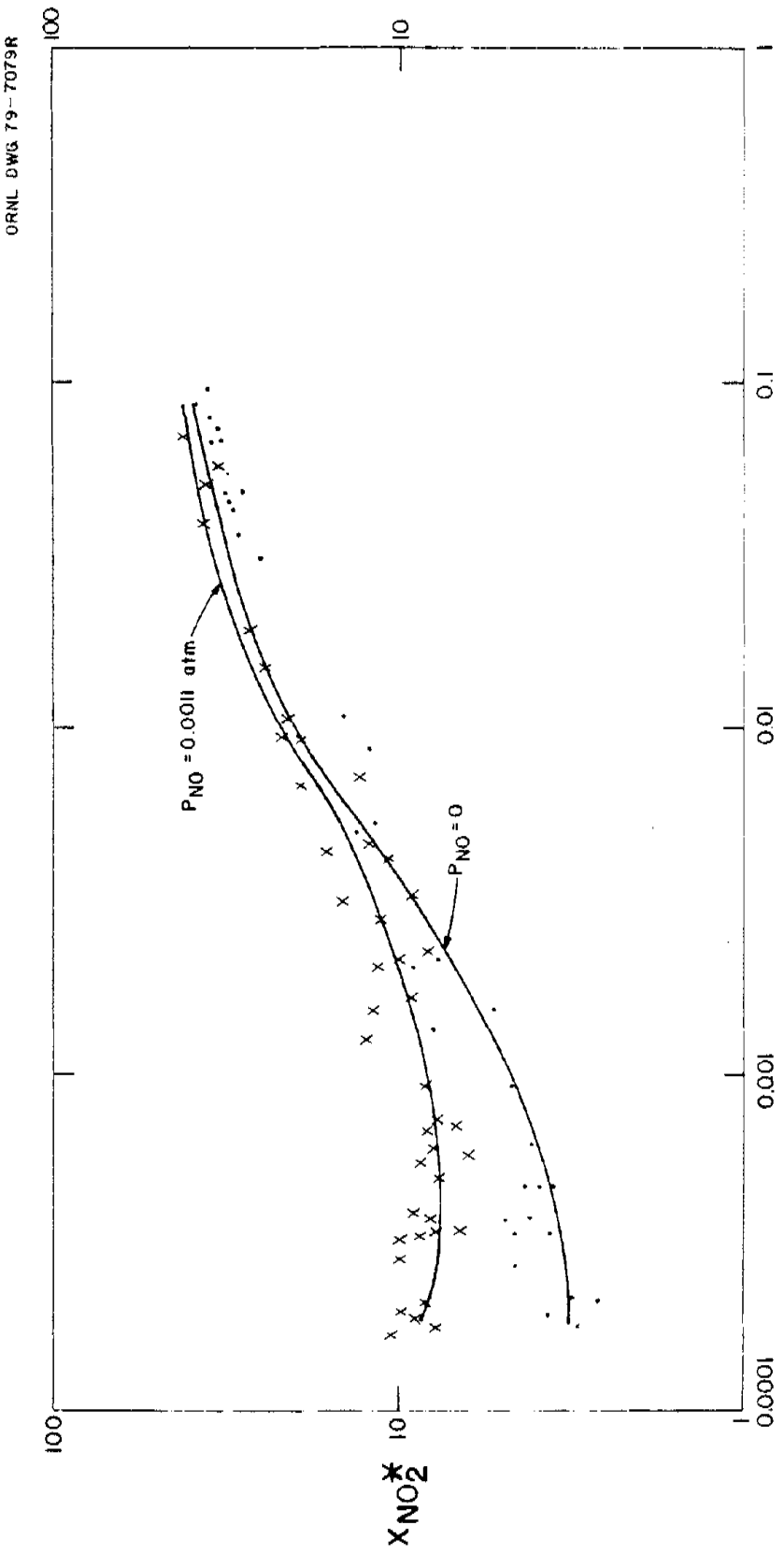

Figure 8. Comparison of measured and predicted conversion of NO_2^* obtained by Andrews and Hanson.

Source: S. P. Andrews and D. Hanson, *Chem. Eng. Sci.* 14: 105 (1961).

Results from a study of a 16-stage crossflow NO_x scrubber used to treat the off-gas from a metal etching facility were reported by First and Viles (1971). This atmospheric pressure scrubber has a face area of 0.116 m^2; each stage is equipped with a spray volume where the gas is sprayed with water, followed by scrubbing with 1.10 m of 37-μ-diam glass packing. For gas rates of 0.052 to 0.078 $m^3\ s^{-1}$, the overall NO_x conversion, X_{NO_x}, varied from 0.90 to 0.97 as the gaseous NO_x concentration in the feed gas varied from one to 33 vol %. The NO_x gases at the scrubber inlet were highly oxidized, 54 to 87% NO_2^*.

Design features of bubble-cap trays for nitrogen oxide scrubbing were investigated by Billet (1972) in both a laboratory-scale and a 1.5-m-diam tray. These studies were conducted at temperatures of 313 to 323 K, pressure of approximately 1.4 atm; the scrubber liquid was approximately 1.15 to 2.03 $kg \cdot mol\ m^{-3}$ HNO_3; and the partial pressure of NO_2^* and NO* assumed to be approximately 0.06 and 0.16 atm. In the laboratory scale studies, two types of bubble caps with cooling elements were studied: (1) a cap with triangular slots surrounded by cooling elements in a rhombic arrangement, and (2) a cap with rectangular slots and cooling elements in a square arrangement surrounding the cap. In studies where the gas load was varied from 30 to 90% of the maximum, tray efficiencies varied from 26 to 47%. From these studies, the cap with rectangular slots surrounded by cooling elements in a square arrangement was 5 to 18% better than the other arrangement. This arrangement was further tested in a 1.5-m-diam tray where similar experimental results were noted. Heat transfer coefficients are also given for the latter studies.

Nitric acid production was examined by Hellmer (1972) who used a semi-industrial-scale sieve-plate column with cooling coils located in

the bubble layer of the plates. The acid concentration was varied along with the NO_2^* concentration. According to Hellmer, it is possible to calculate the number of plates necessary for a given HNO_3 outlet concentration and entering NO_2^* concentration using literature rate constants for Reactions (29) and (5). Murphree plate efficiencies ranged from 23 to 65% for acid concentrations varying from 0 to 15 kg·mol m^{-3} and from 23 to 65% for NO_2^* partial pressures varying from near 0 to 0.25 atm. Hellmer also gives the relative heat transfer coefficient of the bubble layer as a function of the acid concentration.

Bowman, Kulczak, and Shulman (1974) studied the scrubbing of low gas concentrations of NO_2^* in air with water in a packed column. The column was 0.76 m in diam and packed to a height of 1.52 m with No. 2 plastic Intalox saddles. Tests were conducted at atmospheric pressure. Results are reported at a liquid flow rate of 9.46×10^{-4} m^3 s^{-1} for superficial gas velocities of 0.35 to 1.25 m s^{-1} and NO_2 gas concentrations of 1000 to 3750 ppm in Figure 9. Other results are reported at temperatures from 287 to 300 K and NO_2^* concentrations of 750 to 3750 ppm in Figure 10. In general, NO_x conversion increases with increasing gaseous NO_2 concentration, decreasing temperature, and decreasing gas flow rate.

Zhidkov et al. (1974), correlated many different cases of tray efficiency for NO_x removal in sieve plate towers. Their equation could be extremely useful if further parameter definitions were available or could be ascertained.

The absorption of NO_2^* by aqueous nitric acid in concentrations of 15.9 to 18.6 kg·mol m^{-3} was investigated by Karavaev and Visloguzova

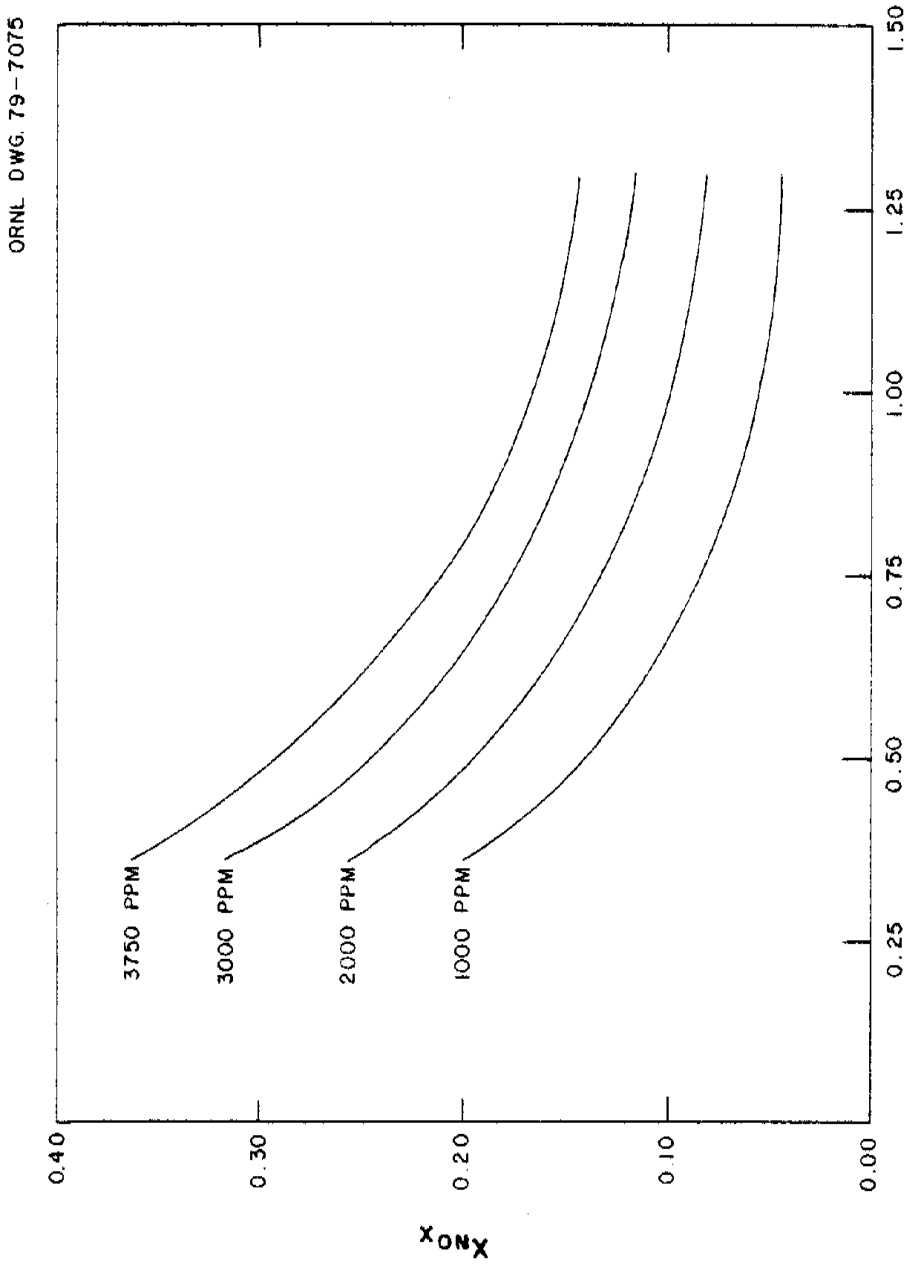

Figure 9. The conversion of NO_x in a packed tower as a function of the superficial gas velocity at a liquid rate of 9.46×10^{-4} m^3 s^{-1} obtained by Bowman, Kulczak, and Shulman.

Source: D. H. Bowman, C. J. Kulczak, and J. J. Shulman, *Pollut. Control Eng.* 6: 38 (1974).

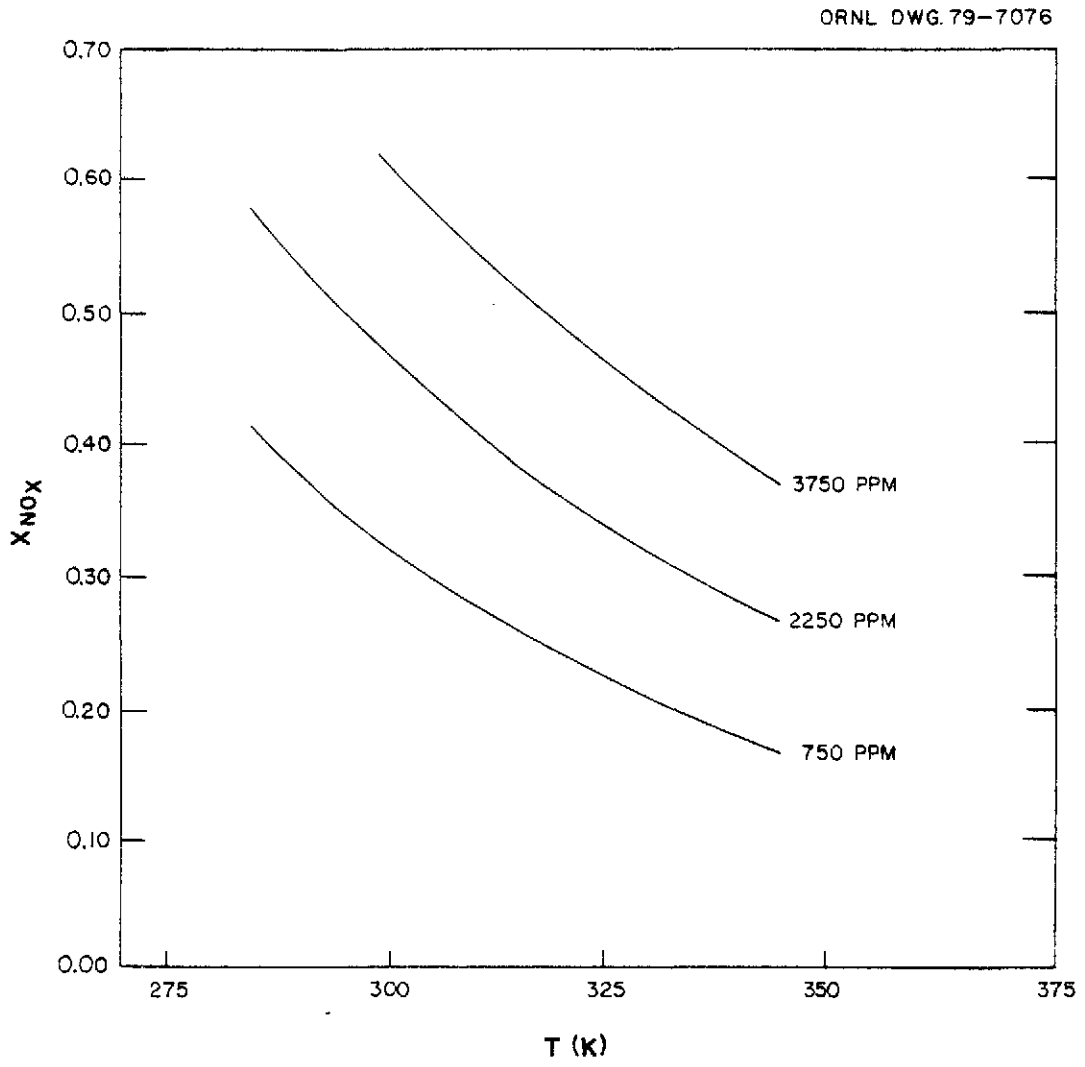

Figure 10. The conversion of NO_x in a packed tower as a function of temperature at gas and liquid rates of 0.156 m^3 s^{-1} and 9.46 × 10^{-4} m^3 s^{-1}, respectively, obtained by Bowman, Kulczak, and Shulman.

Source: D. H. Bowman, C. J. Kulczak, and J. J. Shulman, *Pollut. Control Eng.* 6: 38 (1974).

(1974) in laboratory-scale equipment. The NO_2^* partial pressure was varied from 0.10 to 0.50 atm at a total pressure assumed to be atmospheric; the temperature was varied from 268 to 283 K; nitrogen was the diluent gas. These studies were conducted in a 12.4-mm-diam tower packed to a height of 945 mm with small packing elements. The total packing area was calculated to be 141.3 cm^2; gas residence time variation in the tower was estimated to be between 1.3 and 4.3 s. Standard parameter conditions in these studies were: temperature, 283 K; $P_{NO_2^*}$, 0.36 to 0.42 atm; gas residence time, 2.6 to 2.75 s, liquid loads, 9.78×10^{-4} m s^{-1}, unless otherwise indicated. All parameter effects are over the indicated range of interest. The degree of absorption of NO_2^*, $X_{NO_2^*}$, decreased linearly from 0.46 to 0.33 with a decreasing partial pressure of NO_2^*; the absorption of NO_2^* also linearly decreased with increasing temperatures from 0.84 to 0.34. Overall absorption rate coefficients decrease with increasing NO_2^* partial pressure and temperature. The degree of NO_2^* absorption was also shown to increase proportionally with gas residence time and liquid load. Absorption rate coefficients increased with liquid loads and were not affected by gas residence time. Another interesting conclusion of this study was that the extent of absorption, $X_{NO_2^*}$, and the rate coefficient increased with increasing nitric acid strength.

The initial operating experience with an "extended scrubber column" was presented by Swanson et al. (1978). Extended scrubbing refers to additional scrubbing operations to the off-gas from nitric acid production columns. The device was installed initially to reduce the NO_x emissions from a nitric acid production facility; additional product

recovery and energy conservation benefits are also cited. This 25-plate column (inferred) was 3.66 m in diam., 33.5 m in height, and operates at a pressure of approximately 6 atm. It is designed to treat a 13.2 $m^3\ s^{-1}$ gas stream. The unit was cooled with water at 283 K. The facility has reportedly produced emission concentrations of 178 ppm for a feed gas averaging 3000 ppm.

Results of an experimental study of nitrogen oxide scrubbing in a three-stage sieve-plate column were reported by Counce and Perona (1979a). The column was 0.076 m in diam. with 0.25-m plate spacing. The free area of the plate was 0.6% (Counce and Perona, 1979b). In most of this study, the feed gas was saturated with water at 348 to 356 K. The scrubber liquid, aqueous HNO_3 in concentrations of 1.1 to 3.5 kg·mol m^{-3}, was recirculated in these studies. The total pressure for these studies was approximately 1.1 atm. Several other parameters were investigated: liquid rate, 0.09 to $3.5 \times 10^{-5}\ m^3\ s^{-1}$; partial pressure of NO_2^*, 0.14 to 0.40 atm; noncondensable gas rate (NO_2^* and air), 1.75 to $3.5 \times 10^{-4}\ m^3\ s^{-1}$; and steam flow rate, 0 to 1.08×10^{-3} kg s^{-1}. The presence of HNO_2 in the recirculating liquid was observed to have a deleterious effect on NO_x conversion, X_{NO_x}, in these studies, as is shown in Figure 11. Parameter evaluations were made at steady-state which involves reaching a steady-state HNO_2 concentration. The conversion of NO_x increased with increasing scrubber liquid rate, decreasing gas rate, decreasing acid molarity, and increasing steam rate to a limited extent. The NO_x removal efficiency was also improved by sparging the scrubber liquid in an operation prior to recycle; this apparently decreased the HNO_2 concentration in the scrubber liquid. Overall, the total NO_x removal in

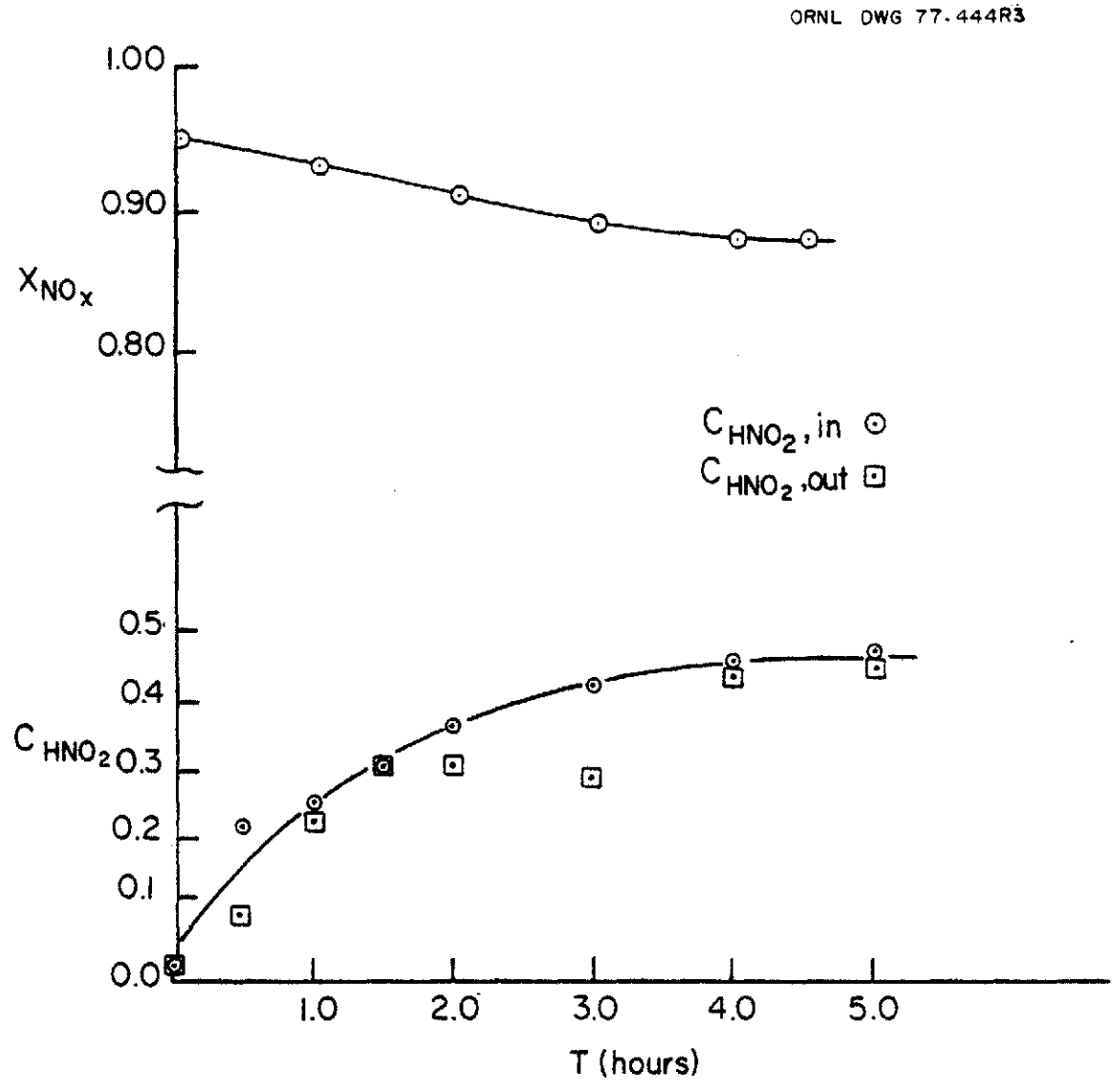

Figure 11. Overall NO_x conversion of a three-stage sieve-plate column with recycle of the scrubber liquid during the approach to steady-state obtained by Counce and Perona.

Source: R. M. Counce and J. J. Perona, *Ind. Eng. Chem. Fundam.* 18: 400 (1979).

the column varied from 75 to 90%. The NO_x conversions for the individual plate and the column were predicted fairly well with a simple mechanistic model that takes into account the effect of aqueous HNO_2 in the scrubbing process (Counce, Groenier, Klein, and Perona, 1978; Counce and Perona, 1980). This model is based on chemical Reactions (1), (21), (25f), (28), and (5):

$$2NO_2\ (g) \leftrightarrow N_2O_4\ (g)\ ,$$

$$N_2O_4\ (g) \leftrightarrow N_2O_4\ (\ell)\ ,$$

$$N_2O_4\ (\ell) + H_2O\ (\ell) \rightarrow HNO_3\ (\ell) + HNO_2\ (\ell)\ ,$$

$$3HNO_2\ (\ell) \leftrightarrow H_2O\ (\ell) + HNO_3\ (\ell) + 2NO\ (g)\ ,$$

and

$$2NO\ (g) + O_2\ (g) \rightarrow 2NO_2\ (g)\ .$$

This model seemed to fit the data better for cases with no steam in the feed gas.

The Bolme NO_x recovery process for the extended scrubbing of gaseous NO_x from the off-gas of conventional nitric acid production columns was discussed in an article by Bolme and Horton (1979). The NO_x removal is accomplished in a multi-stage sieve-plate column (inferred to operate at approximately 6 atm). For the case described, the gaseous NO_x concentration was decreased from 2500 to 85 ppm. Primary NO_x removal was accomplished in a 15-plate scrubber section which uses 4.3 to 5.6 kg·mol m^{-3}

HNO_3 as the scrubber liquid. This concentration of aqueous HNO_3 decreases the absorption of NO_2^* only slightly; however, it will greatly increase the stability of HNO_2 in the liquid phase, and the oxidation of NO to NO_2 will be increased to some extent by the vapor pressure of HNO_3 over the scrub solution. The gas leaving this section was approximately 150 ppm, 70% of which was said to be NO_2^*. The gaseous NO_x concentration is further reduced in a wash section with water as the scrub solution; this solution leaves the extended absorber as liquid feed for the nitric acid production column. The liquid effluent from the scrub section is heated and stripped with steam to remove HNO_2 and any other dissolved NO_x species before recycle; these gaseous NO_x species are fed to the nitric acid production column. This process for extended NO_x recovery appears to be an excellent example of the application of a detailed knowledge of the NO_x-HNO_x-H_2O system chemistry to this scrubbing operation.

An impressive series of experiments on the absorption of NO_x into water and dilute nitric acid was conducted by Koegler using a 0.15-m-diam bubble-cap tower. Other studies also involved the addition of NaOH and H_2O_2 to the liquid phase. The tower had eight trays with one bubble cap per tray and tray spacings of 0.305 m. Gas analysis for NO_2^* and NO* and liquid analysis for HNO_3 and HNO_2 were conducted for each stage from start-up through steady-state. A screening series of experiments was conducted using the variables and ranges given in Table 7. The temperature varied from 297 to 309 K during these tests. The overall NO_2 conversion during these tests ranged from 26 to 83%. At a 95% significance level, only the following variables had an effect on the concentration of NO_2 leaving the absorbers:

Table 7. Assigned system variables for Koegler's studies[a]

Flowsheet parameter	Low value (-)	High value (+)
Total gas flow rate, $m^3\ s^{-1}$	9.4×10^{-4}	2.8×10^{-3}
NO in feed gas, %	1	3
NO_2 in feed gas, %	3	20
O_2 in feed gas, %	11.5	20.2
Flow rate of recycle acid to tray 8, $m^3\ s^{-1}$	2.5×10^{-6}	3.8×10^{-5}
Flow rate of recycle acid to tray 3, $m^3\ s^{-1}$	3.2×10^{-5}	1.3×10^{-4}
Flow rate of water to tray 8, $m^3\ s^{-1}$	9.5×10^{-7}	1.0×10^{-5}
Flow rate of cooling water to tank recycle heat exchanger, $m^3\ s^{-1}$	0	3.5×10^{-4}
Flow rate of cooling water to heat exchanger, $m^3\ s^{-1}$	0	6.2×10^{-4}

[a]Temperature varied from 297 to 309 K during these tests.

Source: S. S. Koegler, *Purex No_x Abatement Pilot Plant*, RHO-CD-702, Rockwell Hanford Operations (July 1979).

1. Percent of NO_2 in the feed gas (positive effect).
2. Total gas flow rate (positive effect).
3. Water to tray 8 (negative effect).

The first two variables increased the NO_2 concentration in the off-gas and decreased column NO_x removal performance; the third (water flow to tray 8) increased column NO_x removal performance by lowering the percent of NO_2 in the off-gas.

A full-factorial test was then run on the variables and ranges indicated in Table 8. The following equation for the 8-tray column is the result of those studies:

$$Y = -0.1067 + 0.2174X_1 + 5.693 \times 10^{-3}X_3 + 0.6219 \log X_1 + 0.02644X_1X_2 - 0.5769X_1X_4 \quad (109)$$

where

$Y = NO_2$ in off-gas, %,

$X_1 = NO_2$ in feed gas, %,

X_2 = total gas flow, std. $ft^2\ min^{-1}$,

X_3 = average column liquid temperature, °F,

and

X_4 = water flow to tray 8, gal min^{-1}.

The results of these experiments showed all four factors tested to be significant at the 99% level. Two strong interactions noted were: cross products of the percent of NO_2 in the feed and the total gas flow,

Table 8. Assigned variables in Keogler's studies — full factorial design

Variable	Low value (-)	Mid value (0)	High value (+)
NO_2 feed gas, %	1	4	7
Total gas flow rate, $m^3\ s^{-1}$	8.2×10^{-4}	1.6×10^{-3}	2.5×10^{-3}
Flow rate of water to tray 8, $m^3\ s^{-1}$	1.3×10^{-6}	1.04×10^{-5}	2.3×10^{-5}
Acid recycle temperature, K	294	311	327

Source: S. S. Koegler, *Purex No_x Abatement Pilot Plant*, RHO-CD-702, Rockwell Hanford Operations (July 1979).

and the percent of NO_2 in the feed and the water flow rate to the column. These interactions were also significant at the 99% level.

The production of HNO_2 in the liquid was also examined as a function of the four system variables in Table 8. The percent NO_2 in the feed gas (positive effect), water flow rate (negative effect), and liquid temperature (negative effect) were found to significantly affect the concentration of HNO_2 in the product/feed tank at the 99% level. The gas flow rate had a smaller positive effect, but was significant at the 95% level. Significant effects also were found for interactions between feed NO_2 concentrations and temperature (negative), feed NO_2 concentration and water flow rate (negative), and temperature and water flow rate (positive).

In conclusion, the NO_x removal efficiency of the scrubber was increased by decreasing the gas rate, increasing the NO_x feed concentration, increasing the water flow to the column, and decreasing column temperatures. The presence of aqueous HNO_2 had a definite deleterious effect on the column NO_x removal. The highest were obtained when scrubbing with 15.2 wt % HNO_3 (no recycle) and with aqueous H_2O_2 or NaOH. These aqueous components tend to stabilize or destroy aqueous HNO_2 before its decomposition results in the production of gaseous NO_x species.

3. Literature Summary

The NO_x-HNO_x-H_2O System

The NO_x-HNO_x-H_2O chemical system can be described for engineering purposes by considering the important species to be NO, NO_2, N_2O_3, N_2O_4, HNO_2, HNO_3, and H_2O.

Reactions (1), (2), (3), and (5) describe the gas-phase distribution of NO_x and HNO_x species:

$$2NO_2\ (g) \leftrightarrow N_2O_4\ (g)\ ,$$

$$NO\ (g) + NO_2\ (g) \leftrightarrow N_2O_3\ (g)\ ,$$

$$NO\ (g) + NO_2\ (g) + H_2O\ (g) \leftrightarrow 2HNO_2\ (g)\ ,$$

and

$$2NO\ (g) + O_2\ (g) \rightarrow 2NO_2\ (g)\ .$$

Usually conditions that maximize the presence of gaseous N_2O_4, such as increased pressure and/or decreased temperature, will produce the maximum NO_x absorption for high gaseous NO_x partial pressures; conditions that maximize the presence of gaseous N_2O_3 and/or HNO_2 provide maximum NO_x absorption efficiency for dilute gaseous NO_x partial pressures. The nature of the gas-phase interaction of NO_2^* and H_2O is poorly understood. The thermodynamic equilibrium at ambient temperatures does not favor gaseous HNO_3 production. However, if the partial pressure of HNO_3 exceeds its equilibrium vapor pressure over aqueous solutions then a fog

or mist is formed, and the overall reaction involving the formation of liquid HNO_3 is favored at ambient conditions.

Whether NO is produced during the depletion of HNO_2 from solution or present in the feed gas, the oxidation of NO in the gas phase is an important phenomena in describing the NO_x-HNO_x-H_2O system. Gaseous NO is not stable in oxygen containing environments at ordinary scrubber temperatures and pressures. The oxidation of NO as expressed in Reaction (5) will proceed almost completely to the right, provided sufficient oxygen is present. The gaseous oxidation of NO is an unusual trimolecular reaction that has an apparent negative temperature dependency. Control of temperature in NO_x scrubbers is not only important for increasing the equilibrium partial pressure and solubility of the more reactive species, but also in promoting the conversion of NO to a more absorbable specie.

The solubilities of NO_2^*-NO* species range over several orders of magnitude. In order of increasing solubility, these species are listed as NO, NO_2, N_2O_3, N_2O_4, and HNO_2. The pressure of HNO_3 over dilute solution may be considered negligible. The importance of the solubilities of these species is somewhat over-shadowed, however, by the fast hydrolysis reactions of N_2O_3 and N_2O_4 in the liquid phase.

In the liquid phase, the following reactions appear to be important to the absorption process:

$$2NO_2\ (\ell) + H_2O\ (\ell) \rightarrow HNO_3\ (\ell) + HNO_2\ (\ell)\ , \qquad (24f)$$

$$N_2O_4\ (\ell) + H_2O\ (\ell) \rightarrow HNO_3\ (\ell) + HNO_2\ (\ell)\ , \qquad (25f)$$

and

$$N_2O_3\ (\ell) + H_2O\ (\ell) \rightarrow 2HNO_2\ (\ell)\ . \qquad (26f)$$

These reactions may be treated irreversibly due to low aqueous concentrations of HNO_2 and HNO_3. The reaction of NO_2 and water is sufficiently slow to be considered as a bulk-phase reaction; thus, the absorption is related to the transfer of NO_2 into the bulk-liquid phase. The hydrolytic reactions of N_2O_4 and N_2O_3 are sufficiently fast to take place in the liquid film. The absorption rate for the ith specie reacting in the liquid film by the film theory coupled with chemical reaction is (Danckwerts, 1970):

$$\bar{R}_i = (\sqrt{Dk}/H)_i\ P_i^*\ . \qquad (110)$$

The absorption and reaction of gaseous oxides and the absorption of gaseous acid species in the NO_x-HNO_x-H_2O system result in the production of aqueous HNO_3 and/or HNO_2. Aqueous HNO_3 is relatively stable in this system, while aqueous HNO_2 is relatively unstable. The depletion chemistry of HNO_2 in aqueous solutions has been the subject of several investigations (see Table 9). The combination of mass transfer and chemical reaction, the variation in the depletion stoichiometry, and the order of the depletion reactions have led in a great deal of confusion in this area.

The best known equation for describing the depletion of aqueous HNO_2 from aqueous solutions is Reaction (60):

$$3HNO_2\ (\ell) \leftrightarrow H^+\ (\ell) + NO_3^-\ (\ell) + H_2O\ (\ell) + 2NO\ (g)\ .$$

Table 9. Results of studies on the depletion of aqueous HNO_2 by various researchers

C_{HNO_2} (kg·mol m^{-3})	C_{HNO_3} (kg·mol m^{-3})	Temperature (K)	Pressure (atm)	Atmosphere	Reactor type	Reaction order	-R*		Other conclusions	Experimenter
0.005	~0	300	1	Open/carbonic acid	Quiescent tank	1	~0.33	Depletion rate drop	Depletion rate constant decreased by 1/3 for each 15 K drop	Montemartini
0.005	0.8-5.6	291	1	H_2	Sparged tank	1	~0.33			Montemartini
0.0003-0.003	~0	284-304	1	Inert	Quiescent tank	2	~0.33	Depletion rate	Depletion rate constant doubled for each 20 K	Yoler
0.1-0.6	~0	291	1	NO	Vibrated tank	2	~0.33	Agitation increased	Agitation increased decomposition rate	Sapozhnikova
0.02 0.08		298	1	N_2	Sparged tank		~0.33	Depletion of aqueous to rate of escape	Depletion of aqueous HNO_2 was thought to be proportional to rate of escape of NO from solution	Trautz
				N_2	Sparged tank	1-3		Order of reaction was depleted	Order of reaction decreased from 3 to 1 as aqueous HNO_2 was depleted	Liebmann
0.032		273-313	1	Air	Quiescent tank	1				Ray et al.
0.05	~0	289	1	Air	Quiescent tank	2	~0.33	Increased surface	Increased surface area increased depletion rate	Knox and Reid
0.05	0-7.25	273-323	1	Air	Vibrated tank	2	~0.33	Depletion rate	Depletion rate increased with agitation, temperature	Knox and Reid
0.05	~0	291	1	Air/CO_2	Sparged tank	2	~0.33	Depletion rate was	Depletion rate was higher for air sparge than CO_2 sparge	Knox and Reid
0.05-0.23	0.3-3.0	273-303	1	N_2	Sparged tank	1*	<0.33	Depletion rate gas velocity, decreased with	Depletion rate constant was proportional to 7/3 power of gas velocity, doubled each 15 K, increased with C_{H^+}, decreased with P_{NO}	Klemenc and Pollak
0.2-0.4		273-298	1	Paraffin	Stirred tank	1	~0.33			Taylor et al.
0.025-0.1		298	0.5, 1	NO	Vibrated tank	4	~0.33[a]	Depletion rate strength	Depletion rate constant increased linearly with ionic strength	Abel et al.
0.001-0.01	0 5	298	1	Air	Stirred tank	1	0.14-0.44	Depletion rate gas-liquid kg·mol m^{-3};	Depletion rate increased with increased agitation rate, gas-liquid interfacial area, and acidity up to 0.01 kg·mol m^{-3}; R* increased with increasing agitation	Lang and Aunis
0.1		298	1	Air	Stirred tank	1-<2	0.33-0.75	As the reactor was decreased, approached 2	As the reactor was partially closed, the depletion rate decreased, R* decreased, and the depletion order approached 2	Lang and Aunis
0.1		298		N_2	Stirred, sparged tank	1	0.27			
0.1		298		Air	Stirred, sparged tank	1	0.475	Depletion rate was for N_2 or air, the sparge rate increased R*	Depletion rate was much higher for the O_2 sparge than for N_2 or air, which were about the same; increasing the sparge rate increased the depletion rate and increased R*	Lang and Aunis
0.1		298		O_2	Stirred, sparged tank	1	0.78			
0 05	0-6	293-308	1	Air	Stirred tank	1	~0	Depletion rate	Depletion rate increased proportional to pH	Kumoro
0.01-0.1	0-2 (pH)	295-313	1	H_2	Stirred tank	1		Depletion rate stirrer speed;	Depletion rate constant increased proportion to pH and stirrer speed; for <283 K, R** = -1/2, >283 K, R** = -1/3	Sutawa et al.
0.05-0.23	0.5-4.5	273-313	1	NO	Agitated tank	2, 4	~0.33			Usabillaga
0.2	0.2	298	1	Inert/NO	Agitated tank			R* increased from cover gas	R* increased from -1/3 to 0 as NO was admitted to the cover gas	Sofin et al.
0.004-0.0004		273-295	1	N_2	Quiescent tank	1	>0	Depletion rate area and ionic	Depletion rate proportional to gas-liquid interfacial area and ionic strength	Kobayashi et al.
0.004-0.0004		273-295	1	N_2	Vibrated tank	1-4/3	>0	The depletion agitation rate	The depletion proportional to ionic strength and agitation rate	Kobayashi et al.
0.005		298	50	O_2	Stirred tank	1	~1			Pogrebnaya
0.004-0.2		288, 298	1	He	Stirred tank	1-4/3	0.136-0.349	R* increased with increased with approached one	R* increased with increasing a[b]; depletion rate increased with increasing agitation; depletion order approached one as agitation rate increased	Komiyama and Inoue
0.005-0.05		288, 298	1	He	Sparged tank	4/3	0.33	Depletion rate and was proportio	Depletion rate increased with increasing sparge rate and was proportional to $(k_La)^{2/3}$	Komiyama and Inoue

[a] Order of depletion mechanism was between first and third at low gas rates; definitely approached first for high gas rates.

[b] $a = (1/k_La)/[(1/k_La) + V_L/G]$.

Sources:

1. C. Montemartini, *Rendiconti IV* (6): 263 (1890).
2. C. Montemartini, *Rendiconti V* (1): 63 (1892).
3. V. H. Yoler, *Proc. Roy. Soc.* 52: 27 (1892).
4. A. V. Sapozhnikova, *Russ. J. Phy. Chem.* 32: 375 (1900).
5. M. Trautz, *Z. Physik. Chem.* 42: 513 (1904).
6. H. Leibmann, Dissertation, University of Dresden, Germany (1914).
7. P. C. Ray, M. L. Dey, and J. C. Ghosh, *J. Chem. Soc.* 3, 411 (1917).
8. J. Knox and D. M. Reid, *J. Chem. Soc.* 38 (9). 1057 (1919).
9. A. Klemenc and P. Pollak, *Z. Physik. Chem.* 101, 150 (1922).
10. T. W. J. Taylor, E. W. Wignall, and J. F. Cowley, *J. Chem. Soc.* 1923 (1927).
11. E. Abel and H. Schald, *Z. Physik. Chem.* 132: 55-64, 64-67 (1928); 134: 249 (1928); E. Abel, H. Schald, and E. Roemer, *Z. Physik. Chem.* 148: 337 (1930).
12. F. H. Lang and G. Aunis, *Bull. Soc. Chem. France* 18(15): 155 (1951).
13. F. H. Lang and G. Aunis, *Bull. Soc. Chem. France* 18(5): 398 (1951).
14. Y. Komuro, *Nippon Kagaku Zasshi*, *Kagaku Zasshi, Tokyo* 74: 47 (1953).
15. T. Sutawa, M. Hondo, O. Hanabe, Hondo, O. Hanabe, and H. Hinokiyama, *Kogyo Kagaku Zasshi* 58(10): 744 (1955).
16. A. Usabillaga, Dissertation, Dissertation, University of Illinois (1962).
17. B. S. Sofin, A. E. Nokhotkin, Nokhotkin, and A. Galeev, *Sb. Aspir. Rab. Kazan. Khim. Tekhnol. Inst. Khim. Kinet.* 1: 166 (1970). (1970).
18. H. Kobayashi, H. Takezawa, Takezawa, K. Hara, T. Hikka, and K. Kitano, *Nippon Kagakkai-shi*, 381 (1976).
19. V. L. Pogrebnaya, A. P. Usov, A. P. Usov, and A. V. Baranov, *J. Appl. Chem. of the USSR* 49(4): 757 (1976).
20. H. Komiyama and H. Inoue, H. Inoue, *J. of Chem. Eng. Japan* 11(1): 25 (1978).

This overall equation was developed by Abel and Schmid (1928a). Working in an NO atmosphere, in a completely batch system and under conditions of extremely high liquid-phase mass-transfer, this decomposition process is fourth order with respect to aqueous HNO_2 (Abel and Schmid, 1928b), Equation (62):

$$r_{HNO_2} = -k_{60} \frac{C^4_{HNO_2}}{P^2_{NO}} .$$

Abel and Schmid (1928b) recognized that the removal of NO from solution could limit the dissociation of aqueous HNO_2; these studies were conducted at conditions which reduced the mass-transfer resistances to the removal of NO from solution. Because of the equilibrium nature of the Abel-Schmid depletion process, as implied in Equation (62), the rate controlling process can shift to the removal of NO from solution,

$$r_{HNO_2} = - (3/2)\ k_L a\ (C_{NO} - C^*_{NO}) , \qquad (111)$$

under mass-transfer limiting conditions. A simplified rate expression based on the work of Abel and Schmid has been obtained by Andrews and Hanson (1961) and later by Komiyama and Inoue (1978) for use when the concentration of NO at the liquid side of the gas-liquid interface was zero, Equation (95):

$$r_{HNO_2} = - (3/2)^{1/6}\ (k_{25f}\ K^2_{88}\ K^2_{89})^{1/3}\ (k_L a)^{2/3}\ C^{4/3}_{HNO_2} .$$

This equation represents the depletion of aqueous HNO_2 under liquid-phase mass-transfer controlling conditions. By working with the

Abel-Schmid kinetics, it has been shown that the order of the aqueous HNO_2 depletion reaction can vary from slightly greater than one to four. The Abel-Schmid stoichiometry also stipulates that the molar ratio of HNO_3 and NO produced to HNO_2 decomposed to be -1/3 and -2/3 respectively. For convenience, these molar ratios have been referred to as R* and R** respectively. This stoichiometry is in general agreement with that found by most researchers in HNO_2 depletion chemistry.

Some researchers, however, have found R* to be greater than -1/3 (R** > -2/3) in studies into the non-oxidixing depletion of aqueous HNO_2. The order (with respect to HNO_2) of the HNO_2 depletion reaction is usually equal to or slightly greater than one for studies when R* is greater than -1/3. The value of R*, found by Komiyama and Inoue (1978), was about -1/3 in studies with a He sparged semi-batch contactor; the corresponding depletion order, with respect to HNO_2, in these studies was about 4/3. In further studies, with an agitated semi-batch gas-liquid contactor featuring a planear interface, R* increased with α, defined as

$$\alpha = (1/k_L a)/[(1/k_G a) + (V_L/G)] \ ;$$

in these studies the order of the depletion reaction approached unity, with respect to HNO_2, as α increased. This increase in R* was also noted by Lang and Aunis (1951a,b) in aqueous HNO_2 depletion studies, as the N_2 rate to a sparged gas-liquid contactor was increased; the depletion order in these studies was about one. The value of R* is also reported by Safin et al. (1970) to increase from -1/3 to 0 as the NO content was increased in the N_2 sparge gas of an aqueous HNO_2 mixture. The order

of the reaction was reported by Liebmann (1914) to decrease from 3 to 1 as aqueous HNO_2 was removed in a N_2 sparged device. Generally, these depletion rates increase with gas sparge rate, agitation, etc.

The increasing value of R* suggests that species other than NO can be desorbed during the depletion of HNO_2 from aqueous solutions. The first-order depletion kinetics and its sensitivity to gas rates and agitation suggest that mass-transfer resistances are involved in this process. The aqueous HNO_2 depletion process might be represented, with respect to the indicated considerations, as

$$r_{HNO_2} = -k_L a \, (C_{N_2O_3} - C^*_{N_2O_3}) = -k_G a \, (P^*_{N_2O_3} - P_{N_2O_3}) \, , \qquad (112)$$

and

$$\bar{R}^a_{HNO_2} = -k_L a \, (C_{HNO_2} - C^*_{HNO_2}) = -k_G a \, (P^*_{HNO_2} - P_{HNO_2}) \, . \qquad (113)$$

The stoichiometry of Equations (112) and (113) produce R* and R** of -1/2 and 0 respectively. This is the other stoichiometric boundary for the non-oxidizing depletion of aqueous HNO_2.

The effect of oxygen on the depletion of aqueous HNO_2 was studied by Lang and Aunis (1951b). The value of R* in these studies decreased with increasing partial pressures of O_2 in the sparge gas of a sparged and stirred gas-liquid semi-batch contactor. The first-order HNO_2 depletion rate constant was changed very little when N_2 or air was used as the sparge gas; however, this rate constant was greatly increased when pure O_2 was used as the sparge gas. The high pressure oxidation of HNO_2 in the liquid phase in a stirred and sparged gas-liquid contactor has also been reported by Pogrebnaya et al. (1976). From the studies of

Lang and Aunis (1951b), liquid-phase oxidation of HNO_2 is not substantial at ambient conditions when the partial pressure of O_2 is that of air.

The Design of NO_x Scrubbers

The existing concepts for NO_x scrubber design were developed primarily for the nitric acid production industry. There has been renewed interest in this area in recent years, stimulated by the need to remove NO_x from gas streams as a pollution abatement and a resource recovery measure. The absorbers used by the nitric acid production industry are fairly well tuned devices, having evolved through several generations of use. However, because of a lack of theoretical understanding of the mechanisms involved in nitric acid production, there is little basis for extrapolation to situations involving different NO_x partial pressures and nitric acid concentrations.

Some experimental studies have been reported over the last 25 years that provide insight into the mechanisms involved in the scrubbing of nitrogen oxides from gas streams. This work has been primarily directed toward the development of plate columns. From an analysis of these studies, it appears that some characteristics of packed columns would make these devices very efficient NO_x scrubbers. A conceptual model of NO_x scrubbing in packed towers, based on the chemistry of the NO_x-HNO_x-H_2O system and on an analysis of scrubber studies conducted with plate columns, was tested in this activity. The development of this model is important not only for the advancement of scientific understanding of the phenomena involved in the aqueous scrubbing of gaseous nitrogen oxides, but also to serve as a reasonable basis for scrubber performance

extrapolation and to provide a credible response function for varied NO_x scrubbing situations.

The NO_x scrubbing models of Andrews and Hanson (1961) and Hoftyzer and Kwanten (1972) assume steady-state with respect to the aqueous HNO_2 concentration — HNO_2 disappears as fast as it is produced. Recent studies by Makhotkin and Shamsutdinov (1976), Counce and Perona (1979a), and Koegler (1979), as well as some observations by Andrews and Hanson and Koval and Peters (1960), have shown that aqueous HNO_3 scrubber solutions have a steady-state capacity for retaining considerable concentrations of HNO_2. The overall stoichiometry of some sparged semi-batch NO_2 absorption studies by Makhotkin and Shamsutdinov were found to be Reaction (27f),

$$3NO_2\ (g) + H_2O\ (\ell) \rightarrow 2HNO_3\ (\ell) + NO\ (g)\ ,$$

only when a steady-state concentration of aqueous HNO_2 was present. During the period of time before steady-state was reached, the molar ratio of production of gaseous NO to NO_2 absorbed is less than 1:3 expected from Equation (27f). In multi-stage NO_x scrubbing studies with a recirculating liquid phase, Counce and Perona, as well as Koegler, have noticed a similar effect. Counce and Perona (1980) have also developed a simple mechanistic model for NO_x removal that takes into account the effect of HNO_2 on the overall scrubbing process, and fitted their data fairly closely during this transient before steady-state and at-steady-state. From these studies, it can be seen that the build-up of aqueous HNO_2 coincides with a loss in NO_x scrubbing efficiency. This can be attributed to a loss in the liquid capitance to retain NO in the

liquid phase as HNO_2. This phenomena was also noted by Andrews and Hanson, who considered only the steady-state NO_x absorption performance of their system. This type of steady-state analysis is probably correct for plate gas-liquid contactors with long liquid hold-up times; however, it is probably incorrect to apply this to a conceptual understanding of packed NO_x absorbers due to the limited liquid hold-up time of these devices.

The scrubbing of NO_x compounds in packed towers with non-recycle of the scrubber liquid will almost certainly be in the transition region, with respect to aqueous HNO_2, for a portion, if not all of the tower. This hypothesis is based on the observed capacity of aqueous HNO_3 for retaining HNO_2 and the limited liquid hold-up time in packed towers. It seems logical to describe the NO_x absorption mechanisms of the liquid phase as well as the gas phase in dynamic terms. The overall column performance will then be a function of total system dynamics, without the restriction of assumed stoichiometric constraints.

Packed Column Model

A model for describing mass-transfer and chemical-reaction phenomena is given in Figure 12. The model allows for calculations in the bulk-gas phase, within the gas film, at the gas-liquid interface, within the liquid film, and the bulk-liquid phase. The gas phase is assumed to be saturated with H_2O, consistent with the temperature and liquid HNO_3 concentration. The partial pressure of HNO_3 is usually small over solutions of low acid molarity compared with the NO_x partial pressures in these experiments and is taken to be zero. The indicated gaseous

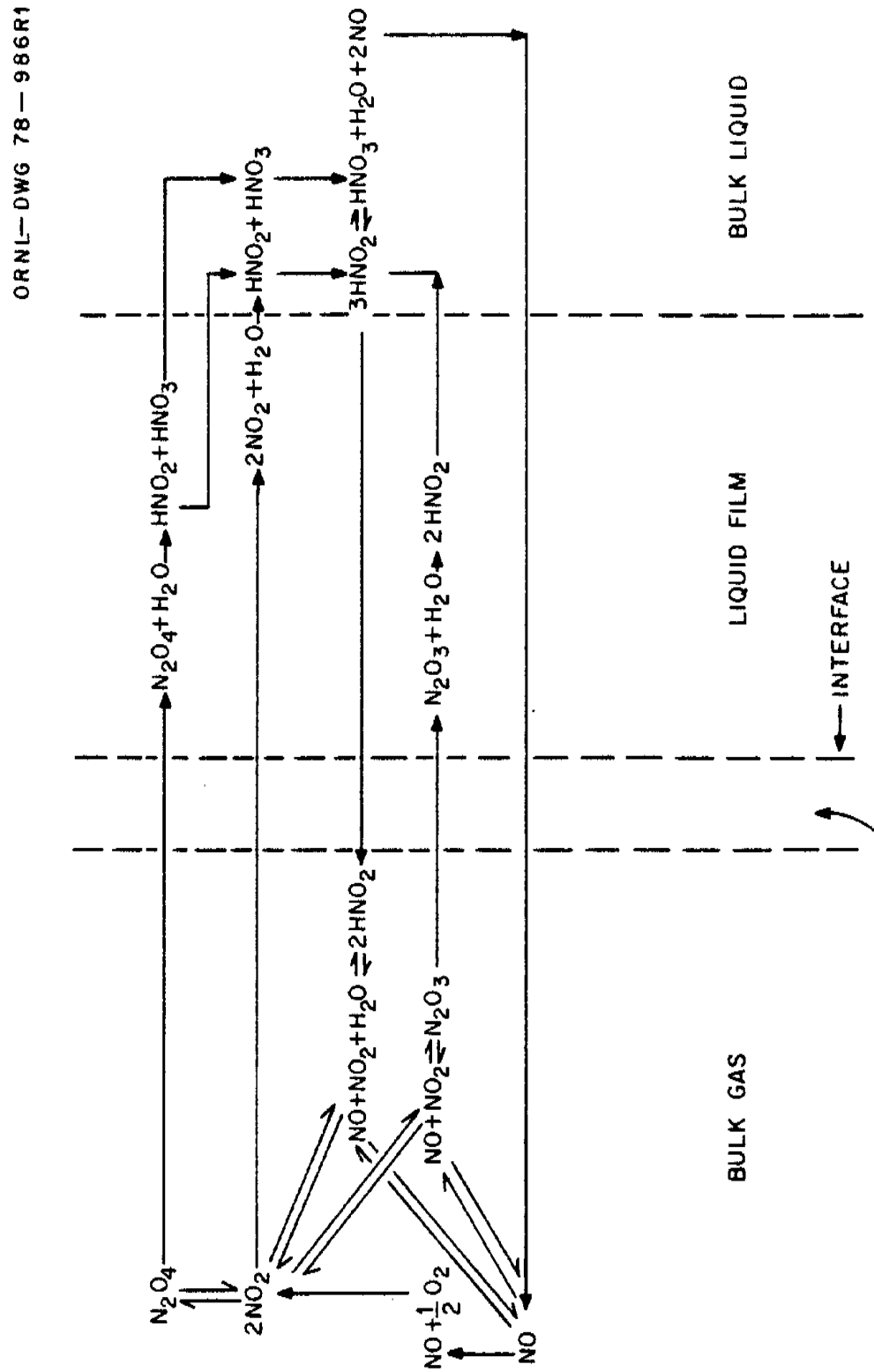

Figure 12. Model for describing mass-transfer and chemical-reaction phenomena.

chemical equilibria are assumed to apply at all times in the bulk-gas phase. The predicted HNO_2 partial pressure is usually small compared with the H_2O partial pressure and is always assumed to be equal to or below the saturation partial pressure. The model accommodates the oxidation of gaseous NO to NO_2 in the bulk-gas phase.

The steady-state transport of each absorbing component, j, across both the gas and liquid films is expressed by (Danckwerts, 1973):

$$\bar{R}_j = -k_G (P_j^* - P_j) = (Ek_L)_j (C_j^* - C_j) \quad . \tag{114}$$

In the case of physical absorption or desorption, the enhancement factor, E, is taken to be unity. The absorbing species are NO_2, N_2O_4, and N_2O_3. From the work of Corriveau (1971), Denbigh and Prince (1947), Koval and Peters (1960), and Peters and Koval (1959), it may be concluded that HNO_2 is not an absorbing specie, although it cannot be ruled out as a desorbing specie. The other desorption specie is NO, which is formed from the bulk liquid-phase decomposition of HNO_2. The resistances involved in the transfer of these absorption/desorption species will be modeled in an attempt to simulate this operation. A material balance on the indicated transport phenomena is possible due to accounting for the production and disappearance of HNO_2 and HNO_3 due to the absorbing and desorbing reactions and mass-transfer operations.

CHAPTER III

THEORETICAL

1. General Development

The absorption/desorption phenomena involved in the scrubbing of nitrogen oxides from gas streams have been simulated for an incremental column volume. This incremental volume is illustrated in Figure 13. The volume of this incremental section is such that the change in component partial pressures and concentrations, as well as gas and liquid flow rates in the increment may be neglected in rate equations for interphase transport. The gas phase is assumed to be ideal, and isothermal conditions are further assumed to prevail. The mathematical model developed in this chapter is designed to be used in the computation of the partial pressures of gas species leaving the increment and concentrations of liquid species entering the increment. This requires known or assumed information about the gas and liquid streams entering and leaving the increment respectively. A schematic absorption model for this calculation was previously presented in Figure 12. The mathematical model developed here is based on mass-transfer data for packed towers and specific chemical reaction information for the NO_x-HNO_x-H_2O system.

The nitrogen oxide species of interest in the gas-phase are NO, NO_2, N_2O_3, N_2O_4, and HNO_2. The partial pressure of "chemical" nitric oxide (NO^*) and nitrogen dioxide (NO_2^*) are defined, consistent with previous usage, as:

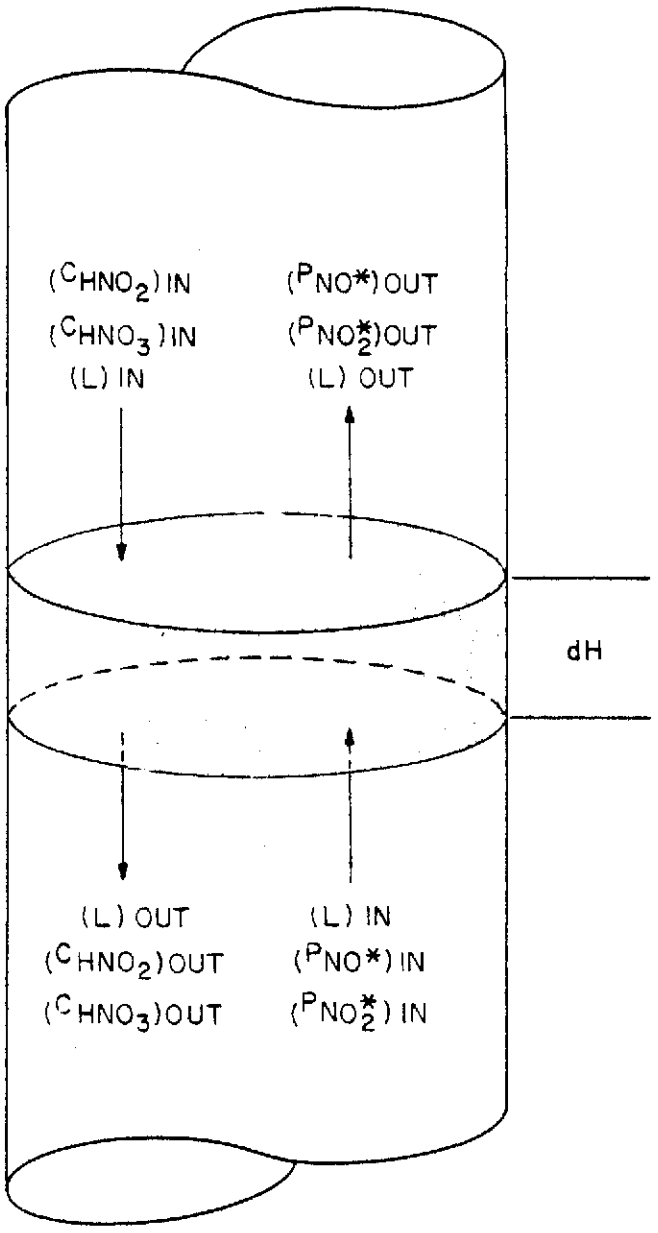

Figure 13. Representation of incremental volume in a packed tower.

$$P_{NO_2^*} = P_{NO_2} + 2P_{N_2O_4} + P_{N_2O_3} + 1/2P_{HNO_2} , \quad (115)$$

and

$$P_{NO^*} = P_{NO} + P_{N_2O_3} + 1/2P_{HNO_2} . \quad (116)$$

The bulk-gas-phase component partial pressures of these species are calculated using existing equilibrium information as:

$$P_{N_2O_4} = K_1 P_{NO_2}^2 , \quad (117)$$

$$P_{N_2O_3} = K_2 P_{NO} P_{NO_2} , \quad (118)$$

and

$$P_{HNO_2} = (K_3 P_{H_2O} P_{NO_2})^{1/2} . \quad (119)$$

These gas-phase equilibrium expressions are assumed to apply throughout the gas phase. The water vapor partial pressure is obtained by assuming the gas phase to be saturated. The component partial pressures are calculated from known partial pressures of NO_2^* and NO*. The derivation of equations used in this computation is given in Appendix A.

The steady-state gas-phase performance equation for the incremental absorption/desorption phenomena of NO_2^* and NO* may be expressed as

$$\text{input} = \text{output} \pm \begin{array}{l}\text{disappearance or} \\ \text{appearance due to} \\ \text{gas-phase reaction}\end{array} \pm \begin{array}{l}\text{disappearance or} \\ \text{appearance due to} \\ \text{absorption or desorption}\end{array} . \quad (120)$$

In the previous equation, the disappearance terms are positive while the appearance terms are negative. The molar input of the ith specie to

the column increment may be represented as $G\ (P_i)_{in}/(RT)$ while the output is $G\ (P_i)_{out}/(RT)$.

The extent of the gas-phase oxidation of NO to NO_2 occurring in the increment, X_{NO}, is computed and used to adjust the molar rates of NO and NO_2 leaving the increment as $\pm\ G\ P_{NO}\ X_{NO}/(RT)$. The term X_{NO} is the conversion of NO to NO_2. The molar rate of O_2 leaving the increment is also corrected. The derivation of the equation used in the calculation of X_{NO} is given in Appendix B.

The disappearance and/or appearance phenomena of NO_2^* and NO* in the gas-phase due to absorption and desorption may be simplified by defining an absorption flux for each gaseous nitrogen oxide component in terms of gas-phase and enhanced liquid-phase mass-transfer coefficients and the partial pressure and concentration driving forces, Equation (114):

$$\overline{R}_i = k_{G,i}\ (P_i - P_i^*) = (Ek_L)_i(C_i^* - C_i)\ .$$

Thus desorption is inverse absorption. The desorbing species are HNO_2 and NO. The reaction producing NO is considered to be sufficiently slow as not to effect the concentration profile in the liquid phase; thus, the enhancement factor, E, is equal to one for both of these cases. The molar rate of disappearance or appearance of NO_2^* and NO* in the incremental gas-phase is obtained as a $\overline{R}_{NO_2^*}\ a\Delta V$ and $\overline{R}_{NO^*}\ a\Delta V$. The term ΔV is the incremental column volume. The fluxes of NO_2^* and NO* are found as

$$\overline{R}_{NO_2^*} = \overline{R}_{NO_2} + 2\overline{R}_{N_2O_4} + \overline{R}_{N_2O_3} + 1/2\overline{R}_{HNO_2}\ , \qquad (121)$$

and

$$\overline{R}_{NO^*} = \overline{R}_{N_2O_3} + 1/2\overline{R}_{HNO_2} + \overline{R}_{NO} \ , \tag{122}$$

noting that the flux of HNO_2 will be restricted to desorptive only.

The total flux of nitrogen oxides is:

$$\overline{R}_{NO_x} = \overline{R}_{NO_2^*} + \overline{R}_{NO^*} \ . \tag{123}$$

Insertion of the developed relationships into the gas-phase performance equation yields:

$$\frac{G(P_{NO_2^*})_{in}}{RT} = \frac{G(P_{NO_2^*})_{out}}{RT} + (\overline{R}_{NO_2} + 2\overline{R}_{N_2O_4} + \overline{R}_{N_2O_3} + 1/2\overline{R}_{HNO_2}) \ a\Delta V$$

$$- \frac{G \ P_{NO} \ X_{NO}}{RT} \ , \tag{124}$$

and

$$\frac{G(P_{NO^*})_{in}}{RT} = \frac{G(P_{NO^*})_{out}}{RT} + (\overline{R}_{N_2O_3} + 1/2\overline{R}_{HNO_2} + \overline{R}_{NO}) \ a\Delta V$$

$$+ \frac{G \ P_{NO} \ X_{NO}}{RT} \ . \tag{125}$$

The partial pressures of NO_2^* and NO^* leaving the increment are

$$(P_{NO_2^*})_{out} = (P_{NO_2^*})_{in} - (\overline{R}_{NO_2} + 2\overline{R}_{N_2O_4} + \overline{R}_{N_2O_3} + 1/2\overline{R}_{HNO_2}) \ (a\Delta VRT/G)$$

$$+ P_{NO} \ X_{NO} \ , \tag{126}$$

and

$$(P_{NO^*})_{out} = (P_{NO^*})_{in} - (\overline{R}_{N_2O_3} + 1/2\overline{R}_{HNO_2} + \overline{R}_{NO})\ (a\Delta V\ RT/G) - P_{NO}\ X_{NO}\ ; \tag{127}$$

in terms of total nitrogen oxide partial pressure,

$$(P_{NO_x})_{out} = (P_{NO_2^*})_{out} + (P_{NO^*})_{out}\ . \tag{128}$$

Further adjustments of the gas flow rate and component partial pressures due to bulk-gas component removal or addition are made before beginning the next incremental calculation.

Focusing on the liquid phase of the incremental column volume, the absorption reactions produce aqueous nitric and nitrous acids. Nitric acid is relatively stable in the liquid phase and has a fairly low vapor pressure at ambient conditions. Aqueous nitrous acid is unstable at ambient conditions and has a substantial vapor pressure. An overall steady-state performance equation for the liquid phase of the incremental absorption/desorption/reaction phenomena with respect to aqueous HNO_2 and HNO_3 may be expressed as:

$$\begin{array}{l}\text{input of} \\ HNO_3\end{array} = \begin{array}{l}\text{output of} \\ HNO_3\end{array} - \begin{array}{l}\text{production from} \\ \text{reactions of} \\ \text{absorbing } NO_x \\ \text{components}\end{array} - \begin{array}{l}\text{production from} \\ \text{liquid phase} \\ \text{decomposition} \\ \text{of } HNO_2\ ,\end{array} \tag{129}$$

and

$$\begin{array}{l}\text{input of} \\ HNO_2\end{array} = \begin{array}{l}\text{output of} \\ HNO_2\end{array} - \begin{array}{l}\text{appearance as product} \\ \text{from reactions of} \\ \text{absorbing } NO_x \\ \text{components}\end{array} + \begin{array}{l}\text{decomposition} \\ \text{of } HNO_2 \text{ in} \\ \text{liquid phase and} \\ \text{physical desorption} \\ \text{of } HNO_2\ .\end{array} \tag{130}$$

The molar inputs of nitric and nitrous acids are $L(C_{HNO_3})_{in}$ and $L(C_{HNO_2})_{in}$ while the outputs are $L(C_{HNO_3})_{out}$ and $L(C_{HNO_2})_{out}$.

The rate of acid production in the liquid phase (also possible removal in the case of nitrous acid) due to the absorption flux of NO_x species from the gas phase is $\sum_{i=1}^{n} \psi_i \overline{R}_i a\Delta V$. The term, ψ_i, is a stoichometric factor. These production rates for nitric acid and nitrous acid are

$$\sum_{i=1}^{n} \psi_i \overline{R}_{HNO_3} a\Delta V = (1/2\overline{R}_{NO_2} + \overline{R}_{N_2O_4})\ a\Delta V\ , \tag{131}$$

and

$$\sum_{i=1}^{n} \psi_i \overline{R}_{HNO_2} a\Delta V = (1/2\overline{R}_{NO_2} + \overline{R}_{N_2O_4} + 2\overline{R}_{N_2O_3} + \overline{R}_{HNO_2})\ a\Delta V\ . \tag{132}$$

The equilibrium as expressed in Equation (28),

$$3HNO_2\ (\ell) \leftrightarrow HNO_3\ (\ell) + H_2O\ (\ell) + 2NO\ (\ell)\ ,$$

is assumed to apply in the liquid phase from the work of Abel and Schmid (1929). This equilibrium reaction proceeds to the right as NO desorbs from the aqueous phase. The absorption of NO is neglected due to its low solubility. The bulk-phase concentration of NO is calculated from a modified Abel-Schmid equilibrium expression,

$$C_{NO} = \frac{P_{NO}}{H_{NO}} = \frac{1}{H_{NO}} \left(\frac{a^3_{HNO_2}}{K_{60} a_{H^+}\ a_{NO_3^-}} \right)^{1/2}\ , \tag{133}$$

or

$$C_{NO} = \left(\frac{a^3_{HNO_2}}{H^2_{NO}\ K_{60}\ a_{H^+}\ a_{NO_3^-}} \right)^{1/2} . \qquad (134)$$

Thus, the production of nitric acid in the increment due to the decomposition may be represented by $1/2k_{L,NO}(C_{NO} - C^*_{NO})$ and the disappearance of nitrous acid by $-3/2k_{L,NO}(C_{NO} - C^*_{NO})$. Incorporating these relationships into the liquid-phase performance equation yields:

$$L(C_{HNO_3})_{in} = L(C_{HNO_3})_{out} - (1/2\overline{R}_{NO_2} + \overline{R}_{N_2O_4})\ a\Delta V + 1/2\overline{R}_{NO}\ a\Delta V \qquad (135)$$

$$L(C_{HNO_2})_{in} = L(C_{HNO_2})_{out} - (1/2\overline{R}_{NO} + \overline{R}_{N_2O_4} + 2\overline{R}_{N_2O_3} + \overline{R}_{HNO_2})\ a\Delta V - 3/2\overline{R}_{NO}\ a\Delta V , \qquad (136)$$

or

$$(C_{HNO_3})_{in} = (C_{HNO_3})_{out} - (1/2\overline{R}_{NO_2} + \overline{R}_{N_2O_4} - 1/2\overline{R}_{NO})(a\Delta V/L) , \qquad (137)$$

and

$$(C_{HNO_2})_{in} = (C_{HNO_2})_{out} - (1/2\overline{R}_{NO_2} + \overline{R}_{N_2O_4} + 2\overline{R}_{N_2O_3} + \overline{R}_{HNO_2} + 3/2\overline{R}_{NO})(a\Delta V/L) . \qquad (138)$$

By knowing or assuming $(P_{NO_2^*})_{in}$, $(P_{NO^*})_{in}$, $(C_{HNO_2})_{out}$, and $(C_{HNO_3})_{out}$, similar quantities may be calculated at the top of the increment provided $\overline{R}_i$, in the liquid phase, may be calculated for the individual NO_x species. The calculation of these individual flux equations is derived

in Appendix C. The desorptive flux of NO was shown by Komiyama and Inoue (1978) to be limited by the decomposition reaction of HNO_2 occurring in the bulk liquid; thus, Equation (95) was used, in an appropriately modified fashion, as an upper bound to the desorption of NO. This is further discussed in Appendix E.

2. Implementation

A computer program, shown in Appendix G, was developed to calculate the entering concentrations of HNO_2 and HNO_3 and effluent partial pressures of NO_2^* and NO* for given liquid and gas streams, column incremental volume, effluent concentrations of HNO_2 and HNO_3, and entering partial pressures of NO_2^* and NO*. Such a differential increment of packing was shown in Figure 13 (see page 102). By using multiple increments, the NO_x removal performance of a packed tower of any finite height can be modeled. An incremental height of 1 cm was determined to be adequate for use in these calculations. The use of smaller increments yielded minimal changes in the overall column NO_x conversion, and these changes were well within the error associated with scatter in the data.

Some further adjustment of the volumetric gas flow rates and component partial pressures is necessitated in the described computations due to removal of gaseous species in bulk quantities. These adjustments are accomplished between the described incremental computations.

CHAPTER IV

EXPERIMENTAL APPARATUS AND PROCEDURE

A flowsheet of the experimental system is presented in Figure 14. Two packed absorption/desorption columns were used in this study with inside diameters of 0.076 and 0.102 m respectively. These columns were packed with ceramic Intalox saddles with diameters of 6 and 13 mm respectively. Other equipment used in the study was associated with the scrubber liquid supply, metering, and sampling systems, and the gaseous supply, metering, and sampling systems.

The scrubber liquid was supplied from the liquid supply tank on a continuous basis or batch or recycle mode. This stream was metered by rotameter to the column in use. The temperature of this stream could be adjusted as necessary by an in-line heat exchanger. The liquid is distributed in the tower approximately 0.03 m above the top of the packing.

In the 0.076-m-diam column, the gas enters the packing through the packing support; the gas is injected directly into the bottom of the packing in the 0.102-m-diam column. A liquid seal in the effluent liquid line is maintained either manually or by a jack-leg in the case of the liquid-recycle mode. Both feed and effluent liquid streams with respect to the packed columns could be manually sampled.

Carrier gases of air, N_2 or O_2, could be metered by rotameter to either of the two packed towers and as a sparge gas to the liquid supply tank. Normally, NO_2^* or NO^*/NO_2^* feed mixtures were produced by blending in the correct portion of these gases. Steam may also be added to this

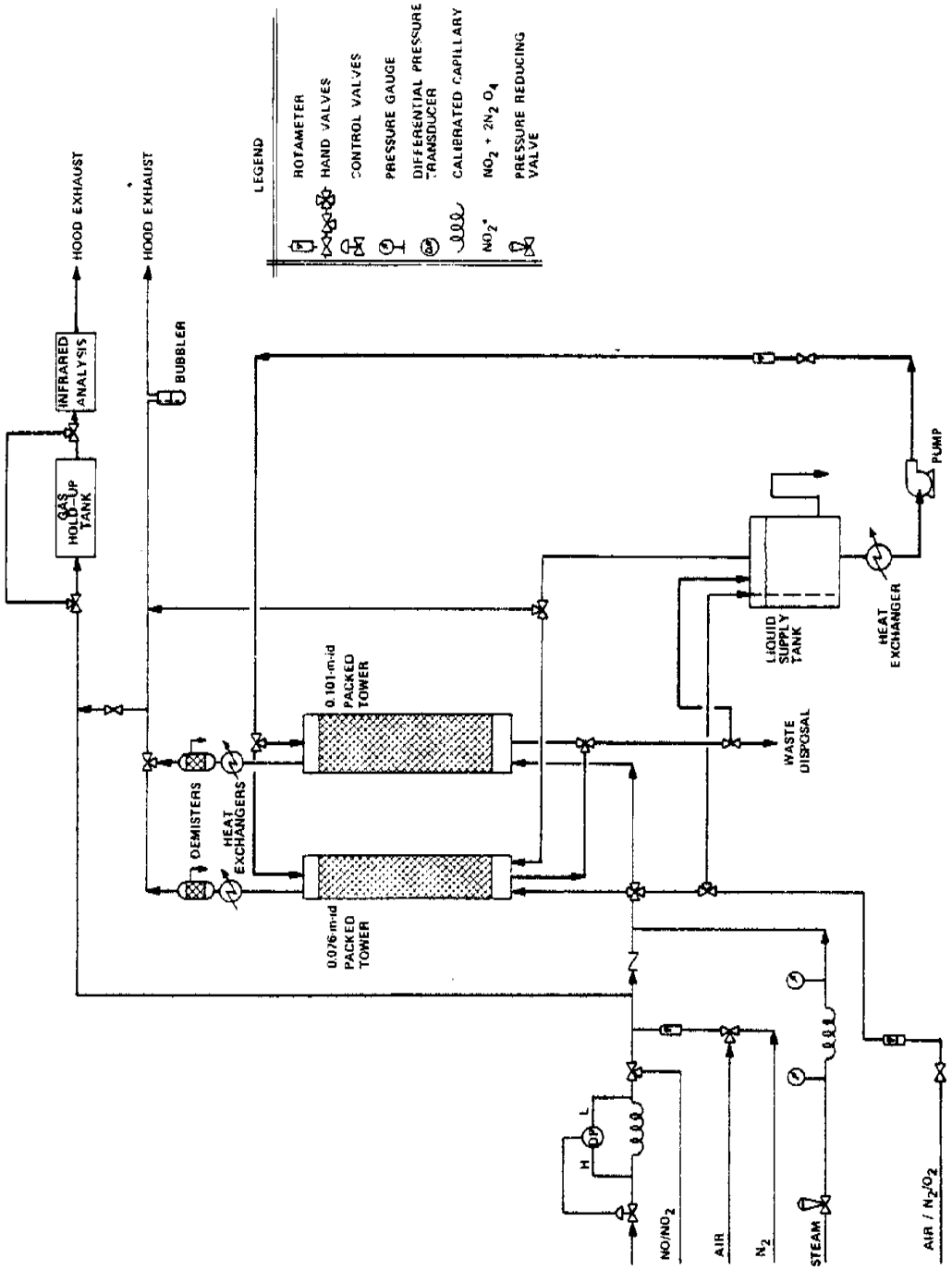

Figure 14. Flowsheet of experimental system.

feed gas. The gas stream leaving the packed tower was cooled and demisted for entrained acid recovery and control of the water content. The volume of this recovered liquid was recorded and the acid content determined analytically. A nitric acid bubble column on the effluent gas stream provided the pressure necessary to route a stream through the gas analysis equipment. Thus, the scrubber column was operated slightly above atmospheric pressure.

The gas analysis for NO^*/NO_2^* could be done by taking gas samples for standard wet chemical analysis or by passing a gas stream through infrared detectors for NO^* and NO_2^* analyses. Liquid samples were stabilized immediately with the addition of hydrogen peroxide and cerric sulfate for later analysis of total acid and nitrous acid respectively. The entire experiment was located in a chemical fume hood in which a constant air flow was maintained.

CHAPTER V

RESULTS

The final evaluation of a model lies in the comparison of the model with the experimental data. This discussion will consider the data and trends in that data, and will also focus the comparison of the model predicted NO_x conversion and that obtained experimentally. After considering a scouting series of nitrogen oxide scrubbing tests conducted in the 0.076-m-ID column, this discussion will consider the data and model predictions from the 0.102-m-ID column, which is considered the most reliable, then return to the data from the 0.076-m-ID column data for conclusion.

A screening series of tests was initially conducted to get a broad understanding of nitrogen oxide absorption in packed towers. The response variable is the conversion of NO_x, X_{NO_x}. This series of tests is presented in Table 10. These data are quite qualitative in nature. The effect of variable i on the NO_x conversion is defined by:

$$\text{Effect of variable i} = \frac{\Sigma[(X_{NO_x} \text{ at high values of i}) - (X_{NO_x} \text{ at low values of i})]}{(\text{half the number of factorial runs})} . \tag{139}$$

The most pronounced effect on the NO_x conversion is produced by variation in the oxidation state of the gas. This is a well known phenomena in nitrogen oxide scrubbing; in general, the NO* species have a much lower solubility and reactivity than the NO_2^* species. The second largest effect was produced by the variation in the partial pressure of nitrogen

Table 10. Data for saturated fractional factorial design for studying seven NO_x scrubbing variables in eight runs

Variables		-(Low)	+(High)
1.	Scrubber liquid flow rate, $m^3\ s^{-1}$	3.5×10^{-5}	5.25×10^{-5}
2.	Scrubber liquid HNO_3 molarity, $kg \cdot mol\ m^{-3}$	0	3.0
3.	Partial pressure of NO_x in feed gas	0.05	0.20
4.	Steam flow rate in feed gas, $kg\ s^{-1}$	0	5.0×10^{-4}
5.	Air or nitrogen as diluent gas	Nitrogen	Air
6.	Scrubber liquid temperature, K	286	306
7.	Oxidation state of NO_x in feed gas	0.5	1.0

	Variable							Overall NO_x conversion
Run	1	2	3	4	5	6	7	X_{NO_x}
A	-	-	-	-	+	-	-	69
B	+	-	-	+	-	-	+	86
C	-	+	-	+	+	+	+	91
D	+	+	-	-	-	+	-	52
E	-	-	+	-	-	+	+	90
F	+	-	+	+	+	+	-	78
G	-	+	+	+	-	-	-	82
H	+	+	+	-	+	-	+	96
Effect	-4.9	-0.6	11.8	7.6	6.4	-5.6	20.6	80

oxides in the feed gas; this variation appears to be explainable by an increase in the driving forces for the absorption phenomena causing increased absorption, also, the higher nitrogen oxide partial pressure should produce a larger proportional amount of the higher molecular weight species which are more absorbable and reactive. The increase in removal efficiency with the addition of steam to the feed gas was previously noted by Counce and Perona (1979a). The increase in removal efficiency with air instead of nitrogen can be attributed to the oxidation of NO* species to the NO_2^* state which increases the solubility and reactivity of these species. The decrease in removal efficiency with increased temperature can be credited to the decrease in higher molecular weight species, such as N_2O_4 and N_2O_3, due to the nature of the gas-phase equilibrium reactions. The decrease in scrubber efficiency with increased gas rate may be attributed to the loss of residence time in the column. The liquid rate apparently had little effect in these studies; this probably indicates some overriding second-order effects because the gas-liquid interfacial area and liquid-phase mass-transfer coefficient are known to increase with liquid rate. These studies provided a qualitative description of nitrogen oxide scrubbing in packed towers. This understanding was useful in deciding the level of complexity required in a mathematical explanation of this operation.

A series of experiments using the 0.102-m-diam tower packed with 13-mm Intalox saddles provides the basis for the model development. These data are presented in Table II. These experiments were conducted in a manner designed to minimize entrance effects as the gas is injected directly into the bottom of the packing. In other studies using the

Table 11. Data from the studies with the 0.102-m-diam column packed with 13-mm Intalox saddles

Run	Column packing height (m)	Column pressure (atm)	Gas phase conditions: Inlet: Total gas flow rate (std $m^3 s^{-1} \times 10^3$)	Gas phase conditions: Inlet: Mole fraction of NO_2^*	Gas phase conditions: Inlet: Mole fraction of NO^*	Gas phase conditions: Inlet: Temperature (K)	Gas phase conditions: Outlet: Mole fraction of NO_x^*	Gas phase conditions: Outlet: Temperature (K)	Liquid phase conditions: Inlet: Temperature (K)	Liquid phase conditions: Inlet: Flow rate ($m^3 s^{-1} \times 10^5$)	Liquid phase conditions: Inlet: Temperature (K)	Liquid phase conditions: Outlet: C_{HNO_2} ($kg \cdot mol\ m^{-3}$)	Liquid phase conditions: Outlet: Total acid ($kg \cdot mol\ m^{-3}$)	Liquid phase conditions: Outlet: Temperature (K)	Experi scrul effici
10-1	0.30	1.09	2.85	0.047	0.000	299	0.021	300	300	5.0	297	0.0224	0.0616	297	0.1
10-2	0.61	1.11	2.95	0.047	0.000	295	0.013	299	299	5.0	298	0.0313	0.0770	298	0.
10-3	0.61	1.06	3.14	0.049	0.000	295	0.013	299	299	5.0	298	0.0367	0.0928	299	0.
10-4	0.91	1.09	3.17	0.050	0.000	295	0.009	297	297	5.0	297	0.0428	0.1061	298	0.
10-5	0.91	1.15	3.24	0.050	0.000	298	0.011	300	300	3.5	298	0.0528	0.1450	299	0.
10-6	0.91	1.15	3.24	0.047	0.000	298	0.011	300	300	3.5	298	0.0518	0.1420	299	0.
10-7	0.87	1.17	3.23	0.047	0.000	299	0.009	300	300	7.3	297	0.031	0.071	298	0.
10-8	0.87	1.16	3.23	0.047	0.000	299	0.008	300	300	7.3	298	0.031	0.068	299	0.
10-9	0.87	1.06	1.58	0.050	0.000	299	0.007	300	300	3.5	298	0.031	0.073	299	0.
10-10	0.87	1.06	1.51	0.050	0.000	299	0.007	299	299	3.5	298	0.032	0.076	299	0.
10-11	0.30	1.12	3.21	0.050	0.000	298	0.021	302	302	3.6	298	0.0306	0.098	298	0.
10-12	0.30	1.12	3.21	0.050	0.000	298	0.021	302	302	3.6	298	0.0307	2.102	298	0.
10-13	0.30	1.07	1.50	0.050	0.000	298	0.014	300	300	3.5	298	0.0215	0.0627	298	0.
10-14	0.30	1.07	1.50	0.050	0.000	298	0.013	301	301	3.6	298	0.0214	0.0606	299	0.
10-15	0.30	1.13	3.23	0.047	0.000	298	0.022	297	297	3.6	298	0.0246	0.0856	298	0.
10-16	0.30	1.10	3.22	0.048	0.000	297	0.019	303	303	3.6	298	0.0451	0.108	299	0.
10-17	0.61	1.11	3.25	0.050	0.000	298	0.017	300	300	3.5	296	0.0558	0.147	296	0.
10-18	0.61	1.12	3.06	0.050	0.000	298	0.012	301	301	3.5	298	0.0526	0.1435	298	0.
10-19	0.61	1.07	1.58	0.050	0.000	298	0.0073	302	302	3.5	298	0.0327	0.0809	298	0.
10-20	0.61	1.07	1.63	0.050	0.000	298	0.0063	303	303	3.5	298	0.0349	0.0905	298	0.
10-21	1.21	1.13	3.26	0.044	0.000	298	0.005	299	299	3.5	297	0.0656	0.1539	297	0.
10-22	1.21	1.13	3.26	0.044	0.000	298	0.005	301	301	3.5	298	0.0599	0.1454	298	0.
10-23	1.21	1.08	1.52	0.044	0.000	298	0.003	299	299	3.5	298	0.0362	0.0776	298	0.
10-24	1.21	1.08	1.52	0.044	0.000	299	0.003	298	298	3.5	298	0.0348	0.0722	298	0.
10-25[a]	1.21	1.08	1.84	0.044	0.000	298	0.007	299	299	3.5	298	0.0385	0.0820	298	0.
10-26[a]	1.21	1.09	1.84	0.044	0.000	298	0.007	299	299	3.5	298	0.0382	0.0828	298	0.
10-27	1.21	1.08	1.49	0.033	0.010	297	0.007	297	297	3.5	290	0.0445	0.0708	291	0.
10-29	1.21	1.10	3.35	0.028	0.018	295	0.015	299	299	3.5	298	0.0685	0.1066	298	0.
10-30	1.21	1.10	1.45	0.032	0.011	298	0.008	300	300	3.5	298	0.0388	0.0584	298	0.
10-31	1.21	1.10	2.28	0.035	0.013	298	0.011	301	301	3.5	298	0.0508	0.0822	298	0.
10-32-2F	0.79	1.11	2.74	0.0100	0.0003	295	0.0037	304	304	3.6	298	0.0100	0.0210	298	0.
10-32-2G	0.79	1.19	2.80	0.0017	0.0083	295	0.0093	304	304	1.8	298	0.0090	0.0095	298	0.
10-32-2H	0.79	1.40	4.95	0.0019	0.0078	294	0.0098	298	298	3.6	298	0.0050	0.0040	298	0.
10-32-2I	0.79	1.34z	5.16	0.0100	0.0001	297	0.0053	306	306	1.8	298	0.0210	0.0615	298	0.

[a]Nitrogen instead of air used as diluent gas.

0.076-m-diam column this precaution was not taken and entrance effects are present in the experimental data. The model development consisted of determining the value of $(\sqrt{Dk}/H)_{N_2O_4}$ that allowed the model prediction to most accurately represent the data. The value of $(\sqrt{Dk}/H)_{N_2O_3}$, obtained by Corriveau (1971), is the only known such constant. The effect of the ionic strength on these constants should be minimal as these studies were conducted using a water-dilute acid scrub solution. The values of K_1, K_2, and K_3 were from the works of Verhoek and Daniels (1931), Beattie and Bell (1957), and Wayne and Yost (1951) respectively. The use of these constants maintained consistency as they have been used in the calculation of $(\sqrt{Dk}/H)_{N_2O_4}$ and $(\sqrt{Dk}/H)_{N_2O_3}$. The Henry's Law constants for NO, NO_2, and HNO_2 are from the International Critical Tables, Loomas (1928), Andrews and Hanson (1961), and Abel and Neusser (1929) respectively. The rate constant for the oxidation of NO used in these calculations was that of Bodenstein (1918). The value of K_{60} was that from the work of Abel and Schmid (1928c). The values of k_G were calculated from a correlation by Onda, Takeuchi, and Okumoto (1968).

$$\frac{k_G\, RT}{a_t\, D_G} = 5.23 \left(\frac{G'}{a_t\, \mu_G}\right)^{0.7} \left(\frac{\mu_G}{\rho_G\, D_G}\right)^{0.33} \left(a_t\, d_p\right)^{-2.0} . \qquad (140)$$

The constant 5.23 is replaced by 2.00 for Raschig rings and Berl saddles smaller than 15 mm. This correlation by Onda et al., is considered accurate to ±30%. The values of a and k_L were taken from experimental results using the 13-mm Intalox saddles (Danckwerts, 1970) and calculated for the 6-mm Intalox saddles, using equations from Puranik and Vogelpohl (1974), and Mohunta, Vaidyanathan, and Laddha (1969):

$$a/a_t = 1.045 \left(\frac{L'}{a_t \mu_G}\right)^{0.041} \left(\frac{(L')^2}{a_t \rho_L \sigma}\right)^{0.133} \left(\frac{\sigma}{\sigma_c}\right)^{0.182} , \quad (141)$$

and

$$k_L a \left(\frac{a_t \mu_L}{g \rho_L}\right)^{2/3} \left(\frac{\mu_L}{g^2 \rho_L}\right)^{1/9} = 0.0025 \left(\frac{\mu_L (L')^3 a_t^3}{g^2 \rho_L^4}\right)^{1/4} \left(\frac{\mu_L}{\rho_L \mathcal{D}_L}\right)^{-1/2} . \quad (142)$$

Both of these correlations are accurate to ±20%. These selections are consistent with recent reviews in these areas by Laurent and Charpentier (1974), and Sherwood, Pigford, and Wilke (1975). The correlations for effective interfacial area and liquid-phase mass-transfer coefficient are the only known such correlations that include data from tests using Intalox saddles. The most critical coefficient is the value of $(\sqrt{\mathcal{D}k}/H)_{N_2O_4}$. These values range from 5.7×10^{-4} (Corriveau, 1971) to 11×10^{-4} kg·mol atm^{-1} m^{-2} s^{-1} (Dekker, Snoeck, and Kramers, 1959). Most of the NO_x absorption efficiency data lies bounded by computations using the model previously presented and the above values of $(\sqrt{\mathcal{D}k}/H)_{N_2O_4}$. Model predictions of X_{NO_x} were calculated using the values of $(\sqrt{\mathcal{D}k}/H)_{N_2O_4}$ obtained by the various researchers. The value of $(\sqrt{\mathcal{D}k}/H)_{N_2O_4}$ that produced the minimum residual sum of squares was that of Dekker, Snoeck, and Kramers (1959). The residual sum of squares is defined as:

$$RMS = \sum_{i=1}^{n} [(X_{NO_x})_{exp} - (X_{NO_x})_{cal}]^2/(n-1) , \quad (143)$$

where n is the number of test cases (experiments) and exp and cal are the experimental and calculated values. The minimum RMS was 0.0040 for

runs 10-1 through 10-31, given in Table 11. The feed gas partial pressures of NO_x were about 0.05 atm.

Data for experiments conducted using the 0.102-m-diam column and a fully oxidized feed gas are shown in a number of plots in Figures 15 through 18. These plots include calculated NO_x conversion at the extremities of $(\sqrt{Dk}/H)_{N_2O_4}$ values. From these plots, it can be seen that the experimental NO_x conversions tend to lie near the maximum observed $(\sqrt{Dk}/H)_{N_2O_4}$ value, which is the value producing the lowest RMS value for this data.

The data for runs with a partially oxidized feed gas, along with the model predictions, are presented in Table 12. In this comparison, the model prediction is consistently lower than the experimentally observed values of X_{NO_x}.

A series of four runs was conducted using the 0.102-m-diam column at NO_x feed partial pressures of about 0.01 atm. A summary of the run conditions and model predictions is presented in Table 13. A comparison between the model predicted and experimental X_{NO_x} shows good agreement.

Additional data were taken using the 0.074-m-diam column (presented in Table 14). Some selected experimental conversions from these data are compared with calculated values and presented in Figure 19. Again, reasonable agreement with the selection of the higher $(\sqrt{Dk}/H)_{N_2O_4}$ value is observed. The value of the RMS for the experiments presented in Table 14 for only runs with all NO_x feed gases in NO_2^* state was calculated to be 0.0009.

Other experimental activities concerned the depletion of nitrous acid from solutions in contact with nitrogen, air, and oxygen. These

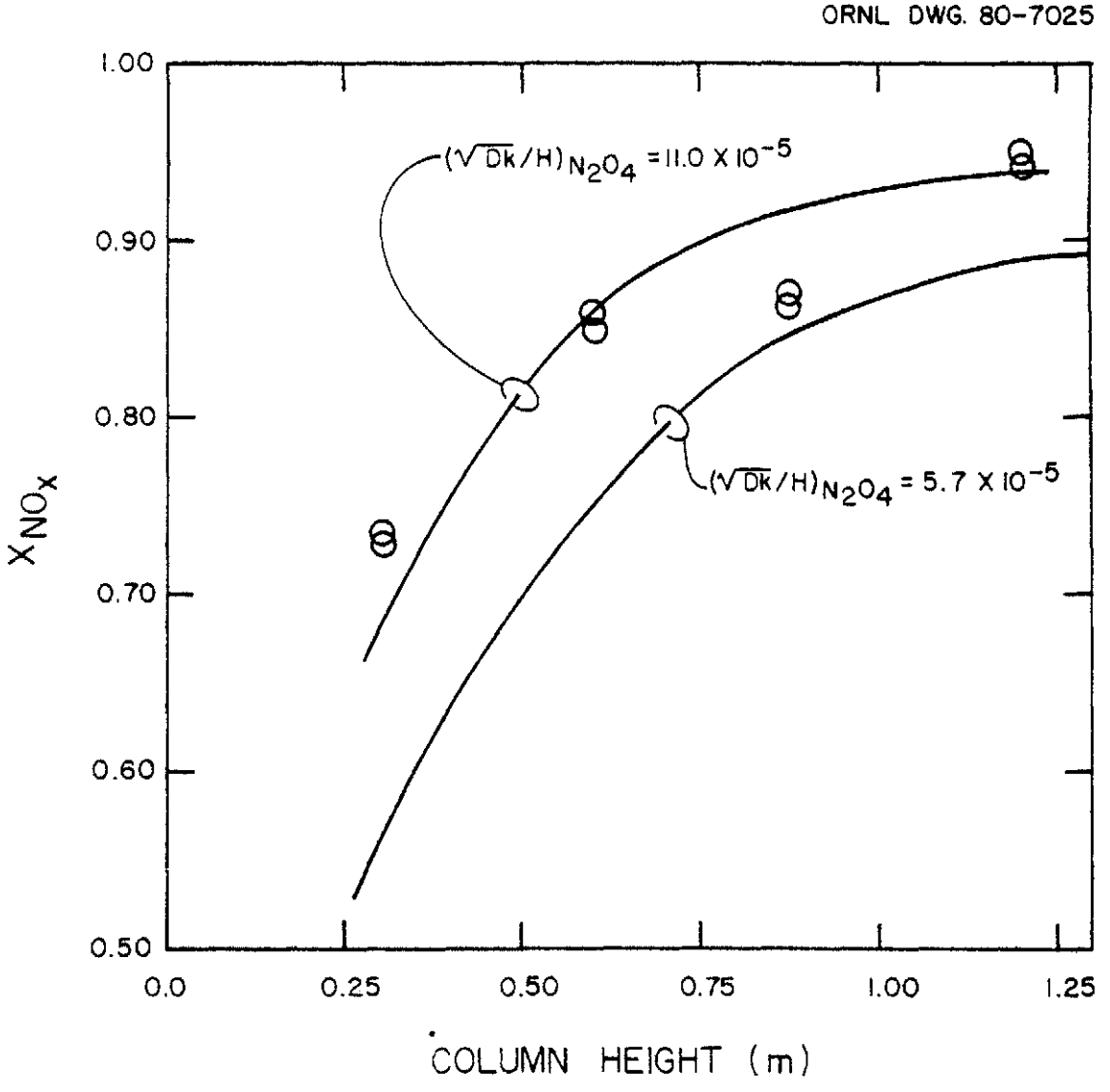

Figure 15. Experimental nitrogen oxide conversions at varying column heights and model predictions over the range of $(\sqrt{Dk}/H)_{N_2O_4}$ values from runs 10-13, 10-14, 10-19, 10-20, 10-9, 10-10, 10-23, and 10-24. The other parameters were $G \cong 1.5 \times 10^{-4}$ std $m^3\ s^{-1}$, $L = 3.5 \times 10^{-5}\ m^3\ s^{-1}$, $Y_{NO_x,in} \cong 0.05$, and $P_T = 1.1$ atm.

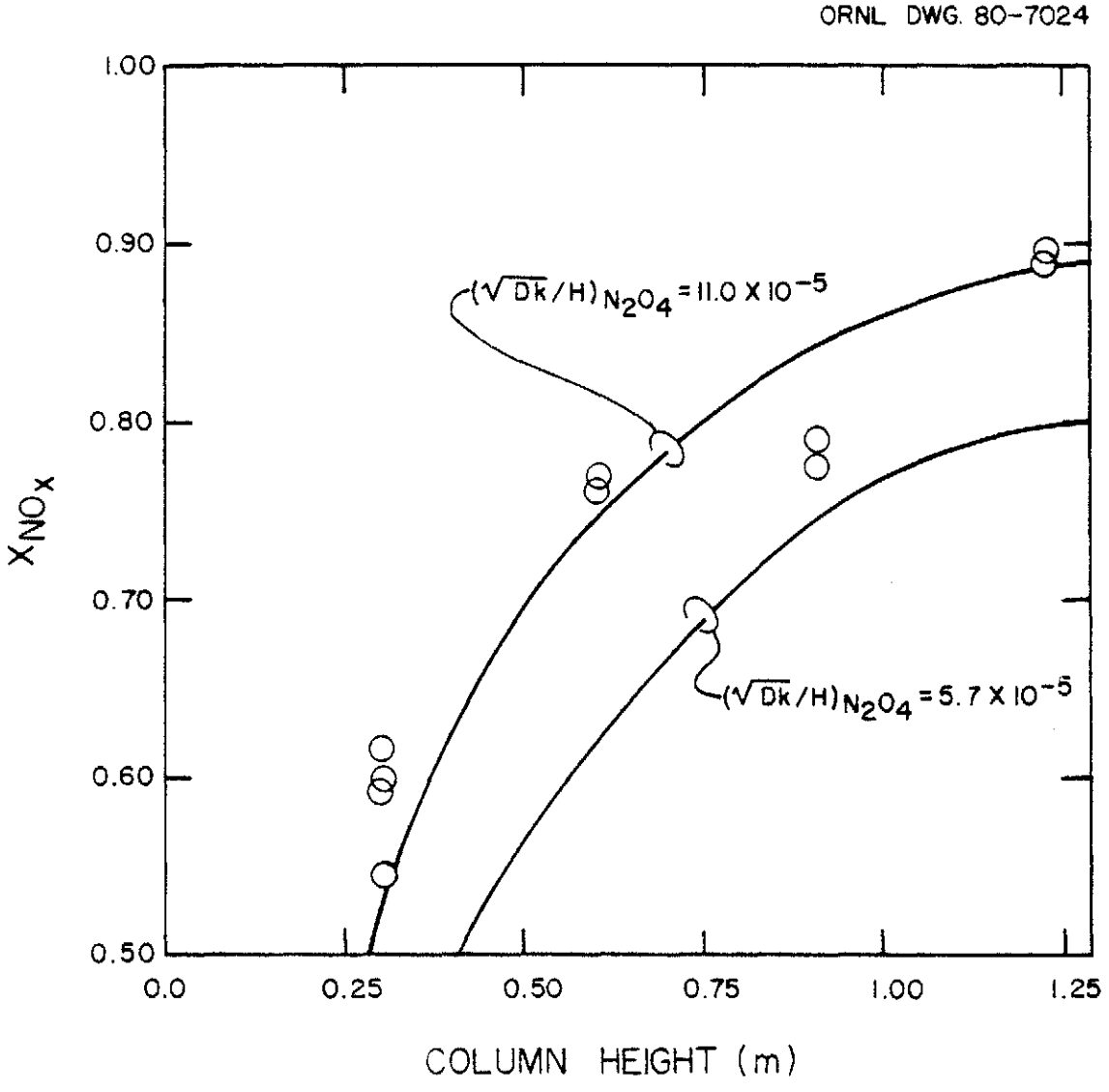

Figure 16. Experimental nitrogen oxide conversions at varying column heights and model predictions over the range of $(\sqrt{Dk}/H)_{N_2O_4}$ values from runs 10-5, 10-6, 10-11, 10-12, 10-15, 10-16, 10-17, 10-18, 10-21, and 10-22. Other parameters were $G \cong 3.2 \times 10^{-4}$ std m^3 s^{-1}, $L = 3.5 \times 10^{-5}$ m^3 s^{-1}, $Y_{NO_x,in} = 0.05$, and $P_T = 1.1$ atm.

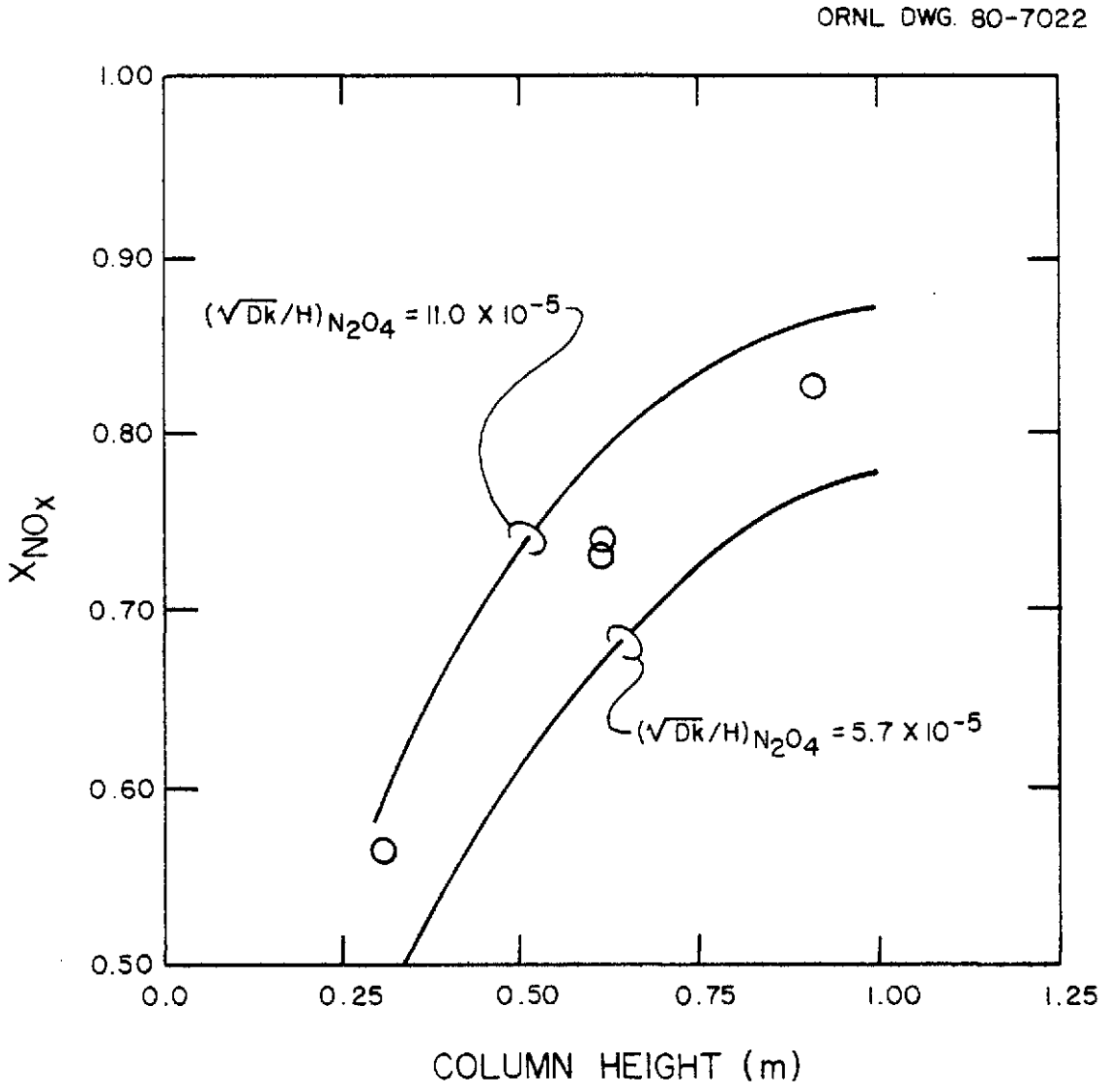

Figure 17. Experimental nitrogen oxide conversions at varying column heights and model predictions over the range of $(\sqrt{Dk}/H)_{N_2O_4}$ values from runs 10-1, 10-2, 10-3, and 10-4. The other parameters were $G \cong 3.2 \times 10^{-4}$ std m^3 s^{-1}, $L = 5.0 \times 10^{-5}$ m^3 s^{-1}, $Y_{NO_X,in} \cong 0.05$, and $P_T = 1.1$ atm.

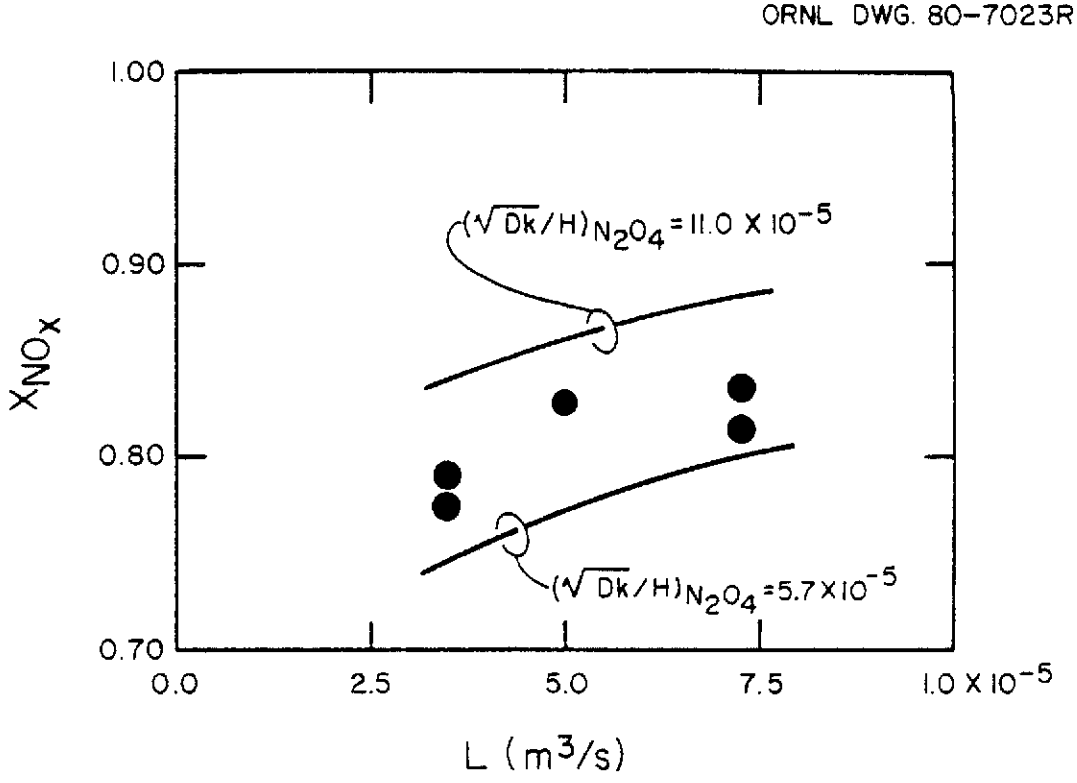

Fig. 18. Experimental nitrogen oxide conversions at varying liquid rates and model predictions over the range of $(\sqrt{Dk}/H)_{N_2O_4}$ values from runs 10-4, 10-5, 10-6, 10-7, and 10-8. Other parameters were $G \cong 3.2 \times 10^{-4}$ std m^3 s^{-1}, H = 0.90 m, $Y_{NO_x,in} \cong 0.05$, and P_T = 1.1 atm.

Table 12. The experimental and model[a] predicted conversion of NO_x for a feed gas containing NO* and NO_2^*

	X_{NO_x}	
Run	Experimental	Calculated
10-29	0.648	0.544
10-30	0.821	0.737
10-31	0.779	0.693

[a]Model prediction is based on $(\sqrt{Dk}/H)_{N_2O_4} = 11.0 \times 10^{-5}$.

Table 13. Experimental and calculated results[a] for runs with the NO_x feed partial pressure at about 0.01 atm

Variables	-(low)	+(high)
1. Gas rate ($m^3\ s^{-1}$)	$\sim 3 \times 10^{-3}$	$\sim 5 \times 10^{-3}$
2. Liquid rate ($m^3\ s^{-1}$)	$\sim 1.8 \times 10^{-5}$	$\sim 3.6 \times 10^{-5}$
3. Per cent of NO_x in +IV state (%)	~20	~100

	Variable				
Run	1	2	3	$(X_{NO_x})_{exp}$	$(X_{NO_x})_{cal}$
10-32-2F	-	+	+	0.64	0.62
10-32-2G	-	-	-	0.10	0.07
10-32-2H	+	+	-	0.00	0.06
10-32-2I	+	-	+	0.48	0.54

[a] Calculated X_{NO_x} is based on $(\sqrt{Dk}/l)_{N_2O_4}$ of 11.0×10^{-5}.

Table 14. Data from the studies with the 0.076-m-diam column packed with 6-mm Intalox saddles[a]

		Gas phase conditions							Liquid phase conditions					
		Inlet				Outlet			Inlet		Outlet			
Run	Column packing height (m)	Total gas flow rate (std $m^3\ s^{-1} \times 10^4$)	Mole fraction of NO_2^*	Mole fraction of NO^*	Temperature (K)	Mole fraction of NO_x	Temperature (K)	Temperature (K)	Flow rate ($m^3\ s^{-1} \times 10^5$)	Temperature (K)	C_{HNO_2} (kg-mol m^{-3})	C_{H^+} (kg-mol m^{-3})	Temperature (K)	Experimental NO_x conversion
PTR-19	0.102	3.27	0.100	0.000	298	0.020	305	305	4.5	298	0.0120	0.0175	298	0.82
PTR-20	0.102	3.27	0.100	0.000	298	0.018	302	302	4.5	298	0.0100	0.0140	298	0.84
PTR-21	0.152	3.27	0.100	0.000	298	0.008	303	303	4.5	298	0.0110	0.0180	298	0.93
PTR-22	0.152	3.23	0.100	0.000	298	0.006	302	302	4.5	298	0.0120	0.0150	298	0.95
PTR-23	0.203	3.26	0.100	0.000	298	0.004	302	302	4.5	298	0.0115	0.0125	298	0.96
PTR-24	0.203	3.26	0.100	0.000	298	0.004	303	303	4.5	298	0.0135	0.0205	298	0.96
MR3	0.406	3.26	0.096	0.000	298	0.004	299	299	5.2	298	0.0114	0.0217	298	0.97
MR4	0.406	3.24	0.104	0.000	298	0.004	299	299	3.5	298	0.167	0.0356	298	0.97
MR5	0.406	3.31	0.060	0.060	297	0.019	303	303	5.2	297		0.0261	297	0.86
MR6	0.406	3.29	0.056	0.056	297	0.021	304	304	5.2	297	0.0175	0.0221	297	0.83
CTC1	0.152	2.73	0.051	0.000	298	0.008	306	306	5.2	298	0.0037	0.0076	298	0.85
CTM3	0.305	3.26	0.204	0.000	298	0.012	304	304	5.2	298	0.0255	0.0470	299	0.96
CTC2	0.152	3.24	0.053	0.000	296	0.009	398	398	5.2	298	0.0043	0.010	299	0.84
CTM4	0.305	3.22	0.200	0.000	299	0.001	305	305	5.2	298	0.0182	0.052	299	0.96
CTH1	0.152	3.21	0.197	0.000	300	0.023	306	306	5.2	299	0.0147	0.0359	300	0.90
CTG1	0.305	3.22	0.051	0.000	299	0.005	305	305	5.2	299	0.0027	0.0076	300	0.91

[a] All runs were conducted at 1.10 atm.

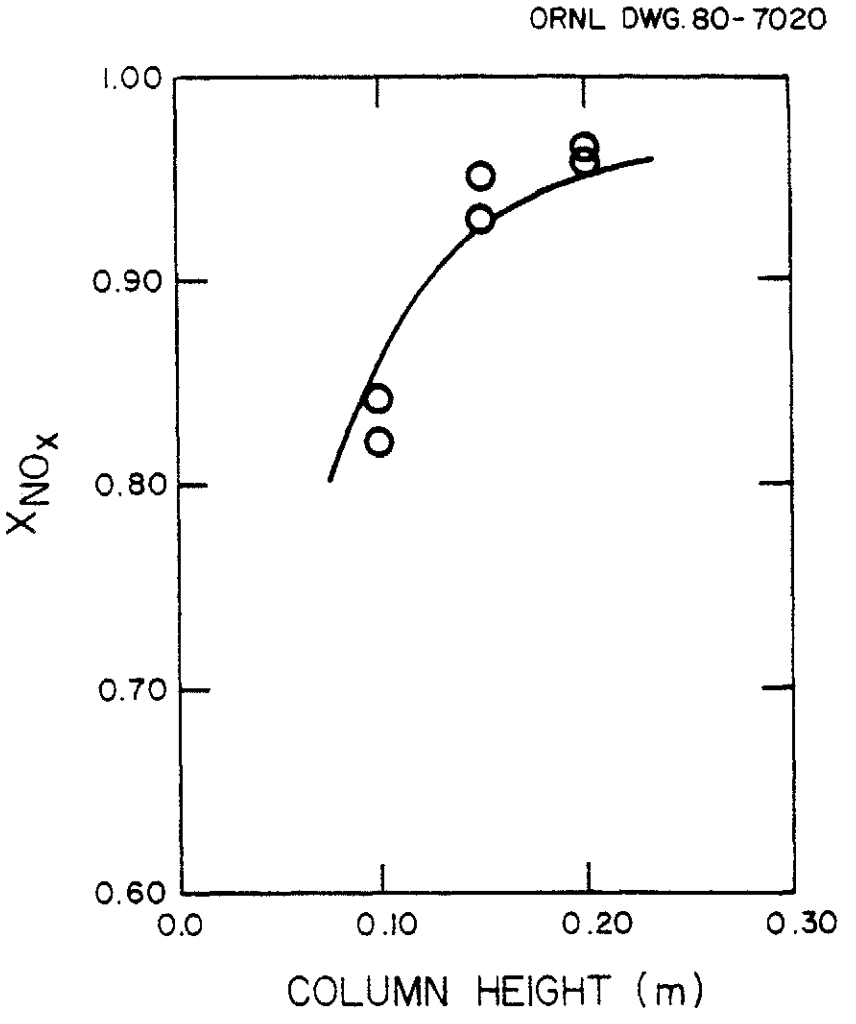

Fig. 19. Experimental and model predicted conversion at varying column heights from runs PTR-19, PTR-20, PTR-21, PTR-22, PTR-23, and PTR-24. Other parameters were $G = 3.3 \times 10^{-4}$ std $m^3\ s^{-1}$, $L = 4.5 \times 10^{-5}\ m^3\ s^{-1}$, $Y_{NO_x,in} = 0.10$, and $P_T = 1.10$ atm.

studies are presented in Appendix D. In depletion studies conducted using the smaller diameter tower at fairly low gas-rate to liquid-rate ratios, the depletion processes seem well described by the Abel-Schmid (1928a) stoichiometry. In depletion studies conducted using the larger diameter column at much higher gas-rate to liquid-rate ratios, the depletion processes apparently involve both the decomposition, described by Abel and Schmid, and physical desorption of HNO_2. The depletion of nitrous acid determined experimentally is compared to that calculated by the absorption/desorption model in Appendix E. Although there is good agreement in this particular comparison, further comparison at a mechanistic level is rather inconclusive.

Overall, predictions using the mathematical model, developed in this activity, compare reasonably with the obtained experimental data.

CHAPTER VI

CONCLUSIONS AND RECOMMENDATIONS

1. Conclusions

1. The mathematical model developed in this activity represents the nitrogen oxide scrubbing results over a wide range of conditions.
2. Moderate depths of packing can achieve fairly high nitrogen oxide removal efficiencies at similar conditions to those studied.
3. The scrubbing of NO_2^* feed gases leads to an almost equal molar production of nitric and nitrous acids.

2. Recommendations

1. The mathematical model developed in this study should be used for the simulation of nitrogen oxide absorption in packed towers under similar conditions to those studied.
2. Further experimental results will be needed at lower nitrogen oxide partial pressures, at lower temperatures, and at higher nitric acid concentrations before further model development may proceed.
3. The future study of nitrogen oxide absorption in packed towers should be done using packing with well-studied mass-transfer characteristics.
4. Studies to determine $(\sqrt{Dk}/H)_{N_2O_3}$, H_{NO_2}, and H_{HNO_2} for a wide range of temperatures and acid concentrations should be conducted.
5. Further studies into the decomposition of nitrous acid at various nitric acid concentrations and temperatures should be conducted.

6. Further model testing and evaluation will be necessary to determine the model's usefulness for predicting nitrogen oxide removal in packed towers when the feed gas contains steam and/or the feed scrubbing liquor contains nitrous acid.

LIST OF REFERENCES

LIST OF REFERENCES

Abel, E., and E. Neusser, *Monatsh. Chem.* 54: 855 (1929).

Abel, E., and Proisl, Z. *Elektrochem.* 35: 712 (1929).

Abel, E., O. Redlich, and B. V. Lengyel, Z. *Physik. Chem.* 132: 189 (1928).

Abel, E., and H. Schmid, Z. *Physik. Chem.* 132: 55 (1928a).

Abel, E., and H. Schmid, Z. *Physik. Chem.* 132: 64 (1928b).

Abel, E., and H. Schmid, Z. *Physik. Chem.* 134: 279 (1928c).

Abel, E., H. Schmid, and S. Babad, Z. *Physik. Chem.* 136: 135 (1928).

Abel, E., H. Schmid, and S. Babad, Z. *Physik. Chem.* 136: 419 (1929).

Abel, E., and H. Schmid, Z. *Physik. Chem.* 136: 430 (1929).

Abel, E., H. Schmid, and E. Romer, Z. *Physik. Chem.* 148: 337 (1930).

Andrews, S. P., and D. Hanson, *Chem. Eng. Sci.* 14: 105 (1961).

Ashmore, P. G., and B. J. Tyler, *J. Chem. Soc.* 1017 (1961).

Astarita, G., *Mass Transfer with Chemical Reaction*, Elsevier, New York (1967), pp. 5, 11-19, 35, 65.

Atroshchenko, V. I., V. I. Konvisar, and E. I. Kordysh, *J. Appl. Chem. USSR* 33: 288 (1960).

Atroshchenko, V. I., V. I. Konvisar, and M. T. Ivakhnenko, *J. Appl. Chem. USSR* 38: 2619 (1965).

Beattie, I. R., and S. W. Bell, *J. Chem. Soc.* 1681 (1957).

Beattie, I. R., *Progress in Inorganic Chemistry*, Interscience, New York (1963).

Billet, R., *Brit. Chem. Engr. & Proc. Tech.* 17 (9): 705 (1972).

Bolme, D. W., and A. Horton, *Chem. Engr. Prog.* 75 (3): 95 (1979).

Bodenstein, M., Z. *Elektrochem.* 24: 183 (1918).

Bodenstein, M., Z. *Elektrochem.* 100: 68 (1922).

Bowman, D. H., C. J. Kulczak, and J. J. Shulman, *Pollut. Control Eng.* 6: 38 (1974).

Box, G. E. P., W. G. Hunter, and J. S. Hunter, *Statistics for Experimenters*, Wiley, New York (1978).

Bunton, C. A., and G. L. Stedman, *J. Chem. Soc.* 240 (1958).

Burdict, C. L., and E. S. Freed, *J. Am. Chem. Soc.* 54: 1003 (1932).

Carrington, T., and N. Davidson, *J. Chem. Soc.* 57: 418 (1953).

Carberry, J., *Chem. Eng. Sci.* 9: 189 (1959).

Caudle, P. G., and K. G. Denbigh, *Trans. Faraday Soc.* 49: 39 (1953).

Chambers, F. S., and T. K. Sherwood, *Ind. Eng. Chem.* 29: 1415 (1937).

Chilton, T. H., *Chem. Eng. Prog. Manag. Ser.* 3: 56 (1960).

Chilton, T. H., and E. W. Knell, *PACHEC 1972, Session 13*, 75 (1972).

Corriveau, C. E., Jr., *The Absorption of N_2O_3 into Water*, Master's Thesis in Chemical Engineering, University of California, Berkeley (1971).

Counce, R. M., W. S. Groenier, J. A. Klein, and J. J. Perona, *Proc. Fifteenth DOE Nuclear Air Cleaning Conf.*, Boston, Mass., (1979).

Counce, R. M., and J. J. Perona, *Ind. Eng. Chem. Fundam.* 18: 400 (1979a).

Counce, R. M., and J. J. Perona, *Ind. Eng. Chem. Process Des. Dev.* 18: 562 (1979b).

Counce, R. M., *A User's Guide to ABNØX, a Computer Program Designed to Simulate the Nitrogen Oxide Removal Efficiency of a Multistage Bubble-Cap Tower*, ORNL/TM-6938 (September 1979).

Counce, R. M., and J. J. Perona, *Ind. Eng. Chem. Proc. Des. Devel.* 19: 426 (1980).

Danckwerts, P. V., *Gas Liquid Reactions*, McGraw-Hill, New York, 1970, 146.

Dekker, W. A., E. Snoeck, and H. Kramers, *Chem. Eng. Sci.* 11: 61 (1959).

Denbigh, K. G., and A. J. Prince, *J. Chem. Soc.* 59: 316 (1947).

England, C., and W. H. Corcoran, *Ind. Eng. Chem. Fundam.* 13: 373 (1974).

Epshtein, D. A., *J. Gen. Chem.* (Russian) 9: 792 (1939).

Fauser, G., *Chem. Metall. Eng.* 35: 474 (1928).

First, M. W., and F. J. Viles, Jr., *J. Air Poll. Control Asso.* 122 (1971).

Forsythe, G. E., M. A. Malcolm, and C. B. Moler, *Computer Methods for Mathematical Computations*, Prentice-Hall, Englewood Clifts, N.J. (1977).

Forsythe, W. R., and W. F. Giauque, *J. Am. Chem. Soc.* 64: 48 (1942).

Greig, J. D., and P. G. Hall, *Trans. Faraday Soc.* 63: 655 (1967).

Gerstacker, *Chem. Eng. Sci.* 14: 124 (1961).

Graham, H. G., V. E. Lyons, and H. L. Faucett, *Chem. Eng. Prog.* 60: 77 (1964).

Graham, R. F., and B. J. Tyler, *J. Chem. Soc.* 68 (4): 683 (1972).

Grätzel, M., A. Henglein, J. Lilie, and G. Beck, *Ber. Bunsenges* 73: 646 (1969).

Goyer, G. G., *J. of Colloid Sci.* 18: 616 (1963).

Gray, P., "The Chemistry of Dinitrogen Tetroxide," *Roy. Inst. Chem.*, London (1958).

Hasche, R. L., and W. A. Patrick, *J. Am. Chem. Soc.* 46: 1207 (1925).

Hellmer, L., *Chem. Eng. Tech.* 44: 420 (1972).

Ho, W. H., *Proceedings of the National Science Council*, No. 10, Part 1, 175 (May 1977).

Hoftyzer, P. J., and F. J. G. Kwanten, *Processes for Air Pollution Control*, 2nd ed., Chemical Rubber Co., Cleveland, 1972, Chap. 5B.

JANAF Thermochemical Tables, 2nd ed., The Dow Chemical Company, Midland, Michigan (1971).

Kaiser, E. W., and C. H. Wu, *J. Phys. Chem.* 81 (18): 1701 (1977).

Kameoka, Y., and R. L. Pigford, *Ind. Eng. Chem. Fundam.* 16: 163 (1977).

Karavaev, M. M., and V. G. Visloguzova, *J. Appl. Chem. USSR* 47 (5): 1001 (1974).

Karavaev, M. M., and G. A. Skvortsov, Russ. *J. Phys. Chem.* 36 (5): 566 (1962).

Klemenc, A., and E. Hayek, *Z. Anorg. U. Allgem. Ch.* 186: 181 (1930).

Klemenc, A., and F. Pollak, *Z. Physik. Chem.* 101: 105 (1922).

Knox, J., and D. M. Reid, *J. Chem. Soc. Ind.* 38 (9): 105T (1919).

Kobayashi, H., N. Takezawa, K. Hara, T. Nikka, and K. Kitano, *Nippon Kagakukai-shi* 383 (1976).

Koegler, S. S., *Purex NO_x Abatement Pilot Plant*, Rockwell Hanford Operations, RHO-CD-702 (July 1979).

Komiyama, H., and H. Inoue, *J. of Chem. Eng. Japan* 11 (1): 25 (1978).

Komuro, Y., *Nippon Kagaku Fasshi*, Tokyo 74: 47 (1953).

Koval, E. J., and M. S. Peters, *Ind. Eng. Chem.* 52: 1011 (1960).

Kramers, H., M. P. P. Blind, and E. Snoeck, *Chem. Eng. Sci.* 14: 115 (1961).

Lang, F. M., and G. Aunis, *Bull. Soc. Chem. de France* 18 15: 135 (1951a).

Lang, F. M., and G. Aunis, *Bull. Soc. Chem. de France* 18 5: 398 (1951b).

Laurent, A., and J. C. Charpentier, *The Chem. Engr. J.* 8: 85 (1974).

Lefers, J. B., F. C. deBoks, C. M. Van den Bleek, and P. J. van den Berg, *Chem. Engr. Sci.* 35: 145 (1980).

Lewis, G. N., and A. Edgar, *J. Amer. Chem. Soc.* 33: 292 (1911).

Lewis, G. N., and M. Randall, *Thermodynamics*, 1st ed., McGraw-Hill, New York (1923).

Liebmann, H., Dissertation, University of Dresden (1914).

Loomis, A. L., *International Critical Tables III*: 255, McGraw-Hill, New York (1928).

Makhotkin, A. F., and A. M. Shamsutdinov, *Khim i Khim. Tekhn.* XIX (9): 1411 (1976).

Menegus, R. L., *Chem. Engr. Sci.* 9: 192 (1959).

Mohunta, D. M., A. S. Vaidyanathan, and G. S. Laddha, *Indian Chem. Engr.* 11: 73 (1969).

Moll, M. J., *The Rate of Hydrolysis of Nitrogen Tetroxide*, Ph.D. Dissertation, University of Washington (1966).

Montemartini, C., *Rendiconti* IV (6): 263 (1890).

Montemartini, C., *Rendiconti* I (1): 63 (1892).

Morrison, M. E., R. C. Rinker, and W. H. Corcoran, *Ind. Eng. Chem. Fundam.* 5: 175 (1966).

Onda, K., H. Takeuchi, and Y. Okumuto, *J. of Chem. Engr.* I: 56 (1968).

Peters, M. S., *University of Illinois Engineering Experiment Report No. 14*, USAEC-COO-1015 (1955).

Peters, M. S., and J. L. Holman, *Ind. Eng. Chem.* 47: 2536 (1955).

Peters, M. S., and E. J. Koval, *Ind. Eng. Chem.* 51: 577 (1959).

Peters, M. S., C. P. Ross, and J. E. Klein, *AIChE J.* 1: 105 (1955).

Pigford, R. L., *Chem. Engr. Prog.* 74 (9): 11 (1978).

Pogrebnaya, V. L., A. P. Usov, and A. V. Baranov, *J. Appl. Chem. of the USSR* 49 (4): 757 (1976).

Puranik, S. S., and A. Vogelpohl, *Chem. Engr. Sci.* 29: 501 (1974).

Ray, P. C., M. L. Dey, and J. C. Ghosh, *J. Chem. Soc.* London 3: 413 (1917).

Safin, R. S., A. F. Makhotkin, and A. F. Galeev, *Sb. Aspir. Rab. Kazan. Khim. Tekhnol. Inst. Khim. Nauk.* 1: 166 (1970).

Sapozhnikova, A. V., *Journal Russ. Phys. Chem.* 32: 375 (1900).

Sapozhnikova, A. V., *Journal Russ. Phys. Chem.* 33: 506 (1901).

Schmid, G., and G. Baehr, *Z. Physik, Chem.* 41: 8 (1964).

Schmid, H., and P. Kremayr, *Monat. Chemie* 48: 417 (1966).

Schwartz, S. E., and W. H. White, *Equilibrium Solubility of the Nitrogen Oxides and Oxyacids in Aqueous Solutions*, Battelle BNL 27102 (January 1980).

Selby, S. M., *Standard Mathematical Tables*, 15th ed., The Chemical Rubber Co., Cleveland (1967), p. 363.

Shah, Y. T., and M. M. Sharma, *Trans. Instn. Chem. Engrs.* 54: 1 (1976).

Sherwood, T. K., R. L. Pigford, and C. R. Wilke, *Mass Transfer*, McGraw-Hill, New York, Chapter 8 (1975).

Smith, J. H., *J. Am. Chem. Soc.* 69: 1742 (1947).

Stedman, G., *Advances in Inorganic Chemistry and Radiochemistry*, Academic Press, New York (1979), p. 142.

Suzawa, T., M. Hondo, O. Manabe, and H. Hinokiyama, *Kogyo Kagaku Zasshi* 58 (10): 744 (1955).

Swanson, G. G., Jr., J. V. Prusa, T. M. Hellman, and D. E. Elliot, *Pollut. Engr.* 10: 52 (1978).

Taylor, G. B., T. H. Chilton, and S. L. Handforth, *Ind. Eng. Chem.* 23: 860 (1931).

Taylor, T. W. J., E. W. Wignall, and J. F. Cowley, *J. Chem. Soc.* 1923 (1927).

Tereshchenko, L. Y., V. P. Panov, and M. E. Pozin, *J. Appl. Chem. USSR* 41 (3): 474 (1968).

Trautz, M., *Z. Physik. Chem.* 47: 513 (1904).

Treacy, J. C., and F. Daniels, *J. Am. Chem. Soc.* 77: 2033 (1955).

Turney, A. J., *J. Chem. Soc.* 4263 (1960).

Turney, A. J., and G. A. Wright, *J. Chem. Soc.* 2415 (1958).

Usabillaga, A., *Kinetics of Nitrous Acid Formation and Decomposition*, Dissertation, University of Illinois (1962).

Valey, V. H., *Proc. Roy. Soc.* 52: 27 (1892).

Verhoek, F. H., and F. J. Daniels, *J. Am. Chem. Soc.* 53: 1250 (1931).

Waldorf, D. M., and A. L. Babb, *J. Chem. Phys.* 40: 1165 (1964), 39: 432 (1963).

Wayne, L. G., and D. M. Yost, *J. Chem. Phys.* 19: 41 (1951).

Wendel, W. M., and R. L. Pigford, *AIChE J.* 4: 249 (1958).

Zhidov, B. A., A. S. Plygunov, V. I. Atroshchenko, M. M. Karaveav, G. A. Bochenko, G. A. Skvortsov, A. G. Udovenko, and A. L. Kontsevoi, *The Soviet Chem. Ind.* 6 (12): 768 (1974).

APPENDIXES

APPENDIX A

THE CALCULATION OF THE GAS-PHASE PARTIAL PRESSURES OF NO, NO_2, N_2O_3, N_2O_4, AND HNO_2

The important gas phase components are NO, NO_2, N_2O_3, N_2O_4, and HNO_2. The important gas-phase equilibrium reactions, as shown in Equations (1), (2), and (3), are:

$$2NO_2\ (g) \leftrightarrow N_2O_4\ (g)\ ,$$

$$NO\ (g) + NO_2\ (g) \leftrightarrow 2N_2O_3\ (g)\ ,$$

and

$$NO\ (g) + NO_2\ (g) + H_2O\ (g) \leftrightarrow 2HNO_2\ (g)\ .$$

These components are calculated from known partial pressures of P_{NO*} and $P_{NO_2^*}$ and defined by Reactions (115) and (116),

$$P_{NO_2^*} = P_{NO_2} + 2P_{N_2O_4} + P_{N_2O_3} + \frac{1}{2} P_{HNO_2}\ ,$$

and

$$P_{NO*} = P_{NO} + P_{N_2O_3} + \frac{1}{2} P_{HNO_2}\ .$$

Additional relationships of the total partial pressure of nitrogen oxides, P_{NO_x}, and the difference between $P_{NO_2^*}$ and P_{NO*}, ξ, are defined by:

$$P_{NO_x} = P_{NO_2^*} + P_{NO*} = P_{NO} + P_{NO_2} + 2P_{N_2O_4} + 2P_{N_2O_3} + P_{HNO_2}\ , \qquad (A.1)$$

and

$$\xi = P_{NO_2^*} - P_{NO^*} = P_{NO_2} + 2P_{N_2O_4} - P_{NO} \quad . \tag{A.2}$$

The component partial pressures may be expressed as functions of P_{NO} and P_{NO_2}, using the equilibrium reactions as expressed in Reactions (117), (118), and (119),

$$P_{N_2O_4} = K_1 \, P_{NO_2}^2 \quad ,$$

$$P_{N_2O_3} = K_2 \, P_{NO} \, P_{NO_2} \quad ,$$

and

$$P_{HNO_2} = (K_3 \, P_{H_2O} \, P_{NO} \, P_{NO_2})^{1/2} \quad .$$

Substituting the previous equations into Equations (A.1) and (A.2) yields:

$$P_{NO_x} = P_{NO} + P_{NO_2} + 2K_1 \, P_{NO_2}^2 + 2K_2 \, P_{NO} \, P_{NO_2} + (K_3 \, P_{H_2O} \, P_{NO} \, P_{NO_2})^{1/2} \quad , \tag{A.3}$$

and

$$\xi = P_{NO_2} + 2K_1 \, P_{NO_2}^2 - P_{NO} \quad . \tag{A.4}$$

The values of P_{NO_x} and ξ can be calculated from P_{NO^*} and $P_{NO_2^*}$. Equations (A.3) and (A.4) now contain a total of two unknowns. These equations are solved numerically using the HYBRD1 subroutine. This subroutine will be described in the MINPACK Documentation Package, currently being developed by the Applied Mathematics Division, Argonne National Laboratory, Argonne, Illinois.

APPENDIX B

DERIVATION OF THE CONVERSION OF NO TO NO_2 IN THE GAS-PHASE OF A PACKED COLUMN

The gas flowing through a packed tower is considered to be in plug-flow. The steady state material balance for NO around a differential gas space is

$$\begin{matrix}\text{input} \\ \text{of NO}\end{matrix} = \begin{matrix}\text{output} \\ \text{of NO}\end{matrix} + \begin{matrix}\text{disappearance} \\ \text{by reaction}\end{matrix} \quad . \tag{B.1}$$

These input, output, and disappearance terms in kg·mol s^{-1} are $G(P_{NO})_{in}/(RT)$, $G(P_{NO})_{out}/(RT)$, and $[-r_5/(RT)]\ dV$. Inserting these terms in Equation (B.1),

$$G(P_{NO})_{in}/(RT) = G(P_{NO})_{out}/(RT) + [-r_5/(RT)]\ dV \ , \tag{B.2}$$

noting that

$$G(P_{NO})_{out}/(RT) = G[(P_{NO})_{in} + d(P_{NO})_{in}]/(RT) \ , \tag{B.3}$$

and

$$d(P_{NO})_{in} = -(P_{NO})_{in}\ dX_{NO} \ , \tag{B.4}$$

and using Equations (B.1), (B.2), and (B.3),

$$G(P_{NO})_{in}/(RT) = G[(P_{NO})_{in} - (P_{NO})_{in} dX_{NO}]/(RT) + [-r_5/(RT)]\ dV \ , \tag{B.5}$$

which after rearrangement and division by RT yields:

$$G(P_{NO})_{in} dX_{NO} = -r_5 \, dV \, . \tag{B.6}$$

Further rearrangement yields an integrable form,

$$\frac{1}{G(P_{NO})_{in}} \int_0^V dV = \int_0^{X_{NO}} \frac{dX_{NO}}{-r_5} \, . \tag{B.7}$$

The reaction rate may be expressed as:

$$-r_5 = k_5 \, P_{NO}^2 \, P_{O_2} = k_5[(P_{NO})_{in} \, (1 - X_{NO})]^2 \, [(P_{O_2})_{in} \times \left(1 - \frac{(P_{NO})_{in}}{2(P_{O_2})_{in}} X_{NO}\right) \, . \tag{B.8}$$

Substituting Equation (B.8) into (B.7) yields:

$$\frac{1}{G(P_{NO})_{in}} \int_0^V dV$$

$$= \int_0^{X_{NO}} \frac{dX_{NO}}{k_5[(P_{NO})_{in}(1 - X_{NO})]^2 \, [(P_{O_2})_{in} \left(1 - \frac{(P_{NO})_{in}}{2(P_{O_2})_{in}} X_{NO}\right)} \, . \tag{B.9}$$

Further rearrangement yields a simplified expression:

$$\frac{k_5(P_{NO})_{in}(P_{O_2})_{in}}{G} \int_0^V dV = \int_0^{X_{NO}} \frac{dX_{NO}}{(1 - X_{NO})^2 \left(1 - \frac{(P_{NO})_{in}}{2(P_{O_2})_{in}} X_{NO}\right)} \, . \tag{B.10}$$

The right-hand side of this equation is in the form of

$$\int \frac{dx}{(a + bx)^2 (a' + b'x)} , \tag{B.11}$$

which is integrated as (Selby 1967):

$$\frac{1}{a\,b' - a'b}\left(\frac{1}{a + bx} + \frac{b'}{a\,b' - a'b} \ln \frac{a' + b'x}{a + bx}\right) . \tag{B.12}$$

Defining

$$a = 1 ,$$

$$b = -1 ,$$

$$a' = 1 ,$$

and

$$b' = -(P_{NO})_{in}/(2P_{O_2})_{in} .$$

The following equation is obtained (retaining b′ for simplicity):

$$\frac{k_5 (P_{NO})_{in} (P_{O_2})_{in} V}{G} = \frac{1}{b' + 1}\left[\frac{1}{1 - X_{NO}} + \frac{b'}{b' + 1} \ln \frac{1 + b' X_{NO}}{1 + X_{NO}}\right] , \tag{B.13}$$

and upon rearrangement,

$$\frac{k_5 (P_{NO})_{in} (P_{O_2})_{in} V}{G} - \frac{1}{1 + b'}\left[\frac{1}{1 - X_{NO}} + \frac{b'}{1 + b'} \ln \frac{1 + b' X_{NO}}{1 - X_{NO}}\right] = 0 . \tag{B.14}$$

Solution of this polynomial involves finding the root, X_{NO}, between zero and 1. This solution is accomplished using a simple bisection routine.

APPENDIX C

CALCULATION OF INTERFACIAL NO_x-HNO_x PARTIAL PRESSURES

The following development proceeds very similarily to that of Corriveau (1971) except that mass-transfer and reaction in the liquid phase is included in the interacting relationships. The gas-phase chemical equilibrium between NO, NO_2, N_2O_3, N_2O_4, HNO_2, and H_2O is assumed to apply in the gas film and at the gas-liquid interface. The important equilibrium considerations are Reactions (1), (2), and (3).

$$2NO_2\ (g) \leftrightarrow N_2O_4\ (g)\ ,$$

$$NO\ (g) + NO_2\ (g) \leftrightarrow N_2O_3\ (g)\ ,$$

and

$$NO\ (g) + NO_2\ (g) + H_2O\ (g) \leftrightarrow 2HNO_2\ (g)\ .$$

The partial pressures of gaseous N_2O_4, N_2O_3, and HNO_2 may be expressed in terms of NO and NO_2, utilizing constants for the previously mentioned equilibrium reactions as Reactions (117), (118), and (119):

$$P_{N_2O_4} = K_1\ P_{NO_2}^2\ ,$$

$$P_{N_2O_3} = K_2\ P_{NO}\ P_{NO_2}\ ,$$

and

$$P_{HNO_2} = (K_3\ P_{NO}\ P_{NO_2}\ P_{H_2O})^{1/2}\ .$$

The partial pressure of NO_2^* and NO* and their difference can be expressed as:

$$P_{NO_2^*} = P_{NO_2} + 2P_{N_2O_4} + P_{N_2O_3} + \frac{1}{2} P_{HNO_2} , \tag{C.1}$$

$$P_{NO^*} = P_{NO} + P_{N_2O_3} + \frac{1}{2} P_{HNO_2} , \tag{C.2}$$

and

$$\xi = P_{NO_2^*} - P_{NO^*} = P_{NO_2} + 2P_{N_2O_4} - P_{NO} . \tag{C.3}$$

A flux of component i through the gas film may be represented by

$$\overline{R}_i = - \frac{\mathcal{D}_{G,i}}{RT} \left(\frac{dP_i}{dx} \right) . \tag{C.4}$$

By multiplying and dividing the right-hand side by the inverse film thickness, $(1/\delta)$, the following equation is obtained:

$$\overline{R}_i = - \frac{\mathcal{D}_{G,i}/\delta}{RT} \left[\frac{dP_i}{d(x/\delta)} \right] , \tag{C.5}$$

Further simplification is obtained by introducing the gas-phase mass-transfer coefficient, $k_{G,i}$, and a dimensionless film thickness, ζ:

$$\overline{R}_i = - k_{G,i} \left(\frac{dP_i}{d\zeta} \right) . \tag{C.6}$$

The local absorption rate of NO_2^* and NO* is expressed in terms of the gas-film mass-transfer coefficient and a dimensionless film thickness, ζ, as

$$\overline{R}_{NO_2^*} = -k_{G,NO_2^*} \frac{dP_{NO_2^*}}{d\zeta} , \tag{C.7}$$

and

$$\overline{R}_{NO^*} = -k_{G,NO^*} \frac{dP_{NO^*}}{d\zeta} . \tag{C.8}$$

Utilizing Equations (C.1) and (C.2),

$$\frac{dP_{NO_2^*}}{d\zeta} = \frac{dP_{NO_2}}{d\zeta} + 2 \frac{dP_{N_2O_4}}{d\zeta} + \frac{dP_{N_2O_3}}{d\zeta} + \frac{1}{2} \frac{dP_{HNO_2}}{d\zeta} , \tag{C.9}$$

and

$$\frac{dP_{NO^*}}{d\zeta} = \frac{dP_{NO}}{d\zeta} + \frac{dP_{N_2O_3}}{d\zeta} + \frac{1}{2} \frac{dP_{HNO_2}}{d\zeta} , \tag{C.10}$$

The gradients of N_2O_4, N_2O_3, and HNO_2 in the gas film may be expressed in terms of NO and NO_2 as:

$$\frac{dP_{N_2O_4}}{d\zeta} = 2K_1 \, P_{NO_2} \frac{dP_{NO_2}}{d\zeta} , \tag{C.11}$$

$$\frac{dP_{N_2O_3}}{d\zeta} = K_2 \, P_{NO} \frac{dP_{NO_2}}{d\zeta} + K_2 \, P_{NO_2} \frac{dP_{NO}}{d\zeta} , \tag{C.12}$$

and

$$\frac{dP_{HNO_2}}{d\zeta} = \frac{1}{2} \left(K_3 \, P_{H_2O} \frac{P_{NO}}{P_{NO_2}} \right)^{1/2} \frac{dP_{NO_2}}{d\zeta} + \frac{1}{2} \left(K_3 \, P_{H_2O} \frac{P_{NO_2}}{P_{NO}} \right)^{1/2} \frac{dP_{NO}}{d\zeta} . \tag{C.13}$$

The fluxes of NO_2^* and NO* through the gas film are calculated using appropriate gas-phase mass-transfer coefficients as:

$$-\overline{R}_{NO_2^*} = \left[k_{G,NO_2} + 4k_{G,N_2O_4} K_1 P_{NO_2} + k_{G,N_2O_3} K_2 P_{NO} + \frac{1}{4} k_{G,HNO_2} (K_3 P_{H_2O} P_{NO}/P_{NO_2})^{1/2} \right] \frac{dP_{NO_2}}{d\zeta}$$

$$+ \left[k_{G,N_2O_3} K_2 P_{NO_2} + \frac{1}{4} k_{G,HNO_2} (K_3 P_{H_2O} P_{NO_2}/P_{NO})^{1/2} \right] \frac{dP_{NO}}{d\zeta} , \quad (C.14)$$

$$-\overline{R}_{NO^*} = \left[k_{G,N_2O_3} K_2 P_{NO} + \frac{1}{4} k_{G,HNO_2} (K_3 P_{H_2O} P_{NO}/P_{NO_2})^{1/2} \right] \frac{dP_{NO_2}}{d\zeta}$$

$$+ \left[k_{G,N_2O_3} K_2 P_{NO_2} + \frac{1}{4} k_{G,HNO_2} (K_3 P_{H_2O} P_{NO_2}/P_{NO})^{1/2} + k_{G,NO} \right] \frac{dP_{NO}}{d\zeta} , \quad (C.15)$$

and

$$-\overline{R}_{\xi} = \left(k_{G,NO_2} + 4k_{G,N_2O_4} K_1 P_{NO_2} \right) \frac{dP_{NO_2}}{d\zeta} - \left(k_{G,NO} \right) \frac{dP_{NO}}{d\zeta} . \quad (C.16)$$

The absorption/desorption of the indicated gas species through the liquid film is represented by:

$$\overline{R}_{NO_2^*} = (Ek_L)_{NO_2} (C^*_{NO_2} - C_{NO_2}) + 2(Ek_L)_{N_2O_4} (C^*_{N_2O_4} - C_{N_2O_4})$$

$$+ (Ek_L)_{N_2O_3} (C^*_{N_2O_3} - C_{N_2O_3}) + \frac{1}{2} (Ek_L)_{HNO_2} (C^*_{HNO_2} - C_{HNO_2}) , \quad (C.17)$$

and

$$\overline{R}_{NO^*} = (Ek_L)_{N_2O_3} (C^*_{N_2O_3} - C_{N_2O_3}) + \frac{1}{2} (Ek_L)_{HNO_2} (C^*_{HNO_2} - C_{HNO_2}) + (Ek_L)_{NO} (C^*_{NO} - C_{NO}) \quad (C.18)$$

Defining E to be 1 for physical absorption and assuming the hydrolysis reactions of N_2O_3 and N_2O_4 to be fast and pseudo-first order, pending justification in Appendix F,

$$\overline{R}_{NO_2^*} = k_{L,NO_2} C^*_{NO_2} + 2(\sqrt{Dk})_{N_2O_4} C^*_{N_2O_4} + (\sqrt{Dk})_{N_2O_3} C^*_{N_2O_3} + \frac{1}{2} k_{L,HNO_2} (C^*_{HNO_2} - C_{HNO_2}) , \quad (C.19)$$

and

$$\overline{R}_{NO^*} = (\sqrt{Dk})_{N_2O_3} C^*_{N_2O_3} + \frac{1}{2} k_{L,HNO_2} (C^*_{HNO_2} - C_{HNO_2}) + k_{L,NO} (C^*_{NO} - C_{NO}) . \quad (C.20)$$

Using the assumption that Henry's Law applies at the gas-liquid interface [$C_i = H_{(i)} P_i$],

$$\overline{R}_{NO_2^*} = (k_L/H)_{NO_2} P^*_{NO_2} + 2(\sqrt{Dk}/H) P^*_{N_2O_4} + (\sqrt{Dk}/H)_{N_2O_3} P^*_{N_2O_3} + \frac{1}{2} (k_L/H)_{HNO_2} P^*_{HNO_2} - \frac{1}{2} k_{L,HNO_2} C_{HNO_2} , \quad (C.21)$$

$$\overline{R}_{NO^*} = (\sqrt{Dk}/H)_{N_2O_3} P^*_{N_2O_3} + \frac{1}{2} (k_L/H)_{HNO_2} P^*_{HNO_2} - \frac{1}{2} k_{L,HNO_2} C_{HNO_2} + (k_L/H)_{NO} P^*_{NO} - k_{L,NO} C_{NO} , \quad (C.22)$$

and

$$\overline{R}_\xi = (k_L/H)_{NO_2} P^*_{NO_2} + 2(\sqrt{\mathcal{D}}k/H)_{N_2O_4} P^*_{N_2O_4} - (k_L/H)_{NO} P^*_{NO} - k_{L,NO} C_{NO} . \quad (C.23)$$

Separating the variables in Equation (C.16) and preparation for integration yields:

$$-\overline{R}_\xi \int_o^\zeta d\zeta = k_{G,NO_2} \int_{P_{NO_2}}^{P^*_{NO_2}} dP_{NO_2} + 4 k_{G,N_2O_4} K_1 \int_{P_{NO_2}}^{P^*_{NO_2}} P_{NO_2} dP_{NO_2} - k_{G,NO} \int_{P_{NO}}^{P^*_{NO}} dP_{NO} . \quad (C.24)$$

Integration of the above equation yields:

$$-\overline{R}_\xi \zeta = k_{G,NO_2} (P^*_{NO_2} - P_{NO_2}) + 2k_{G,N_2O_4} K_1 \left[(P^*_{NO_2})^2 - (P_{NO_2})^2\right] - k_{G,NO} (P^*_{NO} - P_{NO}) . \quad (C.25)$$

Substituting $\overline{R}_\xi$ for the liquid phase, Equation (C.23), into Equation (C.25) yields, after some rearrangement,

$$P^*_{NO} = \frac{aP^*_{NO_2} + b(P^*_{NO_2})^2 - c P_{NO_2} - e P^2_{NO_2} + f P_{NO} + g C_{NO}}{f + h} , \quad (C.26)$$

where

$$a = k_{G,NO_2} + (k_L/H)_{NO_2} ,$$

$$b = 2k_{G,N_2O_4} K_1 + 2(\sqrt{\mathcal{D}}k/H)_{N_2O_4} K_1 ,$$

$$c = k_{G,NO_2} ,$$

$$e = 2k_{G,N_2O_4} K_1 ,$$

$$f = k_{G,NO} ,$$

$$g = k_{L,NO} ,$$

and

$$h = k_{L,NO}/H_{NO} .$$

Equation (C.26) relates P^*_{NO} to P_{NO}, P_{NO_2}, $P^*_{NO_2}$ at a depth ζ in the gas film and is important later in the development.

Rearranging Equation (C.15) yields:

$$-\frac{dP_{NO}}{d\zeta} = \frac{\bar{R}_{NO} + (m)\ (dP_{NO_2}/d\zeta)}{1} , \qquad (C.27)$$

where

$$1 = k_{G,N_2O_3} K_2 P_{NO_2} + \frac{1}{4} k_{G,HNO_2} (K_3 P_{H_2O} P_{NO_2}/P_{NO})^{1/2} + k_{G,NO} ,$$

and

$$m = k_{G,N_2O_3} K_2 P_{NO_2} + \frac{1}{4} k_{G,HNO_2} (K_3 P_{H_2O} P_{NO}/P_{NO_2})^{1/2} .$$

Substitution and rearrangement of Equation (C.27) into Equation (C.14) yields:

$$\frac{dP_{NO_2}}{d\zeta} = \frac{-(1)(\bar{R}_{NO_2^*}) + (m)(\bar{R}_{NO^*})}{(t)(1) - (w)(y)} , \qquad (C.28)$$

where $\bar{R}_{NO_2^*}$ and $\bar{R}_{NO^*}$ are defined in Equations (C.19) and (C.20),

$$t = k_{G,NO_2} + 4\ K_{G,N_2O_4}\ K_1\ P_{NO_2} + k_{G,N_2O_3}\ K_2\ P_{NO} + \frac{1}{4}\ k_{G,HNO_2}(K_3 P_{H_2O} P_{NO}/P_{NO_2})^{1/2} ,$$

$$w = k_{G,N_2O_3}\ K_2\ P_{NO_2} + \frac{1}{4}\ k_{G,HNO_2}\ (K_3 P_{H_2O} P_{NO_2}/P_{NO})^{1/2} ,$$

and

$$y = k_{G,N_2O_3}\ K_2\ P_{NO} + \frac{1}{4}\ k_{G,HNO_2}\ (K_3 P_{H_2O} P_{NO}/P_{NO_2})^{1/2} .$$

This equation for P^*_{NO} has been solved numerically by a "shooting" method using subroutines RKF45 and ZEROIN (Forsythe, Malcolm, and Moler, 1977); this solution process requires the simultaneous solution of Equation (C.26) for P^*_{NO}. The absorption of HNO_2 is not allowable by the mathematical model presented in Chapter V. In order to prevent the absorption of HNO_2, the single component flux of HNO_2 is tested; if the flux is absorptive then k_{L,HNO_2} is made equal to zero. This will allow the desorption of HNO_2 and prevent its absorption.

APPENDIX D

THE DEPLETION OF AQUEOUS NITROUS ACID IN PACKED TOWERS

The depletion of nitrous acid from aqueous nitric–nitrous acid solutions during contact with various gases was investigated using columns packed with Intalox saddles as the contacting device. These studies were conducted at 298 K and near atmospheric pressure. The liquid phase was recirculated in these studies. These studies were designed to estimate the effects of gas flow rate, liquid flow rate, column height, and the oxygen content of the contacting gas on the depletion process(es).

The primary response variable was the conversion or removal efficiency of aqueous nitrous acid in the packed tower,

$$X_{HNO_2} = \frac{C_{HNO_2,in} - C_{HNO_2,out}}{C_{HNO_2,in}} . \qquad (D.1)$$

Other response variables were the molar ratio of HNO_3 produced to HNO_2 disappearing, R*, and the molar ratio of NO produced to HNO_2 disappearing, R**. These parameters are indicators of the extent that Reaction (28f),

$$3HNO_2\ (\ell) \rightarrow HNO_3\ (\ell) + H_2O\ (\ell) + 2NO\ (g)\ ,$$

describes the depletion process. If Reaction (28f) is completely descriptive then R* and R** should be -1/3 and -2/3 respectively. If the depletion involves the desorption of N_2O_3 or HNO_2 as described in terms of an overall reaction by

$$2HNO_2\ (\ell) \rightarrow NO\ (g) + NO_2\ (g) + H_2O\ (\ell)\ , \qquad (D.2)$$

the values of R* and R** will be 0 and -1/2 respectively. In experiments involving the contact of nitrous acid solutions with nitrogen, the hypothesis that R* and R** are -1/3 and -2/3 or that these quantities are 0 and -1/2 will be tested. In other experiments, the extent that the presence of oxygen in the contact gases influence R* and R** will be studied.

The feed gas to the column during these operations contains no NO; an analysis for NO in the effluent gas was conducted during later runs. In all runs, the feed and effluent liquid streams were sampled. These samples were analyzed for total acidity and nitrous acid; the total acidity was assumed to be attributed to the sum of the nitric and nitrous acids. Based on this assumption, the change in total acid concentration can be represented by:

$$dC_{H^+} = dC_{HNO_3} + dC_{HNO_2}\ . \qquad (D.3)$$

The quantity, R*, can be obtained by a rearrangement of Equation (D.3);

$$R^* = \frac{dC_{HNO_3}}{dC_{HNO_2}} = \frac{dC_{H^+}}{dC_{HNO_2}} - 1\ . \qquad (D.4)$$

The rate of change in nitrous acid concentration in the system is related to the production rate of NO in the off-gas from the tower by:

$$V_{L,T}\ \frac{dC_{HNO_2}}{dt} = \left(\frac{1}{R^{**}}\right) \frac{G\ P_{NO,out}}{RT}\ . \qquad (D.5)$$

Thus R** may be obtained by:

$$R^{**} = \left(\frac{G}{V_{L,T}RT}\right) \frac{P_{NO,out}}{dC_{HNO_2}/dt} \quad . \tag{D.6}$$

In these studies, nitrous acid was produced initially by bubbling N_2O_3 through 0.025 m^3 of water in the liquid hold-up tank; nitric acid is produced simultaneously by some decomposition of HNO_2 (see also Chapter IV). This aqueous solution was then metered continuously to the packed column where it was contacted with the selected gas-nitrogen, air, or oxygen. The effluent solution from the column flowed by gravity back to the liquid hold-up tank. Recirculation of this solution provided a means of obtaining information on the depletion process(es) over a range of nitrous acid concentrations. The two packed towers used in these studies were 0.0762-m-ID with 6-mm Intalox saddles and 0.102-m-ID with 13-mm Intalox saddles. The feed and effluent liquid streams were sampled for total acid and nitrous acid. In the studies with the 0.102-m tower, the off-gas was also analyzed for NO. The experimental data for the described studies is presented in Tables D.1 through D.4. The data was usually taken by duplicate sampling.

D.1. Analysis of X_{HNO_2} from the Studies with the 0.0762-m-ID Column

The first series of experiments, A through D, utilized a 2^{3-1} factorial design to study the effect of gas flow rate, liquid flow rate, and packing height (volume) on the extent of nitrous acid conversion, X_{HNO_2}, in the small diameter tower. The concentrations of nitrous acid

Table D.1. Data from the depletion of aqueous nitrous acid studies (runs A-D) conducted in a 0.0762-m-ID tower packed with 6-mm Intalox saddles[a] (Duplication of samples are shown)

Run	Time (s)	L^b ($m^3\ s^{-1} \times 10^5$)	G_{in}^b (std $m^3\ s^{-1} \times 10^4$)	H (m)	Gas (N_2-air-O_2)	$C_{HNO_2,in}$ (kg·mol m^{-3})	$C_{HNO_2,in}$ (kg·mol m^{-3})	$C_{HNO_2,out}$ (kg·mol m^{-3})	$C_{HNO_2,out}$ (kg·mol m^{-3})	$C_{H^+,in}$ (kg·mol m^{-3})	$C_{H^+,in}$ (kg·mol m^{-3})	$C_{H^+,out}$ (kg·mol m^{-3})	$C_{H^+,out}$ (kg·mol m^{-3})
A	0	1.70	3.27	0.15	N_2	0.0478	0.0457			0.0924	0.0719		
	1,800	1.70	3.27	0.15	N_2	0.0445	0.0440	0.0349	0.0393	0.1068	0.1081	0.1036	0.1028
	3,600	1.70	3.27	0.15	N_2	0.0376	0.0375	0.0347	0.0347	0.1036	0.1028	0.1019	0.1020
	5,400	1.70	3.27	0.15	N_2	0.0335	0.0334	0.0309	0.0311	0.0976	0.0968	0.0948	0.0972
	7,200	1.70	3.27	0.15	N_2	0.0293	0.0294	0.0274	0.0273	0.0960	0.0956	0.0948	0.0937
	9,000	1.70	3.27	0.15	N_2	0.0257	0.0257	0.0244	0.0245	0.0936	0.0938	0.0927	0.0926
	10,800	1.70	3.27	0.15	N_2	0.0230	0.0219	0.0222	0.0214	0.0910	0.0898	0.0891	0.0896
B	0	3.45	3.19	0.30	N_2	0.0708	0.0705			0.1507	0.1539		
	1,800	3.40	3.19	0.30	N_2	0.0482	0.0480	0.0429	0.0442	0.1313	0.1293	0.1281	0.1296
	3,600	3.35	3.19	0.30	N_2	0.0346	0.0343	0.0299	0.0319	0.1254	0.1219	0.1184	0.1198
	5,400	3.70	3.19	0.30	N_2	0.0267	0.0273	0.0256	0.0255	0.1165	0.1168	0.1144	0.1161
	7,200	3.70	3.19	0.30	N_2	0.0228	0.0220	0.0207	0.0207	0.1124	0.1110	0.1109	0.1100
	9,000	3.45	3.19	0.30	N_2	0.0185	0.0186	0.0179	0.0189	0.1114	0.1100	0.1041	0.1090
	10,800	3.30	3.19	0.30	N_2	0.0139	0.0149	0.0140	0.0143	0.1079	0.1065	0.1065	0.1065
	12,600	3.30	3.19	0.30	N_2	0.0127	0.0128	0.0112	0.0114	0.1059	0.1051	0.0996	0.1051
C	0	1.25	1.70	0.30	N_2	0.0558	0.0563			0.1332	0.1326		
	1,800	1.05	1.70	0.30	N_2	0.0480		0.0440		0.1464		0.1440	
	3,600	1.55	1.70	0.30	N_2	0.0416		0.0378		0.1413		0.1403	
	5,400	1.70	1.70	0.30	N_2	0.0366		0.0340		0.1387		0.1361	
	7,200	1.60	1.70	0.30	N_2	0.0312		0.0295		0.1352		0.1330	
	9,000	1.75	1.70	0.30	N_2	0.0273		0.0253		0.1322		0.1299	
	10,800	1.60	1.70	0.30	N_2	0.0237		0.0225		0.1284		0.1280	
	12,600	1.60	1.70	0.30	N_2	0.0205		0.0191		0.1276		0.1260	
	14,400	1.60	1.70	0.30	N_2	0.0179		0.0164		0.1250		0.1248	
D	0	3.45	1.70	0.15	N_2	0.0539	0.0549			0.1244	0.1193		
	1,800	3.50	1.70	0.15	N_2	0.0413	0.0409	0.0376	0.0387	0.1188	0.1125	0.1097	0.1044
	3,600	3.40	1.70	0.15	N_2	0.0357	0.0353	0.0339	0.0337	0.1142	0.1107	0.1124	0.1133
	5,400	3.45	1.70	0.15	N_2	0.0198	0.0198	0.0211	0.0191	0.1082	0.1084	0.1056	0.1068
	7,200	3.65	1.70	0.15	N_2	0.0242	0.0241	0.0227	0.0233	0.1036	0.1060	0.1043	0.1032
	9,000	3.50	1.70	0.15	N_2	0.0240	0.0232	0.0227	0.0227	0.1040	0.1032	0.1024	0.1024
	10,800	3.50	1.70	0.15	N_2	0.0215	0.0216	0.0210	0.0206	0.1012	0.1016	0.1012	0.1008
	12,600	3.40	1.70	0.15	N_2	0.0196	0.0195	0.0188	0.0189	0.1012			

[a] Temperature = 298 K; total pressure = 1.10 atm.

[b] The tabulated numbers have been multiplied by the indicated factor.

Table D.2. Data from the depletion of aqueous nitrous acid studies (runs E and F) conducted in a 0.0762-m-ID tower packed with 6-mm Intalox saddles[a] (Duplication of samples is shown)

Run	Time (s)	L^b ($m^3\ s^{-1} \times 10^5$)	$G_{in}{}^b$ (std $m^3\ s^{-1} \times 10^4$)	H (m)	Gas (N_2-air-O_2)	$C_{HNO_2,in}$ (kg·mol m^{-3})	$C_{HNO_2,in}$ (kg·mol m^{-3})	$C_{HNO_2,out}$ (kg·mol m^{-3})	$C_{HNO_2,out}$ (kg·mol m^{-3})	$C_{H^+,in}$ (kg·mol m^{-3})	$C_{H^+,in}$ (kg·mol m^{-3})	$C_{H^+,out}$ (kg·mol m^{-3})	$C_{H^+,out}$ (kg·mol m^{-3})
E	0	1.62	3.33 E-4	0.15	Air	0.0521	0.0552			0.1256	0.1284		
	1,800	1.67	3.33 E-4	0.15	Air	0.0473	0.0473	0.0431	0.0426	0.1152	0.1284	0.1244	0.1280
	3,600	1.67	3.33 E-4	0.15	Air	0.0405	0.0404	0.0368	0.0369	0.1248	0.1268	0.1252	0.1224
	5,400	1.67	3.33 E-4	0.15	Air	0.0353	0.0350	0.0350	0.0326	0.1252	0.1264	0.1220	0.1232
	7,200	1.67	3.33 E-4	0.15	Air	0.0299	0.0307	0.0281	0.0303	0.1240	0.1220	0.1228	0.1228
	9,000	1.62	3.33 E-4	0.15	Air	0.0255	0.0256	0.0238	0.0235	0.1228	0.1238	0.1240	0.1200
	10,800	1.52	3.33 E-4	0.15	Air	0.0221	0.0222	0.0204	0.0215	0.1212	0.1188	0.1208	0.1212
	12,600	1.67	3.33 E-4	0.15	Air	0.0199	0.0199	0.0198	0.0168	0.1212	0.1212	0.1200	0.1200
F	0	1.79	3.30 E-4	0.15	O_2	0.0529	0.0525			0.1154	0.1156		
	1,800	1.79	3.30 E-4	0.15	O_2	0.0435		0.0347		0.1058		0.1005	
	3,600	1.84	3.30 E-4	0.15	O_2	0.0359		0.0322		0.1024		0.0994	
	5,400	1.84	3.30 E-4	0.15	O_2	0.0294		0.0261		0.0993		0.0976	
	7,200	1.84	3.30 E-4	0.15	O_2	0.0243		0.0215		0.0988		0.0980	
	9,000	1.79	3.30 E-4	0.15	O_2	0.0185		0.0166		0.0978		0.0970	
	10,800	1.79	3.30 E-4	0.15	O_2	0.0128		0.0118		0.0965		0.0963	

[a] Temperature = 298 K; total pressure = 1.10 atm.
[b] The tabulated numbers have been multiplied by the indicated factor.

Table D.3. Data from the depletion of nitrous acid studies (run G) conducted in a 0.102-m-ID tower packed with 13-mm Intalox saddles[a] (Duplication of samples are shown)

Time (s)	Temperature (K)	$C_{HNO_2,in}$ (kg·mol m^{-3})	$C_{HNO_2,in}$ (kg·mol m^{-3})	$C_{HNO_2,out}$ (kg·mol m^{-3})	$C_{HNO_2,out}$ (kg·mol m^{-3})	$C_{H^+,in}$ (kg·mol m^{-3})	$C_{H^+,in}$ (kg·mol m^{-3})	$C_{H^+,out}$ (kg·mol m^{-3})	$C_{H^+,out}$ (kg·mol m^{-3})	$P_{NO,out}$[b] (std atm × 10^4)
0	299	0.0190	0.0183	0.0161	0.0164	0.082	0.0800	0.081	0.0770	7.60
1200	299	0.0143	0.0142	0.0120	0.0123	0.080	0.0798	0.079	0.0782	5.00
2400	300	0.0109	0.0110	0.0090	0.0093	0.077	0.0782	0.077	0.0772	3.20
3600	300	0.0085	0.0090	0.0076	0.0073	0.076	0.0766	0.076	0.0770	2.60
4800	300	0.0074	0.0071	0.0064	0.0064	0.075	0.0752	0.075	0.0742	2.00
6000	300	0.0055	0.0052	0.0052	0.0055	0.074	0.0748	0.074	0.0744	1.30
7200	300	0.0044	0.0047	0.0042	0.0047	0.073	0.0752	0.073	0.0750	1.00

[a] The liquid that collected in the off-gas demister at 298 K had a total volume of 2.7×10^{-4} m^3 and a total acid and nitrous acid concentration of 0.14- and 0.0071-kg mol m^{-3} respectively. (Liquid rate = 3.58×10^{-5} m^3 s^{-1}, gas rate = 1.46×10^{-3} std m^3 s^{-1}, contact gas = N_2, height of packing = 0.81 m, total pressure = 1.10 atm.)

[b] The tabulated numbers have been multiplied by the indicated factor.

Table D.4. Data from the depletion of nitrous acid studies (run II) conducted in a 0.102-m-ID column packed with 13-mm Intalox saddles[a]

Time (s)	Temperature (t_{in}) (K)	$C_{HNO_2,in}$ (kg-mol m^{-3})	$C_{HNO_2,out}$ (kg-mol m^{-3})	$C_{H^+,in}$ (kg-mol m^{-3})	$C_{H^+,out}$ (kg-mol m^{-3})	$P_{NO,out}$ atm
0	298			0.28	0.27	0.00615
60				0.279	0.268	
240		0.0701	0.0672			
300		0.0767	0.0658			0.00510
420				0.26	0.26	0.00385
1,080	297			0.262	0.245	
1,140						
1,380		0.0588	0.0619			
1,440		0.0591	0.0584			0.00295
1,800						0.00270
2,100				0.25	0.25	
2,160	297			0.250	0.246	
2,280						0.00220
2,340						
2,460		0.0430	0.0300			
2,580		0.0417	0.0349			0.00190
2,700				0.24	0.24	
3,660	297			0.230	0.236	
3,780						0.00135
3,900		0.0287	0.0252			
4,020		0.0284	0.0241			0.00125
4,140				0.23	0.23	
4,860	297			0.235	0.232	
4,980						0.00095
5,100		0.0222	0.0194			
5,220		0.0210	0.0180			0.00080
5,340				0.23	0.20	
6,060	297			0.228	0.228	
6,240						0.00065
6,300		0.0160	0.0139			
6,360		0.0156	0.0137			0.00062
6,480				0.23	0.22	
7,260	297			0.227	0.226	
7,380						0.00048
7,440						
7,500		0.0122	0.0108			
7,560		0.0119	0.0104			0.00044
7,620				0.22	0.22	
8,400	297			0.225	0.224	
8,460						
8,580		0.0105	0.0095			
8,640		0.0102	0.0085			0.00034
8,700				0.22	0.22	
9,660	297			0.225	0.225	
9,840						
10,020		0.0076	0.0070			
10,200		0.0075	0.0070			0.00026
10,260						

[a] Liquid rate = 3.6×10^{-5} m^3 s^{-1}, gas rate = 1.56×10^{-3} std m^3 s^{-1}, contact gas = N_2, height of packing = 0.81 m, total pressure = 1.41 atm.

in the feed and effluent streams vs experimental time for these runs are shown in Figures D.1 through D.4. The Equation (D.7) was fit to data from runs A, B, and C,

$$\log C_{HNO_2} = a + b\ (t)\ ; \tag{D.7}$$

while Equation (D.8) was used to fit the data from run D,

$$(C_{HNO_2})^{-1} = a = b\ (t)\ . \tag{D.8}$$

The unknown constants, a and b, were estimated by method of least squares and are listed in Table D.5. The calculated values of the inlet and outlet nitrous acid concentrations were used to compare the conversion of nitrous acid at points of equal concentration. The effects shown in Table D.6 were estimated by a Yates algorithm [Box, Hunter, and Hunter (1978)]. A main effect is the average change in response per unit change in process variable.

This analysis shows that as the concentration of nitrous acid entering the tower is increased: (1) the effect of the change in liquid flow rate (L) decreases (actually shown to impede the depletion of nitrous acid at higher nitrous acid concentrations), (2) the effect of gas rate (G) increases, and (3) the effect of the change in height (H) generally decreases.

Another way of viewing the effects of the independent variables is to show the effect in a relative sense. The relative main effects are obtained by dividing the effect given in Table D.6 by the average HNO_2 conversion; the relative main effect of variable i is

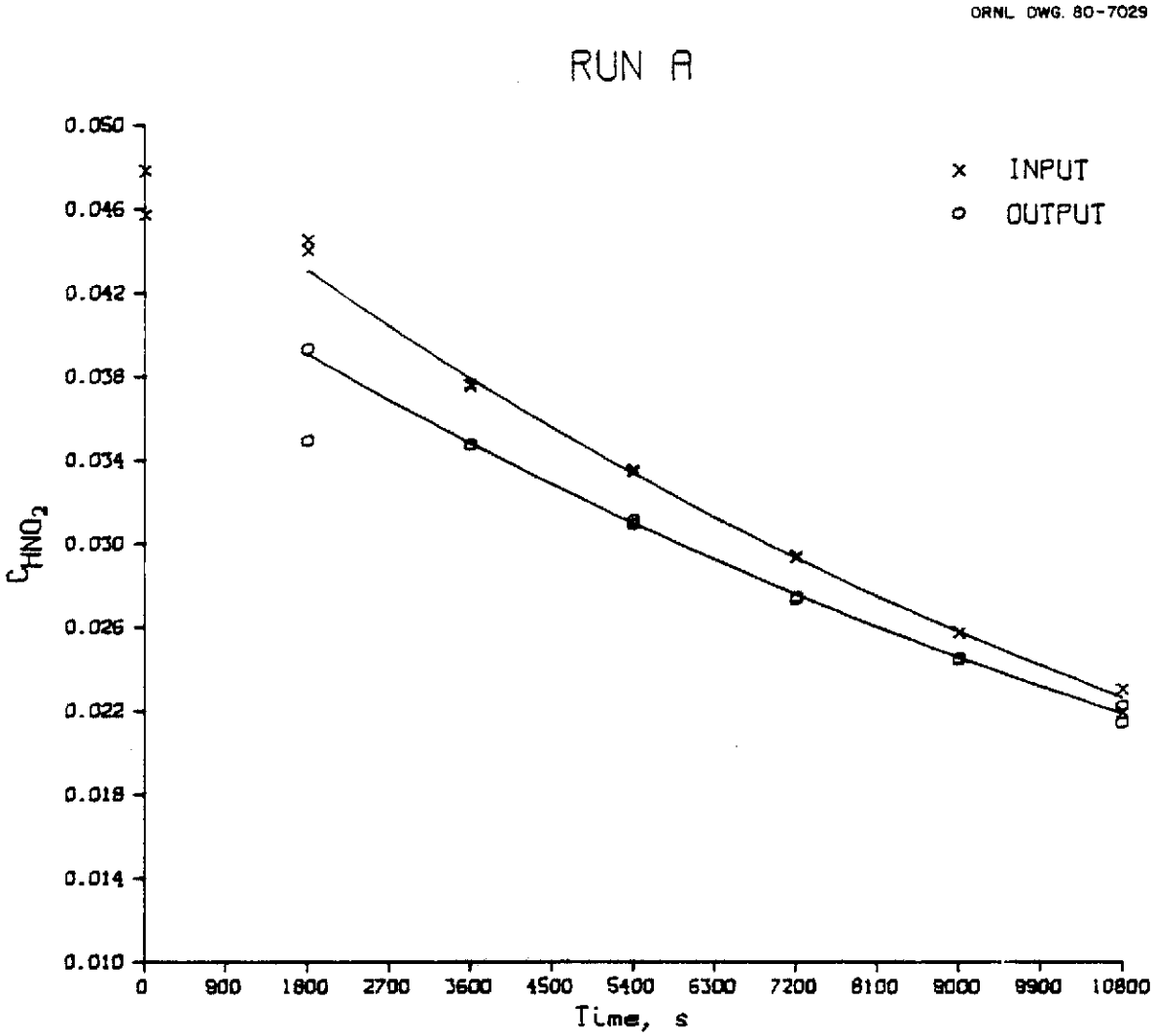

Figure D.1. Column feed and effluent nitrous acid concentrations vs time for experiment A.

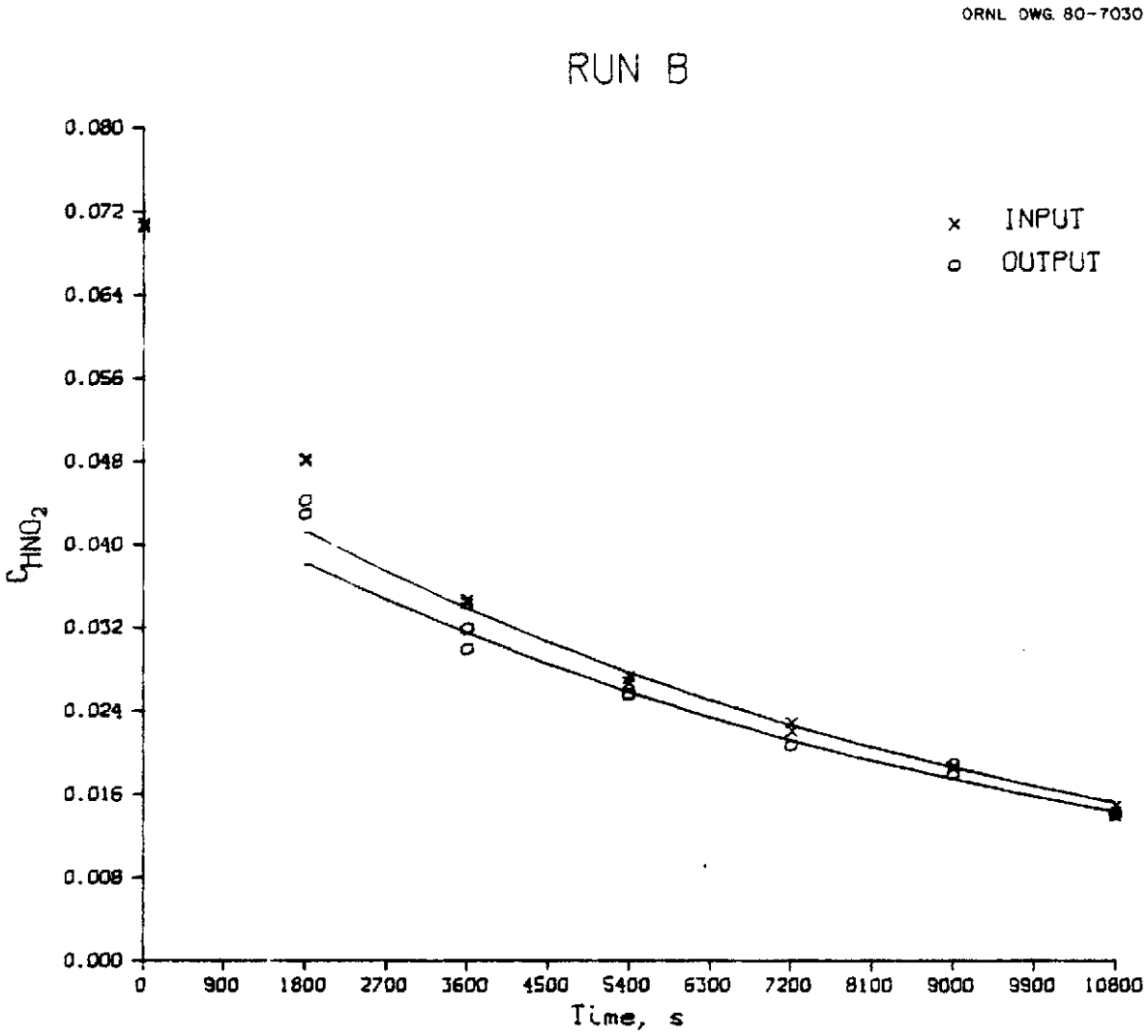

Figure D.2. Column feed and effluent nitrous acid concentrations vs time for experiment B.

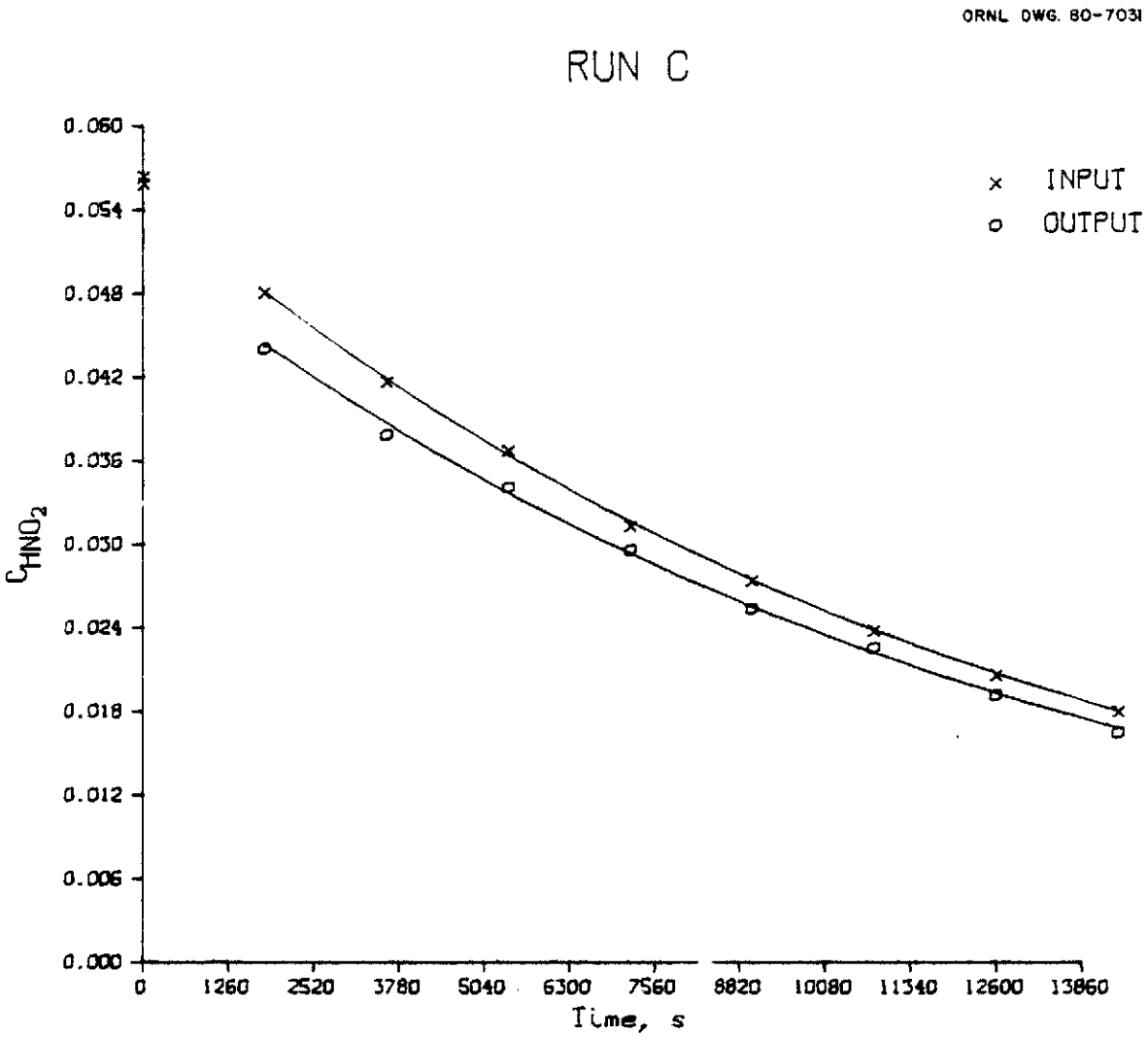

Figure D.3. Column feed and effluent nitrous acid concentrations vs time for experiment C.

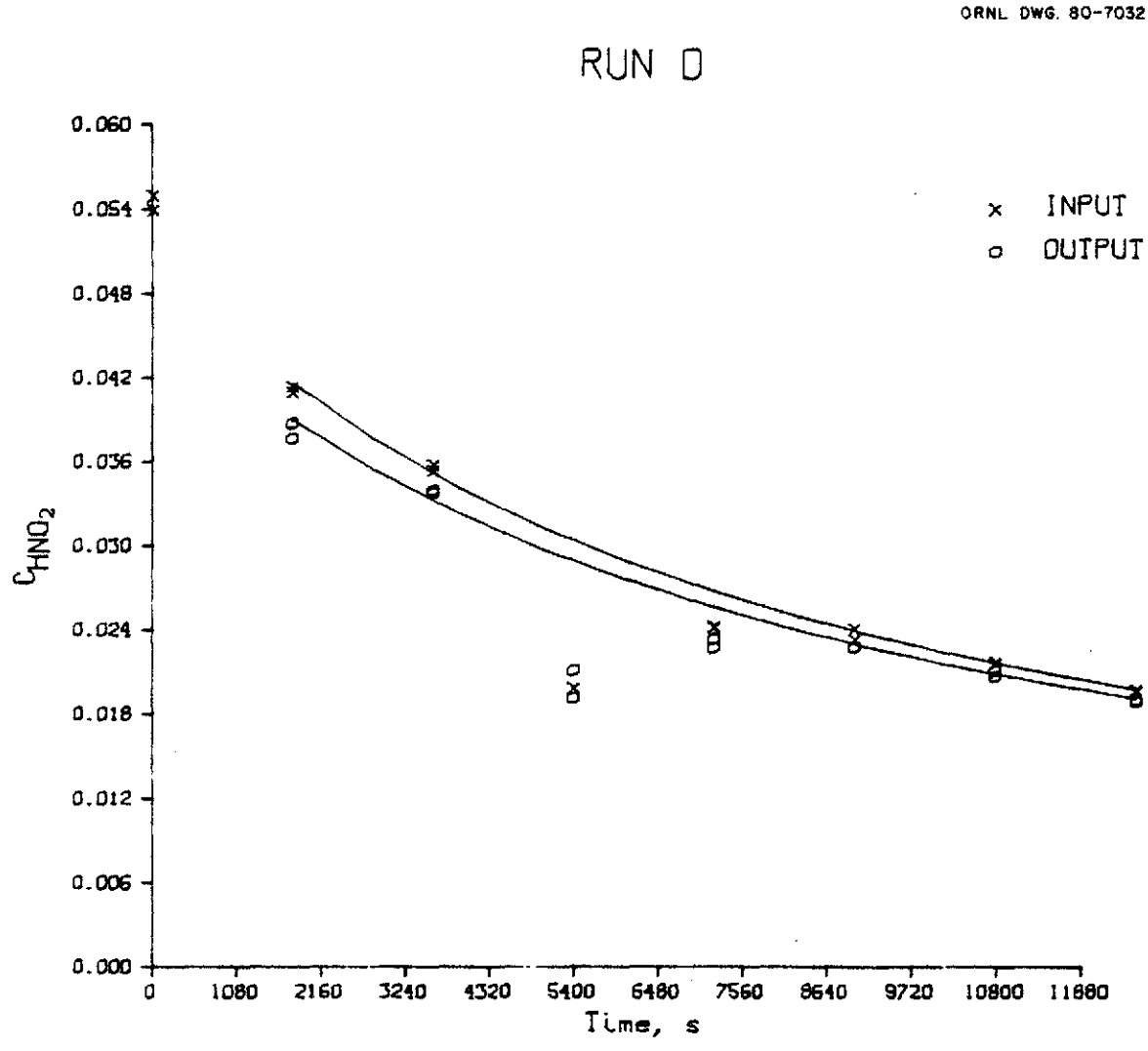

Figure D.4. Column feed and effluent nitrous acid concentrations vs time for experiment D.

Table D.5. Coefficients used in the fitting of the HNO_2 concentrations vs time data

Run	Coefficient	
	a	b
A (inlet)	-1.31	-3.118×10^{-5}
(outlet)	-1.358	-2.816×10^{-5}
B (inlet)	-1.298	-4.856×10^{-5}
(outlet)	-1.333	-4.771×10^{-5}
C (inlet)	-1.257	-3.412×10^{-5}
(outlet)	-1.293	-3.365×10^{-5}
D (inlet)	19.552	0.00250
(outlet)	21.178	0.00252

Table D.6. Experimental depletion conversions of HNO_3 for a 2^{3-1} factorial study of the depletion of nitrous acid in packed towers

Variables	-(low)	+(high)
L (scrubber liquid flow rate), $m^3\ s^{-1}$	1.75×10^{-5}	3.50×10^{-5}
G (feed gas flow rate), $m^3\ s^{-1}$	1.57×10^{-4}	3.24×10^{-4}
H (packing height), m	0.15	0.30

Variable arrangement				Removal efficiencies (X_{HNO_2}) at varied $C_{HNO_2,in}$				
				$C_{HNO_2,in}$				
Run	L	G	H	0.015	0.020	0.025	0.030	0.035
A	-	+	-	-0.0035	0.0240	0.0449	0.0616	0.0750
B	+	+	+	0.0579	0.0626	0.0663	0.0692	0.0718
C	-	-	+	0.0637	0.0674	0.0703	0.0726	0.0746
D	+	-	-	0.0268	0.0340	0.0412	0.0482	0.0551
Average				0.0380	0.0470	0.0557	0.0629	0.0691
Effects of Variable (Yates method):								
			L	+0.009	+0.003	-0.0039	-0.008	-0.012
			G	-0.018	-0.007	-0.002	+0.005	+0.009
			H	+0.049	+0.036	+0.0253	+0.016	+0.008

$$\phi_i = \left(\frac{\text{main effect of i on } X_{HNO_2}}{\text{average } X_{HNO_2}} \right)_{C_{HNO_2}} . \qquad (D.9)$$

The relative effects of L, G, and H, shown in Figure D.5 as ϕ_L, ϕ_G, and ϕ_H, change as a function of the feed concentrations of nitrous acid, $C_{HNO_2,in}$. The relative effect of the change in column height, ϕ_H, decreases from near unity to near zero as the concentration of nitrous acid increases over the range of $C_{HNO_2,in}$. The effect of the liquid rate likewise becomes less prominent with increasing nitrous acid strength. However, the gas rate effect becomes increasingly more pronounced as the concentration of nitrous acid increases.

If it is assumed that mass-transfer is important to some extent in this depletion process, then it seems appropriate to view these experiments from a vantage point that includes how the indicated variable manipulation affects the mass-transfer resistances. The increased column height is directly proportional to interfacial area and liquid- and gas-residence time in the tower. The increase in liquid flow rate increases both the liquid-phase mass-transfer rate constant(s) and the gas-liquid interfacial area. The increase in gas flow rate increases the gas-phase mass-transfer rate constant(s). Based on the assumption of the importance of mass-transfer on the depletion of aqueous nitrous acid, the following theory may be proposed for experiments A through D:
(1) liquid-phase mass-transfer is becoming less important with increasing nitrous acid concentration, while the converse is true for the gas-phase mass-transfer; in other words, the primary mass-transfer resistance is

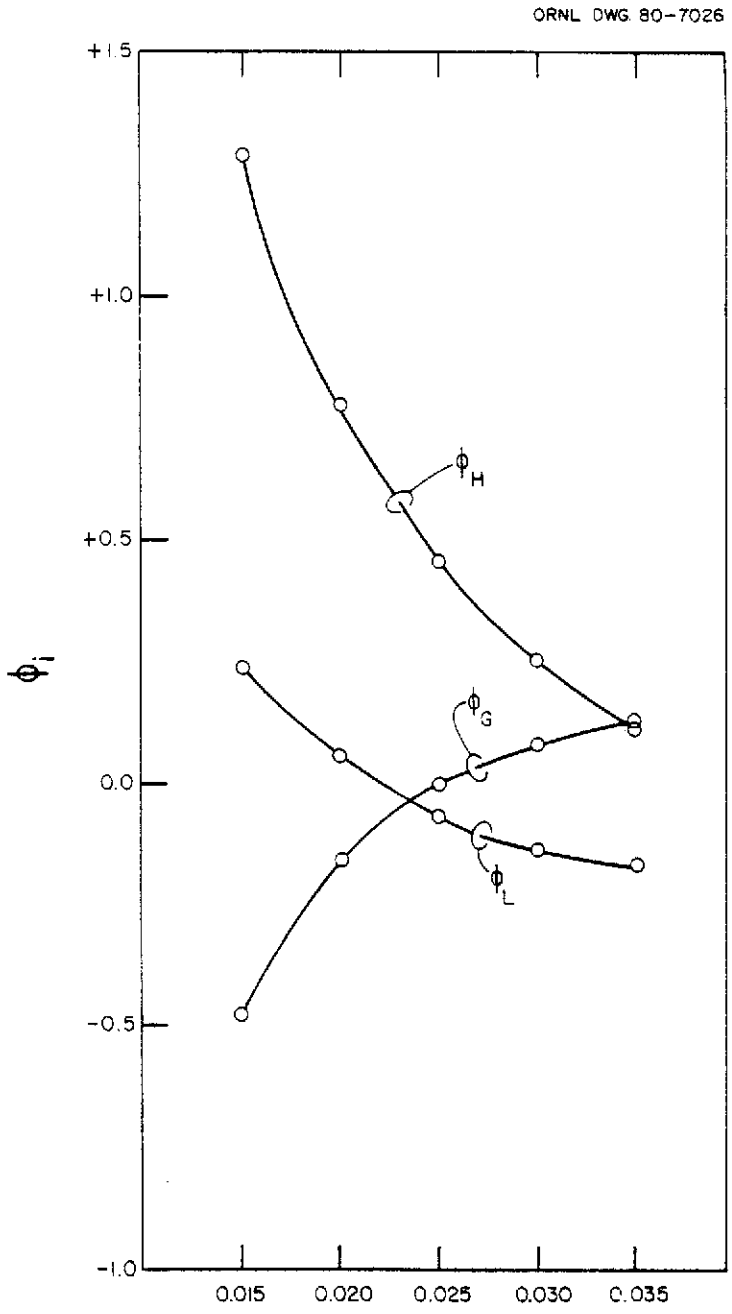

Figure D.5. The relative main effects of the manipulation of L, G, and H on X_{HNO_2} at varying $C_{HNO_2,in}$.

shifting from the liquid to the gas-phase with increased nitrous acid concentration, and (2) the effect of additional interfacial area and residence times becomes of less importance with increasing nitrous acid strength.

D.2. Analysis of R* from the Studies with the 0.0762-m-ID Column

The feed concentrations of total and nitrous acid to the contactor, $C_{H^+,in}$ and $C_{HNO_2,in}$, represent the system concentrations at a given time, assuming that the liquid hold-up tank is well mixed. Thus, the quantity, R*, may be determined from the slope of C_{H^+} as a function of C_{HNO_2}. These plots are presented in Figures D.6 through D.9. The values of R* for experiments A through D and a 95% confidence interval is presented in Table D.7. On the basis of the information in Table D.7, the hypothesis that R* is zero is rejected with 95% confidence; the hypothesis that R* is -1/3 cannot be rejected. From the median values of R*, it would seem to indicate that Reaction (28f) is dominant and Reaction (D.1) is also involved to a limited extent in the depletion of aqueous HNO_2.

D.3. The Effect of Air and O_2 on X_{HNO_2} and R* from the Studies with the 0.0762-m-ID Column

Experiment A was rerun in experiments E and F with air and oxygen as the respective contact gases. The purpose of these runs was to determine the role that oxygen played in the depletion process(es). Since the direct or indirect oxidation of nitrous acid is a known phenomena, it was anticipated that oxygen would affect to some extent the HNO_2

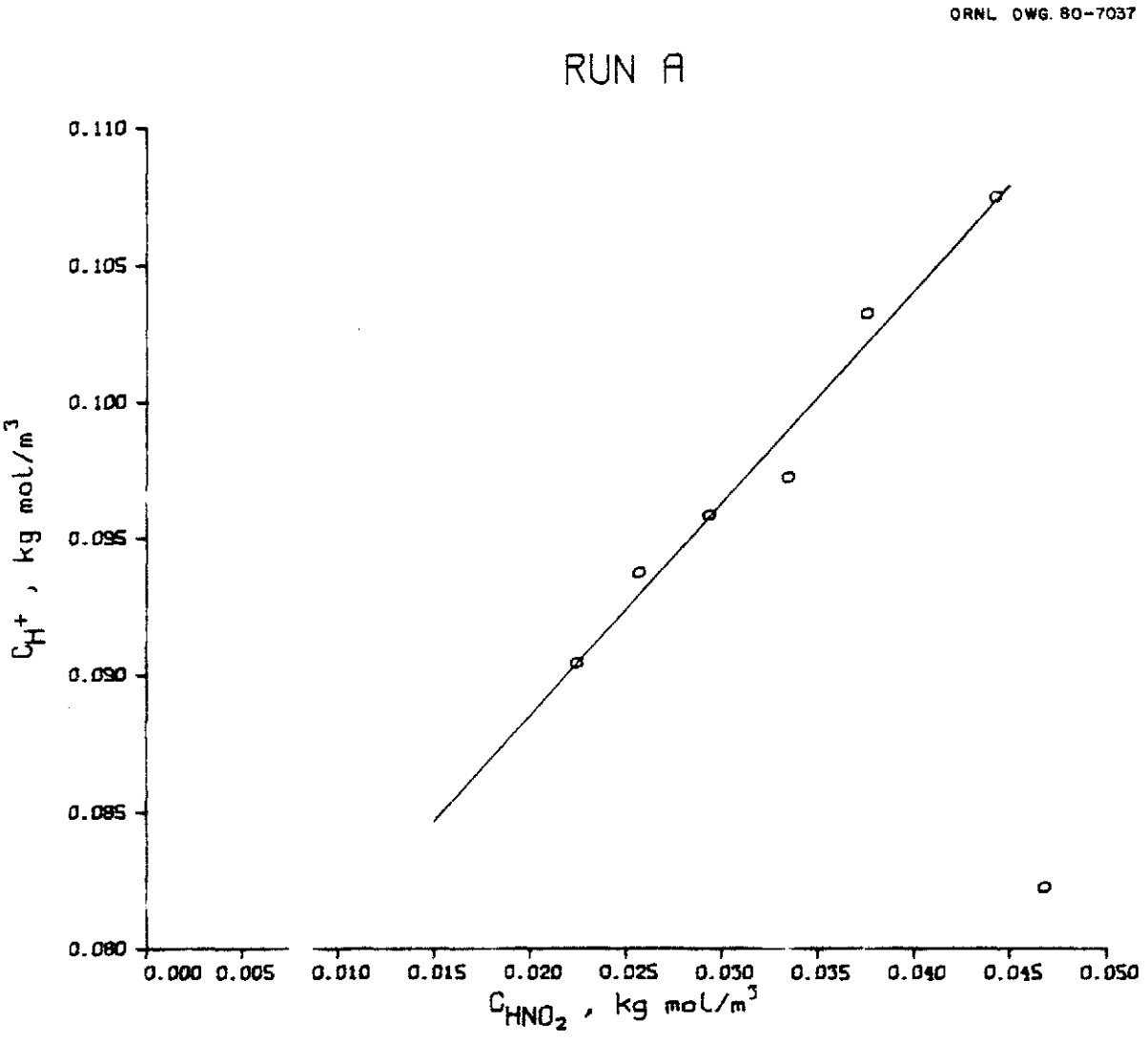

Figure D.6. The change in the system total acid concentration as a function of the changing nitrous acid concentration in experiment A.

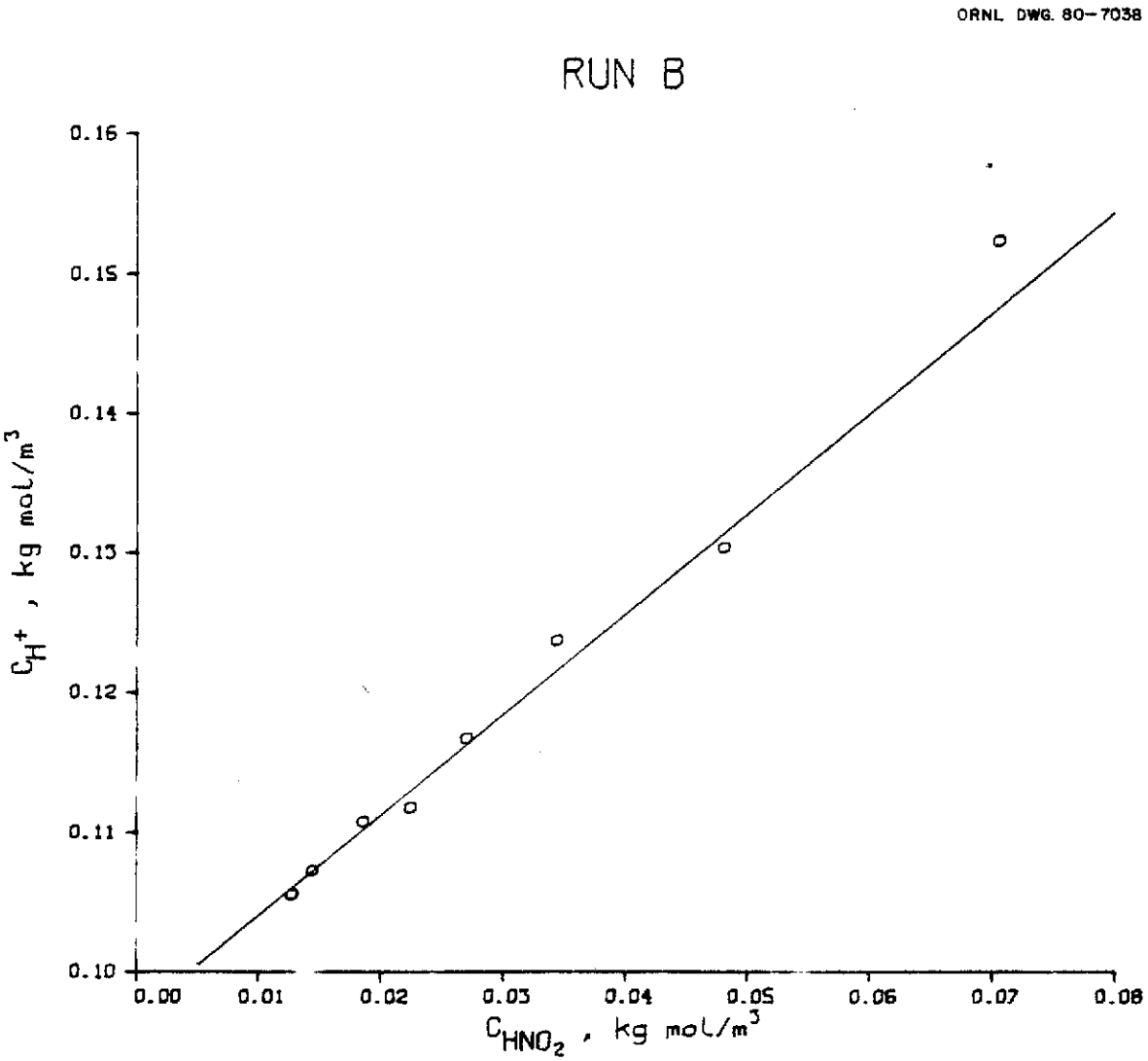

Figure D.7. The change in the system total acid concentration as a function of the changing nitrous acid concentration in experiment B.

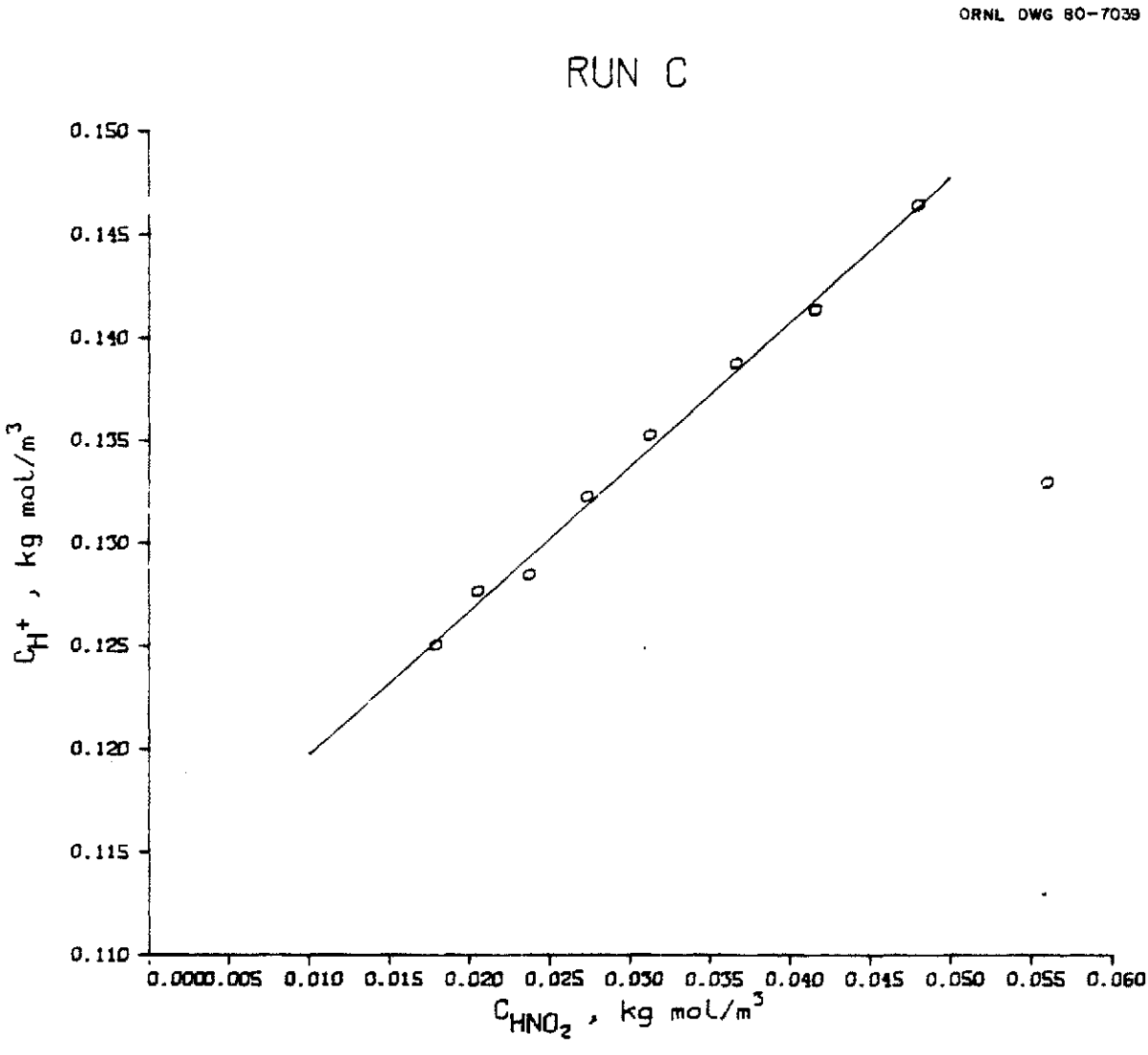

Figure D.8. The change in the system total acid concentration as a function of the changing nitrous acid concentration in experiment C.

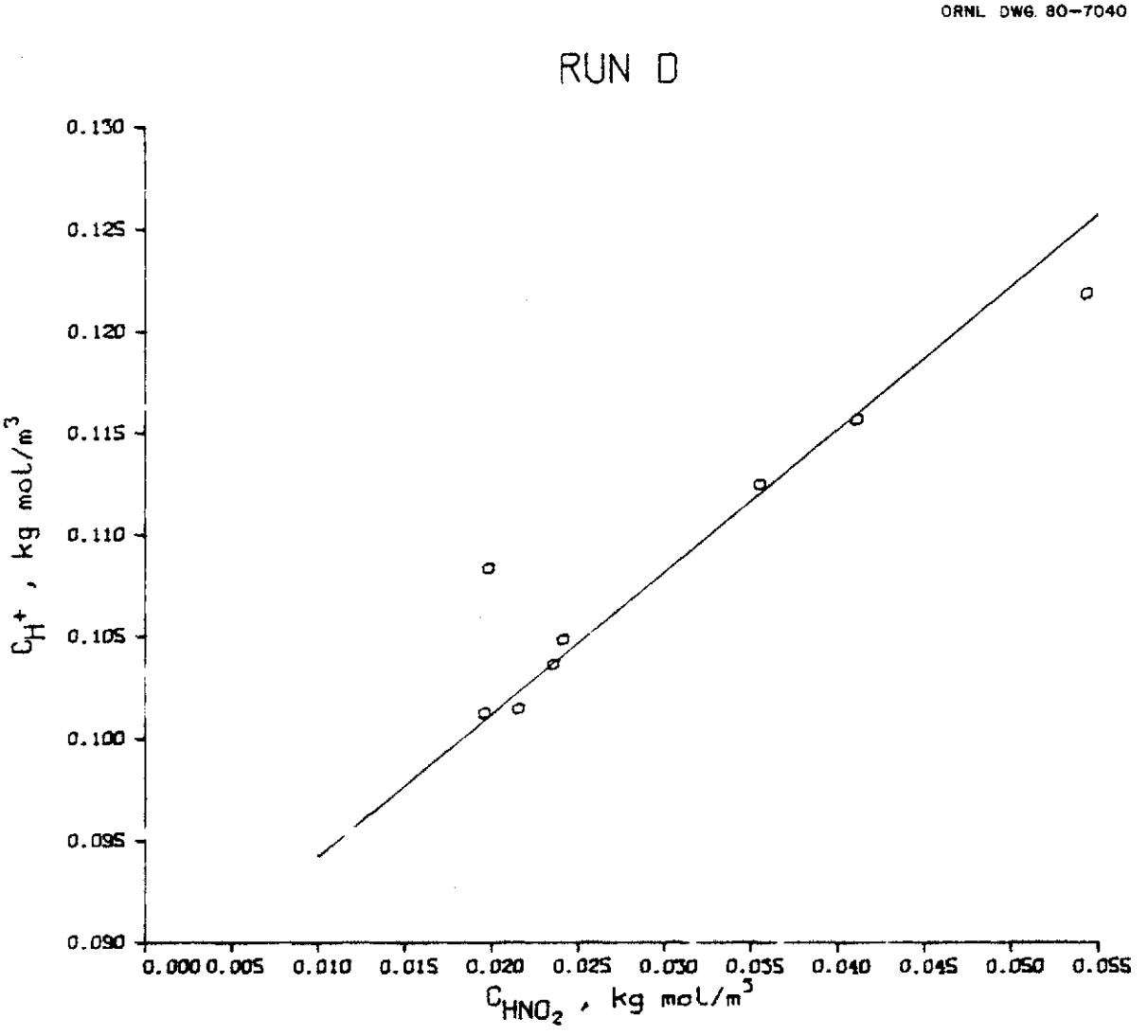

Figure D.9. The change in the system total acid concentration as a function of the changing nitrous acid concentration in experiment D.

Table D.7. Values of R* and a 95% confidence interval for experiments A through D

Run	(dC_{H^+}/dC_{HNO_2})	Degrees of freedom	95% confidence interval about (dC_{H^+}/dC_{HNO_2})
A	0.78	4	(0.61, 0.95)
B	0.72	5	(0.62, 0.82)
C	0.70	6	(0.65, 0.75)
D	0.70	4	(0.61, 0.79)

Run	R*	95% confidence interval about R*
A	-0.22	(-0.39, -0.05)
B	-0.28	(-0.39, -0.18)
C	-0.30	(-0.35, -0.25)
D	-0.30	(-0.39, -0.21)

conversion, X_{HNO_2}, or the ratio of nitric acid produced to nitrous acid disappearing, R*.

The feed and effluent nitrous acid concentrations vs time are shown in Figures D.10 and D.11 for runs E and F respectively. The unknown constants in Equation (D.6) were estimated from the concentrations in experiments E and F and are listed in Table D.8. From the slope of the logarithm of $C_{HNO_2,in}$ vs time, the following observations were made: (1) Little effect of oxygen on the conversion of nitrous acid was noted when comparing runs A and E (Tables D.5 and D.8); however, the conversion is remarkably different for runs A and F. (2) This data indicate that oxygen has little effect on the depletion rate at air concentrations but can have a substantial impact on the rate when pure oxygen is used as the constant gas.

The ratio of the production of nitric acid to the depletion of nitrous acid was also studied in experiments E and F. Plots of the change in total acidity vs nitrous acid are presented in Figures D.12 and D.13. The value of R*, as shown in Table D.8, increases to about 0.8 in these experiments as the partial pressure of oxygen in the contact gas is increased to near 1. This effect is significantly different from 0 or -1/3 at a 95% level and indicates that nitrous acid is being oxidized by the overall equation,

$$2HNO_2\ (\ell) + O_2\ (\ell) \rightarrow 2HNO_3\ (\ell)\ , \qquad (D.10)$$

to an increasing extent as the partial pressure of oxygen increases.

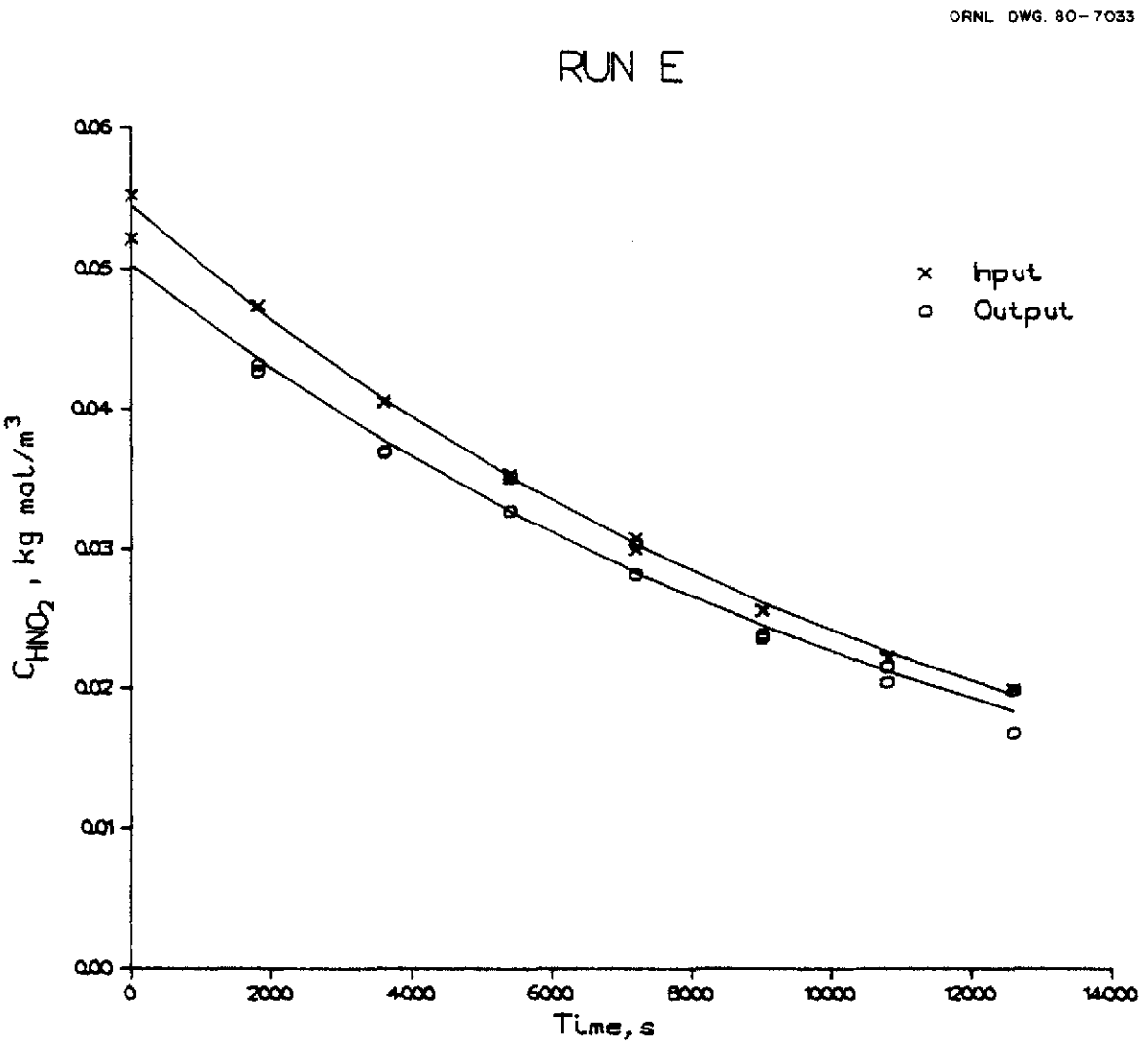

Figure D.10. Column feed and effluent nitrous acid concentrations vs time for experiment E; a rerun of experiment A with air instead of nitrogen as the contact gas.

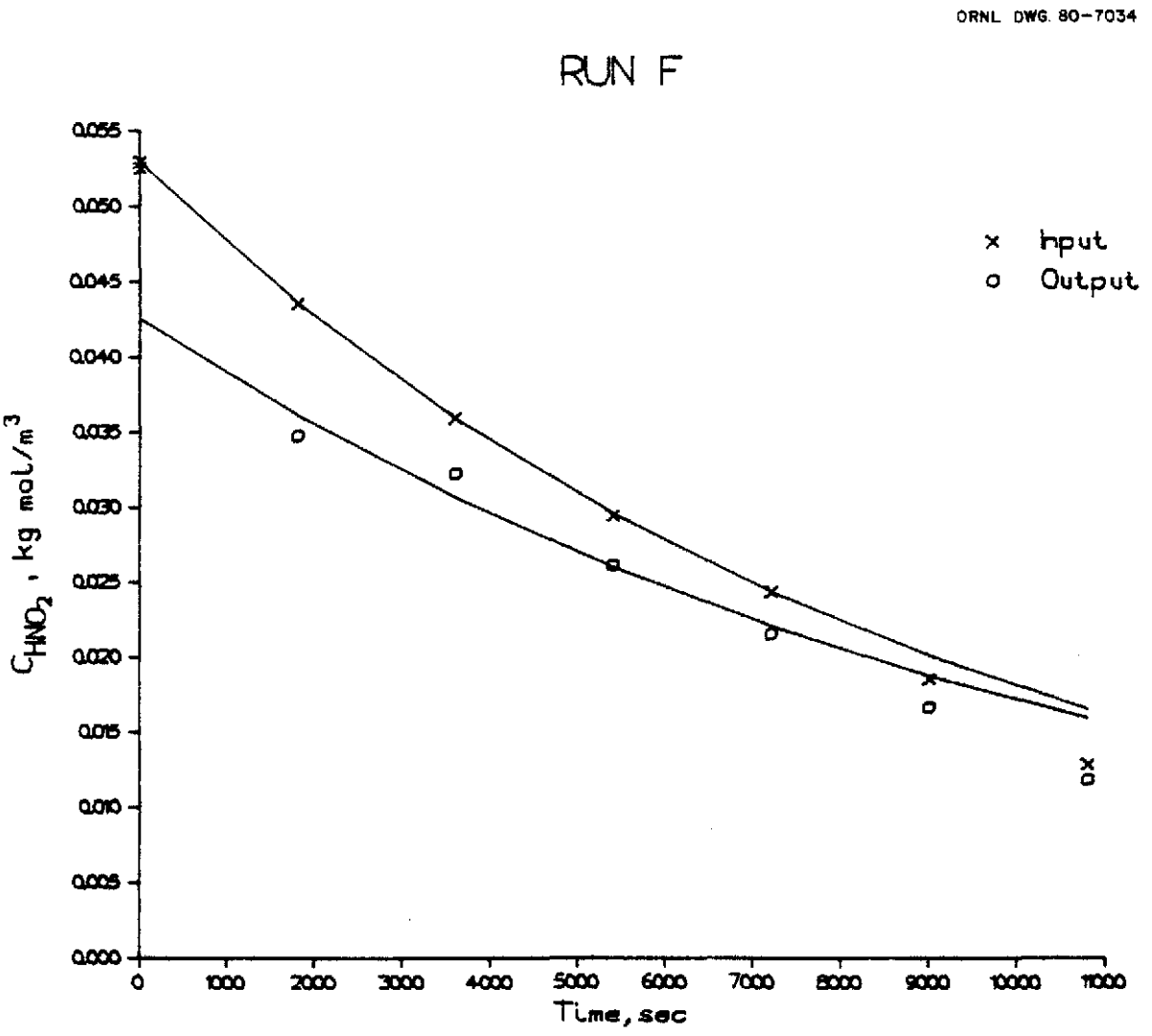

Figure D.11. Column feed and effluent nitrous acid concentrations vs time for experiment F; a rerun of experiment A with oxygen instead of nitrogen as the contact gas.

Table D.8. Results from experiments E and F

Coefficients used in the fitting of the nitrous acid concentrations vs time data for experiments E and F using Equation (D.6).[a]

Run	Coefficient a	Coefficient b
E (inlet)	-1.264	-3.55×10^{-5}
(outlet)	-1.299	-3.48×10^{-5}
F (inlet)	-1.277	-4.697×10^{-5}
(outlet)	-1.372	-3.972×10^{-5}

R* and a 95% confidence interval for experiments E and F

Run	(dC_{H^+}/dC_{HNO_2})	Degrees of freedom	95% confidence interval
E	0.27	4	(0.44, 0.11)
F	0.20	2	(0.16, 0.23)

Run	R*	Degrees of freedom	95% confidence interval
E	-0.73	4	(-0.56, -0.89)
F	-0.80	2	(-0.84, -0.77)

[a]The slope at the higher C_{HNO_2} values of run F was used in this analysis as two slopes are indicated.

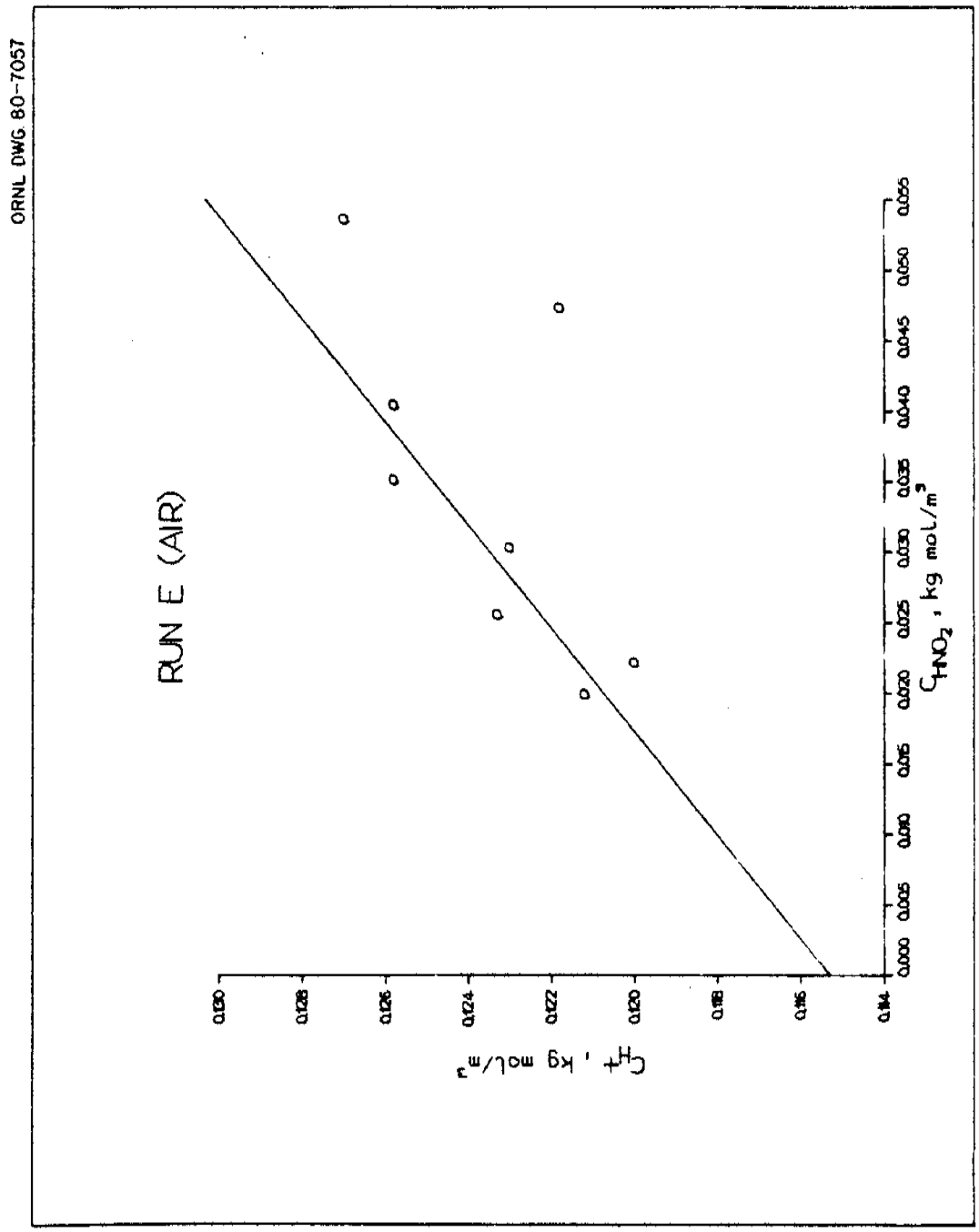

Figure D.12. The change in the system total acid concentration as a function of the changing nitrous acid concentration in experiment E.

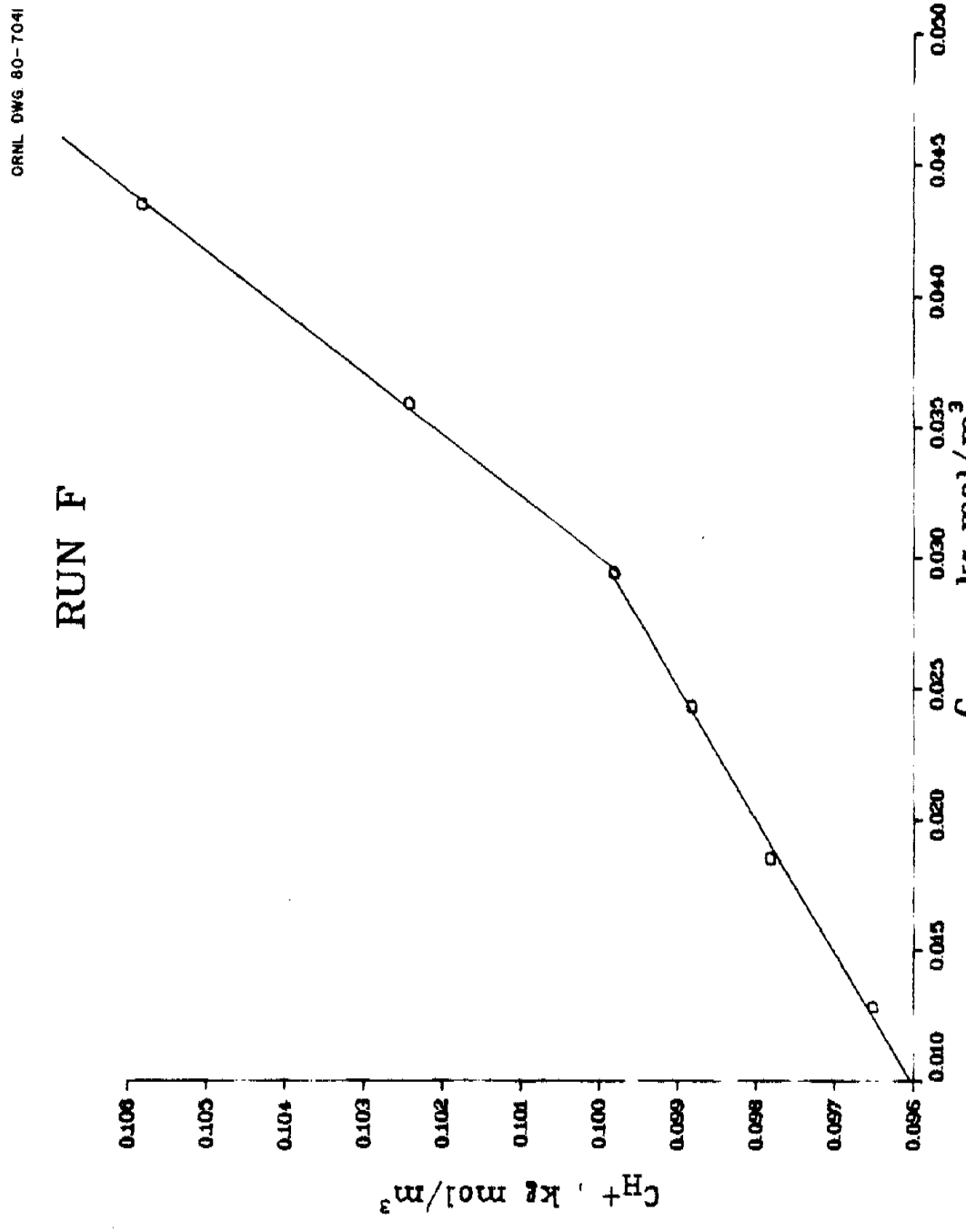

Figure D.13. The change in the system total acid concentration as a function of the changing nitrous acid concentration in experiment F.

D.4. Analysis of the Data from the Studies with the 0.102-m-ID Column

The desorption of nitrous acid was further investigated in a 0.102-m-ID tower packed with 13-mm Intalox saddles. These experiments were conducted much in the same manner as previously mentioned experiments with N_2 as the contact gas, except that the mole fraction of nitric oxide in the effluent gas was also determined.

The concentrations of nitrous acid in the feed and effluent liquid streams are shown in Figures D.14 and D.15. Logarithmic Equation D.7 was used to fit the data from these runs and is also shown in Figures D.14 and D.15. Experiment H covers a wider range of nitrous acid concentrations and could not be fit well with either Equation D.7 or D.8.

The feed concentrations of nitric and total acids are plotted in Figures D.16 and D.17. From the slope of C_{H^+} as a function of C_{HNO_2}, the quantity, R*, is determined in Table D.9. The value of R* for experiment G is apparently in error. The value of R* for experiment H and its confidence interval does not include 0 or -1/3 but lies between these values. This indicates that the desorption reaction mechanisms probably includes both Equations (28f) and (D.2).

The partial pressure of nitric oxide in the column effluent gas is related to the disappearance of system nitrous acid for experiments G and H in Figures D.18 and D.19. From the slope of P_{NO} vs dC_{HNO_2}/dt, the values of R** may be computed. Two slopes representing two values of R** for experiment H seem plausible. The confidence interval for R** at higher nitrous acid concentrations in experiment H does not include 2/3, but it is fairly close. The value of R** for the lower nitrous acid concentrations

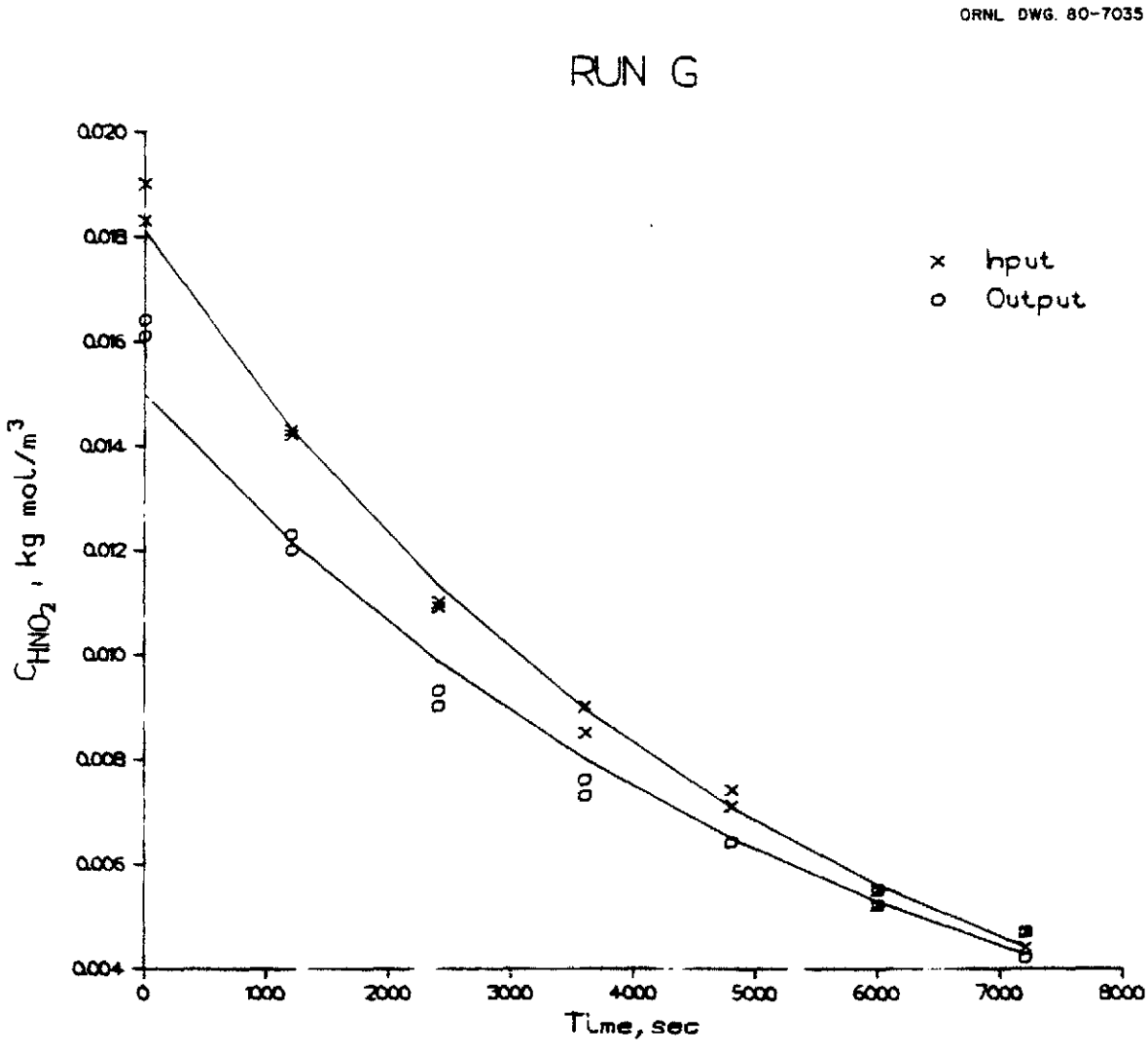

Figure D.14. Column feed and effluent nitrous acid concentrations vs time for experiment G.

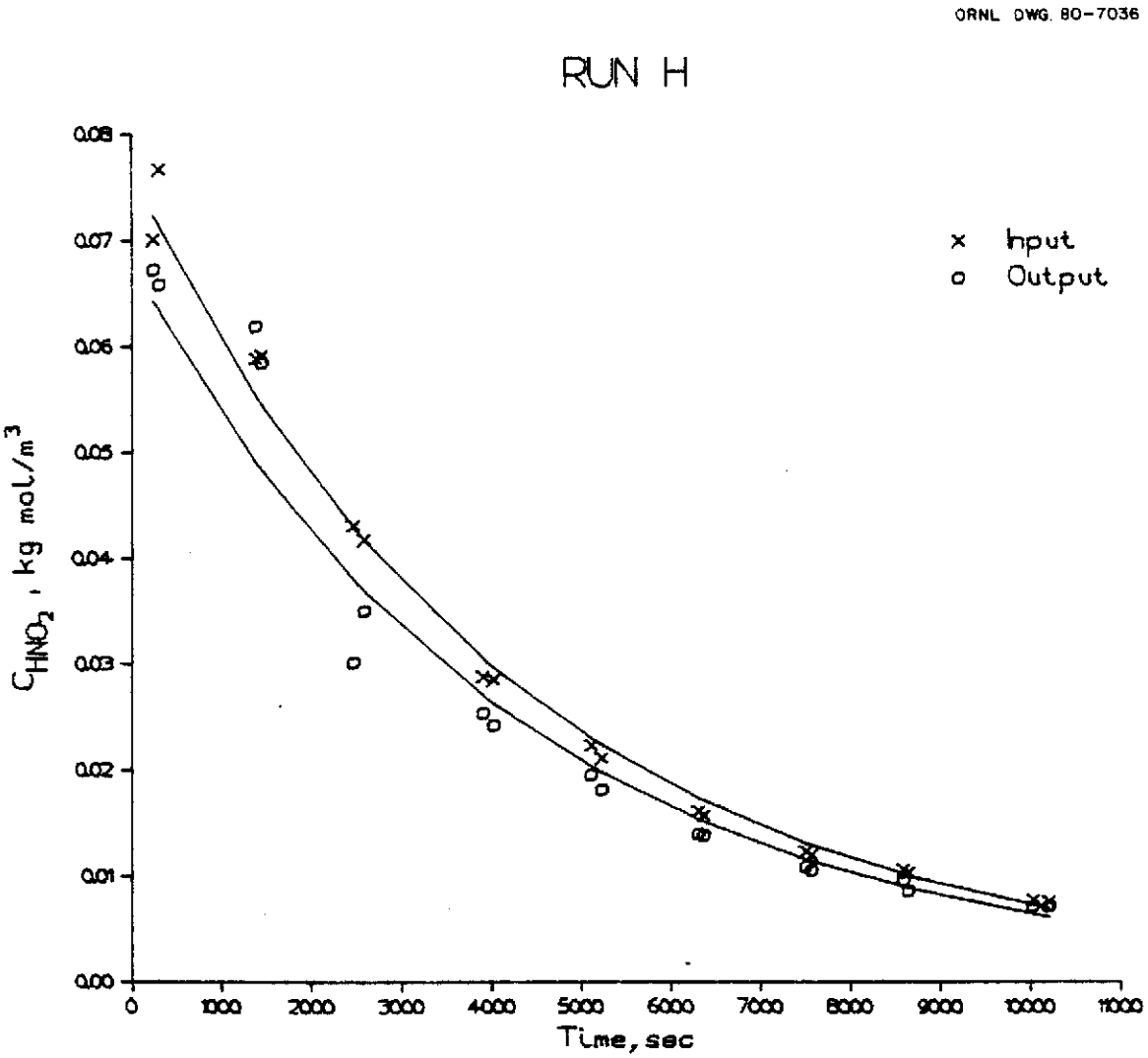

Figure D.15. Column feed and effluent nitrous acid concentrations vs time for experiment H.

Table D.9. Values of R^{*} and R^{**} and a 95% confidence interval for experiments G and H

Experiment	Degrees of freedom	$\frac{dC_{H^+}}{dC_{HNO_2}}$	Confidence interval	R^{*}	Confidence interval
G	5	0.528	(0.438, 0.619)	-0.472	(-0.562, -0.381)
H	16	0.777	(0.833, 0.721)	-0.223	(-0.167, -0.279)

Experiment	Degrees of freedom	$\frac{P_{NO}}{dC_{HNO_2}/dt}$	Confidence interval	R^{**}	Confidence interval
G	5	-237.1	(-203.3, -270.9)	-0.566	(-0.486, -0.647)
H_1[a]	5	-302.6	(-280.3, -324.9)	-0.772	(-0.715, -0.829)
H_2[a]	16	-189.9	(-182.6, -197.2)	-0.485	(-0.466, -0.503)

[a]Experiment H appears to have two values of R^{**}; H_1 is the experimental data at higher HNO_2 concentrations, and H_2 is the experimental data at lower HNO_2 concentrations.

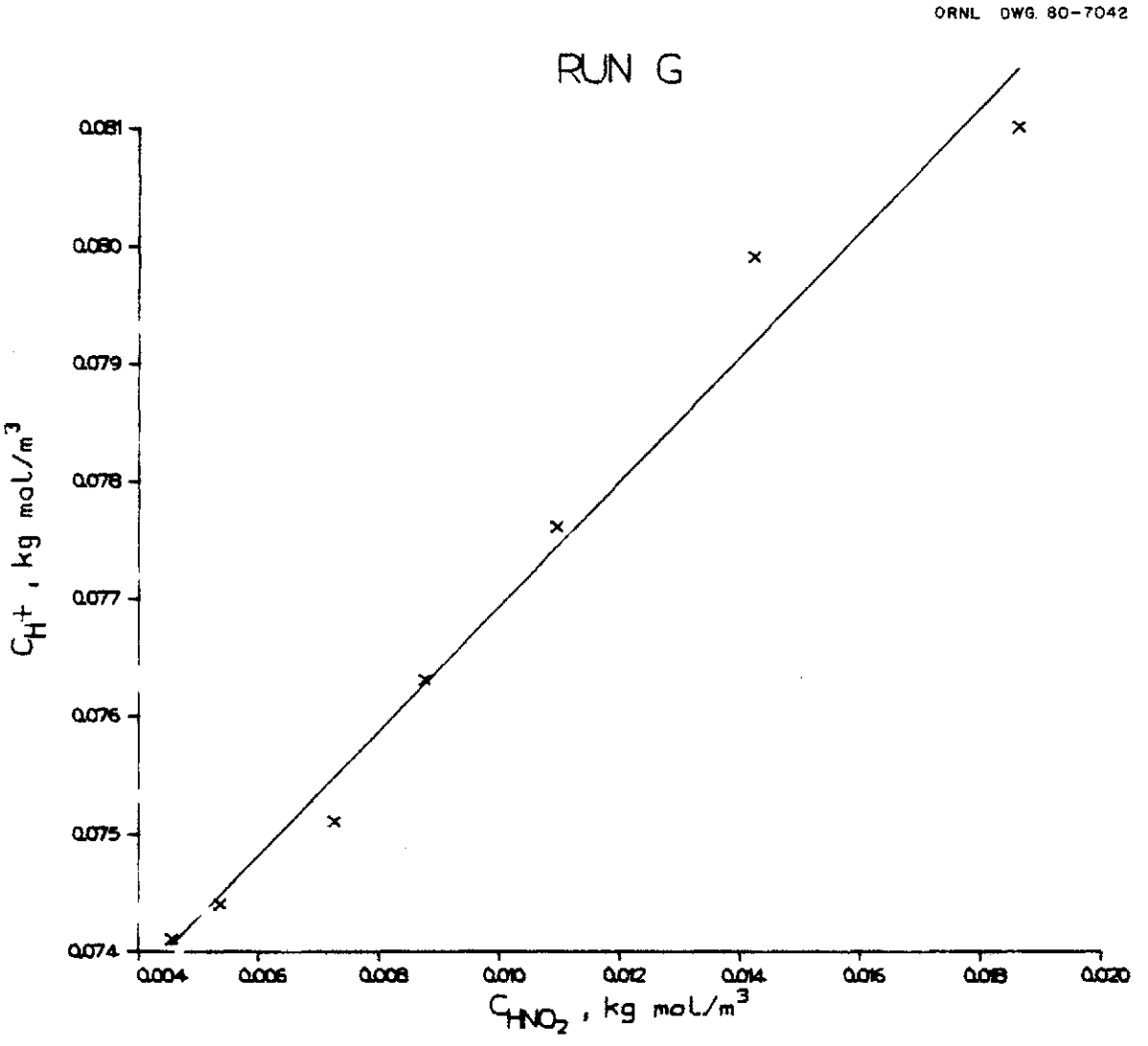

Figure D.16. The change in the system total acid concentration as a function of the changing nitrous acid concentration in experiment G.

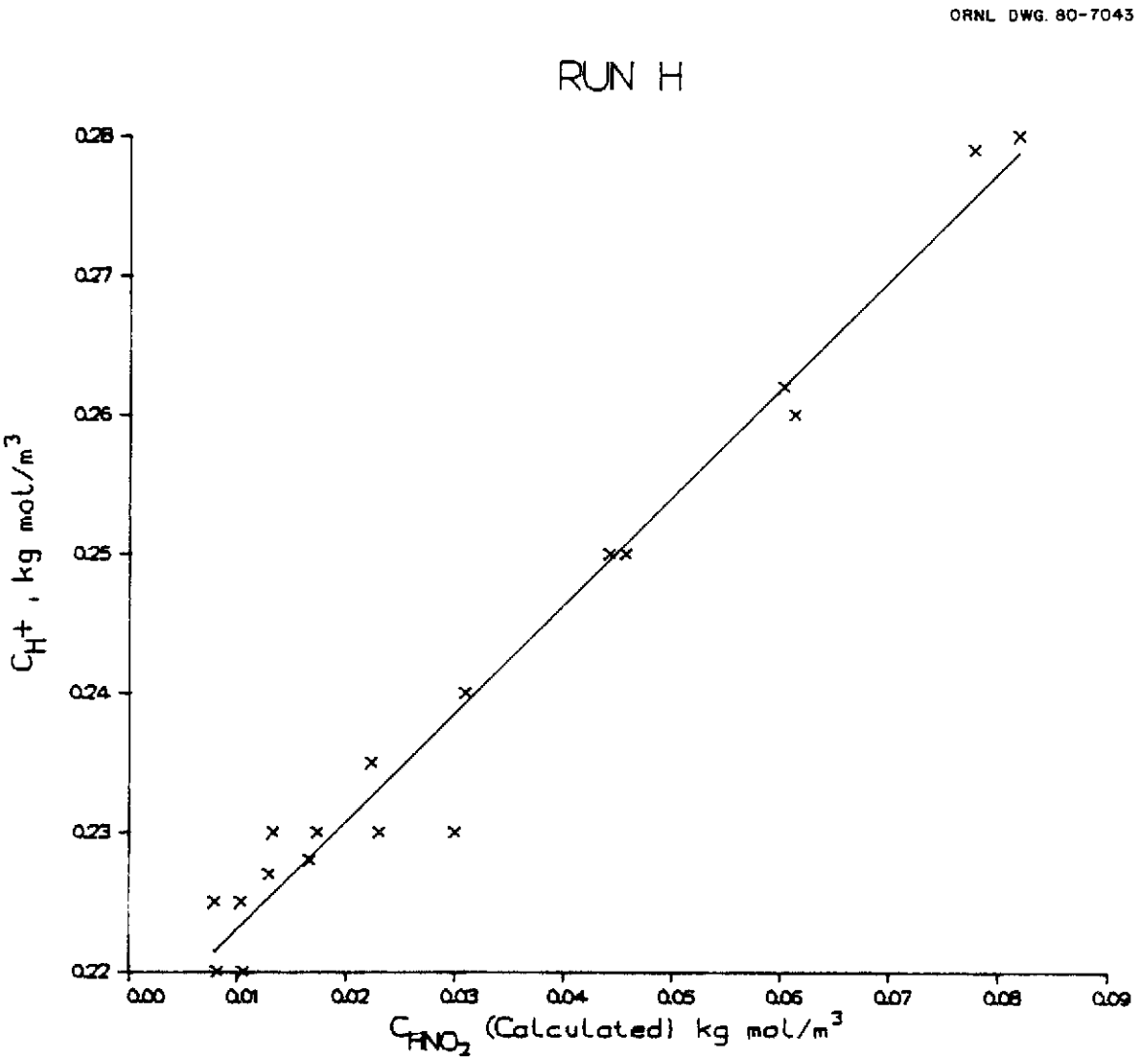

Figure D.17. The change in the system total acid concentration as a function of the changing nitrous acid concentration in experiment H.

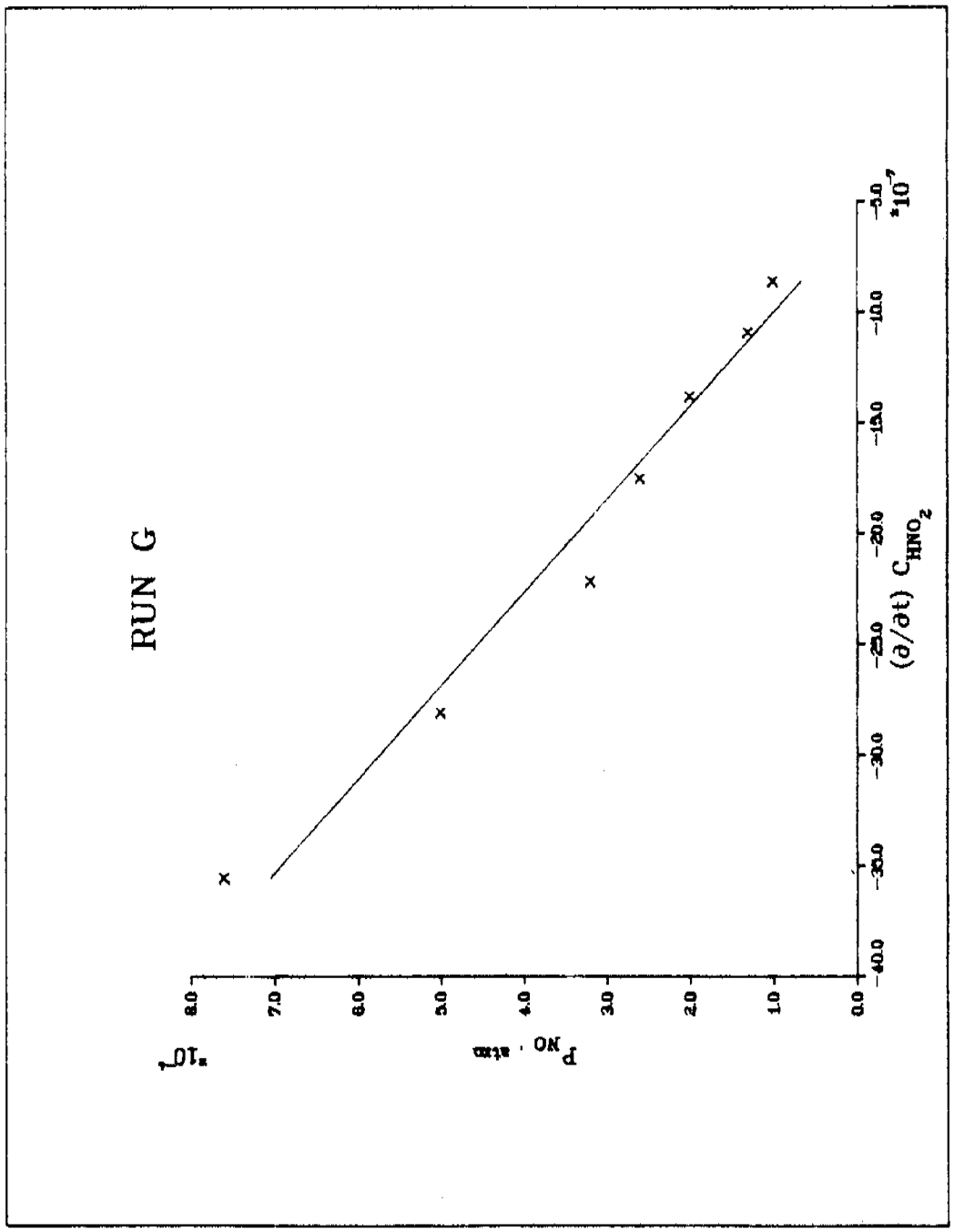

Figure D.18. The change in the partial pressure of nitric oxide in the column effluent gas as a function of the disappearance of the system nitrous acid concentration for experiment G.

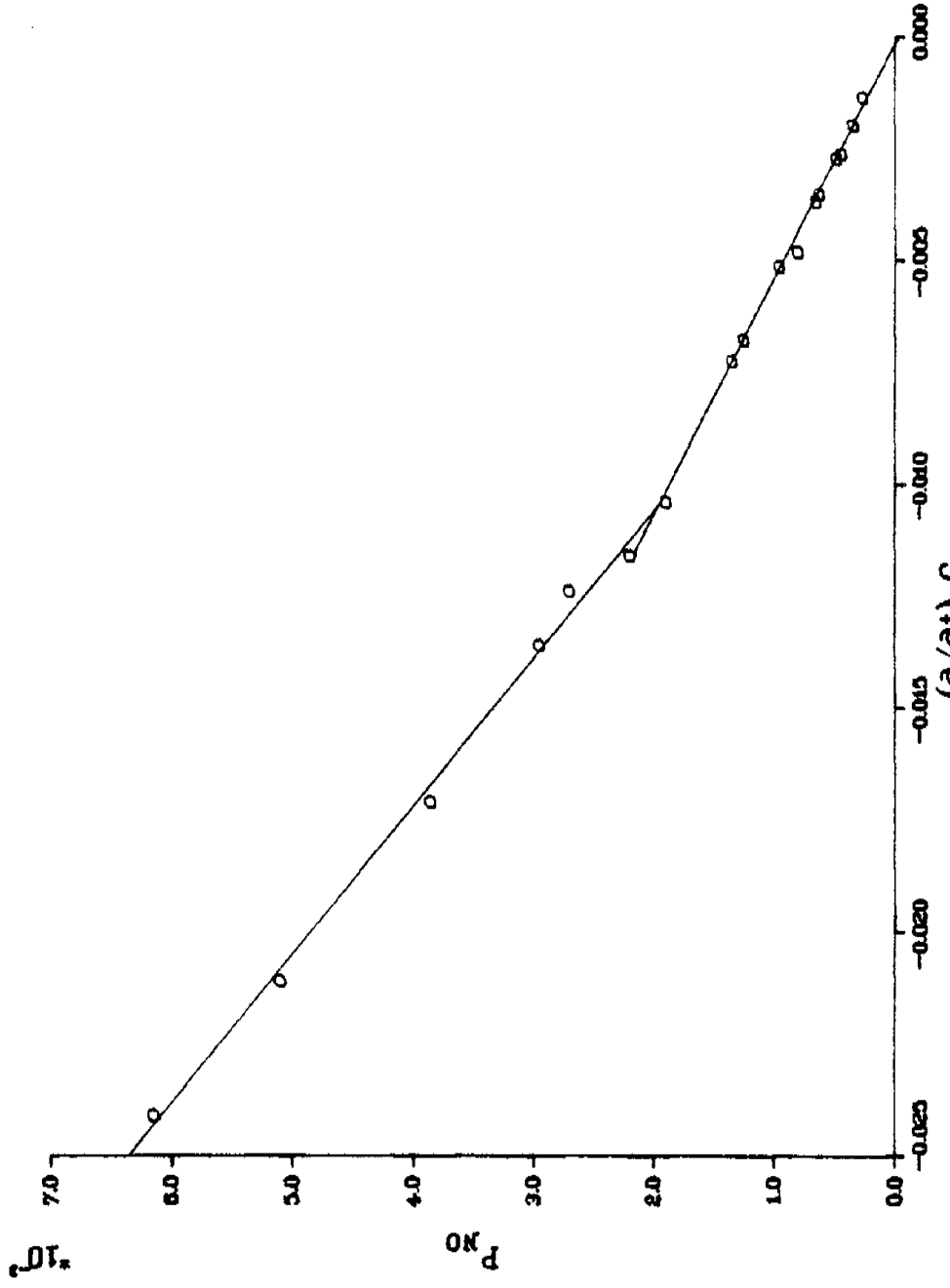

Figure D.19. The change in the partial pressure of nitric oxide in the column effluent gas as a function of the disappearance of the system nitrous acid concentration for experiment H.

in both experiments G and H includes 1/2, indicating that Equation (D.2) represents the mechanism of HNO_2 desorption at lower nitrous acid concentrations.

D.5. Summary

The desorption of nitrous acid in packed towers involves both Reactions (28f) and (D.2) respectively,

$$3HNO_2\ (\ell) \rightarrow HNO_3\ (\ell) + H_2O\ (\ell) + 2NO\ (g)\ ,$$

and

$$2HNO_2\ (\ell) \rightarrow H_2O\ (\ell) + NO_2\ (g) + NO\ (g)\ .$$

The data clearly indicate that Reaction (28f) predominates in the results from the smaller diameter tower. In the results from the larger diameter tower, the conclusions are less clear; apparently, Reaction (28f) predominates at the higher HNO_2 concentrations, and Reaction (D.2) predominates at the lower HNO_2 concentrations. It should be emphasized that the gas rate to liquid rate ratio was much larger in the larger diameter column than the smaller column.

From the smaller diameter column data it appears that as the nitrous acid concentration varies from low to high concentrations, the mass-transfer resistance shifts from the liquid to the gas phase.

APPENDIX E

THE MODEL PREDICTION IN THE DESORPTION MODE AND COMPARISON WITH EXPERIMENTAL DATA

The mathematical model which was developed in Chapter V was used to predict the depletion of HNO_2 for conditions similar to those in run H. The experimental data from this run are given in Table D.4. The model prediction of X_{HNO_2} vs the experimental results are presented in Figure E.1.

The model predicts R* and R** values of 0 and -1/2. This indicates that the model predicted depletion of nitrous acid in these studies was entirely due to the desorption of HNO_2. This is in disagreement with the experimental results, which indicates that both the desorption and the bulk liquid decomposition of HNO_2 was occurring. The bulk liquid-phase decomposition rate in the model was bounded by Equation (86), developed by Komiyama and Inoue (1978). The liquid volume was approximated by the term $\varepsilon_L V_{col}$ for use in the model. Further research in the depletion phenomena in packed towers appears to be necessary to improve the credibility of the model predictions for aqueous HNO_2 depletion calculations.

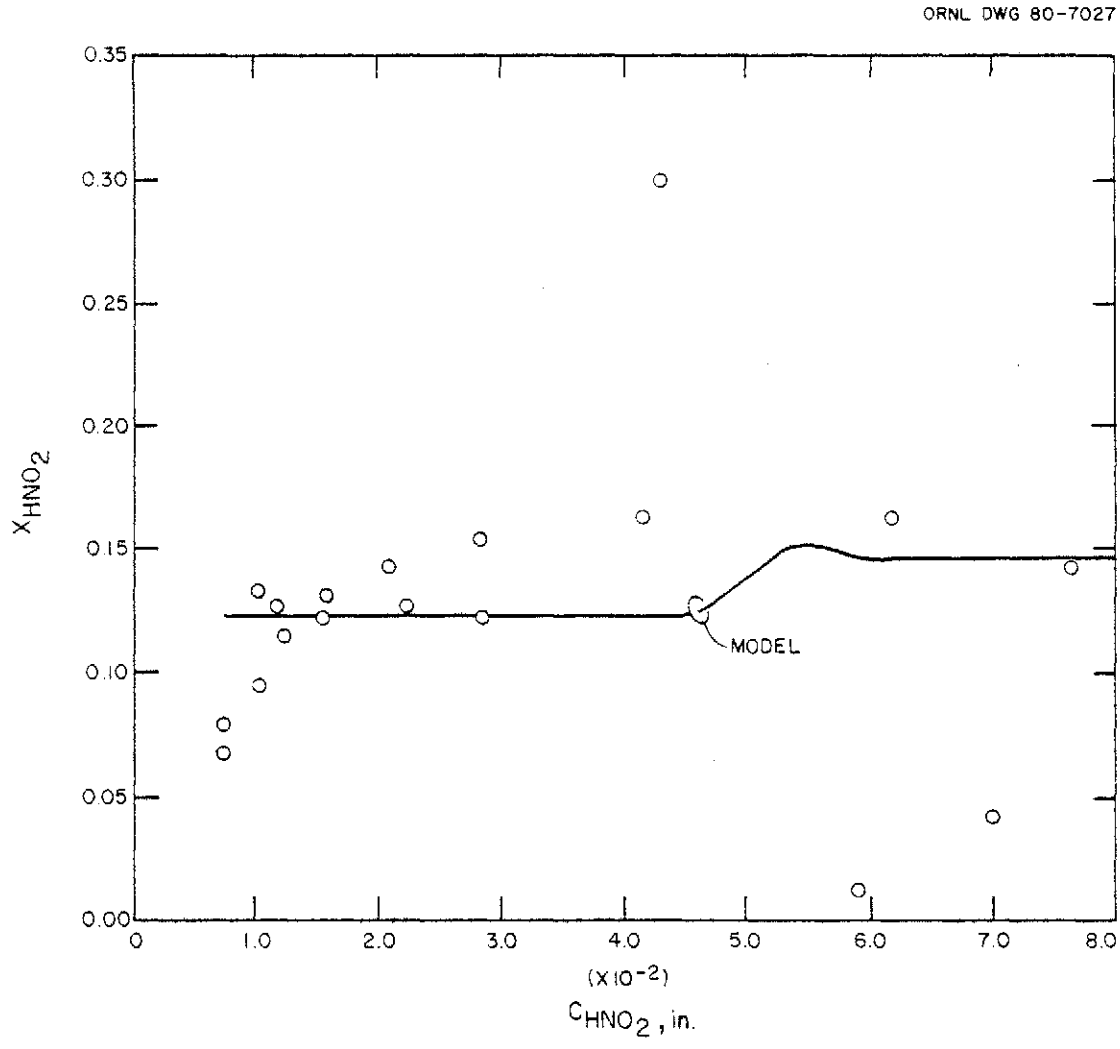

Figure E.1. A comparison of the model prediction vs experimental data for desorption run H.

APPENDIX F

REACTION REGIME FOR THE HYDROLYSIS OF N_2O_4 AND N_2O_3 IN COLUMNS PACKED WITH 6- AND 13-MM INTALOX SADDLES

The criteria for a fast pseudo-first-order reaction of component A dissolving in and reacting with B are (Danckwerts, 1970):

$$3k_L < \sqrt{\mathcal{D}k\ C_B} < 1/2\ k_L \left(1 + \frac{\mathcal{D}_B B}{Z\mathcal{D}_A\ C_A^*}\right) . \qquad (F.1)$$

The liquid-phase mass-transfer coefficient usually varies between 4×10^{-5} to 9×10^{-5} m s^{-1} for the bulk of these studies. For dilute solutions, B is nearly unity, and the value of $\sqrt{\mathcal{D}k}$ for N_2O_4 and N_2O_3 are 8.4×10^{-4} and 6.2×10^{-4} m s^{-1} (Dekker et al., 1959; Corriveau, 1971). The diffusivity of N_2O_4 and N_2O_3 are approximated by 1.4×10^{-9} and 1×10^{9} m^2 s^{-1} (Kramers et al., 1961; Corriveau, 1971). The diffusivity of water is estimated at 2.6×10^{-9} m^2 s^{-1}. Upper limits for interfacial partial pressures for N_2O_4 and N_2O_3 are estimated at 1×10^{-2} and 3×10^{-4} atm. Utilizing the Henry's Law constant for these species (given in Table 3), the interfacial concentration of these species is estimated at 1.3×10^{-2} and 1.26×10^{-4} kg·mol m^{-3}. Evaluating Equation (F.1) at the high values of k_L for N_2O_4 and N_2O_3 absorption and reaction yields:

$$2.7 \times 10^{-4} < 6.4 \times 10^{-4} < 6.5 \times 10^{-3} ,$$

and

$$2.7 \times 10^{-4} < 6.2 \times 10^{-4} < 9.1 \times 10^{-3} ;$$

similarily evaluated at low values of k_L,

$$1.2 \times 10^{-4} < 8.4 \times 10^{-4} < 2.9 \times 10^{-3} ,$$

and

$$1.2 \times 10^{-4} < 6.2 \times 10^{-4} < 9.1 \times 10^{-3} .$$

It appears that for the bulk of the work (the studies conducted in the larger diameter tower) the criteria for a fast reaction are met. This test is important because at the lower limits of mass-transfer coefficients in packed towers, the fast reaction assumption is questionable. There is some uncertainty in the validity of this assumption for the smaller diameter column and its 6-mm packing. However, in view of the uncertainty in calculating the mass-transfer coefficients for this packing, the fast-reaction regime is assumed to apply.

APPENDIX G

COMPUTER PROGRAM

This computer code, which is written in FORTRAN, consists of a main program and a number of subroutines. This program was used to predict the NO_x scrubbing results at conditions similar to those of the experiments.

```
      IMPLICIT REAL*8(A-H,O-Z)
      REAL*8 K,KG,MUGAS,KL
      DIMENSION K(3),DELP(10),RATE(10),H(10),P(10),PSTAR(10)
     *,F(3),POUT(10),KG(10)
C     THIS PROGRAM IS IN CGS UNITS
C     A IS THE GAS-LIQUID INTERFACIAL AREA
C     ACOL IS THE AREA OF THE COLUMN
C     CHNO3 IS THE CONCENTRATION OF HNO3 IN THE LIQUID PHASE
C     CHNO2 IS THE CONCENTRATION OF HNO2 IN THE LIQUID PHASE
C     COMPONENT 1 IS NO2*
C     COMPONENT 2 IS NO*
C     COMPONENT 3 IS O2
C     COMPONENT 4 IS N2
C     COMPONENT 5 IS NO2
C     COMPONENT 6 IS N2O4
C     COMPONENT 7 IS N2O3
C     COMPONENT 8 IS HNO2
C     COMPONENT 9 IS NO
C     COMPONENT 10 IS H2O
C     DP IS THE DIAMETER OF THE PACKING
C     DELZ IS THE INCREMENTAL COLUMN HEIGHT
C     EPIDRY IS THE VOID FRACTION OF THE DRY COLUMN
C     EPI IS THE VOID FRACTION OF THE COLUMN
C     FACTOR IS USED TO ACCOUNT BULK LOSS OF GAS PHASE
C     FLUX IS A PARTIAL PRESSURE FLUX
C     K IS AN EQUILIBRIUM CONSTANT
C     KG IS THE GAS PHASE MASS TRANSFER COEFFICIENT
C     KL IS THE LIQUID PHASE MASS TRANSFER COEFFICIENT
C     H IS HENRY'S LAW CONSTANT
C     P IS THE BULK PHASE PARTIAL PRESSURE OF COMPONENT I
C     PSTAR ISINTERFACIAL PARTIAL PRESSURE OF COMPONENT I
C     POUT IS PARTIAL PRESSURE OF COMPONENT I LEAVING INCREMENT
C     R IS UNIVERSAL GAS LAW CONSTANT
C     RCOL IS THE RADIUS OF THE COLUMN
C     T IS TEMPERATURE (KELVIN)
C     VCOL IS THE INCREMENTAL VOLUMN OF THE COLUMN
      NPASS=1
      K(1)=6.76D0
      K(2)=0.522D0
      K(3)=1.74D0
      SQRTK4=169.4D0
      H(5)=24.4D3
      H(6)=2.59D3
      H(7)=0.769D3
      H(8)=0.0305D3
      H(9)=531.D3
      P(10)=0.031D0
      AKPRIM=K(3)*P(10)
      SQRAKP=DSQRT(AKPRIM)
      EN2O3=1.59D-4
      EN2O4=11.0D-5
      ERRR=0.0D0
      COMP=0.0D0
      READ(5,101)NCASE
  101 FORMAT(I2)
      DO 100 II=1,NCASE
```

```
      ERRR=ERRR+DABS(COMP)
      READ(5,9) RUN,HCOL,GIN,AL,T,Y1I,Y2I,Y120
      READ(5,9) C2IN,C3IN,CHNO2,CHNO3,PT,RCOL,DP,AIR
 9    FORMAT(8D7.3)
      WRITE(6,92)
 92   FORMAT(10X,'RAW DATA',/)
      WRITE(6,91) RUN,HCOL,GIN,AL,T,Y1I,Y2I,Y120
      WRITE(6,91) C2IN,C3IN,CHNO2,CHNO3,PT,RCOL,DP,AIR
 91   FORMAT(8D14.4)
      FL=Y1I+Y2I
      PSI=Y120/FL
      XNOXE=(1.0D0-PSI)/(1.0D0-PSI*FL)
      CHNO2=1.0D-4*CHNO2
      CHNO3=1.0D-4*CHNO3
      CHNO2I=1.0D-4*C2IN
      CHNO3I=1.0D-4*C3IN
      R=85.05D0
      AMG=XNOXE*GIN*FL/(R*T)
      AML=AL*(CHNO2+CHNO3-CHNO2I-CHNO3I)
      AMATBL=AML/AMG
      DELZ=1.000D0
      RINC=HCOL/DELZ
      NINCT=RINC
      GIN=GIN/PT
      RHOLIQ=1.0D0
      DELPNO=0.0D0
      P(1)=PT*Y1I
      P(2)=PT*Y2I
      P120UT=Y120*PT
      PNO2IN=P(1)
      PNOIN=P(2)
      NPASS=0
C     SPECIFIC FOR 6MM PACKEDG
      EPIDRY=0.74
      IF(DP.GT.1.0D0) EPIDRY=0.73D0
      C2OUT=CHNO2
      C3OUT=CHNO3
C     NEW CONVERGANCE FROM HIGH ACID SIDE
C
      CHNO2=1.5D0*CHNO2
      CHNO3=1.5D0*CHNO3
      XC2=CHNO2
      XC3=CHNO3
C
      CNO=SQRTK4*CHNO2**1.5/(CHNO3*H(9))

      R=82.05D0
      ADRY=9.8D0
      IF(DP.GT.1.0D0) ADRY=4.8D0
      PI=3.14159265D0
      ACOL=PI*RCOL**2.
      VCOL=ACOL*DELZ
      PSUMO=PT
      IF(DP.GT.1.0D0) GOTO181
      CALL HOLDUP (DP,AL,RHOLIQ,ACOL,EPIL)
      GOTO182
```

```
  181   CONTINUE
        EPIL=0.07D0
        IF(AL.GT.40.0D0)EPIL=.09D0
        IF(AL.GT.60.0D0)EPIL=.11D0
  182   CONTINUE
        EPI=1.0D0-EPIDRY-EPIL
        VLIQ=EPIL*VCOL
        VGAS=(1.0D0-EPI)*VCOL
        AGAS=ACOL*(1.0D0-EPI)
        PAIR=PT*(1.0D0-P(1)-P(2)-P(10))
        CAIR=0.21D0
        IF(AIR.LT.1.5D0)CAIR=0.0D0
        P(3)=CAIR*PAIR
        P(4)=(1.0D0-CAIR)*PAIR
        PO2IN=P(3)
        PN2IN=P(4)
        G=GIN*PT/(PT-P(10))
        GIN=G
C       IF(DP.GT.1.0D0)GOTO2
        IF (P(3) .LE. 0.0D0)GO TO 2
        IF (P(2) .LE. 0.0D0)GO TO 2
        CALL NOOXID (2,T,P(2),P(3),1100.0D0,G,XNO)
        P(3)=P(3)*(1.0D0-P(2)*XNO/(2.0D0*P(3)))
        P(1)=P(1)+P(2)*XNO
        P(2)=P(2)*(1.0D0-XNO)
        GO TO 6
  2     XNO=0.0
  6     CONTINUE
        AG=G
        CALL GPMTC (AG,AL,T,P,PT,ACOL,RHOLIQ,ADRY,DP,KG)
        CALL VISCOS (PT,P,T,MUGAS)
        AL=AL
        IF(DP.GT.1.0D0)GOTO176
        CALL IAREA (MUGAS,RHOLIQ,AL,ADRY,ACOL,A)
        CALL LPMTC (ACOL,AL,RHOLIQ,A,ADRY,DP,KL)
        GOTO177
  176   KL=6.4D-3
        A=2.25D0
        IF(AL.GT.40.0D0)KL=6.5D-3
        IF(AL.GT.40.0D0)A=2.7D0
        IF(AL.GT.60.0D0)KL=7.2D-3
        IF(AL.GT.60.0D0)A=2.95D0
  177   CONTINUE
       WRITE (6,21) EPIL,A,KL,KG(5),KG(6),KG(7),KG(8),KG(9)
        BETA=A*VCOL/DELZ
    3   CONTINUE
        PA=P(1)
        PB=P(2)
        CALL GGCON(P)
  88    CONTINUE
C       WRITE (6,21) EPIL,A,KL,KG(5),KG(6),KG(7),KG(8),KG(9)
   21   FORMAT(8D12.4)
C       WRITE(6,4)NICRE,G,P(1),P(2),P(3),P(4),P(5),P(6),P(7),P(8),P(9)
    4   FORMAT (I3,2X,F5.0,9(2X,F7.6))
        PSUMN=P(3)+P(4)+P(5)+P(6)+P(7)+P(8)+P(9)+P(10)
        FACTOR=(PSUMO-PSUMN)/PSUMO
```

```
      G=G*(1.-FACTOR)
      GV=G/AGAS
      DO 1 I = 2,8
      P(I)=P(I)/(1.-FACTOR)
    1 CONTINUE
      XNO=1.1D0
      IF (P(9) .LE. 0.0D0) XNO=0.0D0
      IF (P(3) .LE. 0.0D0) XNO=0.0D0
      IF (XNO .LE. 0.0D0) GO TO 17
      CALL NOOXID (2,T,P(9),P(3),VGAS,G,XNO)
      P(3)=P(3)*(1.0D0-P(9)*XNO/(2.0D0*P(3)))
      DELPNO=P(9)*XNO
   17 CONTINUE
   13 CONTINUE
      IF (CHNO3 .LE. 1.0D-6) CNO=0.0D0
      IF (CHNO2 .LE. 0.0D0) CNO=0.0D0
      IF (CNO .LE. 0.0D0) GO TO 16
      CNO=SQRTK4*CHNO2**1.5/(CHNO3*H(9))
   16 CONTINUE
      IF(CHNO2.LE.0.0D0) REXN=0.0D0
      IF(CHNO2.LE.0.0D0) GO TO 178
      AKKI=2.39D-3
      TESTK=0.667D0*AKKI*KL**.667*CHNO2**1.333*EPIL/A**.333
  178 CONTINUE
C     ABELK=.027D6
C     TESTK=0.667D0*ABELK*EPIL*CHNO2*CHNO3**2/A
      CALL FLUX (K,P,EN2O3,EN2O4,KG,H,KL,CHNO2,CNO,TESTK,PSTAR)
      RATE(5)=KL*PSTAR(5)/H(5)
      RATE(6)=EN2O4*PSTAR(6)
      RATE(7)=EN2O3*PSTAR(7)
      RATE(8)=KL*(PSTAR(8)/H(8)-CHNO2)
      RATE(9)=KL*(PSTAR(9)/H(9)-CNO)
      IF(RATE(8).GT.0.0D0) RATE(8)=0.0D0
      IF(RATE(9).GT.0.0D0) RATE(9)=0.0D0
      GOTO111
      IF(NPASS.GT.2) GOTO111
      WRITE(6,112) NICRE,RATE(5),RATE(6),RATE(7),RATE(8),RATE(9)
      WRITE(6,4) NICRE,G,P(1),P(2),P(3),P(4),P(5),P(6),P(7),P(8),P(9)
      WRITE (6,4) NICRE,G,PSTAR(1),PSTAR(2),PSTAR(5),PSTAR(6),
     * PSTAR(7),PSTAR(8),PSTAR(9)
      WRITE (6,4) NCRE,G,XNO,DELPNO,DELC3A,DELC3,DELC2,CHNO2,CHNO3,
     * VCOL,CNO
  112 FORMAT(I3,5D14.5)
  111 CONTINUE
C     RATE(5)=KG(5)*(P(5)-PSTAR(5))
C     RATE(6)=KG(6)*(P(6)-PSTAR(6))
C     RATE(7)=KG(7)*(P(7)-PSTAR(7))
C     RATE(8)=KG(8)*(P(8)-PSTAR(8))
C     RATE(9)=KG(9)*(P(9)-PSTAR(9))
C     WRITE (6,4) NICRE,G,PSTAR(1),PSTAR(2),PSTAR(5),PSTAR(6),
C    * PSTAR(7),PSTAR(8),PSTAR(9)
   99 CONTINUE
      IF(NPASS.LE.1) GOTO126
C     ABELK=.027D6
C     TESTK=0.667D0*ABELK*EPIL*CHNO2*CHNO3**2
      TESTD=KL*A*(CNO-PSTAR(9)/H(9))
```

```
      IF(TESTD.GT.TESTK)GOTO125
      GO TO 126
C 125 CONTINUE
  125 WRITE(6,127)NICRE,TESTK,TESTD
  127 FORMAT(I3,2D14.7)
  126 CONTINUE
      VLIQ=EPIL*VCOL
      VGAS=(1.0D0-EPI)
      DO 44 I=5,9
      DELP(I)=RATE(I)*A*VCOL*R*T/G
      P(I)=P(I)-DELP(I)
      IF(P(I).LE.0.0D0)P(I)=0.0D0
   44 CONTINUE
      DELC3A=0.5D0*G*(DELP(5)+2.0D0*DELP(6))/(R*T)
      DELC2A=DELC3A+G*(2.0D0*DELP(7)+DELP(8))/(R*T)
      DELC2=DELC2A+1.5D0*G*DELP(9)/(R*T)
      DELC3=DELC3A-0.5D0*G*DELP(9)/(R*T)
      CHNO3=CHNO3-DELC3/AL
      CHNO2=CHNO2-DELC2/AL
      XC2=XC2-DELC2/AL
      XC3=XC3-DELC3/AL
      IF(CHNO2.LE.0.0D0)CHNO2=1.0D-9
      IF(CHNO3.LE.0.0D0)CHNO3=1.0D-9
C     WRITE (6,4)NCRE,G,XNO,DELPNO,DELC3A,DELC3,DELC2,CHNO2,CHNO3,
C    * VCOL,CNO
      P(1)=P(5)+2.0D0*P(6)+P(7)+P(8)/2.0D0+DELPNO
      P(2)=P(7)+P(8)/2.0D0+P(9)-DELPNO
      NICRE=NICRE+1
      IF (NICRE .LT. NINCT)GO TO 3
      CALL GGCON(P)
      PSUMN=P(3)+P(4)+P(5)+P(6)+P(7)+P(8)+P(9)+P(10)
      FACTOR=(PSUMO-PSUMN)/PSUMO
      G=G*(1.-FACTOR)
      GV=G/AGAS
      DO 11 I = 2,8
      P(I)=P(I)/(1.-FACTOR)
   11  CONTINUE
      XNOXC=(GIN*(PNO2IN+PNOIN)-G*(P(1)+P(2)))/(GIN*(PNO2IN+PNOIN))
      COMP=XNOXC-XNOXE
      WRITE (6,149)
  149 FORMAT('      G, PNO2, PNO, CHNO2, CHNO3',/)
      WRITE (6,150)GIN,PNO2IN,PNOIN,C2OUT,C3OUT,XNOXC,AMATBL
  150 FORMAT (7D14.4)
      WRITE (6,150)G,P(1),P(2),CHNO2,CHNO3,XNOXE,COMP
      CHNO2I=0.0D0
      CHNO3I=0.0D0
C     ADJ2=CHNO2I-CHNO2
C     ADJ3=CHNO3I-CHNO3
      ADJ2=CHNO2I-XC2
      ADJ3=CHNO3I-XC3
      AADJ2=DABS(ADJ2)
      AADJ3=DABS(ADJ3)
      IF(NPASS.LE.1)GOTO152
      IF(NPASS .GT. 10)GO TO 15
      IF(AADJ2 .LE. 5.0D-7)GO TO 151
      GO TO 152
```

```
 151     IF(AADJ3 .LE. 5.0D-7)GO TO 15
 152     CONTINUE
         NPASS=NPASS+1
C
C        NEW CONVERGENCE
C        CASAB=GIN*XNOXE*(PNO2IN+PNOIN)/(R*T)
C        ACIDPR=AL*(C2OUT+C3OUT)
C        COMP=CASAB-ACIDPR
C        ACOMP=DABS(COMP)
C        IF(ACOMP.LE.0.05D0)GOTO15
C        CHNO2=C2IN+0.33D0*COMP/AL
C        CHNO3=C3IN+0.33D0*COMP/AL
         CHNO2=C2OUT+0.333D0*ADJ2
         CHNO3=C3OUT+0.333D0*ADJ3
C
         G=GIN
         P(1)=PNO2IN
         P(2)=PNOIN
         P(3)=PO2IN
         P(4)=PN2IN
         C3OUT=CHNO3
         C2OUT=CHNO2
          XC3=C3OUT
         XC2=C2OUT
         NICRE=1
         GO TO 3
 15      CONTINUE
 100     CONTINUE
         WRITE(6,9)ERRR
         STOP
       END
```

```
      SUBROUTINE GPMTC (G,AL,T,P,PTOT,ACOL,RHOLIQ,ADRY,DPACK,KG)
      REAL*8 AAA,G,AL,L,T,P,PTOT,ACOL,RHOLIQ,ADRY,DPACK,KG,A,DG,
     *  AA,BB,CC,DD,EE,FF,GG,MUGAS,R,SURTEN,MWAVG,RHOGAS
      DIMENSION P(10),DG(10),KG(10)
      COMMON RHOGAS,MWAVG
      GR=980.0D0
      SURTEN=70.0D0
      CALL VISCOS (PTOT,P,T,MUGAS)
      CALL GASDIF (PTOT,T,DG)
      G=G*RHOGAS/ACOL
      L=AL*RHOLIQ/ACOL
      R=82.05D0
      AA=.85
      BB=L/(ADRY*MUGAS)
      CC=L**2.*ADRY/(RHOLIQ**2.0D0*GR)
      DD=L**2./(RHOLIQ*SURTEN*ADRY)
      A=ADRY*(1.-DEXP((-1.45)*AA**.75*BB**.1*CC**(-.05)*DD**.2))
      EE=ADRY*DPACK
      FF=G*DPACK/MUGAS
      DO 1 I=5,9
      GG=MUGAS/(RHOGAS*DG(I))
      AAA=5.23D0
C     IF(DPACK.LT.1.0D0)AAA=2.3
      KG(I)=AAA*G/(PTOT*MWAVG)*EE**(-1.7)*FF**(-.3)*GG**(-.667)
    1 CONTINUE
      RETURN
      END
```

```
      SUBROUTINE VISCOS (PTOT,P,T,MUGAS)
      REAL*8 P,T,MUGAS,A,B,C,MU,SQRTMW,MW,MWTOT,MWAVG,SUMN,
     *  SUMD,RHOGAS,PTOT
      DIMENSION MW(10),A(5),B(5),C(5),MU(5),P(10),SQRTMW(5)
      COMMON RHOGAS,MWAVG
C     NO*=COMPONENT 1
C     NO*=COMPONENT 2
C     O2 =COMPONENT 3
C     N2=COMPONENT 4
      R=82.05
      A(2)=56.77D0
      A(3)=18.11D0
      A(4)=30.43D0
      B(2)=.4814D0
      B(3)=.6632D0
      B(4)=.4989D0
      C(2)=-.8434D-4
      C(3)=-1.879D-4
      C(4)=-1.093D-4
      DO 1 I = 2,4
      MU(I)=(A(I)+B(I)*T+C(I)*T**2.)/1.0D6
    1 CONTINUE
      MU(1)=(138.D0+.49D0*(T-273.0D0))/1.0D6
      SQRTMW(1)=5.48D0
      SQRTMW(2)=6.79D0
      SQRTMW(3)=5.66D0
      SQRTMW(4)=5.29D0
      MW(1)=30.D0
      MW(2)=30.0D0
      MW(3)=32.0D0
      MW(4)=28.0D0
      MWTOT=0.0D0
      MWAVG=0.0D0
      SUMN=0.0D0
      SUMD=0.0D0
      DO 2 I=1,4
      MWTOT=MWTOT+P(I)/PTOT*MW(I)
      SUMN=SUMN+P(I)/PTOT*MU(I)*SQRTMW(I)
      SUMD=SUMD+P(I)/PTOT*SQRTMW(I)
    2 CONTINUE
      MUGAS=SUMN/SUMD
      MWAVG=MWTOT
      RHOGAS=PTOT*MWAVG/(R*T)
      RETURN
    END
```

```
      SUBROUTINE GASDIF (PTOT,T,DG)
      REAL*8 PTOT,T,DG,VAAIR,MW,MWAIR,VA
      DIMENSION DG(10),VA(10),MW(10)
      VA(5)=30.4D0
      VA(6)=60.8D0
      VA(9)=23.6D0
      VA(8)=43.3D0
      VA(7)=53.4D0
      VAAIR=29.9D0
      MW(5)=46.0D0
      MW(6)=92.0D0
      MW(9)=30.0D0
      MW(8)=47.0D0
      MW(7)=76.0D0
      MWAIR=29.0D0
C     GILLAND EQUASION FOR CALCULATING GASEOUS DIFFUSION COEF.
      DO 1 I=5,9
      DG(I)=0.0043*T**1.5*DSQRT(1./MW(I)+1./MWAIR)/
     *  (PTOT*(VA(I)**.333+VAAIR**.333)**2.)
    1 CONTINUE
      RETURN
      END
```

```
      SUBROUTINE LPMTC (ACOL,AL,RHOLIQ,A,ADRY,DPACK,KL)
      REAL*8 ACOL,AL,KL,AA,BB,CC,DD,RHOLIQ,L,A,MULIQ,DL,ADRY,DPACK,GR
      L=AL*RHOLIQ/ACOL
      GR=981.0D0
      MULIQ=.010D0
      DL=1.8D-05
      AA=RHOLIQ/(MULIQ*GR)
      BB=L/(A*MULIQ)
      CC=MULIQ/(RHCLIQ*DL)
      DD=ADRY*DPACK
C     KL=0.0051D0*AA**(-.333)*BB**.667*CC**(-.5)*DD**0.4
    1 FORMAT (D14.6)
      EE=ADRY*MULIQ/(GR*RHOLIQ)
      FF=MULIQ/(GR**2*RHOLIQ)
      GG=MULIQ*L**3*ADRY**3/(GR**2*RHOLIQ**4)
      KL=.0025*GG**.25*CC**(-.5)*EE**(-.667)*FF**(-.111)/A
      RETURN
      END
```

```
      SUBROUTINE HOLDUP (DPACK,AL,RHOLIQ,ACOL,EPIL)
      REAL*8 L,AL,RHOLIQ,ACOL,DPACK,EPIL,DE
      L=AL*RHOLIQ/ACOL
      DE=0.68*DPACK**.85
      EPIL=0.145D0*(L/DE)**0.6
      RETURN
    END
```

```
      SUBROUTINE IAREA (MUGAS,RHOLIQ,AL,ADRY,ACOL,A)
      REAL*8 L,AL,RHOLIQ,ACOL,ADRY,A,SURTEN,RHOGAS,AA,BB,CC,DD
     *  ,MUGAS
      COMMON RHOGAS,MWAVG
      SURTEN=70.0D0
      GR=980.0D0
      L=AL*RHOLIQ/ACOL
      AA=.85
    2 FORMAT (D14.6)
      BB=L/(ADRY*.01D0)
      CC=L**2.*ADRY/(RHOLIQ**2.0D0*GR)
      DD=L**2./(RHOLIQ*SURTEN*ADRY)
C     A=ADRY*(1.-DEXP((-1.45)*AA**.75*BB**.1*CC**(-.05)*DD**.2))
      RE=BB
      WE=DD
      A=1.045*ADRY*RE**.041*WE**.133*AA**(-.182)
      RETURN
      END
```

```
      SUBROUTINE GGCON(P)
      COMMON AK(3),AKPRIM,PHIA,P12
     REAL*8 FCN,PHIA,PHI,P12,F,Y,WA,FTOL,YTOL,ALPHA,AK,AKPRIM,P,AAK
    *  ,AAA,ERR,COMPA,COMPB
     EXTERNAL FCN
     DIMENSION Y(2),F(2),WA(13),P(10)
       P(10)=.031D0
       AK(1)=6.76D0
       AK(2)=0.522D0
       AK(3)=1.74D0
       AKPRIM=AK(3)*P(10)
       PHI=P(1)-P(2)
       PHIA=PHI
       P12=P(1)+P(2)
     LWA=13
      N=2
     Y(1)=P(1)
     Y(2)=P(2)
       IF (Y(1) .LE. 0.0D0)GO TO 620
       IF (Y(2) .LE. 0.0D0)GO TO 630
       IF (Y(1) .LE. 1.0D-4)GOTO632
       IF (Y(2) .LE. 1.0D-4)GOTO631
     FTOL=1.0D-6
     YTOL=1.0D-6
     MAXFEV=1000
     CALL HYBRD1(N,FCN,Y,F,FTOL,YTOL,MAXFEV,IER,LWA,WA)
       IF(Y(1) .LT. 0.0D0)GO TO 710
       IF(Y(2) .LT. 0.0D0)GO TO 710
       IF (IER .GT. 1)GO TO 710
       GO TO 720
710      WRITE(6,600)IER
 600 FORMAT(' IER=',I2)
     WRITE(6,610)MAXFEV,Y(1),F(1),Y(2),F(2)
 610 FORMAT(' AFTER ',I5,' ITERATIONS',/
    1 ,10X,'P5= ',D18.11,5X,'F1= ',D18.11,/
    2 ,10X,'P9= ',D18.11,5X,'F2= ',D18.11)
       WRITE (6,609)P(1),P(2)
609    FORMAT(10X,'P1= ',D18.11,5X,'P2= ',D18.11)
720    CONTINUE
       GO TO 690
620    Y(1)=0.0D0
       IF(Y(2).LE.0.0D0)Y(2)=0.0D0
       GO TO 640
630    P(2)=0.0D0
631    P(9)=P(2)
       P(8)=0.0D0
       P(7)=0.0D0
       AAK=1.0D0/AK(1)
       ALPHA=(AAK*DSQRT(1.0D0+8.0D0*Y(1)/AAK)-AAK)/(4.0D0*Y(1))
       P(5)=P(1)*ALPHA
       P(6)=P(1)*(1.0D0-ALPHA)/2.0D0
       GOTO680
632    P(5)=P(1)
       P(6)=0.0D0
       P(7)=0.0D0
       P(8)=0.0D0
```

```
      P(9)=P(2)
      GOTO680
 640  CONTINUE
C 640 WRITE (6,650)Y(1),Y(2)
 650  FORMAT('    ',2D14.6)
 690  CONTINUE
      P(9)=Y(2)
      P(5)=Y(1)
      IF(P(5) .LT. 0.0D0)GO TO 660
      P(6)=AK(1)*P(5)**2
      IF (P(9) .LE. 0.0)GO TO 670
      P(7)=AK(2)*P(5)*P(9)
      P(8)=DSQRT(AK(3)*P(10)*P(5)*P(9))
      GO TO 680
 670  P(7)=0.0D0
      P(8)=0.0D0
      GO TO 680
 660  P(6)=0.0D0
      P(7)=0.0D0
      P(8)=0.0D0
 680  CONTINUE
C     WRITE (6,700) P(1),P(2),P(5),P(6),P(7),P(8),P(9),P(10)
 700  FORMAT ('    ',8D14.6)
      RETURN
     END
```

```
C
C
C
      SUBROUTINE FCN(N,Y,F,IER)
      IMPLICIT REAL*8(A-H,O-Z)
        COMMON AK(3),AKPRIM,PHIA,P12
      DIMENSION F(2),Y(2)
        PHI=PHIA
C       WRITE(6,100) Y(1),Y(2),AK(1),AK(2),AKPRIM,PHI,P12
  100   FORMAT(7D14.6)
      F(1)=Y(1)+2.0D0*AK(1)*Y(1)*Y(1)+2.0D0*AK(2)*Y(1)*Y(2)+
     1     DSQRT(DABS(AKPRIM*Y(1)*Y(2)))+Y(2)-P12
      F(2)=Y(1)+2.0D0*AK(1)*Y(1)*Y(1)-Y(2)-PHI
        IF(Y(2).GT.0.0D0)GO TO 200
        F(1)=1.0D6*Y(2)
  200   CONTINUE
      RETURN
      END
```

```
      SUBROUTINE FLUX (K,P,EN2O3,EN2O4,KG,H,KL,ACHNO2,ACNO,REXN,PS)
C   PROGRAM TO USE THE SHOOTING METHOD TO SOLVE A
C   DIFFERENTIAL EQN WITH AN UNKNOWN BOUNDARY CONDITION.
C   THIS DIFF EQ INVOLVES ABSORPTION FLUX ACROSS A GAS-
C   LIQUID INTERFACE AND WAS DERIVED BY P COUNCE.
C   PROGRAM BY C EMERSON.  24OCT79.
C
C
      IMPLICIT REAL*8 (A-H,O-Z)
        REAL*8 K,KG,KL
        COMMON /CCPASS/PNOB,PHI(13),CHNO2,CNO,PNOS
        COMMON /CPASS/PNO2S,PNO2B
        DIMENSION K(3),H(10),P(10),PS(10),KG(10)
      EXTERNAL F
      EXTERNAL DERV
      B=.100D0
      A=0.1D-4
      TOL=1.0D-3
        CHNO2=ACHNO2
        CNO=ACNO
        PNOB=P(9)
        PNO2B=P(5)
        SQARKP=DSQRT(K(3)*P(10))
        PHI(1)=KL/H(5)
        PHI(2)=2.0D0*EN2O4*K(1)
        PHI(3)=EN2O3*K(2)
        PHI(4)=0.5D0*KL*SQARKP/H(8)
        PHI(5)=0.5D0*KL
        PHI(6)=1.11D0*KL/H(9)
        PHI(7)=KL
        PHI(8)=KG(5)
        PHI(9)=4.0D0*KG(6)*K(1)
C       PHI(11)=0.0D0
        PHI(10)=KG(7)*K(2)
        PHI(11)=0.25D0*KG(8)*SQARKP
        PHI(12)=KG(9)
        PHI(13)=0.0D0
        FLUX=(P(8)-H(8)*CHNO2)/(1.0D0/KL+1.0D0/(H(8)*KG(8)))
        IF(FLUX.LT.0.0D0)PHI(4)=0.0D0
        IF(FLUX.LT.0.0D0)PHI(5)=0.0D0
      Z=ZEROIN(A,B,F,TOL)
        IF(Z .LT. 0.0D0)GO TO 301
        IF (PNOS .LT.0.0D0)GO TO 301
        GO TO 302
 301    CONTINUE
      WRITE(6,300)Z,PNOS
  300 FORMAT(' ','PNO2S= ',E18.11,'PNOS= ',E18.11)
 302    CONTINUE
        DIFF=KL*(CNO-PNOS/H(9))
C       IF(DIFF.GT.REXN)GOTO303
        IF(REXN.GT.DIFF)REXN=DIFF
        GOTO306
 303    PHI(6)=0.0D0
        PHI(7)=0.0D0
        PHI(13)=REXN
        Z=ZEROIN(A,B,F,TOL)
```

```
      IF(Z.LT.0.0D0)GO TO305
      IF(PNOS.LT.0.0D0)GOTO305
      GOTO306
305   WRITE(6,300)Z,PNOS
306   CONTINUE
      PS(5)=Z
      PS(9)=PNOS
      PS(6)=K(1)*PS(5)*PS(5)
      PS(7)=K(2)*PS(5)*PS(9)
      IF(P(5) .LE. 0.0D0)GO TO 1
      IF(P(9) .LE. 0.0D0)GO TO 1
      PS(8)=SQARKP*DSQRT(PS(5)*PS(9))
      GO TO 2
1     PS(8)=0.0D0
2     CONTINUE
      RETURN
      END
```

```
C
C
C
      SUBROUTINE DERV(T,Y,YP)
      IMPLICIT REAL*8 (A-H,O-Z)
        COMMON /CCPASS/PNOB,PHI(13),CHNO2,CNO,PNOS
      COMMON /CPASS/PNO2S,PNO2B
        DATA ZERO/1.D-6/
        PHIA=PHI(1)
        PHIB=PHI(2)
        PHIC=PHI(3)
        PHID=PHI(4)
        PHIE=PHI(5)
        PHIF=PHI(6)
        PHIG=PHI(7)
        PHIH=PHI(8)
        PHII=PHI(9)
        PHIJ=PHI(10)
        PHIK=PHI(11)
        PHIL=PHI(12)
        PHIM=(-1.0D0)*PHI(13)
      PNO2=Y
C       WRITE (6,100)PHIA,PHIB,PHIC,PHID,PHIE,PHIF,PHIG,PHII,PHIJ,PHIK
C 100   FORMAT (10D14.4)
        IF(PNOB.LE.ZERO)PNOB=ZERO
        IF(PNO2B.LE.ZERO)PNO2B=ZERO
      IF(PNO2.LT.ZERO)PNO2=ZERO
      PNOS=((PHIH+PHIA)*PNO2S+(.5D0*PHII+PHIB)*
     1     PNO2S*PNO2S-PHIH*PNO2B-.5D0*PHII*PNO2B*PNO2B+PHIL*PNOB+
     2     PHIG*CNO-PHIM)/(PHIL+PHIF)
      IF(PNOS.LT.ZERO)PNOS=ZERO
      PNO=1.D0/PHIL*((PHIA*PNO2S+PHIB*PNO2S*PNO2S-PHIF*PNOS
     1    -PHIM+PHIG*CNO)*T+PHIH*PNO2+.5D0*PHII*PNO2*PNO2
     2    -(PHIH*PNO2B+.5D0*PHII*PNO2B*PNO2B-PHIL*PNOB))
      IF(PNO.LT.ZERO)PNO=ZERO
      IF(T.GT..99D0) PNO=PNOS
      A=PHIH+PHII*PNO2
      B=PHIJ*PNO+PHIK*DSQRT(PNO/PNO2)
      C=PHIJ*PNO2+PHIK*DSQRT(PNO2/PNO)
      D=PHIL
      RNO2S=PHIA*PNO2S+PHIB*PNO2S*PNO2S+
     1      PHIC*PNOS*PNO2S+PHID*DSQRT(PNOS*PNO2S)-
     2      PHIE*CHNO2
      RNOS=PHIC*PNOS*PNO2S+PHID*DSQRT(PNOS*PNO2S)+
     1     PHIF*PNOS-PHIE*CHNO2-PHIG*CNO+PHIM
      YP=((-C-D)*RNO2S+C*RNOS)/((A+B)*(C+D)-C*B)
      RETURN
      END
```

```
C
C
C
      DOUBLE PRECISION FUNCTION F(C)
      IMPLICIT REAL*8 (A-H,O-Z)
      EXTERNAL DERV
      DIMENSION WORK(9),IWORK(5)
      COMMON /CPASS/PNO2S,PNO2B
      PNO2S=C
      NEQN=1
      Y=PNO2B
      RELERR=1.0D-3
      ABSERR=0.0D0
      IFLAG=1
      T=0.0D0
      TOUT=1.0D0
      CALL RKF45(DERV,NEQN,Y,T,TOUT,RELERR,ABSERR,IFLAG,WORK,IWORK)
      F=Y-PNO2S
      IF(IFLAG.GT.2) WRITE(6,200) IFLAG
  200 FORMAT(' IFLAG= ',I2)
      RETURN
      END
```

```
      SUBROUTINE NOOXID (NFLOW,T,PNO,PO2,VGAS,G,XNO)
        IMPLICIT REAL*8 (A-H,O-Z)
C-----VGAS IS VOLUME OF FREE SPACE
      REAL*8  K
      NPASS = 0
      CXZ = 0.0D0
      XL = 0.000D0
      XR = .9990D0
      XTEST=2*PO2/PNO
      IF (XTEST .LE. XR) XR=XTEST
      B=PNO/PO2
      EPI = .0001D0
      R = .08205D0
      K=10**(652.1D0/T-0.7356D0)
        TAW=VGAS/G
C       WRITE (6,52) PNO,PO2,TAW,K
      A = K*TAW *PNO*PO2
 101  FORMAT (2(4X,E10.3))
      CALL EVALG (NFLOW,B,A,XR,FXR)
      CALL EVALG (NFLOW,B,A,XL,FXL)
      AFXL = DABS(FXL)
      AFXR = DABS(FXR)
      IF(AFXL - EPI) 20,20,10
 10   IF(AFXR - EPI) 21,21,11
 11   IF (FXL * FXR .LT. 0.0) GO TO 12
      WRITE (6,13)
 13   FORMAT(5X,' A ROOT BETWEEN 0 AND 1 IS NOT FOUND IN GAS')
      WRITE (6,51) XL,XR,FXL,FXR
 51     FORMAT ('XL,XR,FXL,FXR=',4D10.3)
        WRITE (6,52) PNO,PO2,TAW,K
 52     FORMAT ('  PNO,PO2,TAW,K=',4D10.3)
      XNO=0.0D0
      GO TO 23
 12   IF(XR-XL) 14,14,15
 14   XZ = (XL - XR)/2.0D0
      CALL EVALG (NFLOW,B,A,XZ,FXZ)
      XNO=XZ
      GO TO 23
 15   TXL = XL
      TXR = XR
 16   NPASS = NPASS + 1
      XZ = (TXL + TXR)/2.0D0
      XNO=XZ
      CONV = DABS(XZ -CXZ)
      IF (CONV .LT. EPI) GO TO 40
      IF (NPASS .GT. 1000) GO TO 40
      GO TO 30
 40   CONTINUE
      GO TO 100
 30   CONTINUE
      CXZ = XZ
      CALL EVALG (NFLOW,B,A,XZ,FXZ)
      AFXZ = DABS (FXZ)
      ADXZ = DABS (TXL - TXR)
      IF (AFXZ .LE. EPI) GO TO 24
      IF (ADXZ .LE. EPI) GO TO 24
```

```
      IF (FXL * FXZ .LT. 0) GO TO 25
      TXL = XZ
      FXL=FXZ
      GO TO 16
 20   CONTINUE
      XNO=XL
      GO TO 23
 21   CONTINUE
      XNO=XR
      GO TO 23
 24   CONTINUE
 25   TXR = XZ
      FXR=FXZ
      XNO=XZ
      GO TO 16
  23  CONTINUE
100   CONTINUE
      RETURN
      END
```

```
      SUBROUTINE EVALG (NFLOW,B,A,X,FX)
        IMPLICIT REAL*8(A-H,O-Z)
C       IF NFLOW EQ 2,THE MODEL USED IS PLUG FLOW
C       IF NFLOW EQ 1, THE FLOW IS ASSUMED TO BE MIXED
      IF (NFLOW .EQ. 2) GO TO 2
        IF (X .LE. 0.0D0)FX=A
        IF (X .LE. 0.0D0)GO TO 1
      FX=A*(1.0D0-((B/2.0D0)+2.0D0)*X+(B+1.0D0)*X**2-(B/2.0D0)*X**3)-X
      GO TO 1
    2 CONTINUE
        IF (X .LE. 0.0D0)FX=A
        IF (X .LE. 0.0D0)GO TO 1
        BB=(-1.0D0)*B/2.0D0
      FX=A-(1.0D0/(1.0D0+BB))*(1.D0/(1.D0-X)+(BB/(1.0D0+BB))
     *  *DLOG((1.D0+BB*X)/(1.D0-X)))
    1 CONTINUE
      RETURN
      END
```